OULU 2023
D 1732

ACTA UNIVERSITATIS OULUENSIS

Jyri-Johan Paakki

BOLD FMRI DETECTABLE ALTERATIONS OF BRAIN ACTIVITY IN CHILDREN AND ADOLESCENTS ON THE AUTISM SPECTRUM

UNIVERSITY OF OULU GRADUATE SCHOOL;
UNIVERSITY OF OULU,
FACULTY OF MEDICINE;
MEDICAL RESEARCH CENTER OULU;
OULU UNIVERSITY HOSPITAL

ACTA UNIVERSITATIS OULUENSIS
D Medica 1732

JYRI-JOHAN PAAKKI

BOLD FMRI DETECTABLE ALTERATIONS OF BRAIN ACTIVITY IN CHILDREN AND ADOLESCENTS ON THE AUTISM SPECTRUM

Academic dissertation to be presented with the assent of the Doctoral Programme Committee of Health and Biosciences of the University of Oulu for public defence in Auditorium 7 of Oulu University Hospital, on 18 August 2023, at 12 noon

UNIVERSITY OF OULU, OULU 2023

Acta Univ. Oul. D 1732, 2023

Supervised by
Professor Vesa Kiviniemi
Professor Osmo Tervonen

Reviewed by
Docent Veikko Jousmäki
Docent Simo Vanni

Opponent
Professor Juhana Hakumäki

ISBN 978-952-62-3741-1 (Paperback)
ISBN 978-952-62-3742-8 (PDF)

ISSN 0355-3221 (Printed)
ISSN 1796-2234 (Online)

Cover Design
Raimo Ahonen

PUNAMUSTA
TAMPERE 2023

Paakki, Jyri-Johan, BOLD fMRI detectable alterations of brain activity in children and adolescents on the autism spectrum.

University of Oulu Graduate School; University of Oulu, Faculty of Medicine; Medical Research Center Oulu; Oulu University Hospital

Acta Univ. Oul. D 1732, 2023

University of Oulu, P.O. Box 8000, FI-90014 University of Oulu, Finland

Abstract

The dissertation consists of three peer-reviewed publications and is related to the basic research of autism spectrum disorder (ASD), especially the assessment of changes in brain function using functional magnetic resonance imaging (fMRI). The purpose was to discover possible differences in cued and spontaneous brain activity in autistic child and adolescent participants compared to typically developing controls.

We used blood oxygen level dependent (BOLD) fMRI imaging of the brain, with which the participants were examined at rest and while looking at facial expressions. The resting state (RS) fMRI data artifacts were reduced, and brain networks were identified using independent component analysis. In addition, the RS was analyzed 1) over the entire measurement period using the regional homogeneity (ReHo) method, which measures local connectivity, and 2) based on the states of different brain networks grouped into shorter periods using the co-activation patterns (CAP) method. Statistically significant differences between groups were found in RS, more clearly with the CAP method. Also, significant differences in brain activity were found between the groups regarding the observation of facial expressions.

The dissertation increases the understanding of changes in brain networks related to the autism spectrum, strengthening and supplementing previous research results. Based on our results, analyses of brain networks grouped into similar activation phases of shorter duration are worth further development. The new information can help develop earlier and more accurate imaging diagnostics, tentatively recognizing possible intervention target brain networks and evaluating therapeutic effects.

Keywords: adolescent, autism spectrum disorder, brain, CAP, co-activation patterns, emotional facial expressions, face processing, fMRI, functional MRI, hierarchical clustering, ICA, independent component analysis, mirror neuron system, regional homogeneity, ReHo, resting state networks, valence

Paakki, Jyri-Johan, Veren happipitoisuudesta riippuvaisella toiminnallisella magneettikuvauksella havaittavat aivotoiminnan muutokset lasten ja nuorten autismikirjossa.
Oulun yliopiston tutkijakoulu; Oulun yliopisto, Lääketieteellinen tiedekunta; Medical Research Center Oulu; Oulun yliopistollinen sairaala
Acta Univ. Oul. D 1732, 2023
Oulun yliopisto, PL 8000, 90014 Oulun yliopisto

Tiivistelmä

Väitöskirja koostuu kolmesta vertaisarvioidusta julkaisusta ja liittyy autismikirjon kehityshäiriön perustutkimukseen, erityisesti aivotoiminnan muutosten arviointiin toiminnallisen magneettikuvauksen (functional MRI, fMRI) avulla. Tutkimuksen tarkoituksena oli selvittää stimuloidun ja spontaanin aivotoiminnan mahdollisia eroavaisuuksia lasten ja nuorten autismikirjossa neurotyypillisiin verrokkeihin nähden.

Tutkimusmenetelmänä käytettiin veren happipitoisuudesta riippuvaista aivojen fMRI-kuvausta, jolla osallistujia tutkittiin levossa sekä heidän katsellessaan kasvojen ilmeitä. Itsenäisten komponenttien analyysilla (ICA) vähennettiin lepotilan fMRI-datan häiriöitä ja tunnistettiin aivoverkostoja. Lisäksi lepotilaa analysoitiin 1) koko mittausjakson ajalta signaalien alueellista homogeenisuutta ts. aivojen paikallista kytkennällisyyttä mittaavalla regional homogeneity (ReHo) -menetelmällä ja 2) eri aivoverkostojen tilojen perusteella lyhyemmiksi ajanjaksoiksi ns. yhtäaikaisten aktivaatioiden kuvioihin (co-activation patterns; CAP) ryhmiteltyinä. Näissä löydettiin tilastollisesti merkittäviä ryhmien välisiä eroja, selkeämmin CAP-menetelmällä. Myös kasvojen ilmeiden tarkkailuun liittyen havaittiin tilastollisesti merkittäviä aivotoiminnan eroja ryhmien välillä.

Väitöskirja lisää ymmärrystä autismikirjoon liittyvistä aivoverkostojen muutoksista vahvistaen ja täydentäen aiempia tutkimustuloksia. Sen perusteella samankaltaisiin lyhempikestoisiin aktivaatiovaiheisiin ryhmiteltyjen aivoverkostojen analyyseja kannattaa kehittää. Uusi tieto voi auttaa varhaisemman ja tarkemman kuvantamisdiagnostiikan kehittämisessä, tarvittaessa oikeisiin aivoverkostoihin kohdennetuissa interventioissa ja niiden vaikutusten arvioinnissa ja seurannassa.

Asiasanat: aivot, aivoverkostot, alueellinen homogeenisuus, ASD, autismikirjon kehityshäiriö, CAP, emotionaaliset kasvojen ilmeet, fMRI, hierarkinen klusterointi, ICA, lepotilaverkosto, peilisolujärjestelmä, ReHo, toiminnallinen magneettikuvaus, valenssi, yhteisaktivaatiokuviot

Emmalle, Fiialle ja Karoliinalle

"Do you know what you are? You are a marvel. You are unique. In all the years that have passed, there has never been another child like you."
"You must work, we must all work, to make the world worthy of its children."
-Pablo Casals

"Never give up on a dream just because of the time it will take to accomplish it. The time will pass anyway."
-Earl Nightingale

"If I had not lived until I was 90, I would not have been able to write this book."
"God knows what other potentials lurk in other people if we could only keep them alive well into their 90s."
-Harry Bernstein

Acknowledgements

This dissertation was carried out alongside clinical work at the Department of Diagnostic Radiology, Oulu University Hospital (OUH), during 2008–2023. The studies have received financial support from the Alma and K.A. Snellman Foundation (Oulu, Finland), Emil Aaltonen Foundation (Tampere, Finland), Finnish Academy Grants #117111 and #123772, Finnish Medical Foundation, Juhani Aho Foundation for Medical Research (Espoo, Finland), Lundbeck Foundation (Turku, Finland), Sigrid Juselius Foundation (Helsinki, Finland), OUH, University of Oulu, and Radiological Society of Finland. I thank all the participants in the study and their parents.

I express my deepest gratitude to a black belt, neuroradiologist, professor, and tango aficionado Vesa Kiviniemi. You have patiently supported and guided my intermittent and winding scientific path since the advanced studies thesis at the medical school. It is in you to kindle your students' spirits, and when analyses "failed," you always had the next one up your sleeve. You have, and continue to, set incredible milestones in brain research. I need to thank another visionary and deep thinker: musculoskeletal radiologist, professor, the former head of our department, and the current dean of Medical Faculty, Osmo Tervonen. I have learned a lot from you, and I thank you for, towards the end, the push that you gave me and the pragmatic advice on how to finish the thesis.

I want to thank pre-examiners Docent Veikko Jousmäki and Docent Simo Vanni for their excellent remarks and advice when reviewing this dissertation. I am very grateful to Professor Juhana Hakumäki for agreeing to be the opponent of this dissertation.

In the beginning, I was really lucky to get a chance to work with two world-class neuroscientists: Research Associate Dr Xiangyu Long and esteemed Professor Yu-Feng Zang. 我最卑微的感謝!

Like countless other researchers, I am deeply indebted to a child psychiatrist, pediatrician, and psychotherapist, Emerita Professor Irma Moilanen, the primus motor behind the seminal and impactful northern Finland ASD studies. I have been very fortunate to research and co-author with adolescent and child psychiatrist, entrepreneur, psychotherapist, and specialist in general medical practice, Dr Jukka Rahko. My warmest thanks to Jukka. I also humbly thank other researcher colleagues and collaborators at that time for their efforts then, and for all the diligent preparations even earlier: Professor Sven Bölte, Emerita Professor Alice Carter, Emerita Professor Hanna Ebeling, Adjunct Professor Tuula Hurtig, Docent Eira Jansson-Verkasalo, Dr Katja Jussila, Dr Aija-Riitta Kotila, Dr Sanna Kuusikko-Gauffin, Dr Jari Kätsyri, Dr Marja-Leena Mattila, Dr Helena Miettunen,

Docent Juha Nikkinen, Emerita Professor David L. Pauls, Emerita Professor Mikko Sams, Dr Tuomo Starck, and Dr Jukka Remes.

I admire my long-term superior, musculoskeletal radiologist, professor, and the chief executive officer of OUH service center Jaakko Niinimäki for his authenticity, effectiveness, innovation, integrity, intelligence, and leadership. I thank my current direct supervisor and head of imaging at OUH, emergency radiologist Dr Marko Nikki, for his warm humoristic attitude, guidance, and effectiveness in helping our many imaging sub-specialties despite administrative pressures. Thanks to both for instilling hope through tough times and leading by example. For similar efforts, I thank the head of diagnostics at OUH, pathologist Docent Saila Kauppila. I also want to warmly remember my former superiors, musculoskeletal radiologist Dr Ilkka Hannila and neuroradiologist Docent Ari Karttunen, as well as the medical director of Pohde well-being services and interventional radiologist Dr Terhi Nevala. I warmly thank my fellow administrative and responsible colleagues Docent Airi Jartti, Dr Elina Järvenpää, Dr Salla-Maarit Kokkonen, Dr Ilkka Lindgren, Professor Miika Nieminen, Dr Marja Perhomaa, Dr Annina Sipola, and Dr Elias Vaattovaara.

To expert senior colleagues, Docent Eija Pääkkö and Docent Eero Ilkko: thank you for forming the monitoring group of my Ph.D. studies. I also thank you for teaching me the fascinating art of radiology and correcting my study reading mistakes as well as possible. For those two qualities, I also owe my gratitude to each and every colleague at the Department of Diagnostic Radiology, OUH. Radiant thanks. Sticks or roses, I still appreciate all the feedback. Many thanks to the knowledgeful and skilled help of Riitta Käkelä, Sanna Mertaniemi, Meri Ojakangas, Reetta Rajala, Teija Ronkainen, Leila Salo, and Arja Väänänen. This dissertation was fortunate to receive the final linguistical touches from Emeritus Senior Lecturer Gordon Roberts.

I especially want to remember my past and present colleagues and co-workers at the Avohoitotalo and G-röntgen for bearing with me (Anna Kaisa, Heli, Heljä, Johannes, Katri, Kirsi, Marjatta, Mauno, Mika, Mikko, Nina, Riina, Sannamari, Seija, Tarja, Tiina, Timo, Tuomas, Pieta, and Veli-Pekka to name just a few). Particularly I am indebted and grateful for the friendship of the chief musculoskeletal radiologist at OUH, Dr Jyri Järvinen. Shout-outs to skilled radiologists (Markus, Aku, Ville, Jarkko, Juha, Eeva, Sari, Sirpa, Suvi, Tuija …) and radiographers who visited or still work in the Central Finland Hospital, Jyväskylä and remembering us juniors (Tatu, T-J, Ilkka), acquiring the base of our skills in radiology and having fun in and out of work.

Without the support of my dear friends Pekka Kerimaa, Heli Kerimaa, Mikko Ylikulju, and Jenni Ranta-Ylikulju, this would have been a dreary lonesome path.

I thank you for all the family gatherings and holiday trips together. I want to thank all my cursus Huusko and Harmainen colleagues and other Oulu Med School fellow students, friends, and past and present motorcycle enthusiasts: what wild fun times and rides we had!

I cannot thank enough my old (are we old?) flatmate Markus Suvanto for everything. Sorry that I once burnt your rice and tried to lie about it. I also warmly pinch two other diploma engineers, Vesa Hyvönen and Markus Kannala.

I consider myself very privileged to have experienced the coming of age with my oldest friend Kari Kyläkoski and our great classmates of 93'. This work would not have been possible without the coding skills and mindset acquired then in Silver Spirit and Wizzcat crews. I wish a pdf scroller with cool effects was possible. Dr. Gold would send greetings to Amigaman, Darkie, Florist, Hazy Mind, Jeddie, Kissarobotti, Pygmy Projects, and other talents whose handles I forgot.

Though I left my home town Rovaniemi, it has a special place in my brain, and the same goes for many places in Lapland and their residents, especially the family branches of Paakki and Pekkala.

Ritva and Raimo Paalimäki, you have been essential to the well-being of our family during the years and have helped us countless times, sometimes at very short notice. We love you.

Heartfelt thanks to my one and only sister Maaria (and her family: Jussi, Onni-Matias, Fanni, and Aaro) for their support and all those important family celebrations.

I thank my parents, Lauri and Sirkku, for giving me life, and I also send a warm hug to their great supportive spouses, Pirkko and Heikki. You have always warmly welcomed us for a visit and taken care of us. We love you.

My magnificent daughters Emma and Fiia, what can I say? I tried to minimize the lost time together due to the dissertation. Still, I often failed or was irritated because it was difficult to tolerate unfinished things and to work on them while tired. I regret every second of those moments. You have given me more than I thought possible, a new purpose and unwavering pursuit to correct my ways and be the best I can be. Thanks for honing my edges; I love you more than anything. And because of you, we have Säde, whom I know can't read but is the most adorable Japanese spitz in the world.

Finally, I thank my beloved wife, Karoliina, for our girls, encouragement ("Hyvä kulta!"), faith, forgiveness, laughs, and love.

12.6.2023 Jyri-Johan Paakki

Abbreviations

3D	Three-Dimensional
4D	Four-Dimensional
ABIDE	Autism Brain Imaging Data Exchange
ADHD	Attention Deficit Hyperactivity Disorder
ADI-R	Autism Diagnostic Interview-Revised
ADOS	Autism Diagnostic Observation Schedule
ACC / ACG	Anterior Cingulate Cortex / Gyrus
AG	Angular Gyrus
ALFF	Amplitude of Low-Frequency Fluctuations
Amy	Amygdala
ASD	Autism Spectrum Disorder(s)
AS	Asperger Syndrome
ASSQ	Autism Spectrum Screening Questionnaire
AFNI	Analysis of Functional NeuroImages
APA	American Psychiatric Association
AQ	Autism Quotient
B_0	Main Magnetic Field
B_1	Radiofrequency Field
BA	Brodmann Area
BET	Brain Extraction Tool
BOLD	Blood Oxygen Level Dependent
CAP	Co-Activation Pattern
CBF	Cerebral Blood Flow
CBV	Cerebral Blood Volume
CC	Corpus Callosum
CEN	Central Executive Network
CG	Cingulate Gyrus
CSF	Cerebrospinal Fluid
DAN	Dorsal Attention Network
dFC	Dynamic Functional Connectivity
DFE	Dynamic Facial Expression
dHb	Deoxyhemoglobin
DMN	Default Mode Network
DMN-A	DMN Anterior Component
DMN-D	DMN Dorsal Component

DMN-V	DMN Ventral Component
DP	Developmental Prosopagnosia
DSM	Diagnostic and Statistical Manual of Mental Disorders
E-I	Excitation-to-Inhibition
ECoG	Electrocorticography
EEG	Electroencephalography
EF	Executive Function
EPI	Echo Planar Imaging
fALFF	fractional ALFF
FC	Functional Connectivity
FDR	False Discovery Rate
FFA	Fusiform Face Area
FFG	Fusiform Gyrus
fMRI	Functional Magnetic Resonance Imaging
FMRIB	fMRI of the Brain Analysis Group, Oxford University, England
FOC	Fronto-Orbital Cortex
FP	Frontal Pole
FPC-L/R	Frontoparietal Cognitive Control, Left / Right Component
FPN	Frontoparietal Network
FSIQ	Full-Scale Intelligence Quotient
FSL	FMRIB's Software Library
FWHM	Full Width at Half Maximum
GICA	Group Independent Component Analysis
GLM	General Linear Model(ing)
GM	Gray Matter
GRE	Gradient-Echo
GSR	Global Signal Regression
Hem	Hemisphere
HFA	High Functioning Autism
HRF	Hemodynamic Response Function
i.e.	Id Est
ICD	International Classification of Diseases
ICN	Intrinsic Connectivity Network
IFG	Inferior Frontal Gyrus
INS	Insula
IOG	Inferior Occipital Gyrus
IPL	Inferior Parietal Lobule

ISLL	Inferior Semi-Lunar Lobule
ITG	Inferior Temporal Gyrus
KCC	Kendall's Coefficient of Concordance
Lat	Lateral
M	Net Magnetization
M_z	Longitudinal Magnetization
M_{xy}	Transverse Magnetization
MCC	Middle Cingulate Cortex
Med	Medial
MEG	Magnetoencephalography
MFG	Medial Frontal Gyrus
MidFG	Middle Frontal Gyrus
MI	Maximum Intensity
ML	Machine Learning
MNI	Montreal Neurological Institute
MOG	Middle Occipital Gyrus
mPFC	medial Prefrontal Cortex
MTG	Middle Temporal Gyrus
MRI	Magnetic Resonance Imaging
NMR	Nuclear Magnetic Resonance
OR	Optic Radiation
OWOB	Overweight and Obesity
PFC	Prefrontal Cortex
PCC	Posterior Cingulate Cortex
PCG	Paracingulate Gyrus
PET	Positron Emission Tomography
PG	Precentral Gyrus
PMC	Premotor Cortex
POC	Parietal Opercular Cortex
p.op	pars opercularis
pSTS	posterior Superior Temporal Sulcus
PT	Planum Temporale
p.tr	pars triangularis
RSN	Resting State Network
S1	Primary Somatosensory Cortex
S2	Secondary Somatosensory Cortex
SE	Spin-Echo

SG	Subcallosal Gyrus
SFG	Superior Frontal Gyrus
SMA	Supplementary Motor Area
SMG	Supramarginal Gyrus
SOG	Superior Occipital Gyrus
SPM	Statistical Parametric Map
STG	Superior Temporal Gyrus
STS	Superior Temporal Sulcus
T1	Spin-Lattice Relaxation Time
T2	Spin-Spin Relaxation Time
T2*	T2 Star
TD	Typically Developing
TL	Temporal Lobe
TP	Temporal Pole
TPN	Task-Positive Network
TVFC	Time-Varying Functional Connectivity
ReHo	Regional Homogeneity
RF	Radiofrequency
RS	Resting State
RS-fMRI	Resting State fMRI
RSN	Resting State Network
RSFC	Resting State Functional Connectivity
Up Med	Upper Medial
VAN-A/P	Ventral Attention Network, Anterior / Posterior component
VASO	Vascular Space Occupancy
Visual Med	Visual network, Medial component
Visual Lat	Visual network, Lateral component
Visual Up Med	Visual network, Upper Medial component
VLF	Very Low Frequency
VPL	Ventral Posterolateral Nucleus (of Thalamus)
W	Kendall's coefficient of concordance
WM	White Matter
WHO	World Health Organization

List of original publications

This thesis is based on the following publications, which are referred to throughout the text by their Roman numerals I – III:

I Rahko, J. S., Paakki, J.-J., Starck, T. H., Nikkinen, J., Pauls, D. L., Kätsyri, J. V., Jansson-Verkasalo, E. M., Carter, A. S., Hurtig, T. M., Mattila, M.-L., Jussila, K. K., Remes, J. J., Kuusikko-Gauffin, S. A., Sams, M. E., Bölte, S., Ebeling, H. E., Moilanen, I. K., Tervonen, O., & Kiviniemi, V. (2012). Valence scaling of dynamic facial expressions is altered in high-functioning subjects with autism spectrum disorders: an fMRI study. *Journal of Autism and Developmental Disorders*, *42*(6), 1011–1024. https://doi.org/10.1007/s10803-011-1332-8

II Paakki, J.-J., Rahko, J., Long, X., Moilanen, I., Tervonen, O., Nikkinen, J., Starck, T., Remes, J., Hurtig, T., Haapsamo, H., Jussila, K., Kuusikko-Gauffin, S., Mattila, M.-L., Zang, Y., & Kiviniemi, V. (2010). Alterations in regional homogeneity of resting-state brain activity in autism spectrum disorders. *Brain Research*, *1321*, 169–179. https://doi.org/10.1016/j.brainres.2009.12.081

III Paakki, J.-J., Rahko, J. S., Kotila, A., Mattila, M.-L., Miettunen, H., Hurtig, T. M., Jussila, K. K., Kuusikko-Gauffin, S. A., Moilanen, I. K., Tervonen, O., & Kiviniemi, V. J. (2021). Co-activation pattern alterations in autism spectrum disorder – a volume-wise hierarchical clustering fMRI study. *Brain and Behavior, 2021;11:e02174.* https://doi.org/10.1002/brb3.2174

Author's contribution

Our research groups and I contributed to the study designs and conducted the MRI imaging. The study-specific contributions are listed below.

Study I: I contributed as a co-author in analyzing the results, and writing and reviewing the manuscript.

Study II: I preprocessed and analyzed the data with help from X. Long. I was responsible for writing the manuscript with contributions from my co-authors.

Study III: I preprocessed and analyzed the data. I was responsible for writing the manuscript with contributions from my co-authors.

Contents

1 Introduction

Autism spectrum disorder (ASD) is a neurodevelopmental condition that typically manifests in early childhood, but affects social communication and behaviors throughout life (American Psychiatric Association, 2013; Lord et al., 2022; World Health Organization, 2020). The Lancet commission on the future of care and clinical research in autism (Lord et al., 2022) states that "autism is a condition of global importance because of its prevalence and the degree to which it can affect individuals and families". Worldwide, at least 78 million people are estimated to have autism, most of whom do not receive adequate support (Lord et al., 2022).

The term neurodiversity describes the natural variability within human brains and minds (Pukki, 2022; Walker, 2014). The neurodiversity movement considers autism to be a neurological difference rather than a disorder. The movement challenges autism researchers and clinicians to reconsider the goals of early intervention, and it is sometimes associated with opposition to efforts to find a cause or cure (Dawson et al., 2022; Lord et al., 2022; Ne'eman, 2021; Robison, 2020; Walker, 2014, 2016; Wallis, 2022). Nowadays, autism may refer to a heterogeneous and broad spectrum of phenotypes, from only autistic personality traits with high intelligence to severe profound autism. A profoundly autistic individual requires around-the-clock access to an adult caregiver due to being unable to be left alone in residence and unable to take care of basic daily adaptive needs. Based on three datasets, the Lancet commission estimated that from 18 to 48 percent of the autism population falls into the category of profound autism, associated with a substantial intellectual disability (e.g., an intelligence quotient below 50), minimal language (e.g., limited ability to communicate with a stranger using comprehensible sentences), or both (Lord et al., 2022).

Neurodevelopmental conditions can require highly specialized pathology-specific treatment when one exists, but the need for individual care, support, services, and educational strategies should always be determined as an essential requirement. Society's failure to accommodate autistic individuals can have devastating effects, primarily on autistic people and their families (Bottema-Beutel et al., 2021; Lord et al., 2022). Autistic individuals, especially women, have a significantly higher risk of psychiatric diagnoses, hospitalizations (Martini et al., 2022), and suicide (Hirvikoski et al., 2020). According to the latest Finnish Client and Patient Safety Strategy Plan 2022–2026, clients, patients, and their close ones are the best experts on their situation, and shared decision-making with them is the primary course of action in healthcare to reach a common understanding (Ministry

of Social Affairs and Health, 2022). Healthcare practice must be based on evidence and good clinical and policy practices, and must promote physical, mental, and social wellbeing while causing as little harm as possible (Ministry of Social Affairs and Health, 2022). Treatment or support starting early is generally thought to be more effective, and, on the other hand, methods for monitoring the effectiveness of interventions should be further developed. Today, an optimal intervention outcome is reached through common goal setting without necessarily conforming to typical behavior (Dawson et al., 2022; Ne'eman, 2021). Early detection can help decide therapy and improve the quality of life for patients and their close ones, positively affecting social communication, language, and adaptive behavior (Lord et al., 2022).

In neurodevelopmental, neurological, and psychiatric diagnostics, the brain's structural magnetic resonance imaging (MRI) is often a basic examination to assess possible anatomical abnormalities related to the condition and exclude other pathology (A. N. Anderson et al., 2019; Dubois et al., 2021; Guo et al., 2022). Often with mild disorders or in the early stages, the neuroradiological findings are normal. In the workup of autism, imaging currently plays a limited role, predominantly assessing other conditions that may be associated with developmental delay or providing etiological insights (Lord et al., 2022; Tang, 2022). There are no unambiguous diagnostic features on MRI, though various structural features have been reported (Rafiee et al., 2022; Tang, 2022), and machine learning (ML) methods may be trained to recognize autism (Ali et al., 2022; Guo et al., 2022; Khodatars et al., 2021).

Functional MRI (fMRI) offers the opportunity to expand the diagnostic "toolbox" of physicians by also imaging brain activity. As our knowledge of the brain's functional networks and their characteristics in different conditions increase, at best, a few minutes of additional neuroimaging in conjunction with brain MRI could provide additional objective diagnostic information, even if the anatomical finding turns out to be normal. Neuroimaging in profound autism represents a distinct challenge, as participants with a higher severity of symptoms have a lower success rate of completing the MRI (DeMayo et al., 2022). While shortcuts to provide objective and inarguable diagnostic answers are enticing, the proper intention of the diagnostic procedures is to provide the clinician with standardized information to formulate an optimal individual care plan (Lord et al., 2022). Whether autism is viewed from the neurodiversity or pathology paradigm (Walker, 2016), studying brain activity in individuals and groups benefits understanding the different forms of neurodivergence.

When this research commenced, the dynamic facial expressions essential for social interaction had not been utilized in brain activity studies of ASD (Study I). On the other hand, the differences in resting state brain activity and especially local connectivity had not been extensively mapped (Study II).

The fluctuations of a person's mental state and attention shifts between internal and external events are continuous. Thus, Study III examined the fMRI time series in shorter periods instead of the more common whole time series approach. We also focused on different brain networks and their co-activations instead of anatomical brain areas only (Study III). While writing this dissertation, Studies I and II were partially re-examined via such a network approach.

2 Literature review

2.1 Magnetic resonance imaging (MRI)

Though nowadays a routine method within medical diagnostics, MRI took decades and several Nobel Prize-earning seminal discoveries to develop.

Atomic nuclei in a strong magnetic field rotate with a frequency dependent on the magnetic field's strength. Their energy can be increased if they absorb radio waves with the same frequency (resonance). When the atomic nuclei return to their previous energy levels, radio waves are emitted. This phenomenon, called nuclear magnetic resonance (NMR), was first described and measured in molecular beams by Isidor Rabi (Rabi et al., 1938), who was awarded the Nobel Prize in Physics in 1944. Applying NMR on liquids and solids, Felix Bloch and Edward Mills Purcell were awarded a Nobel Prize in Physics in 1952 "for their development of new methods for nuclear magnetic precision measurements and discoveries in connection therewith" (Bloch, 1946; Nobel Prize Outreach AB, 2023a; Purcell et al., 1946).

Paul Lauterbur discovered the possibility of creating a two-dimensional image by introducing gradients in the magnetic field. Through analysis of the characteristics of the emitted radio waves, he could determine their origin (Lauterbur, 1973). Peter Mansfield further developed the utilization of gradients in the magnetic field with selective RF irradiation of the sample (Garroway et al., 1974). He showed how the signals could be mathematically analyzed, which made developing useful and fast imaging techniques possible. Lauterbur and Mansfield were awarded the Nobel Prize in Physiology or Medicine in 2003 for their discoveries concerning MRI (Nobel Prize Outreach AB, 2023b).

In neurodevelopmental brain imaging, MRI is the most widely used tool. In a typical diagnostic setting, it can best separate normal soft brain tissue types such as gray or white matter (GM, WM) and cerebrospinal fluid (CSF) or pathologic tissue types like inflammation or different tumors (Plewes & Kucharczyk, 2012; Wardlaw et al., 2012). Simplified, an MRI image gives a density map of hydrogen nuclei in a brain. While hydrogen originates mainly from the high water content of the brain with some contribution from fat tissue protons, especially in WM, there is enough variation in the magnetic properties (namely T1 spin-lattice and T2 spin-spin relaxation times) of each tissue type to stand out with its typical proportions of hydrogen among other elements (Bojorquez et al., 2017; Plewes & Kucharczyk,

2012). However, the resulting voxel (the smallest single unit of a three-dimensional image, equivalent to a pixel of a two-dimensional image) intensities depend heavily on the parameters of the MRI sequence and the timing of measurements (Bojorquez et al., 2017; Plewes & Kucharczyk, 2012).

The magnet in the MRI scanner produces a strong magnetic field B_0 (in a clinical setting, usually 1.5 or 3.0 Tesla units) that forces nuclei of hydrogen atoms in a brain to align their spins (a fundamental property of subatomic particles representing intrinsic angular momentum) to the field's direction, producing the sum of their magnetic properties averaged together and creating net magnetization (M) (Bojorquez et al., 2017; Plewes & Kucharczyk, 2012). Additional gradient coils are used to create a slight augmentation to the B_0 field as a function of left-right or anterior-posterior location in the gantry, a frequency and phase manipulation used for spatial encoding (Gruber et al., 2018; Plewes & Kucharczyk, 2012). When a radio frequency (RF) magnetic field B_1 or pulse with a head RF coil is applied perpendicular to the B_0 field, M is tilted out of alignment. An optimal rotation frequency of the B_1 field must be used for this to occur (Bojorquez et al., 2017; Gruber et al., 2018). This so-called Larmor frequency is derived as the product of nucleus specific gyromagnetic ratio γ and the strength of the B_0 field. For example, hydrogen's Larmor frequency in a homogenous magnetic field is approximately 64 MHz at the 1.5T or 128 MHz at the 3.0T field (Elster, 2023; Gruber et al., 2018; Plewes & Kucharczyk, 2012; Wardlaw et al., 2012)

After the nuclei exciting RF pulse is turned off, M starts to return to be parallel to B_0. Two main mechanisms are at hand: the relatively slower T1 relaxation for regrowth of longitudinal magnetization (M_z) and the faster T2 decay of spin phase coherence for transverse magnetization (M_{xy}) (Goldman, 2001; Plewes & Kucharczyk, 2012). A receiver head RF coil sensitive to magnetic flux changes in the transverse plane can then detect the M_{xy} components as hydrogen nuclei oscillating at the Larmor frequency return to their previous state and emit a resonance wave (Elster, 2023; Plewes & Kucharczyk, 2012). A small signal current is generated in the RF coil via the Faraday-Lenz induction principle (Elster, 2023). A grid of raw data obtained from collecting these signals is called k-space, and it consists of an array of numbers representing spatial frequencies in the MRI image. After sufficient RF pulse and signal measurement repetitions, the k-space includes enough measurements, and an inverse 2D Fourier transform is utilized to achieve a human-readable image (Elster, 2023; Gruber et al., 2018; Plewes & Kucharczyk, 2012).

The magnetic field strength of the MRI scanner influences the image quality. A higher field strength increases image quality, resolution, and signal-to-noise-ratio or can speed up imaging (Gruber et al., 2018; Wardlaw et al., 2012). A higher field strength can also lead to deterioration of image quality by introducing increased susceptibility artifacts causing spatial distortion and signal attenuation near the skull base and paranasal sinuses, increased dielectric artifacts causing signal heterogeneity, and a higher specific absorption rate causing unwanted heating and limiting the size of the imaged area (number of slices) and the duration of the study (Elster, 2023; Wardlaw et al., 2012).

2.2 Functional MRI (fMRI) and neurovascular coupling

Blood oxygen level dependent (BOLD) fMRI relies on the same general principles as MRI but exploits the T2* relaxation caused by a combination of spin-spin ("true" T2) relaxation and magnetic field inhomogeneity. T2* relaxation is seen only with gradient-echo (GRE) echo planar imaging (EPI) because with T2-weighted spin-echo (SE) imaging, transverse relaxation caused by magnetic field inhomogeneities is eliminated by the 180° pulse. Our study used GRE due to the 1.5T magnet and technology at the time, but at higher field strengths, SE BOLD contrast could also be viable (Han et al., 2022; Miao et al., 2023; Raimondo et al., 2021). Repeated BOLD signal measurements via fMRI detect changes in blood oxygen saturation across different brain regions over time and allow indirect non-invasive localization of the neuronal activity in humans and animals. These changes in local T2*-based contrast are elicited because the hemoglobin in the red blood cells is diamagnetic when oxygenated and paramagnetic when deoxygenated (deoxyhemoglobin; dHb). During the brain's neuronal activation, a modest increase in the cerebral metabolic rate of oxygen is accompanied by a much larger increase in local blood flow (P. T. Fox & Raichle, 1986). Due to this imbalance, local capillary and venous blood are more oxygenated during activation. The relative decrease in local dHb leads to a slight increase in the local T2* signal (Buxton et al., 1998; Chavhan et al., 2009; S.-G. Kim & Ogawa, 2012; Oliveira et al., 2021). This BOLD response signal change is 1–5% in 1.5T and 2–10% in 3.0T magnet, i.e., higher field strength increases the BOLD response (Hale et al., 2010; Krasnow et al., 2003; Krüger et al., 2001; Ogawa et al., 1990, 1992).

Oxygen is one of the main ingredients needed in cell metabolism. Even at rest, our brain consumes about 20% of oxygen transported from the lungs by the arterial flow. When a group of neurons activates, a local pulsatile blood surge provides

them with oxygen, glucose, and other necessary ingredients. Waste removal and heat regulation are additional proposed roles for this functional hyperemia. Neurovascular coupling is the essential regulator of metabolism based on the energy demands of neuronal function. This coupling requires a concomitant interplay between the metabolic state of a neuron and the serving capillary network section surrounded by an astrocytic process and its interrelated metabolic pathways (Howarth et al., 2021; Koehler et al., 2009; Ludwig et al., 2021; Marina et al., 2020; Meigel et al., 2019; Ray et al., 2019).

A typical unfiltered T2* weighted fMRI voxel of 55 µl (approx. 4 x 4 x 4 mm^3) contains 5.5 million neurons, 2.2–5.5 x 10^{10} synapses, 22 km of dendrites and 220 km of axons (Logothetis, 2008). Based on the balance of the oxygen supply and consumption in a brain area and the resulting BOLD fMRI signal changes, the measured voxel intensities can be used as a proxy to monitor the fluctuations in induced, mainly excitatory, neuronal responses to some sensory input, task or to track the intrinsic brain activity at rest. (Hillman, 2014; Howarth et al., 2021; Logothetis, 2008; Moon et al., 2021; Oliveira et al., 2021; Schmid et al., 2019)

Though BOLD signal changes indicate neural activity changes in specific brain areas, in a standard fMRI setting, it is impossible to distinguish between inhibitory or excitatory activity (Howarth et al., 2021; Logothetis, 2008). As inhibitory neurons decrease nearby excitatory neuron activity and connect to nearby arterial vasculature, they also play a significant role in BOLD response (Moon et al., 2021). In addition, several supporting cell types, such as glial and vascular cells, contribute to metabolism and hemodynamic changes. Excitatory neurons, however, comprise the largest group of all neurons with a share of 80–90% and are a major consumer of oxygen and energy (Howarth et al., 2012, 2021; Meyer et al., 2011; Moon et al., 2021). An imbalance between excitation and inhibition has been one of the longstanding hypotheses in some neurodevelopmental conditions: self-evidently in epilepsy (Sarlo & Holton, 2021) but also in ASD (Antoine, 2022; Berto et al., 2022; Contractor et al., 2021; Manyukhina et al., 2022; Nelson & Valakh, 2015; Port et al., 2019; Rubenstein & Merzenich, 2003). Increasing the excitation-to-inhibition (E-I) ratio caused a significant reduction of long-range fMRI connectivity in a mouse model, demonstrating an approach toward inferring cortical microcircuit abnormalities from fMRI measurements (Markicevic et al., 2020).

The mathematical function representing neurovascular coupling dynamics is the hemodynamic response function (HRF). The hemodynamic response is several times slower than the neuronal response, comparing seconds to milliseconds. Correspondingly, the classical temporal resolution of fMRI relying on this indirect

measure is lower than electrophysiological methods such as electrocorticography (ECoG), electroencephalography (EEG), or magnetoencephalography (MEG) directly measuring neuronal activity (Sadaghiani et al., 2022). While HRF may differ between individuals and across cortical regions, in a generic form, two combined gamma functions approximate it: a standard positive function at normal lag and a small delayed inverted gamma attempting to model the late undershoot (Friston, Holmes, et al., 1994; Friston, Jezzard, et al., 1994). In a mouse study, excitatory and inhibitory neurons produced slightly differing BOLD responses: stimulation of inhibitory neurons led to biphasic responses at the stimulation site, initial positive and later negative BOLD signals, and negative BOLD responses at downstream sites (Moon et al., 2021). The initial positive BOLD response was due to vasodilation induced by inhibitory neuronal activity, while the negative BOLD response was likely due to vasoconstriction by reduced excitatory activity. The HRF of inhibitory neurons peaks earlier than that of excitatory neurons, which may imply that the often-observed early BOLD fMRI overshoot is due to increased inhibitory neural activity (Moon et al., 2021). The modeling of HRF has evolved gradually from a linear (Friston, Holmes, et al., 1994) to more complex models (Buxton, 2012; Buxton et al., 1998, 2004; Friston et al., 2000; Stephan et al., 2007). The fast fMRI (e.g. whole brain imaged in 100 ms) study results with higher temporal and spatial resolution have shown the limits of canonical HRF models and the need for an update (J. E. Chen et al., 2021; Lewis et al., 2018; Polimeni & Lewis, 2021). Data-driven HRF estimation provides one solution (E. J. Allen et al., 2022; Wu et al., 2021).

Thus, progress has been made over the three decades since the beginning of BOLD imaging (Kwong et al., 1992; Ogawa et al., 1992). However, the complex relationship between neuronal activity and the BOLD signal is still not yet perfectly modeled or understood. The both linear and nonlinear properties of the BOLD signal have been demonstrated with task variations depending on the stimulus modality, duration, and frequency rate (J. E. Chen et al., 2021; Lewis et al., 2018). Logothetis et al. (2001) measured that the BOLD contrast mechanism reflects a given area's input and intracortical processing rather than its spiking output. Combined ECoG and BOLD fMRI studies show a close to linear relationship between neuronal population activity measured by ECoG and BOLD responses (B. J. He et al., 2008; Kucyi et al., 2018; Miller et al., 2009). Still, oxygen consumption by active neurons reduces positive BOLD signals and confounds the accuracy of positive BOLD response as a readout of neuronal activity (Howarth et al., 2021). On the other hand, responses plateau with high stimulus rates or when

the blood flow is increased to the point that all dHb in the venous vasculature is washed out (Bright et al., 2020; Oliveira et al., 2021).

Cerebral blood volume (CBV) measurements based on the differences between T1 relaxation times of blood and tissue combined with a blood signal nulling inversion pulse, known as the vascular space occupancy (VASO) contrast, provide an alternative fMRI contrast mechanism to BOLD. VASO contrast is sensitive to arteriole and post-arterial CBV changes, leading to better microvasculature level localization than BOLD, which also suffers from the draining vein contamination effect. Simultaneous BOLD and VASO-CBV imaging demonstrates a tight response relationship strengthening the putative neuronal origin of the plateauing effects and further elucidating the nonlinear properties of the neurovascular coupling phenomenon (Oliveira et al., 2021). Also, recently, a novel cardiohemodynamic envelope technique from ultrafast fMRI detected the vasodilation response some 1.3 sec prior to the BOLD signal response (Huotari et al., 2022).

Other physiological factors such as cardiac and respiratory control and CSF cycles also affect the magnetic field and the detected T2* signal changes as, for example, measurements in CSF spaces devoid of hemoglobin show (Delaidelli & Moiraghi, 2017; Dreha-Kulaczewski et al., 2015; Kiviniemi et al., 2016; Ludwig et al., 2021). Brain-wide and heterogeneous dynamics coupled only to respiratory and heart rate variation can produce "physiological networks" that resemble previously reported resting state (RS) networks (RSNs) of putatively neuronal origin (J. E. Chen et al., 2020). Functional brain networks may be split into two spatially similar networks; one dominated by the neuronal stimulus, and the other by vasodilatory responses to changes in arterial CO_2 levels. Vascular regulation may be coordinated across long-distance brain regions, or neurovascular relationships vary in a network-specific manner (Bright et al., 2020; Stiernman et al., 2021).

As some noise sources (e.g., head motion, cardiac and respiratory activity) may be generated by the same underlying brain networks that give rise to functional signals, the distinction between signal and noise is not always straightforward (T. T. Liu, 2017). Though context dependent, many methods for cleaning the BOLD signal from non-neuronal fluctuations of instrumental, physiological, or subject-specific origin have been developed in an attempt to isolate the optimal signal with the best correspondence to neuronal activity (Caballero-Gaudes & Reynolds, 2017). In both RS- and task fMRI studies, the neuronal activation appears in the very low frequency (VLF) range (~0.01–0.15 Hz) of the BOLD signal (Huotari et al., 2019; Kiviniemi et al., 2016; Tong et al., 2019). Task activation can be modeled, leading

to more robust neuronal activity associations. In contrast, the RS studies are vulnerable to confounding noise as the neuronal firing is spontaneous and of an unknown time course (Tong et al., 2019).

2.3 Functional connectivity networks in the brain

2.3.1 Analysis methods

Typically, a statistical dependency such as a correlation or covariance of signals is used to constitute a connection between brain regions for a functional network (M. D. Fox & Raichle, 2007; Friston, 1994; Uddin et al., 2019). Stable functional networks are likely underpinned by WM connections (Lu et al., 2011). Most functional neuroscience studies until the end of the 2000s focused on the brain's response to a task or stimulus, which was represented to the study subject during fMRI via appropriate MRI-compatible stimulus devices. Calculating the level and probability of stimulus related brain activation for a single participant is typically achieved using a linear model of the signal together with a Gaussian noise model for the residuals, commonly known as a general linear model (GLM; Friston, Holmes, et al., 1994; Woolrich et al., 2001). The traditional analysis involves correlating BOLD data with a stimulation time course across multiple time blocks, the so-called block design. Contrasting the stimulus and rest conditions in the GLM model design, in effect, averages across each condition and performs a subtraction, minimizing "noise" in the BOLD signal and revealing brain regions modulated by the stimulus or task (Amaro & Barker, 2006; M. D. Fox & Raichle, 2007). Besides subtraction, other condition comparison strategies include factorial (Gurd et al., 2002), parametric, or conjunction (Bremmer et al., 2001) types. In addition to the standard block design, event-related and mixed designs became necessary in assessing higher cognitive functions due to the less predictable timing of stimuli or tasks (Amaro & Barker, 2006; Stark & Squire, 2001). The collection of functional scan(s) for each subject and the development of multi-level mixed effects GLM enabled studying group-level activation effects (Beckmann et al., 2003; Woolrich, Behrens, Beckmann, et al., 2004). Such mass-univariate model-based analysis represents classical statistical inference and is standard in fMRI research. Advancing computing power and software development led to more flexible and sensitive multivariate and model-free statistical methods (Hanke et al., 2009; Kauppi et al., 2014; Kiviniemi et al., 2011; Mahmoudi et al., 2012). Multivariate

methods combined with ML have become powerful tools, and the design and testing of explicit models of neural presentations represent the current state-of-the-art research (Breedlove et al., 2020; Gu et al., 2022; Naselaris & Kay, 2015; Saarimäki et al., 2022; Vanni et al., 2005, 2015).

Analysis of RSNs

The notion that task-related increases in neuronal metabolism are small (<5%) and the observations of organized spontaneous BOLD activity in somatomotor cortices (Biswal et al., 1995) and other regions of the brain (Damoiseaux et al., 2006; M. D. Fox et al., 2005; M. D. Fox & Raichle, 2007; Lowe et al., 1998) generated a new study field of resting state (RS-) fMRI. It was found that brain networks were discernible even without external stimuli while study subjects just rested in the scanner. The major brain networks and their subnetworks were shown to have close correspondence between the independent analyses of resting and activation brain dynamics (Smith et al., 2009). Networks have also been identified with other modalities, such as EEG, ECoG, and MEG (Bourguignon et al., 2011; Bray et al., 2015; De Tiège et al., 2020; Jousmäki, 2000; Sadaghiani et al., 2022).

Nowadays, fMRI during a patient's rest is an applicable option. It can be implemented in connection with typical diagnostic anatomical MRI study without complex preparations, rehearsal, or additional MRI-compatible stimulus hardware. RS data obtained through the scans can be analyzed with a variety of methods, e.g., functional connectivity (Cherkassky et al., 2006; Kennedy & Courchesne, 2008b), regional homogeneity (Zang et al., 2004), co-activation pattern (X. Liu et al., 2018) and independent component (Kiviniemi et al., 2003) analyses, to name but a few. Recently, a range of empirical phenomena, including functional connectivity gradients, the task-positive/task-negative anti-correlation pattern, the global signal, time-lag propagation patterns, the quasiperiodic pattern, and the functional connectome network structure, were presented as manifestations of three spatiotemporal patterns (Bolt et al., 2022). These patterns combining zero-lag representations of functional connectivity structure and time-lag representations of traveling wave structure explain a large portion of the variance in spontaneous BOLD fluctuations and account for much of the large-scale structure underlying all FC analysis (Bolt et al., 2022).

Functional connectivity (FC)

Traditionally RS-fMRI analysis has relied on a temporally stationary, i.e., static FC measure, in which the correlations between the voxel time series of brain regions are examined as unchanging over time. A cross-correlation coefficient map is obtained by correlating the average time course of the seed voxels with other brain areas' voxels' time courses. The most used measure for the degree of correlation is probably the Pearson correlation coefficient, a normalized measurement of the covariance. When the covariance is divided by the two samples' standard deviations, the range of the covariance is rescaled to the interval between -1 and +1 (Rodgers & Nicewander, 1988). It reflects the linear correlation of variables, but ignores many other types of association between signals.

Regional homogeneity (ReHo)

ReHo is a particular case of FC, measuring the local synchronization of spontaneous fMRI signals by calculating the similarity of dynamic fluctuations of voxels within a given cluster, and without any a priori assumptions regarding the hemodynamic model or the signals' probability distributions (Long et al., 2008; Zang et al., 2004; Zou et al., 2009).

In ReHo, a non-parametric statistic Kendall's *W*, i.e., Kendall's coefficient of concordance (KCC; Kendall & Gibbons, 1990; Legendre, 2010), is calculated to represent the similarity of the BOLD time series $v_i(t)$ of each *K* nearest neighboring voxels (Jiang & Zuo, 2016; Maximo et al., 2013; Song et al., 2011; Zang et al., 2004). The KCC is given to the center voxel;

$$W = \frac{\sum_{i=1}^{n} R_i^2 - n(\bar{R})^2}{\frac{1}{12}K^2(n^3 - n)} \quad (1)$$

where *W* (ranging from 0 to 1 and representing no concordance to complete concordance) is the KCC among given voxels; $R_{i=1,\ldots,n}$ represents the ranks of $v_i(t)$, and *n* is the number of temporal observations in the time series (e.g., in Study II, *n* = 249, the number of BOLD volumes - 1); $\bar{R} = ((n+1)K)/2$ is the overall mean rank across all the *K* neighbors and all temporal observations; *K* is the number of time series within a measured cluster (e.g., in Study II, *K* = 27, one given voxel plus the number of its neighbors) (Jiang & Zuo, 2016; Zang et al., 2004).

Zou et al. (2009) investigated the static and dynamic characteristics of cerebral blood flow (CBF) in the RS using an arterial spin labeling (ASL) perfusion imaging

technique. Consistent with previous results from another functional imaging method measuring metabolic changes, positron emission tomography (PET), static CBF measured by ASL was significantly higher in the PCC, thalamus, insula/superior temporal gyrus (STG), and medial prefrontal cortex (mPFC) than the average CBF of the brain. These brain regions also had high temporal synchrony, as measured by ReHo. Higher ReHo in the default mode network (DMN; Buckner et al., 2008; Raichle et al., 2001) is not simply due to the high CBF baseline or SNR, but rather reflects the local synchrony (Zou et al., 2009). Long et al. (2008) used three methods to analyze RS-fMRI data; ReHo, linear correlation, and independent component analysis (ICA). All three methods depicted the DMN. Since the BOLD fMRI reflects neural activity (Logothetis & Wandell, 2004), abnormal ReHo is related to changes in the temporal aspects of the spontaneous neural activity in the regional brain and is a sign of disrupted local functionality. Analysis of ReHo has been utilized in detecting alterations in subjects with attention deficit hyperactivity disorder (ADHD; N. He et al., 2022), depression (Iwabuchi et al., 2015), schizophrenia (Jin et al., 2021; Qiu et al., 2021), obsessive-compulsive disorder (Qing et al., 2021), Parkinson's (Pan et al., 2017) and Alzheimer's diseases (Y. Liu et al., 2008).

The aforementioned volume-based method can also be called 3dReHo, but in this dissertation, it is referred to as ReHo (Fig. 1). In a volume space, the voxel's neighbors may not be close to the voxel across the cortical mantle. Based on the two-dimensional nature of the laminar cerebral cortex, a surface-based ReHo variant is then called 2dReHo (Jiang et al., 2015).

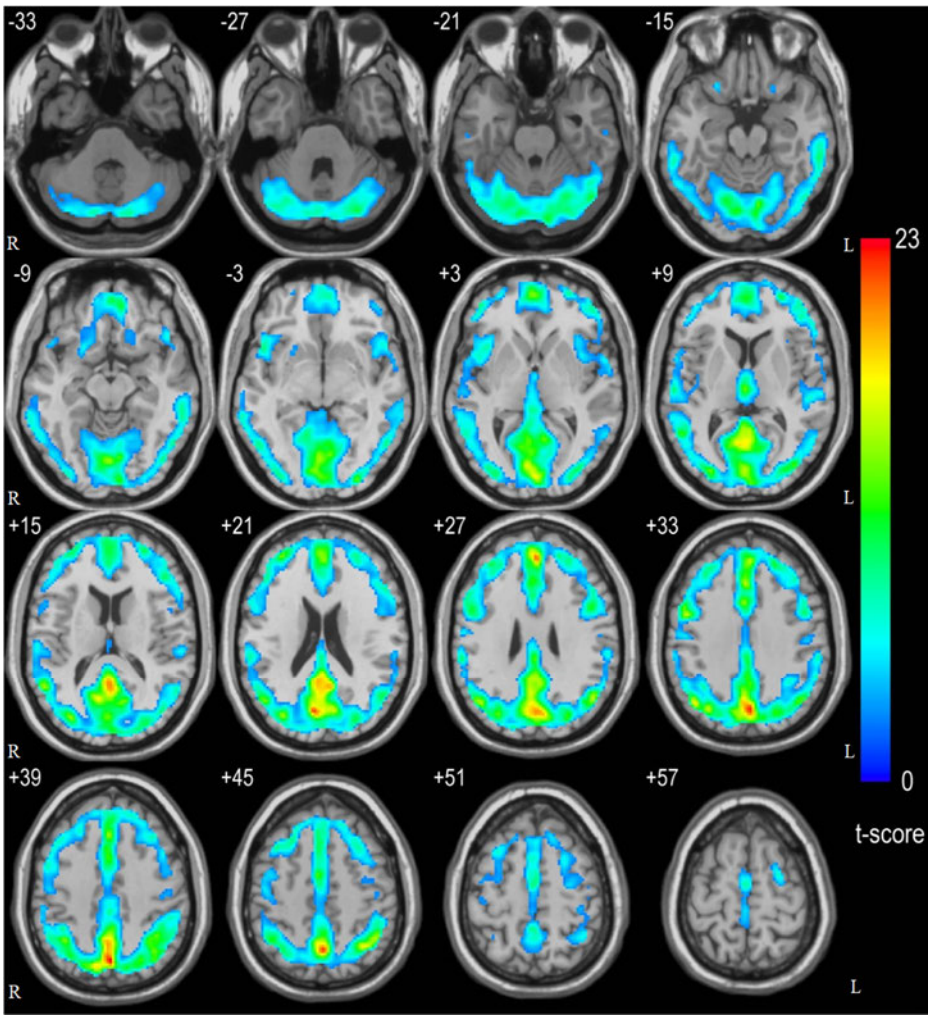

Fig. 1. Results of regional homogeneity (ReHo) are shown as a Kendall's coefficient of concordance (KCC) map across all typically developing (TD) controls in the resting state (one-sample t-test; $p < 0.01$, corrected for the minimum volume of 456 mm^3). The image's left-side corresponds to the brain's right-side. Z-coordinates, according to Talairach space, are shown in the upper left corner of the slices. Reprinted with permission of Elsevier from Study II © 2010 Elsevier.

Co-activation pattern analysis (CAP)

It is important to recognize that the same static FC pattern could result from many different combinations or sequences of shorter spatiotemporal patterns of underlying time-varying FC (TVFC; Lurie et al., 2020). Since the seminal work of Chang and Glover (2010), the last decade has seen a growing trend and a deliberate effort to characterize dynamic changes in brain connectivity as a function of time, dynamic FC (dFC), or TVFC. It has been suggested that greater intraindividual dynamic variance is a potential biomarker of not only ASD but also other mental disorders, such as schizophrenia and ADHD, and that it may underlie confusing static FC measures (H. Chen et al., 2017; Falahpour et al., 2016; J. Zhang et al., 2016). The most widely used TVFC method, temporal sliding window analysis, has been used to demonstrate that FC in the brain possesses time-varying properties (E. A. Allen et al., 2014; Chang & Glover, 2010; Hutchison et al., 2013; Kiviniemi et al., 2011; Lurie et al., 2020; Preti et al., 2017), but simulations and critical review suggest that the stationarity of the RS data cannot be concluded solely using sliding window FC (Hindriks et al., 2016; Laumann et al., 2017), nor CAP analyses (Matsui et al., 2022).

Among the existing TVFC methods, the CAP approach deviates from conventional time-domain approaches by regarding single fMRI volumes at individual time points, instead of fMRI time courses, as the basic units of analysis (X. Liu et al., 2018). Hindriks et al. (2016) suggest that CAPs could be the building blocks of spontaneous BOLD activity and that dFC is a reflection of these. As Tagliazucchi et al. (2016) state: "Instead of asking whether two voxels are engaged in synchronized fluctuations over a relatively long period of time, the question is shifted to whether two voxels become jointly activated (i.e., present high activity above their baseline levels) and what are the timings and properties of these co-activations". The beginning of the development of CAP analysis can be traced back to when Tagliazucchi et al. (2012) established their point process analysis and observed that the timing of high-activity events in BOLD signals allows the reconstruction of major RS networks (RSNs). Soon after, Liu and Duyn (2013) applied k-means clustering (Jain, 2010) to arrange single fMRI volumes into groups and averaged this data group-wise to produce distinct spatial CAPs. Related studies have been conducted by other groups using CAP (Bolton et al., 2020; J. E. Chen et al., 2015; Di Perri et al., 2017; Gutierrez-Barragan et al., 2019; Kupis et al., 2020; X. Liu et al., 2018; Maltbie et al., 2022; X. Zhang et al., 2020; Zhuang et al., 2018) or other terms such as activation spatial maps (Iraji et al., 2022), coincident

threshold crossings (Hudetz et al., 2015) and modes (X. Li et al., 2015). There is also the similarly named iCAPs model (innovation-driven co-activation patterns), which, however, processes the BOLD signal more with a deconvolution for the HRF, leading to a block-type activity-inducing signal and its further derivative "the innovation signal" representing transient activations (Besseling et al., 2018; Karahanoğlu & Van De Ville, 2015).

Constellations of different intrinsic connectivity network (ICN) patterns have previously been referred to as brain states (E. A. Allen et al., 2014). Although in our study CAPs are not calculated as time-varying FC matrix representations, as illustrated by Allen et al. (2014), they can be seen as representing the same brain states as a timeline of various spatiotemporal clusters of (de)activation patterns of independent ICNs/RSNs (Maltbie et al., 2022; Preti et al., 2017). It has been shown that averaging sparse activation events produces ICN patterns that are similar to the conventional seed-based correlation map, which requires the entire dataset (X. Liu & Duyn, 2013; Tagliazucchi et al., 2016). Activation events can be further divided into several distinct subgroups, with specific spatial patterns suggesting dynamic organization. These brain states are visualized as a mean image of multiple volumes (Fig. 2) in which ICNs (Fig. 3) are in similar activation phases, as determined by a clustering algorithm. If the number of states or CAPs depicting the same data is increased, the amount of time for which one CAP is represented grows proportionately shorter. In CAP analysis, the gathered volumes do not have to be sequential, and voxel signal levels per se can be evaluated. These two issues present differences from most sliding window TVFC analyses (X. Liu et al., 2018; Lurie et al., 2020; Preti et al., 2017). Neither sliding windows FC, nor CAP analysis proves the non-stationarity of RS brain activity (Matsui et al., 2022).

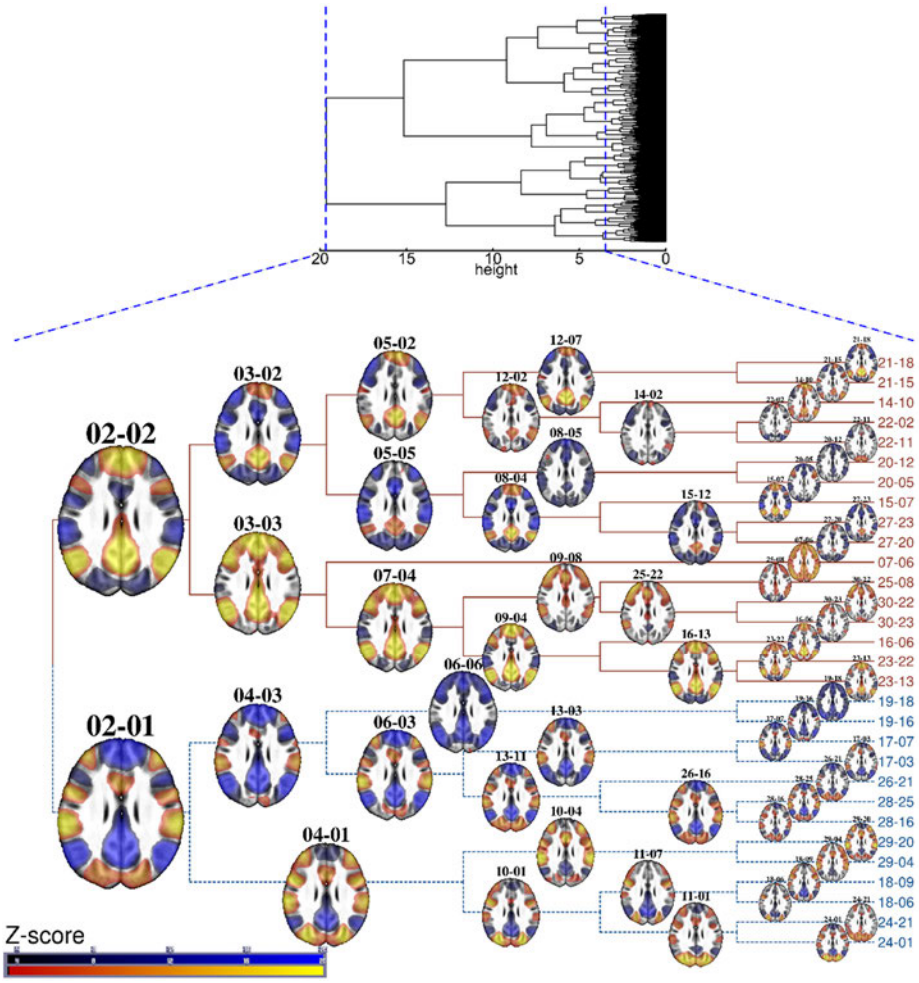

Fig. 2. Co-activation patterns (CAPs) as a hierarchical clustering result dendrogram (Study III). Top, hierarchical clustering (cosine distance, Ward's method) result dendrogram of 11 930 resting state (RS) fMRI volumes of 55 adolescent participants. The X-axis shows the study-specific distances between the clusters as height h. When h = 0, each volume forms its own cluster, and h ≈ 3.48 (dashed blue line on the right) corresponds to splitting the volumes into 30 clusters. Due to image resolution limitations, the volumes were merged as the thickened black column on the Y-axis. The lower part of the figure highlights the cluster levels from 02 to 30 as a cladogram, which shows the relations between the CAPs. The first number indicates the total cluster count at that level. The second number was determined by the clustering algorithm that showed the cluster's ordinal number for only that hierarchical level. For visualization,

the branch lengths have been scaled equal in the cladogram, as opposed to a dendrogram. Each CAP's z-statistic map slice is shown from the same level of anterior and dorsal nodes of the default mode network (DMN). The lower DMN-negative or "task-positive" branches of the cladogram comprise 4658 volumes (39%), and the upper DMN-positive branches 7272 volumes (61% of the whole data) of the RS-fMRI data. Further CAP volume distributions (Figures S1a–b) are detailed in Supporting Information S1 of Study III (https://onlinelibrary.wiley.com/doi/full/10.1002/brb3.2174). The z-statistic color keys range from -20 to -3.5 and 3.5 to 20. Reprinted under CC BY 4.0 license from Study III © 2021 The Authors.

From among the CAP methods, the following can be distinguished: 1) seed-based methods (e.g., Amico et al., 2014; J. E. Chen et al., 2015; Di Perri et al., 2017; Liu & Duyn, 2013), in which the volumes for analysis are selected via predefined seed voxel or region thresholds and in which interactions with the rest of the brain are probed; and 2) seed-free analyses, such as ours, in which the clustering algorithm is applied to all volumes in an entirely data-driven way (e.g., Bolton et al., 2020; Liu et al., 2013, 2018); or 3) studies utilizing both approaches (Gutierrez-Barragan et al., 2019; Iraji et al., 2022). Further, 4) it is possible to form simplified CAPs derived from a limited number of key network ROIs, disregarding the rest of the brain (Kupis et al., 2020). Some researchers interpret that most of the information in the RS-fMRI time courses is carried by a much smaller set of discrete events, which in turn reflect discrete local field potential power events (Karahanoğlu & Van De Ville, 2015; Tagliazucchi et al., 2016; X. Zhang et al., 2020), and can provide directed information of the functional correlations and temporal lags across regions (Cifre et al., 2021). Others argue that focusing on peak events discards important information about transient patterns of connectivity and network reconfigurations (Iraji et al., 2022). Another relevant distinction between studies is that many studies have focused on temporal properties or CAP metrics, such as the occurrence rate, dwell time, and transition probability (e.g., Bolton et al., 2020; Chen et al., 2015), whereas the most salient findings in our Study III, concentrate on the spatial differences across the groups (also see Amico et al., 2014; Di Perri et al., 2017).

In CAP analysis, BOLD fMRI volumes are described by their voxels' signal amplitudes, and their relation to other volumes can be defined via a suitable function, such as the Pearson correlation coefficient (J. E. Chen et al., 2015; Di Perri et al., 2017; X. Li et al., 2015; X. Liu & Duyn, 2013; Rodgers & Nicewander, 1988; Yao et al., 2016), or cosine distance (Karahanoğlu & Van De Ville, 2015; Manning et al., 2008). Among the many unsupervised learning methods, fMRI

studies have also utilized hierarchical clustering for FC analysis (Kam et al., 2017) and for voxel-wise approaches (X. Liu et al., 2012; Thirion et al., 2014; Y. Wang et al., 2016; Y. Wang & Li, 2013). As opposed to k-means clustering, hierarchical agglomerative algorithms are deterministic, and do not require a predetermined number of clusters. To decide which data objects (fMRI volumes here and in Study III) are combined during hierarchical clustering, we chose Ward's method. This belongs to minimum variance methods and uses one variant of the Lance-Williams dissimilarity update formula, sharing the total error sum of squares criterion with k-means clustering (Jain, 2010; Murtagh & Legendre, 2014) and thus builds on earlier CAP research (Bolton et al., 2020; J. E. Chen et al., 2015; Di Perri et al., 2017; X. Liu et al., 2013; X. Liu & Duyn, 2013). While there is a wide temporal gap to cross between EEG and BOLD fMRI phenomena, a new EEG study demonstrated brain-wide intrinsic networks and CAPs also in neuronal-timescale dynamics (Ding et al., 2022).

Independent component analysis (ICA)

One of the most widely used methods to reveal intrinsic connectivity networks is ICA. It does not assume a hemodynamical model but is a blind source separation technique that assumes the observed signals are linear combinations of independent underlying signal sources (Hyvärinen & Oja, 2000). ICA decomposes individual or group-related linearly mixed BOLD fMRI data into components with associated time courses and spatial maps that are, in a statistical sense, maximally independent. ICA can be used both individually and group-wise over a temporal or spatial domain. In spatial ICA, each component is associated with a spatial map depicting the signal locations in the brain. In raw fMRI data, even up to 70–90% of these components may be considered noise, but others reflect neuro-anatomical systems (Abou-Elseoud et al., 2011; M. D. Fox & Raichle, 2007; Griffanti et al., 2017; Hyvärinen & Oja, 2000; Kiviniemi et al., 2003).

ICA cannot determine the absolute number of functional networks (Uddin et al., 2019), but results are sensitive to the model order (chosen number of components), which should be adjusted depending on the study goals (Abou-Elseoud et al., 2010, 2011; Kiviniemi et al., 2009). A model order that is too low may lead to inappropriate fusion of signal sources. Fine-grained parceling requires high model orders, which break larger components into smaller ones, yielding information regarding network hierarchies (Kiviniemi et al., 2009; Smith et al., 2009). This dimensionality also influences the naming of networks. With high

model orders, the variation in decomposition inherent to the ICA method may further hamper the naming.

2.3.2 Brain networks

Major primary brain networks, such as visual, motor, and somatosensory networks are quite stable and their naming at a coarse level is straightforward. However, the network nomenclature associated with higher cognitive functions varies concerningly, but has fortunately also led to descriptions grounded on meta-analysis and proposals for a common taxonomy (Uddin et al., 2019; Urchs et al., 2019; Witt et al., 2021). Uddin et al. (2019) propose six ubiquitous large-scale functional systems referred to by their anatomical names as a reasonable starting point: 1) the occipital network (ON, most commonly associated with visual domain), 2) the pericentral network (PN, somatomotor), 3) the dorsal frontoparietal network (D-FPN, attention), 4) the lateral frontoparietal network (L-FPN, control), 5) the midcingulo-insular network (M-CIN, salience) and 6) medial frontoparietal network (M-FPN, default). These cortical networks also have less well charted subcortical, cerebellar, and brainstem counterparts (Ji et al., 2019; Uddin et al., 2019). In Study III (Fig. 3), we chose a 14-dimensional approach to promote pragmatic visual inspection and to cover the major networks in line with earlier studies (Castellazzi et al., 2014; Starck et al., 2013; Thornburgh et al., 2017; Whitehead & Armony, 2018; Yeo et al., 2015).

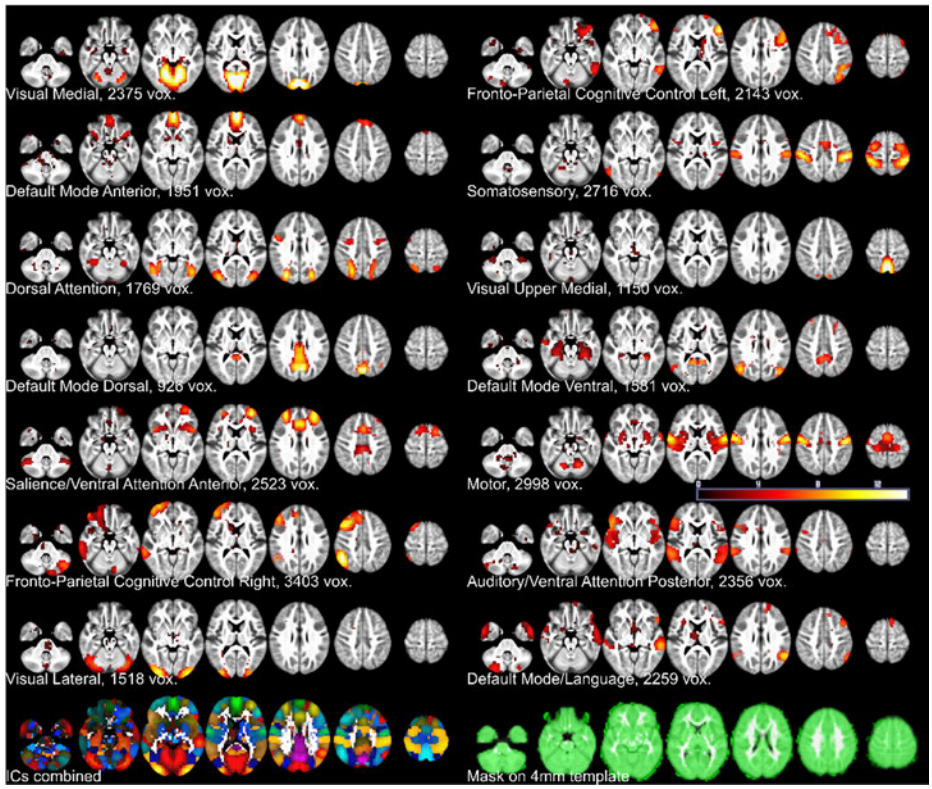

Fig. 3. Study-specific cores of 14 resting state networks (FSL MELODIC group ICA components). The components are ordered column-wise according to the explained variance. Overlapping areas were removed by assigning each 4x4x4 mm^3 voxel to only one IC, with the highest absolute z-statistic over the other ICs. The component areas were used as voxel-wise masks and an atlas to label brain areas when interpreting results. Images of the combined 14 components and study mask are also displayed. The z-statistic color key ranges from 0 (black) to 14 (white). Reprinted under CC BY 4.0 license from Study III © 2021 The Authors.

Default mode network (DMN)

Early brain PET imaging showed that when participants are not engaged in cognitive or other external tasks, certain brain areas (medial posterior cingulate cortex, ventromedial prefrontal cortex, medial temporal lobe, and angular gyrus) tend to become more activated (Shulman & Fiez, 1997). This network was later labeled the default mode network (DMN) (Buckner et al., 2008; Greicius et al.,

2003; Raichle et al., 2001). The DMN is also one of the three fundamental poles of cerebellar functional neuroanatomy, alongside the motor and attentional/executive processing (Guell & Schmahmann, 2020). On a large-scale connectivity view, the DMN sits at the opposite end of a hierarchy equidistant from the primary sensory and motor regions, characterizing its role in cognition and processing transmodal information (Margulies et al., 2016). The two main aspects of DMN are self-referential processing and autobiographic memory (Davey et al., 2016; Gusnard et al., 2001). Deactivation has been thought to indicate an interruption of mental activity (Kennedy et al., 2006), and failure to deactivate the DMN has been associated with increased attentional lapses, reduced task performance in aging, Alzheimer's disease, and schizophrenia (Stiernman et al., 2021). Recent work has begun to study the DMN's role in the regulation and reconfiguration of brain states in varying contexts and highlighted its functional heterogeneity (Groot et al., 2021; Stiernman et al., 2021). The precuneus, a hub inside the posterior DMN (Fig. 3: Default Mode Dorsal or DMN-D), interacts with both the DMN and the frontoparietal networks (Utevsky et al., 2014). Precuneus is a functional core of DMN with a heightened specialization for resting state cognition, but is also more broadly engaged under various processing states (Utevsky et al., 2014). Distinct DMN connectivity patterns can be observed in different amplitude time points, likely related to transient patterns of connectivity embodying dynamic integration and segregation of ICNs (Iraji et al., 2022). Continuous switching between internal and external modes in the brain appears necessary for generating models of the self and the world (M. Kim et al., 2021).

Executive function networks

Executive function (EF) refers to a set of higher-order cognitive processes comprising distinct but highly intercorrelated components necessary for goal-directed behavior. EF includes three core components: inhibitory control, cognitive flexibility, and working memory (Diamond, 2013; Sung et al., 2022). In the fMRI realm, the central executive network (CEN) can be considered in some regards the opposite of the DMN, as they often show contrasting patterns of activation (van der Linden et al., 2021), though the transfer of information and modulatory interaction has been speculated during momentary integration (Iraji et al., 2022). The CEN becomes activated in situations requiring attention, focus, or concentration, such as active maintenance of working memory, switching between tasks, or inhibiting irrelevant information (van der Linden et al., 2021). However, the inconsistent use

of EF network labels and varying spatial topography are a source of confusion. Image-based meta-analysis by Witt et al. (2021) identified nine labels that are frequently used to describe topographically or functionally similar executive brain networks: the central executive network (CEN), the cognitive control network (CCN), the dorsal attention network (DAN), the executive control network (ECN), the executive network (EN), the frontoparietal network (FPN), the working memory network (WMN), the task-positive network (TPN), and the ventral attention network (VAN). Their clustering analysis of group level statistical parametric maps (SPMs) identified four separable network clusters. Two lateralized FPNs contributed to all four clusters. SPMs labeled ECN contributed most to the third cluster. SPMs labeled DAN and TPN were found to contribute to the fourth cluster. Respective new anatomy-based label recommendations for these four clusters were left and right lateral frontoparietal networks (left/right L-FPN, with a secondary label of left/right CEN), dorsomedial frontoparietal network (dM-FPN, with a secondary label of anterior control network) and dorsal frontoparietal network (D-FPN, with a secondary label of dorsal attention network, DAN). (Witt et al., 2021)

Interestingly, the FPN is 2.3-fold overrepresented in the cerebellum compared to the cortex and occupies more cerebellar volume than any other RSN, supporting our executive and adaptive capabilities (Marek et al., 2018; Van Overwalle et al., 2020).

Salience network

The salience network has also been characterized as a VAN, a cingulo-opercular network, and a M-CIN (Uddin et al., 2019). Core regions are the bilateral anterior insula and anterior midcingulate cortex, which are also active in almost all cognitive demands or tasks, likely serving broad functions (Bird et al., 2010; Kana et al., 2007; Simmons et al., 2008; Sridharan et al., 2008; Uddin, 2015; Uddin et al., 2019). For example, the insula is known to activate automatically during both subjective feeling and during other persons' feeling of disgust (Wicker et al., 2003), integrating multimodal responses to novelty or temporal mismatch (Bamiou et al., 2003; Naghavi et al., 2007), intolerance of uncertainty (Simmons et al., 2008) and so on. However, on a greater scale, the salience network is involved in the general role of switching between other networks, particularly the DMN and the CEN, thus related to mind-wandering and task concentration (Sridharan et al., 2008; Uddin & Menon, 2009; van der Linden et al., 2021). The label "salience" denotes its broad

role in identifying important, i.e., salient information. This descriptor is consistent with findings from task fMRI of homeostatic, emotional, and cognitive factors associated with subjective salience, worthy of further attention and processing (Uddin, 2015; Uddin et al., 2019).

Network interplay during higher cognitive functions: attention, mindfulness

In healthy adults, a network graph study found that optimal sustained attention arose from reduced network cross-talk and greater within-network communication in task-relevant networks such as salience, cingulo-opercular, dorsal attention, and visual (Zuberer et al., 2021). In contrast, optimal attention predicted greater network cross-talk, reduced within-network communication in auditory and sensorimotor networks, and lower within-network communication in the subcortical and ventral attention networks (Zuberer et al., 2021). The relationship between network graphs and brain (de)activations needs clarification.

Fluctuations in attentional stability are tracked over time in task-positive (e.g., DAN and VAN) and task-negative (e.g., DMN) regions, and vary in specific ways before attention lapses or concerning reaction time and performance (Fortenbaugh et al., 2018). The DMN contributions are not unambiguous, but also modulated, for example, by motivation (Fortenbaugh et al., 2018).

Concentration or sustained attention and mind-wandering or task-unrelated thoughts are two general mind states alternating with varying frequency and duration during some task. In a study by Scheibner et al. (2017), mindful attention was characterized by less activity in the DMN than mind-wandering, independent of attention type (internal breathing or external sound). The activation difference was greater in inner attention meditation than in external attention meditation. While the ability to concentrate or uphold sustained attention is not equal to mindfulness, these concepts are related, and mindfulness-based interventions can increase attention (Trautwein et al., 2020). The typical definition of mindfulness is the ability to stay aware of and focus attention on experiences in the present moment in an accepting, nonjudgmental manner (Bishop et al., 2004). These transient cognitive states may be captured better in dynamical temporal analysis than in static methods. Marusak et al. (2018) showed that trait mindfulness in youths is related to dynamic but not static RS connectivity. The more mindful youths transitioned more between brain states, spent less time in a particular connectivity state, and showed a state-specific reduction in connectivity between

salience and central executive (i.e., frontoparietal cognitive control) networks (Marusak et al., 2018).

Parallel top-down volitional attention is influenced by the DAN, which has key nodes in the bilateral intraparietal sulcus, superior parietal lobule, and frontal eye fields (Vossel et al., 2014; Yamasaki et al., 2017). Research has demonstrated that these dorsal frontoparietal areas can causally modulate visual areas' activity (Vossel et al., 2014). Much of the research has focused on visuospatial attention, but studies in other sensory modalities have led to the proposal that the DAN and VAN are potentially supramodal attention systems (Vossel et al., 2014).

2.4 Autism spectrum disorder (ASD)

According to the latest 11th revision of the World Health Organization's (WHO) International Classification of Diseases (ICD; ICD-11), ASD is a neurodevelopmental disorder characterized by persistent deficits in one's ability to initiate and sustain reciprocal social interaction and social communication, as well as by a range of restricted, repetitive, and inflexible patterns of behavior and interests. These usually pervasive deficits are sufficiently severe to cause impairment in the individual’s functioning, observable in all settings, although they may vary contextually in personal, family, social, educational, and occupational interactions (World Health Organization, 2020).

The two primary official sources for autism diagnosis are the ICD above, published by WHO, and the Diagnostic and Statistical Manual of Mental Disorders (DSM; latest 5th edition DSM-5, 2013), published by the APA. The DSM is favored in the USA, while the ICD is widely used in Europe; both are influential globally. Both diagnostic criteria incorporate autism, Asperger syndrome (AS), and pervasive developmental disorder – not otherwise specified (PDD-NOS) under a single category of ASD. Both highlight impairments in two areas – social communication and restricted interests and repetitive behaviors – as characteristics of the condition. Both are similar in their conceptualization of autism as a broad category or spectrum comprising many different presentations and are intended to identify the same people, but ICD-11 focuses on this diagnostic concept and provides examples of manifestations, while DSM-5 is more prescriptive (First et al., 2021). The manuals also have other differences. While ICD-11 does not mention sensory abnormalities such as over- or undersensitivity to sound and touch, DSM-5 includes these features.

On the other hand, ICD-11 details subcategories specifying whether an autistic individual also has an intellectual disability and the degree of possible language impairment, while DSM-5 merely acknowledges that autism and intellectual disability can co-occur (American Psychiatric Association, 2013; World Health Organization, 2020). In addition to the two aforementioned official diagnostic systems, by 2020 there were almost two hundred data-driven studies aimed at recognizing subtypes of ASD (Agelink van Rentergem et al., 2021). Usually, in such a study, two to four subtypes described the data well, but the variability of the used measures prevented reasoning whether new subtypes were discovered in each study or whether these were different perspectives on the same subtypes (Agelink van Rentergem et al., 2021).

The prevalence of ASD depends on the diagnostic criteria, but for example, in an epidemiological study of 5484 eight-year-old Finnish children, the prevalence according to DSM-IV-TR criteria was 8.4 per 1000 (Mattila et al., 2011). There has been a notable increase in the prevalence of ASD in the last decades – currently, 18.5 per 1000 in the USA, according to DSM-5 (Maenner, 2020). The etiology of ASD has been widely studied, but the whole process, with many biological and environmental factors, is difficult to grasp. Hundreds of gene variants and de novo mutations affecting transcriptional regulation have been associated with ASD (Herrero et al., 2020). In a multinational cohort study, the estimated heritability of ASD was 80%, ranging from Finland's 51% to Israel's 87% (Bai et al., 2019). Still, none of the individual genes identified to date account for more than 1% of ASD cases (Panisi et al., 2021). A recent review argues that the epidemiological and clinical findings in ASD cannot be explained by the traditional linear genetic model alone, hence the need to move towards a more fluid conception, integrating genetics, environment, and epigenetics as a whole (Panisi et al., 2021). At least 25 different etiological mechanisms and models for ASD have been proposed, each accounting for some aspects of the findings related to ASD (Sarovic, 2021). A recently suggested unifying theory deconstructs autism into three contributing features: an autistic personality dimension, cognitive compensation, and neuropathological risk factors. These interact to cause a maladaptive behavioral phenotype that may require a clinical diagnosis (Sarovic, 2021).

2.5 Face processing in ASD

2.5.1 Development

Brain network development takes advantage of antenatal and neonatal prewiring. Already in neonates, occipital and fusiform face areas (FFA) show biased FC with foveal V1, while the parahippocampal place area and retrosplenial complex are biased toward peripheral V1. These differential inputs may facilitate or even guide the development of domain-specific processing in each network (Kamps et al., 2020). Early visual experience primes not only visual but cross-modal face specialization in the FFA (Dai et al., 2022). Infants show shifting patterns of visual engagement to faces over the first years of life, related to the onset of spoken language. Once toddlers begin learning how to talk, they change focus from the eyes to the mouth. As phrase speech and more complex spoken communication continue to develop, they again increase eye-looking (Habayeb et al., 2021). The ability to recognize faces improves further into adulthood. The development of face-selective brain regions, but not place-selective regions, results from cortical tissue proliferation rather than from pruning exclusively (Gomez et al., 2017).

While ASD generally does not affect the ability to detect and orient to faces (Guillon et al., 2014), face detection may be slower (Georgopoulos et al., 2022; Kala et al., 2021), and interpretation of gaze cues problematic (Del Bianco et al., 2021). Eye-tracking studies have shown that when people look at photographs depicting social scenes, they first look at faces, and then their gaze wanders to other parts of the image. Neurotypical adults are likely to return their gaze to the faces after a few seconds, whereas ASD participants have a low probability of returning to the face (Del Bianco et al., 2021). Further, the reduction of gaze on eyes is consistent across different ages and cultures in ASD (X. Ma et al., 2021). Two different mechanisms may drive the early and late looking patterns, with ASD affecting only the latter. Interest in faces grows with age in neurotypical people but not in ASD (Del Bianco et al., 2021), though gaze on the mouth may increase as ASD individuals age (X. Ma et al., 2021).

ASD participants with the most distinct eye movements pattern also have the poorest communication skills (Del Bianco et al., 2021). Better face recognition ability predicts better affective theory of mind ability and, thus, social cognition in ASD, but not in schizophrenia or typical development (Altschuler et al., 2021). Selective activation of reward and motivation linked areas of the ventral striatum and nucleus accumbens when viewing and responding to happy faces was detected

in controls but not in ASD participants (Shafritz et al., 2015). The lack of motivation to engage in social interaction, perhaps due to different maturation and function of the subcortical pathways, associates with the diminished rewards and pleasure value for faces (Hari & Kujala, 2009; Johnson et al., 2005; Neufeld et al., 2019).

2.5.2 Associated fMRI research

Problems in recognizing facial expressions are considered as one of the core features of ASD (Campatelli et al., 2013; Kuusikko et al., 2009; Sigman et al., 2004), though ASD participants were able to discriminate between happy and fearful faces without any performance lack (Shafritz et al., 2015). It has been suggested that the social problems in ASD may result from a lack of fundamental appreciation of the commonality between self and others (Gopnik & Meltzoff, 1994; Uddin et al., 2008). Brain imaging studies suggest that typically developing (TD) individuals automatically share the emotions of others, probably due to shared affective neuronal networks (de Vignemont & Singer, 2006).

Brain simulation mechanisms and the mirror neuron system (MNS) may be relevant to social functioning in everyday life (Hari et al., 2014; Pfeifer et al., 2008; Rizzolatti & Sinigaglia, 2010). The MNS consists of the brain regions which activate both when participants act and when they observe another person performing the same action, the core regions being IFG (see Fig. 3: FPC L – left IFG pars triangularis [p.tr] & opercularis [p.op] upper half; DMN/Lang – left IFG lateral lower half between p.tr & p.op; Auditory / Ventral attention posterior – left IFG lower medial part, most of the right IFG; FPC R – right IFG p.tr upper anterior), and inferior parietal lobule (IPL) (see Fig. 3: Posterior FPC R – IPL Pfm R; somatosensory; rostrocaudal parts of motor; Auditory / Ventral attention posterior – IPL Pfm lower & posterior parts) (Caspers et al., 2013; Hamilton, 2013; Iacoboni, 2005; Iacoboni et al., 1999; Johnson-Frey et al., 2003; Numssen et al., 2021). A broader MNS definition may also incorporate the somatosensory and premotor cortex (PMC), possibly the anterior insula (Caspers et al., 2010; Hamilton, 2013). Schultz et al. (2000) were the first to provide direct neurofunctional evidence for atypical face processing in ASD. Dapretto and colleagues (2006) found that MNS activity in the IFG p.op was absent during observing facial expressions and inversely related to symptom severity in the social domain in participants with ASD. However, later studies have shown mixed results with increased and normal activity, and no overall evidence of abnormal MNS responses in ASD (Bastiaansen et al.,

2011; Di Martino et al., 2009; Grèzes et al., 2009; Martineau et al., 2010; Philip et al., 2012; Schulte-Rüther et al., 2011). Instead, an alternative model with abnormal social top-down response modulation of MNS has been suggested (Hamilton, 2013). It seems that MNS dysfunction is not a principal feature of ASD, but variations in mirroring may be related to differential expressions of ASD symptom severity (Prinsen & Alaerts, 2022).

Increasing emphasis has been put on the dynamic aspects of facial expression processing. Dynamic information may be integral to the mental representation of faces (Freyd, 1987). Moreover, dynamic facial stimuli may provide a more naturalistic and robust approach to examining face processing. It has been shown that dynamic stimuli activate brain areas related to facial expressions more extensively than static stimuli (LaBar et al., 2003; Sato et al., 2004; Trautmann et al., 2009). In fMRI studies with TD individuals, dynamic facial expressions (DFEs) dominantly activate the right occipital and temporal gyri, fusiform gyri (FFG), the amygdala (Amy; Amy lower half – Auditory/VAN-P; Amy upper half – Motor; minimal DMN-A, FPC L&R, DMN-V), parahippocampal areas, the IFG, ventral PMC and intraparietal sulcus (ant IPL – somatosensory; post IPL – DAN; IPL – FPC R & L) (LaBar et al., 2003; Sato et al., 2004). According to the Harvard-Oxford cortical structural atlas, the FFG has four parts: temporal fusiform cortex anterior (minimal DMN-D, salience/VAN-A, FPC R, FPC L), posterior (DMN-V), temporal occipital fusiform cortex (DAN occipital caudal parts, minimal Visual Up Med) and occipital FFG (partly Visual Medial, partly Visual Lateral).

Pelphrey et al. (2007) were the first to use DFE stimuli morphed from static facial images in fMRI in adults with high-functioning autism (HFA). They concluded that key components of the human face processing system of the social brain areas, i.e., the Amy, FFG, and posterior superior temporal sulcus regions (pSTS – Auditory/VAN-P), showed less activation in individuals with HFA. However, such differences were not observed in regions outside the face processing system (Pelphrey et al., 2007).

Functional neuroimaging provides one avenue for investigating the neural implementation of emotions (Cao et al., 2018; Viinikainen et al., 2010). Another focus of interest in functional neuroimaging of visual processing has been the inclusion of valence, or pleasantness, versus the unpleasantness of facial information. Dimensional theories consider that emotions are represented in N-dimensional space, where the two cardinal dimensions explaining most of the emotional variation are commonly referred to as valence and arousal (Russell & Barrett, 1999). The strength of the BOLD signal has a quadratic relation with the

evaluated valence of an image, showing an inverted U-shape correlation to the subjective reported valence dimension, negative with valence ratings for pleasant pictures and positive with valence ratings for unpleasant pictures in multiple brain regions (Viinikainen et al., 2010).

We have previously combined the use of dynamic expressions with opposing valences in analyzing facial expression processing in TD participants (Rahko et al., 2010). Valence-related differences were detected in brain activation and de-activation in TD participants on passive viewing of dynamic fearful and happy facial expressions (Rahko et al., 2010). In TD participants' opposing-valence DFEs, the positive valence both activates less and deactivates more than the negative valence. We also demonstrated that the MNS was activated more during viewing fearful than during viewing happy expressions (IFG and STS) in a left-dominant manner (Rahko et al., 2010). We also detected more deactivation in the ventral anterior cingulate gyrus (ACG – DMN-A), suggesting more automated attentional processing of fearful expressions during passive viewing (Rahko et al., 2010).

Some investigators (Best et al., 1994; Davidson & Irwin, 1999; Morris et al., 1998, 1999; Nomura et al., 2004) have reported right hemispheric dominance concerning unconscious negative emotional processing or lateralized presentation in both valences (Cao et al., 2018), although other studies of emotional valence have failed to detect hemispheric dominance (Viinikainen et al., 2010). Sato and Aoki (2006) have speculated that right hemispheric dominance in unconscious negative emotional processing may not be specific to facial stimuli.

Observable perceptional alterations in cortical functioning in early parts of the visual system might suggest that a local bias may be characteristic of autism (Caron et al., 2006). Participants with ASD show a reduced "face composite effect" (Teunisse & de Gelder, 2003) and a reduced whole-face advantage for eyes and noses (Joseph & Tanaka, 2003). The impairment for faces in ASD might thus result from the tendency to represent and encode visual information locally, on a part-by-part basis rather than holistically (Behrmann et al., 2006). Deruelle et al. (2008) explained that it is probably the functional interactions between the Amy, as a limbic/emotional structure, and other cerebral regions, such as the dorsolateral prefrontal cortex involved in cognition and/or attention, that are dysfunctional in ASD. Pelphrey et al. (2007) also showed that static images morphed into DFEs show increases in activity in participants with ASD in the Amy, FFG, and STS areas. Some studies address co-occurring alexithymia as the cause of the weaker recognition of emotional facial expressions rather than ASD per se (Bird et al., 2010; R. Cook et al., 2013; Lassalle et al., 2019). An increased rate of ASD is associated

with developmental face recognition impairment prosopagnosia (DP; Fry et al., 2022). The Autism Quotient questionnaire (AQ; Baron-Cohen et al., 2001; Baron-Cohen & Wheelwright, 2001) was used to assess autism traits in DP participants. The Reading the Mind in the Eyes Test (RMET; Baron-Cohen et al., 2001; Baron-Cohen & Wheelwright, 2001) tested DP participants' ability to decipher the emotions of others by viewing only the eyes. Compared to controls, face memory, and perception were similarly deficient in the high- and low-AQ DPs, with the high-AQ DP group additionally showing deficient face emotion recognition (Fry et al., 2022). Task fMRI revealed reduced occipitotemporal face selectivity in both groups, with high-AQ DPs additionally demonstrating decreased pSTS selectivity. RS fMRI showed similar reduced face-selective network connectivity in both DP groups compared to controls (Fry et al., 2022).

2.6 Brain activity and functional connectivity in ASD

2.6.1 Static functional connectivity

Task-based BOLD fMRI studies have revealed abnormalities in the patterns of brain BOLD activations in participants with ASD (G. Allen & Courchesne, 2003; Clements et al., 2018; Courchesne & Pierce, 2005; Dapretto et al., 2006; Di Martino et al., 2009; Hughes, 2007; Iarocci & McDonald, 2006; Just et al., 2007; Kana et al., 2007; Kennedy et al., 2006; Kleinhans et al., 2008; Mizuno et al., 2006; Müller et al., 2003; Picci et al., 2016; Redcay, 2008). Similarly, RS brain activity with fMRI BOLD scans has been able to identify group-level differences in cognitive disorders for nearly two decades (e.g., Greicius et al., 2004; Y. Liu et al., 2008), but the challenge remains to predict individual-level diagnosis correctly in heterogeneous larger populations (M. Liu et al., 2021; Santana et al., 2022). RS data obtained through the scans can be analyzed using various methods, some of which were discussed in the previous chapters. Higher sensitivity and specificity are achieved when RS-fMRI data is complemented with other imaging (task fMRI or structural MRI) or phenotypic data (M. Liu et al., 2021; Santana et al., 2022). However, compared to task-based studies, RS studies evade the problem of different paradigms and difficulties in executing them and do not lose the baseline information with subtraction techniques (Q. Wang et al., 2021).

Among the pioneering RS ASD studies was Cherkassky et al. (2006), who used fixation block data between tasks for functional connectivity analyses, detected

similarities in the volume and organization in RS networks in autism and control groups, but functional underconnectivity was observed in the anterior-posterior connections. Kennedy & Courchesne (2008a) used RS-fMRI to reveal that in autism, the DMN involved in social and emotional processing was disrupted, particularly in the mPFC and left angular gyrus (AG). The DAN was intact and similar to that of the control group. A more detailed view of the DMN abnormality suggested that the ventral mPFC/ventral anterior cingulate cortex (ACC) dysfunction is task-independent and pervasive. However, deficits in the dorsal mPFC and retrosplenial/posterior cingulate cortex (PCC) are task-specific (Kennedy & Courchesne, 2008a).

In a meta-analysis of ten seed-based or ICA method RS datasets, the participants with ASD showed increased connectivity in the cerebellum, right middle temporal gyrus (MTG), superior occipital gyrus (SOG), right supramarginal gyrus (SMG), supplementary motor area (SMA), FFG and putamen (Q. Wang et al., 2021). Decreased connectivity was discovered in some nodes of the DMN, such as the mPFC, precuneus, and AG. Interestingly, compared to seed-based methods, ICA subgroup analysis only revealed decreased RS FC in the DMN (Q. Wang et al., 2021). Also, a previous multilevel model order ICA study found hypoconnectivity in the anterior-posterior DMN interplay on the network level, whereas local functional connectivity in the DMN seemed relatively unaltered (Starck et al., 2013).

In conclusion, ASD is affiliated with altered RS static FC, and the literature supports a diffuse pattern of both rather than only under- or over-connectivity. Even a thorough review of RS FC in ASD with nearly 70 analysis citations found it challenging to draw direct conclusions about the nature of FC in ASD (Hull et al., 2017; See also Harikumar et al., 2021). In addition to the intrinsic heterogeneity of ASD, variation and progress in methodology, such as seed-based vs. ICA FC, may confound the static RS FC results. The on-going advancements in fMRI temporal sampling (Huotari et al., 2019), noise modeling and regression (Keilholz et al., 2017; T. T. Liu, 2017; D. Ma et al., 2023; Scheel et al., 2022), motion correction (Ciric et al., 2017; Parkes et al., 2018; Raval et al., 2022) and in other phases of preprocessing (Bowring et al., 2022) may help to confirm if the FC pattern is really that diffuse or not.

ReHo

The first local connectivity ReHo studies of ASD (Study II; Shukla et al., 2010) reported divergent results, which was not surprising due to crucial methodological differences (e.g., resting state vs. task data, treatment of motion, size of local clusters tested - 27 vs. 7). But methodologically more similar later studies have shown inconsistencies also. The large-sample Autism Brain Imaging Data Exchange (ABIDE; http://fcon_1000.projects.nitrc.org/indi/abide/) showed extensive resting state local overconnectivity in ASD in the right frontal cortex (Di Martino et al., 2014), whereas studies in smaller samples indicated local overconnectivity in posterior regions (Keown et al., 2013; Maximo et al., 2013) that was not seen in the ABIDE study. A study using a subset of the ABIDE data reported underconnectivity in posterior regions, with additional age-related changes and a positive correlation between the mean global ReHo and the Social Communication Questionnaire (SCQ) (Dajani & Uddin, 2016). However, this study applied more liberal movement criteria and included RS data from both eyes-open and eyes-closed states, which are associated with substantial differences in ReHo (D. Liu et al., 2013). Similarly, another ABIDE study reporting decreased ReHo in the DMN, and the visual cortex did not specify the state of the eyes (T. Li et al., 2019). An eyes-open state affects local connectivity, highlighting ASD-related overconnectivity in the posterior, visual regions and underconnectivity in the cingulate gyrus (CG) (Nair et al., 2018). With eyes closed, the pattern was different: local underconnectivity in some visual regions and overconnectivity in the posterior CG (Nair et al., 2018).

Nair et al. (2018) also suggest that local connectivity measures may be susceptible to site and cohort variability. Thomas et al. (2020) calculated static ReHo, the amplitude of low-frequency fluctuations (ALFF), the fractional ALFF (fALFF), degree centrality, eigenvector centrality, local FC density, entropy, voxel-mirrored homotopic connectivity, and auto-correlation lag, for each ~2000 brain volumes in the ABIDE I-II data sets. They trained a three-dimensional convolutional neural network (3D-CNN) to classify the RS-fMRI images as being from ASD or control participants. When all the measures were combined, the result (~ 66%) was still only as good as that of the best single measure, ReHo (Thomas et al., 2020). In a smaller sample (86 ASD, 54 TD) of sedated preschool (3-5 year old) boys, the ReHo value in the right calcarine of the primary visual cortex was increased with ASD and decreased in the language-related brain region (left IFG operculum, left MTG, and left AG) and right mOFC (Lan et al., 2021). No

significant correlation was found between the abnormal brain regions and the Childhood Autism Rating Scale or the Autism Behavior Checklist scores or age. Prepubertal boys (34 ASD, 49 TD) aged from 7 to 10 years had decreased ReHo in the left lingual gyrus (LG), left superior temporal gyrus (STG), left middle occipital gyrus (MOG), and right cuneus (Yue et al., 2022). There were negative correlations between ReHo values in the left LG and left STG and the ADOS social affect score, and a negative correlation between ReHo values in the left STG and the calibrated severity total ADOS score (Yue et al., 2022).

ASD traits exist on a continuum and are more common in males than females, with the male-to-female ratio close to 3:1, though the underlying causes are still unclear (Loomes et al., 2017). An adult TD population (42 females, 43 males) studied with AQ scoring, ICA, fALFF, ReHo, and seed-based FC, revealed a significant negative correlation between the DMN RS FC of the anterior mPFC seed (with MOG and with temporal pole [TP]) and AQ scores in males, but not in females (Jung et al., 2015). Only males showed altered (increased) ReHo in the IFG and cerebellum, but differences were not correlated with ASD traits (Jung et al., 2015). Later, and with a bigger ABIDE sample (92 females and 102 males with ASD; 92 TD females and 104 TD males), Kozhemiako et al. (2020) found increases in local connectivity in the somatomotor and limbic networks (the right primary motor cortex, left and right supplemental motor areas, left operculum, posterior cerebellum, and bilateral TPs) and decreased local connectivity within the DMN (bilaterally in the mPFC, MidFG, PCC, precuneus, and right supramarginal area). These alterations were more pronounced, and the correlations between local connectivity, the SRS, and ADOS were more robust in females (Kozhemiako et al., 2020), thus demonstrating that the ReHo alterations in ASD are present in both sexes. In general, males had higher ReHo than females with and without ASD, especially in the DAN, DMN, and somatomotor network, whereas females had higher ReHo within the VAN (Kozhemiako et al., 2020). Females with ASD showed a stronger age-related positive correlation in visual networks, weaker negative correlation in the limbic network and the VAN, and stronger negative correlation in frontoparietal control and the DMN. In contrast, males with ASD had stronger negative correlations in the somatomotor network (Kozhemiako et al., 2020). An even larger (ASD: 362 males, 82 females; TD: 409 males, 166 females) ABIDE study examined five whole-brain RS FC metrics and detected ASD-related hypo-connectivity for (1) PCC seed intrinsic FC, voxel-mirrored homotopic connectivity (VMHC) and ReHo within the bilateral paracingulate cortex and frontal pole, (2) VMHC and ReHo in the bilateral PCC and precuneus, and (3)

ReHo in the right insula and central operculum (Floris et al., 2021). These results were consistent with prior reports of atypical intrinsic organization of the DMN in ASD. ASD ReHo hyper-connectivity was not found. Males showed decreased ReHo localized in the PCC and precuneus. In females, decreased ReHo was evident in the left AG and lateral occipital cortex (Floris et al., 2021).

Integrating mean regional ReHo and ALFF measurements from ABIDE cohorts with datasets of gene expression in the brains of TD and ASD individuals showed a differential developmental trajectory in a subset of genes in ASD (Berto et al., 2022). These genes are enriched in voltage-gated ion channels and inhibitory neurons, supporting the altered E-I ratio hypothesis. From the 11 cortical areas (including 20 Brodmann areas [BAs]) analyzed, the primary visual cortex (BA17) was the most affected region in ASD, and changes were also found in the inferior temporal cortex (BA20/37) (Berto et al., 2022). Atypical local connectivity may precede disruptions in long-range FC, as neonates with a first-degree relative with ASD had only higher ReHo within multiple RSNs, but normal long-range FC compared to age-matched controls (Ciarrusta et al., 2020). The same research group had earlier demonstrated higher ReHo in regional ROIs associated with social processing in a similar neonatal sample (Ciarrusta et al., 2019). Later in the development, the evidence of general local overconnectivity in ASD disappears as studies have only detected region-specific mixtures of increased and reduced local connectivity (Dajani & Uddin, 2016; Di Martino et al., 2014; Floris et al., 2021; Jao Keehn et al., 2018; Jiang et al., 2015; Kozhemiako et al., 2020; Lan et al., 2021; G. Li et al., 2018; T. Li et al., 2019; Liu J. et al., 2018; L. Ma et al., 2022; Maximo et al., 2013; Nair et al., 2018; Study II; Shukla et al., 2010; Yue et al., 2022; Zhao et al., 2022). Age-related developmental changes were also evidenced by an ABIDE dataset (443 ASD and 435 TD males) classification study utilizing ReHo, which showed a classification performance improvement of up to 10% by considering adults and adolescents separately, and indicating that still developing adolescents were much more difficult to classify correctly (Vigneshwaran et al., 2015).

2.6.2 Time-varying functional connectivity

We found only four eligible ASD CAP studies (excluding our Study III) in August 2022. Kupis et al. (2020) derived five simplified CAPs from six key nodes of M-FPN (DMN, internally oriented cognition), L-FPN (CEN, goal-directed behaviors), and M-CIN (salience, dynamic switching between M-FPN and L-FPN). These

CAPs were examined in children with and without ASD during tasks and RS (Kupis et al., 2020). Inflexibility and reduced differentiation between task and intrinsic brain states among the above networks have been shown to be associated with restricted and repetitive behaviors (RBBs) in ASD (Uddin et al., 2015). A related CAP metric known as dwell time (DT) is the average number of volumes that were continuous on the time distribution and classified as the same state, representing the duration of each state (Yao et al., 2016). Greater M-FPN DT was associated with stronger social abilities, indicating that the dynamics of the M-FPN network may be important in understanding social dysfunction in ASD and the general population. Kupis et al. (2020) conclude: "Group differences between children with ASD and TD children were evident in brain states consisting of the L-FPN and M-CIN specifically during the fourth task run, suggesting atypical between-network coordination in children with ASD during prolonged periods of task engagement. Atypical between-network coordination may underlie neural compensation in children with ASD, enabling comparable behavioral performance as TD children."

In an ABIDE data RS study, ICA-derived M-CIN (salience) components were used as the seed area for the top 20% peak amplitudes of time points to extract five CAPs. A CAP characterized by coactivation of the M-CIN with L-FPN (CEN) and M-FPN (DMN) networks appeared less frequently in children with ASD compared with TD children (Marshall et al., 2020). The reduced communication among these three networks observed in ASD could be related to cognitive and behavioral inflexibility symptoms commonly observed in children with the disorder (Marshall et al., 2020; Uddin et al., 2015).

Children with ASD have higher rates of overweight and obesity (OWOB) than TD children. Brain functional connectivity differences have been shown in both ASD and OWOB. Still, little is known regarding the neural mechanisms associated with the higher prevalence of OWOB and its behavioral impacts on ASD. Kupis et al.(2021) examined the interaction between body mass index (BMI) and diagnosis in predicting dynamic CAP metrics (DT, frequency of occurrence, and transitions between states) as well as dimensional brain-behavior relationships. The relationship between BMI and brain dynamics was moderated by diagnosis (ASD, TD), particularly among the frequency of CAP 4, characterized in this study by coactivation of lateral frontoparietal, temporal, and frontal networks. This pattern was negatively associated with parent-reported inhibition skills. Children with ASD had a shorter CAP 1, characterized by co-activation of the subcortical, temporal, sensorimotor, and frontal networks, and CAP 4 DTs compared with TD children. CAP 1 DT was negatively associated with cognitive flexibility, inhibition,

social functioning, and BMI. Cognitive flexibility moderated the relationship between BMI and brain dynamics in the visual network. These findings provide novel evidence of neural mechanisms associated with OWOB in children with ASD. Further, poorer cognitive flexibility may increase the vulnerability of children with ASD and co-occurring OWOB. Individuals with autism may be more vulnerable to the effects of obesity on brain function (Kupis et al., 2021).

To our knowledge, no studies have enabled definitive inferences between FC and CAP analysis. However, Cifre et al. (2021) have evolved CAP methodology and defined a measure of nonlinear dynamic directed functional connectivity (nldFC) across regions of interest. "This provides directed information of the functional correlations, as well as a measure of temporal lags across regions. The correlations are computed from events identified either as sources or targets, allowing for a straightforward definition of directed graphs (i.e., asymmetric correlation matrices)". The Pearson correlation, computed between the left ventral agranular insula and postcentral gyrus, did not show any differences between ASD and TD, while it has been reported that the postcentral gyrus has differential connectivity in ASD when analyzing large samples (Cheng et al., 2015). However, when Cifre et al. (2021) computed the delays from the insula to other regions, differences between the two groups in the postcentral gyrus appeared, leading them to think that this differential connectivity may be expressed on a spatiotemporal domain: "Another example is the additional difference found between the two groups concerning a weaker functional connectivity between precuneus cortex and ventral agranular insula, which is accompanied by the above-mentioned differences in delay." (Cifre et al. 2021)

2.6.3 Functional connectivity and machine learning

We only utilized unsupervised learning via hierarchical clustering in Study III. ML and deep learning (DL) models for diagnosis and rehabilitation are rapidly advancing (Khodatars et al., 2021). In the near future, it will likely become possible to differentiate among a wide range of cognitive disorders or distinct states of neurodiversity by different stimuli, tasks, or just RS-fMRI protocols. Even today, various ML/DL models can predict with improving accuracy which group an individual belongs to, and identify clinically relevant FC alterations and RSNs (Lanka, Rangaprakash, Dretsch et al., 2020; Lanka, Rangaprakash, Gotoor et al., 2020; Santana et al., 2022). While ASD scorings can be predicted from RS-fMRI data (D'Souza et al., 2020), using behavioral measures such as the SRS exceeds the

classification accuracy achieved with RS-fMRI data (Plitt et al., 2015). In addition, behavioral measures are more readily available and less expensive than MRI.

Many fMRI studies compare group differences between some cognitive disorder and TD controls. A recent meta-analysis of RS-fMRI and ML across 55 ASD studies indicated overall summary sensitivity and specificity of 73.8% and 74.8%, respectively (Santana et al., 2022). In another review with 47 RS and task studies, the classification accuracy ranged from 48.3% to 97%, with higher classification accuracies for task studies (M. Liu et al., 2021). Still, most ML models differentiate only between two clinical groups (Feczko et al., 2018; Jin et al., 2021; Just et al., 2014; Liang et al., 2021; Plitt et al., 2015; Santana et al., 2022; Supekar et al., 2022; Thomas et al., 2020; Vigneshwaran et al., 2015), and rarely more (Du et al., 2022; Mahmood et al., 2020); we are not aware of studies separating more than five groups (Lanka, Rangaprakash, Dretsch, et al., 2020; Lanka, Rangaprakash, Gotoor, et al., 2020). Classification accuracy tends to drop when the size of the dataset increases because achieving good generalization performance in heterogeneous clinical populations is difficult (Lanka, Rangaprakash, Dretsch et al., 2020; Santana et al., 2022). Such a heterogeneity would appear especially in growing infants, children, and adolescents: populations that would particularly benefit from the examination. Larger public pediatric imaging datasets are needed (Ali et al., 2022; Khodatars et al., 2021; M. Liu et al., 2021). Similar issues need to be solved in structural MRI studies utilizing ML (Ali et al., 2022; Guo et al., 2022).

Explainable artificial intelligence (XAI) is an emerging research topic seeking solutions to explain how and why decisions inside algorithms are made (Supekar et al., 2022; Yang et al., 2022). Many studies have been unable to or, for other reasons, did not report the discriminating features (e.g., Vigneshwaran et al., 2015), which is part of the so-called black box problem in the artificial intelligence world. Those studies that do report discriminating features have highlighted the DMN, the ECN, the human voice processing system, and the visual network as the most discriminative brain regions in ASD (Liang et al., 2021; Supekar et al., 2022).

3 Aims of the present study

One of the hallmarks of ASD is the differences in social interactions. Interpreting facial expressions is an essential part of these interactions. We hypothesized that ASD participants might process facial expressions differently from typically developing controls, and the aim of Study I was to evaluate:

1. *Are there valence-associated differences in brain activity during dynamic facial expression viewing in ASD? (Study I)*

Instead of the task state, Studies II and III aimed to explore the resting state. Study II concentrated on regional brain connectivity in the ASD participants to provide a proof of concept about ReHo in this context.

2. *Is regional resting state brain connectivity altered in ASD? (Study II)*

Study III used the co-activation pattern and independent component analysis tools to explore changes in dynamic time-varying functional connectivity.

3. *How does ASD alter time-varying co-activation patterns in spontaneously active brain networks? (Study III)*

4 Materials and methods

4.1 ASD participants

Thirty high-functioning adolescents with ASD were gathered from two partly overlapping studies: a community-based study conducted between 2000–2005 (Mattila et al., 2007, 2011, 2012), and a clinic-based study conducted in 2003 (Kuusikko et al., 2008; Mattila et al., 2009; Weiss et al., 2009). The Regional Ethics Committee of the Northern Ostrobothnia Hospital District approved the study protocols. In accordance with the Helsinki Declaration, written informed consent was obtained from all parents in the screening and diagnostic phase of the studies. All participants and their parents gave written informed consent prior to the fMRI study.

4.1.1 Diagnosis of ASD in the community-based sample

The community-based study was divided into a screening and a diagnostic phase. In screening, all 8-year-old children born in 1992 and living in the Northern Ostrobothnia Hospital District in the autumn of 2000 were chosen to be the target population (n = 5,484). The screening instrument was the Autism Spectrum Screening Questionnaire (ASSQ) (Ehlers et al., 1999). Parents were asked to complete the ASSQ and a developmental questionnaire. Teachers completed the ASSQ. Of the 4,422 (participation rate 81%) children with parents' consent having parents' and/or teachers' ratings, 125 with a reported full-scale IQ (FSIQ) ≥ 50 were invited to further examinations. All 73 screening-positive (parent ASSQ being ≥ 19 and/or teacher ASSQ being ≥ 22; Ehlers et al., 1999) children were invited, and a sample of screening-negative children (n = 52) was selected based on two Swedish publications: (1) all who had teacher ASSQ scores of 17–21 (n = 28) (Kadesjö et al., 1999), and (2) all who had teacher ASSQ scores of 9–16 and parent ASSQ scores of 7–18 (n = 24) (Ehlers et al., 1999). Of the 125 subjects invited, 110 (participation rate 88%) participated in the diagnostic examinations.

The diagnostic examinations included the Autism Diagnostic Interview-Revised (ADI-R) (Lord et al., 1995), the Autism Diagnostic Observation Schedule (ADOS; Lord et al., 2000), module 3, the Wechsler Intelligence Scale for Children –Third revision (WISC-III) (Wechsler, 1991), a school-day observation, and a review of patient records. The ADI-R and ADOS were administered by a

pediatrician trained in using the ADI-R and ADOS for research purposes. Intelligence quotients were measured by a clinical psychologist and a research psychologist using means of the WISC-III. Early development was checked from the patient records of Oulu University Hospital in those cases where verification was considered to be essential after the ADI-R interviews. School-day observations were carried out for 24 participants for whom verification was regarded necessary, 22 of them completely including observation of the child, and structured (ASSQ) and nonstructured teacher interviews.

After these examinations, 82 of the 110 children remained for the final evaluation, including all ASSQ screening-positive (n = 61) and a sample of ASSQ screening-negative children (n = 21). Of the ASSQ screening-negative children, 15 had been scored at or above the thresholds in one or more areas in the ADI-R. At the same time, a second opinion was considered necessary regarding six of them, who had been scored below the thresholds in all areas in the ADI-R, to ensure reliability in diagnosis. The ADI-R and ADOS diagnostic algorithms were not used to make diagnostic classifications but to obtain structured information from parents and for semi-structured child observation. DSM-IV-TR criteria (American Psychiatric Association, 2000) were used in detail to construct clinical consensus diagnoses of ASD, based on all information gathered (ASSQs, ADI-R, ADOS tapes, WISC-III, school day observations, patient records), between a pediatrician with extensive clinical experience of ASD and other developmental disorders, and a child psychiatrist with long-term clinical experience of ASD and other psychiatric disorders (Mattila et al., 2007, 2011).

4.1.2 Diagnosis of ASD in the clinic-based sample

The target population included all registered outpatients with ASD or suspected ASD at Oulu University Hospital who had been diagnosed in the child psychiatric clinic or the child neurological department supervised by a child psychiatrist or a child neurologist. In the autumn of 2002, hospital records were initially evaluated for the clinic-based study's genetic part in high-functioning children and adolescents with ASD (FSIQ $\geq$ 80, WISC-III; Weiss et al., 2009). Severe developmental disorders (e.g., specific language impairment or Fragile-X syndrome) were used as exclusion criteria. Those outpatients who had already been diagnosed with ASD in the community-based study (Mattila et al., 2007) were removed from the diagnostic confirmation of ASD in the clinic-based study.

To define the diagnosis of ASD, the ADI-R and ADOS, module 3, were administered by a research psychologist trained in using the ADI-R and ADOS for research purposes, and early development in all cases was verified from the patient records of Oulu University Hospital. Neither the ADI-R nor ADOS diagnostic algorithms were used in the clinic-based study. The definite diagnoses of ASD were determined according to DSM-IV-TR in detail by the research psychologist, based on all information gathered, including consultation with the pediatrician in the cases of participants for whom a second opinion was considered essential.

4.1.3 Co-occurring conditions and eligibility for fMRI

To identify co-occurring psychiatric disorders, the participants with ASD and their parents were interviewed twice. First in 2005 (Mattila et al., 2010), with an update in 2007, using the Schedule for Affective Disorders and Schizophrenia for School-Age Children (K-SADS-PL) (Kaufman et al., 1997), following DSM-IV-TR criteria. The participants with ASD and severe Tourette's disorder or hyperkinesia were excluded because of the potential difficulty of remaining still throughout the long 45-min study scan. In addition, the participants with ASD were not allowed to have any medications to avoid confounding factors.

Thirty participants with ASD accepted the invitation to participate in the neuroimaging study. One participant with ASD refused to undergo scanning after the first visit because of the high noise level. One fMRI dataset was lost due to a computer storage error.

The facial expression task fMRI data of three participants with ASD were discarded because of excessive movement, e.g., > 1 mm translational or > 1° rotation in any of the planes during neuroimaging. Finally, 25 participants with ASD (19 AS and 6 HFA; 8♀, 17♂; mean age 14.8, range 11.7–17.6, SD 1.6; mean FSIQ (n = 22) 106.4, SD 17.53, range 76–155) were included in the facial expression task fMRI study. The FSIQ of three participants with ASD from the clinic-based study was missing. The participants with ASD were predominantly right-handed; only three were left-handed.

The RS-fMRI data from 28 participants (19 AS and 9 HFA; 8♀, 20♂; age 14.6 ± 1.6) was analyzed as described in later chapters.

4.2 Control participants

Thirty age and gender-matched TD controls were recruited in 2006 from mainstream schools in Oulu (Jansson-Verkasalo et al., 2005; Kuusikko et al., 2008, 2009). The TD controls were first screened using the ASSQ to exclude those with clinically significant ASD symptoms. Secondly, control participants and their parents were interviewed using the K-SADS-PL to exclude those with other psychiatric disorders. We did not measure the IQ of the TD adolescents. However, they all attended mainstream education, and their mean score for school performance was 8.24, a range of 7.00–9.75, on a scale where 4 indicates the lowest and 10 is the best possible school performance.

Two controls were discarded from the study because of high ASSQ scores (>7; Ehlers et al., 1999; Mattila et al., 2009). One control participant had orthodontic braces that could not be removed, and the resulting imaging artifacts inhibited fMRI. Consequently, 27 TD controls (9♀, 18♂, mean age 14.5; range 11.7–17.3, SD 1.5) were scanned. The participants in the control group were predominantly right-handed; only two were left-handed. Handedness was determined through clinical observation and participant reports.

4.3 fMRI data acquisition

MRI imaging was carried out in 2007 using 1.5 T GE Signa HDx with an eight-channel parallel imaging head-coil. Before the imaging, all study participants were shown an introductory video about fMRI scanning, including preparing a child for the procedure. All participants had normal or corrected-to-normal vision with MRI-compatible plastic spectacles. The hearing was protected using earplugs, and the motion was minimized using soft pads fitted over the ears.

Structural data were acquired using a T1-weighted 3D FSPGR sequence covering the whole brain (TR 12.4 ms, TE 5.2 ms, FOV 24 cm × 24 cm, 256 × 256 matrix with 1 mm oblique axial slices, flip angle 20°) for co-registration of the fMRI data to the standard space coordinates.

Within the MRI session, the RS was scanned before task-fMRI scans. The participants were asked to lie still, remain relaxed and awake, and look at a white cross in the middle of a dark-gray screen. The 7 min 35 s long RS BOLD fMRI scanning consisted of 253 whole brain volumes. The parameters of the GRE EPI were: TR 1.8 s, TE 40 ms, flip angle 90°, FOV 25.6 x 25.6 cm, 64 × 64 in-plane

matrix, 4 × 4 × 4 mm voxel size, and 28 oblique axial slices with a 0.4 mm gap and interleaved acquisition order.

The facial expression task scanning covered the whole brain with the following GRE EPI sequence parameters: TR 3.2 s, TE 45 ms, flip angle 90°, FOV 25.6 x 25.6 cm, 128 x 128 in-plane matrix, 2 x 2 x 2.9 mm voxel size, 37 oblique slices with 0.3 mm gap and 153 volumes. The first three images of GRE EPI sequences were excluded because of T1 equilibrium effects.

Facial expression stimuli

DFE stimuli (happy and fearful) were selected from the ‘‘Helsinki University of Technology (TKK) video sequence collection’’ containing facial expressions of six basic emotions recorded using six Finnish student actors. The stimulus preparation and evaluation details are in Kätsyri (2006) and Kätsyri & Sams (2008). In short, the TKK dynamic facial stimuli were carefully designed to portray facial expressions as naturally as possible. The presentations were imaged after thorough rehearsal sessions. The most recognizable facial expression videos were selected from several video recordings of the actors. The TKK collection was compared with Ekman’s Face collection (Ekman & Friesen, 1978) by evaluating overall recognition and naturalness measurements. No significant difference was found between the recognition of emotions from the TKK and EF collections (Kätsyri, 2006), suggesting good overall recognition of emotions from the TKK stimuli (Kätsyri, 2006; Kätsyri & Sams, 2008).

The stimuli were presented during fMRI in semi-randomly alternating (4 happy, 4 fearful) 30-s blocks of 12 × 2.5 s jittered facial expressions. Changing mosaic images of the same faces were presented at baseline to remove primary visual activation (Rahko et al., 2010). The idea of mosaic images was adopted and modified from Sato et al. (2004), see Fig. 4. We initially used dynamic mosaic images, but found the flickering of the continuous mosaic video to increase participants’ eye blinks and gaze wandering, and thus increase the probability of motion artifacts. Therefore, we chose to use stable mosaic images to minimize stress on participants with ASD in the challenging fMRI environment.

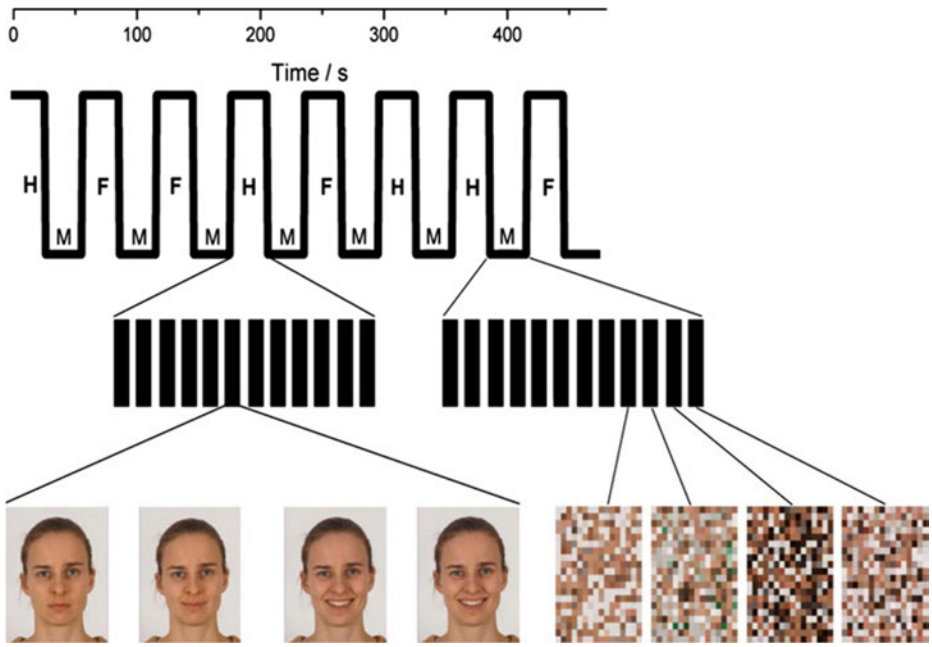

Fig. 4. The stimuli were presented during fMRI in semi-randomly alternating (4 happy, 4 fearful) 30 s blocks of 12 × 2.5 s jittered facial expressions. Changing mosaic images of the same faces were presented as a baseline to remove primary visual activation. This idea of mosaic images was adopted and modified from Sato et al. (2004). Reprinted with permission of Springer Nature from Study I © 2012 Springer Nature.

The dynamic part of each facial expression video was jittered and lasted 1.2 ± 0.3 s (mean ± SD.; range 0.7–1.8 s), and the last frame was shown for 1.5–1 s in such a way that the total duration of each stimulus was 2.5 s. Each block of happy dynamic expressions consisted of six persons' dynamic videos randomized two times for each actor. In fearful expressions, each block consisted of five persons' dynamic videos randomized two or three times for each actor. The imaging session lasted 8 min 10 s (Rahko et al., 2010).

During fMRI, participants watched the stimuli on a translucent screen through a mirror system installed in the head coil. The video projector system was placed in the scanner room by incorporating a secondary Faraday cage inside the scanner Faraday cage. The participants were asked to lie still, relax, and look at what they saw on the screen.

Post-scanning behavioral verification tests

After fMRI scanning, two different methods were used to evaluate how well the participants recognized static and dynamic facial expressions. The participants were instructed to answer based on their first impression (no limits on the response time). The participants chose the correct option from four basic emotions written by the computer (anger, fear, happiness, and surprise). The fifth choice was neutral. In the dynamic and static tests, the participant's task was to name the videos expressing emotions they had seen during fMRI imaging.

4.4 fMRI data preprocessing and analysis

4.4.1 General linear modeling (GLM; Study I)

FSL software versions 3.3 and 4.0 (FMRIB Centre, University of Oxford, www.fmrib.ox.ac.uk/fsl) were used to preprocess and analyze the structural and functional data. FSL is a comprehensive library of analysis tools for brain fMRI, MRI, and diffusion tensor imaging (DTI) data (Jenkinson et al., 2012). FMRIB is the Analysis Group at the Oxford Centre for Functional MRI of the Brain.

Preprocessing and analysis of imaging data

Brain extraction was carried out as preprocessing for structural data using the Brain Extraction Tool (BET) (Smith, 2002). As preprocessing steps for functional data, the translational and rotational motion was corrected using MCFLIRT (Jenkinson et al., 2002) and skull removal with BET. MCFLIRT is an intra-modal motion correction tool. In addition, spatial smoothing using a 5 mm full width at half maximum (FWHM) Gaussian kernel, grand-mean intensity normalization of the entire 4D dataset by a single multiplicative factor, and high-pass temporal filtering (Gaussian-weighted least-squares straight line fitting, with sigma = 90 s) were performed. The stimulus paradigms were used as separate happy and fear blocks, and data processing was carried out using FEAT (FMRI Expert Analysis Tool) version 5.90 (Woolrich, Behrens, & Smith, 2004; Woolrich et al., 2001). Individual time-series GLM was carried out using FMRIB's Improved Linear Model with local autocorrelation correction (Woolrich, Behrens, Beckmann, et al., 2004), and Z (Gaussianized T/F) statistic images were threshold-adjusted at $p = 0.005$ (uncorrected). Registration to high-resolution structural and standard space images

(Montreal Neurological Institute [MNI] avg152T1 template included in FSL) was carried out using the Linear Image Registration Tool (Jenkinson et al., 2002; Jenkinson & Smith, 2001). Higher-level analysis was carried out using FLAME (FMRIB's Local Analysis of Mixed Effects) stage 1 only (Woolrich, Behrens, Beckmann, et al., 2004), and Z (Gaussianized T/F) statistic images were threshold-adjusted using a voxel-level Z-score > 2.3 and a cluster significance threshold of $p < 0.05$ corrected for multiple comparisons (Jenkinson & Smith, 2001). FSL4 (Harvard-Oxford, Juelich, MNI) and AFNI (Talairach & Tournoux, 1988) atlases were utilized to recognize activated areas and differences in activated areas. Motion exclusion criteria were > 1 mm translational or > 1° rotation in any of the planes.

At the individual level, in addition to the happy and fear activation/deactivation contrasts, we also modeled direct valence differences (happy > fear and fear > happy contrasts). At the group level, in our opinion, the valence difference maps between the expressions (happy > fear and fear > happy) show both relative activation and deactivation between the groups.

4.4.2 Regional homogeneity (ReHo; Study II)

Preprocessing

Head motion in fMRI data was corrected using multi-resolution rigid body co-registration of volumes as implemented in FSL 3.3 MCFLIRT software (Jenkinson et al., 2002). The default settings were: middle volume as the reference, three-stage search (8 mm rough + 4 mm initialized with 8 mm results + 4 mm fine grain initialized with previous 4 mm step results) with final trilinear interpolation of voxel values and normalized spatial correlation as the optimization cost function. Brain extraction was carried out for motion-corrected BOLD volumes with optimization of deforming smooth surface model as implemented in FSL 3.3 BET software (Smith, 2002) using threshold parameters $f = 0.5$ and $g = 0$ and for 3D FSPGR volumes using parameters $f = 0.25$ and $g = 0$. The BOLD data were temporally band-pass filtered ($0.01 < f < 0.08$ Hz) with AFNI (Cox, 1996) to reduce physiological noise (Greicius et al., 2003; Lowe et al., 1998) and to remove any linear trend.

Multi-resolution affine co-registration, as implemented in FSL 4.0 FLIRT software (Jenkinson et al., 2002), was used to co-register mean non-smoothed fMRI volumes to 3D FSPGR volumes of corresponding participants and 3D FSPGR

volumes to an MNI standard structural space template (MNI152_T1_2mm_brain included in FSL). Trilinear interpolation was used, the correlation ratio was calculated as the optimization cost function, and the search was conducted in the full [$-\pi$ π] rotation parameters range. The resulting transformations and trilinear interpolation were used to spatially standardize filtered BOLD volumes to 2 mm MNI standard space.

ReHo analysis

A within-subject analysis was first performed using the ReHo approach. The individual ReHo map was obtained by calculating the KCC in a voxel-by-voxel way using the Resting-State fMRI Data Analysis Toolkit (REST) (Song et al., 2011). Each individual ReHo map was divided by this subject's global mean KCC value within the brain mask. This is a similar standardization procedure to that used in PET studies (Raichle et al., 2001). Standardized maps were smoothed with a Gaussian kernel (FWHM = 4 mm) for better anatomical comparability of ReHo values on the group level.

To obtain a visual impression of ReHo, one sample t-test (against 1, i.e., the global mean KCC value after the standardization procedure) was performed within each group (Figures 7 & 8). The differences between ASD subjects and TD controls were examined with two sample t-tests (AFNI 3dttest) between the two groups to create a group difference map. These statistical maps were then transformed into Talairach space (Talairach & Tournoux, 1988) using AFNI hand-landmarking for reporting results and for multiple comparison correction. The AFNI Monte Carlo-simulation program AlphaSim (cluster connection radius 3 mm, individual voxel threshold probability 0.01, 1000 iterations) was used to obtain a corrected significance level of $p < 0.05$ for a minimum volume of 50 voxels (400 mm^3) in the group difference map (Fig. 9) (Cox, 1996). This enabled the identification of significant changes in the ReHo of ASD patients compared to the TD controls. AFNI 3dclust was used to obtain the clusters' sizes, locations, and their respective t-values. Anatomical atlases included in AFNI were used to help locate anatomical areas corresponding to clusters (Eickhoff et al., 2007). Statistical maps were superimposed on the high-resolution anatomical template available in MRIcro (Rorden & Brett, 2000; https://people.cas.sc.edu/rorden/).

4.4.3 Co-activation patterns (CAPs; Study III)

Preprocessing

For anatomical data, we used FSL-VBM FNIRT to register individual T1 structural head volumes and to generate a study-specific template (Andersson et al., 2007; Douaud et al., 2007; Good et al., 2001; Smith et al., 2004). The FSL-VBM was repeated twice using a new target template from a previous analysis. After skull stripping, the FSL's FIRST segmented the structural data into the CSF, WM, and GM (Patenaude et al., 2011).

For the functional data, we ran the AFNI's (Cox, 1996; Cox & Hyde, 1997; Gold et al., 1998) "afni_proc.py" program to produce preprocessing pipeline scripts adapted according to the program's help page examples 9b and 10 (https://afni.nimh.nih.gov/pub/dist/doc/program_help/afni_proc.py.html) and following the guidelines of Jo et al. (2013). We removed the first three images to avoid T1 effects, and computed the outlier fractions for each volume. Motion correction was applied to align the volumes with the average time series, and the skull was stripped. Exploiting the results of our earlier FSL-VBM procedure and the study-specific average template, we applied a non-linear transformation to functional data. The final functional volume size was 42 x 52 x 43 voxels, consisting of 4 x 4 x 4 mm voxels.

After these steps, we interrupted the AFNI pipeline and ran the independent component (IC) analysis-based automatic removal of motion artifacts (ICA-AROMA) for the functional data at the individual level. After inspecting the preliminary results, we prepared custom brain edge and CSF masks fitted for our study-specific adolescent brain template. We inspected the ICA-AROMA results to exclude sporadic RSN removals. Additional ICs were removed if the IC's temporal waveform was monotonously serrated or dominated by high amplitude spikes, or if the spatial distribution represented other scanner noises such as random speckles, or represented mainly WM, arteries, vena sinuses or edge areas (Griffanti et al., 2017). The excluded ICs were spatially cross-correlated with the FSL's fslcc among the participants and group-level ICs to keep the removal process systematic. The median number of ICs left after removal was 14.5 in the ASD and 13 in the TD group (Wilcoxon rank-sum test p-value $\approx$ 0.41). The nonaggressive option was implemented in the participant-wise removal of artifact components (Pruim, Mennes, Buitelaar, et al., 2015; Pruim, Mennes, van Rooij, et al., 2015).

After ICA-AROMA, the AFNI pipeline continued with despiking. The volumes with a framewise displacement of > 0.2 mm were labeled for censoring. We calculated individual volume signal levels from the unprocessed fMRI data using the standardized version of the DVARS-script (Nichols, 2013) and tagged the volumes with a normalized signal level of over 1.29 (outlying 10% of expected SD) for censoring (Aurich et al., 2015; Power et al., 2014, 2015). On average 13.2% (min. 0%, max. 45.6%) of the time series were censored. The shortest time left was 4 minutes and 5 seconds, which was still considered adequate (White et al., 2014). After censoring, 13 750 volumes were reduced to 11 930: the TD participants had an average of 223 volumes, and the ASD participants had 210 volumes left (Wilcoxon rank-sum p-value ≈ 0.34).

We extracted the Region of interest (ROI) time series regressor from the once-eroded CSF mask. Although global signal regression (GSR) is one of the most efficient eliminators of motion-induced artifacts (Power et al., 2014), it may remove the signal of interest and introduce artificial anti-correlations between regions (M. D. Fox et al., 2009; Gotts et al., 2013; Murphy & Fox, 2017). We were interested in the spatial similarity of the volumes (discussed later in the text) and thus did not regress the global signal. We performed spatial smoothing with an 8 mm (~ 2 voxels) FWHM kernel (Z. Chen & Calhoun, 2018) and calculated high-pass temporal filtering regressors for frequencies of < 0.005 Hz. Legendre polynomials of the fourth order were used to model slow baseline fluctuations (i.e., removal of trends). They were combined with censoring, temporal filtering, motion, CSF, and local WM (ANATICOR) regressors into a regression matrix with AFNI 3dDeconvolve. The regression matrix was then projected out of the smoothed data in one step, using the AFNI 3dTproject to remove any possible residual noise left in the data after the earlier application of ICA-AROMA (Jo et al., 2010, 2013).

Group independent component analysis (GICA)

We created uncensored, but otherwise similarly preprocessed datasets with FSL MELODIC multi-session temporal concatenation analysis (Beckmann et al., 2005; Beckmann & Smith, 2004; Jenkinson et al., 2012) and estimated 14 group-level ICs. When interpreting the CAP results, these were used as masks and a simple atlas to label brain areas inside CAPs. As stated earlier, we chose the low-dimensional approach for the sake of pragmatic visual pattern analysis, but still covered major networks in line with earlier studies (Castellazzi et al., 2014; Smith et al., 2009; Starck et al., 2013; Thornburgh et al., 2017; Yeo et al., 2011, 2015).

Hierarchical clustering and extraction of CAPs

The preprocessing continued in MATLAB® (MathWorks®, 2016; Shen, 2014). The fMRI signal was temporally normalized voxel-wise for each participant by subtracting the mean and then dividing by the temporal SD (X. Liu et al., 2018). The individual datasets were masked using combined GICA components and GM voxels (Fig. 3). These volumes and masks were later used with FSL randomise.

The volumes were reshaped, concatenated, and the resulting data matrix was transferred to the R environment (Bengtsson, 2016; R Core Team, 2017). We applied clustering to all the BOLD fMRI volumes acquired from the 55 participants that had survived censoring. As mentioned earlier, the volumes are described by their voxels' signal amplitudes, and their relation to other volumes must be defined via a suitable function. Here, individual volumes were represented as 29 684-dimensional vectors, and a matrix containing the pairwise cosine similarity among all the 11 930 vectors was calculated.

As we were interested in the spatial similarity of the volumes and the corresponding "directionality" of the voxels' signals (above or below average) rather than their absolute amplitude strength, we chose to use the cosine similarity, which is invariant to the scaling of the data. In other words, by excluding anti-correlated patterns, we tried to prevent spatially similar patterns in different phases and with different signal amplitudes from going into different clusters. The Pearson correlation coefficient and cosine similarity are related measures, but the Pearson correlation is also invariant to adding any constant to all data elements, which we considered to possibly have a GSR type of effect on clustering (Manning et al., 2008; Murtagh & Contreras, 2011; Singhal, 2001).

A cosine similarity matrix was converted to a distance matrix, as we performed hierarchical clustering (Murtagh & Contreras, 2011; Murtagh & Legendre, 2014) implemented as the hclust-function (method = "ward.D2") in the fastcluster R-package (Müllner, 2013). The results from 30 to 2 clusters (in total, 58 clusters or CAPs) were evaluated. We aggregated the fMRI volumes assigned to each cluster. The mean image of such a cluster's volumes provided an overall view of the resulting CAP and were then normalized by the standard error (within-cluster and across fMRI volumes) to generate *z*-statistic maps, which quantify the degree of significance to which the CAP map values for each voxel deviate from zero (Liu et al., 2013, 2018).

Group comparison t-tests

The 11 930 RS-fMRI volumes concatenated into one file were input for randomise, a nonparametric permutation inference tool in FSL (M. J. Anderson & Robinson, 2001; Nichols & Holmes, 2002; Winkler et al., 2014). The voxel-wise differences between the ASD and TD groups were assessed for each CAP using two-sample unpaired t-tests (10 000 permutations). The design matrix for each hierarchy level included all the volumes as rows and all the clusters, that is, CAPs existing at that level of the hierarchy, as columns, with separate columns for the TD and ASD participants. We created within-group and between-group contrast files for the CAPs and used participant-wise exchangeability block labels. The resulting Threshold-Free Cluster Enhancement (TFCE) uncorrected p-value maps were merged, and the false discovery rate (FDR) corrected across all the contrasts as implemented in FSL's fdr tool ($q = 0.05$), which gave a p-value threshold of 0.004, corrected for two-tailed results at $p < 0.002$ (M. J. Anderson & Robinson, 2001; Benjamini & Hochberg, 1995; Genovese et al., 2002). We used MRIcron (Rorden & Brett, 2000) and R packages ape (Paradis & Schliep, 2018), dendextend (Galili, 2015), dendsort (Sakai et al., 2014), dplyr (Wickham et al., 2020), ggtree (Yu et al., 2017), ggplot2 (Wickham, 2016), gplots (Warnes et al., 2020), plyr (Wickham, 2011) and RColorBrewer (Neuwirth, 2014) to aid data visualization.

5 Results

5.1 Task state fMRI

In the post-scanning behavioral verification tests, there were no significant group differences in dynamic ($t = -0.93$, $p = 0.36$, df 50) or static facial stimuli ($t = -1.39$, $p = 0.17$, df 50). Static expressions were recognized by 81.20% of the participants with ASD and 85.80% of the TD controls. Dynamic expressions were recognized by 87.50% of the participants with ASD and 93.75% of the TD controls. Although the groups did not differ in expression recognition, DFEs were more recognizable than static expressions. There were no gender differences in the naming of dynamic ($p = 0.81$) or static ($p = 0.22$) emotions depicting prototypical expressions of happiness and fear.

5.1.1 Dynamic facial expressions (DFEs): Fear and happiness

DFE stimuli activated many brain areas in both groups compared to alternating mosaic images reconstructed from the dynamic facial video images. Importantly, limbic regions such as the (bilateral) Amy, hippocampi (DMN-V), thalami, and medial parts of the lentiform nuclei were strongly activated in both groups during the viewing of happy stimuli (Fig. 5). Cortical areas such as the occipitotemporal V2 (Visual Med) and V5 (DAN) regions and FFA were also strongly activated in both groups. Activation was dominant in the right hemisphere in a large cluster extending from the inferior to the medial frontal gyrus (MFG) and V5 in angular and opercular gyri in both groups (Figures 5 & 6; Tables 1 & 2).

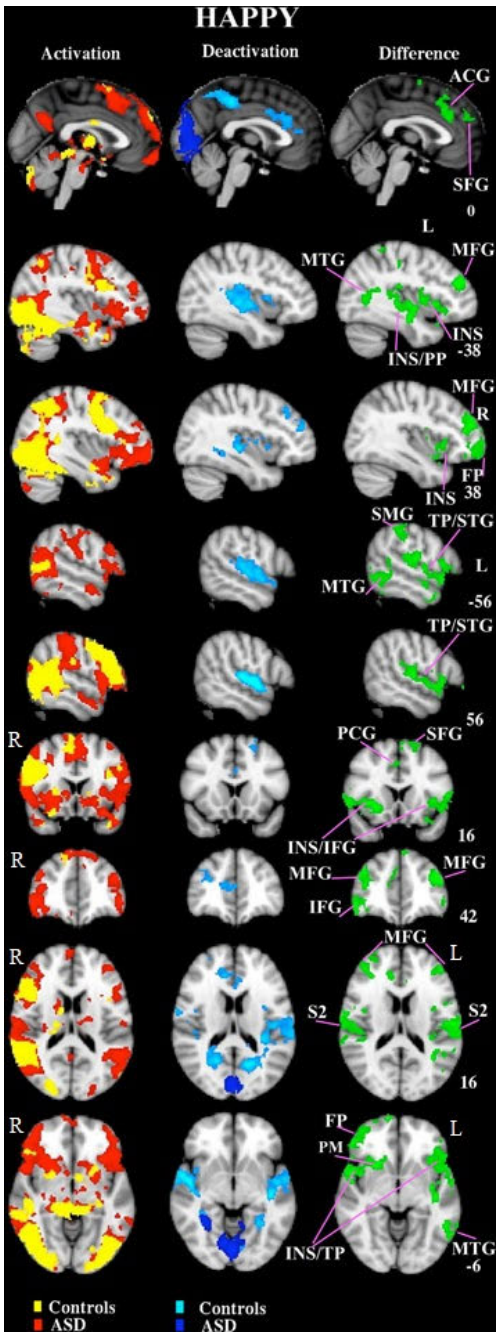

Fig. 5. Significant group activations (warm colors), deactivations (cold colors), and the

between-group differences (green, ASD > TD) during the viewing of dynamic, happy expressions. The visual V5 area in the left occipital cortex was more activated in participants with ASD than in TD controls. When viewing happy facial expressions, participants with ASD showed reduced deactivation compared to TD controls. Voxel levels were threshold-adjusted using a Z-score of > 2.3, a cluster level of p < 0.05 (corrected), and the MNI coordinates are shown on the right. *Abbreviations ACG* anterior cingulate gyrus, *FP* frontal pole, *IFG* inferior frontal gyrus, *INS* insula, *MFG* medial frontal gyrus, *MTG* middle temporal gyrus, *PCG* paracingulate gyrus, *PM* putamen, *PP* planum polare, *S2* secondary somatosensory, *SFG* superior frontal gyrus, *SMG* supramarginal gyrus, *STG* superior temporal gyrus, *TP* temporal pole. Reprinted with permission of Springer Nature from Study I © 2012 Springer Nature.

Differences between groups during happy expressions

Activation (stimulus > mosaic)

Activation was the dominant source of difference between the groups. During dynamic, happy expressions, participants with ASD had stronger activity in cortical and subcortical structures, resulting in a large putamen-insula difference cluster in the right hemisphere between the groups. In the left hemisphere, only an insular difference was observed. Frontal poles at the MFG (salience/VAN-A) were symmetrically more activated in the ASD group. The superior temporal gyrus (STG) on the right (motor) and the primary somatosensory area on the left were more activated in participants with ASD compared with the TD controls. Notably, other structures linked to expression identification, such as the Amy, thalamus, and FFA (Adolphs, 2002), did not show significant differences, even though these areas were strongly activated in both groups. The temporal pole (TP; medial part – DMN-A; posterior – FPC R/L) and PMC BA6 were also more active in participants with ASD. The visual V5 area in the left occipital cortex was more activated in participants with ASD compared with the TD controls (Fig. 5, Table 1).

Deactivation (mosaic > stimulus)

Participants with ASD showed reduced deactivation compared with the TD controls when viewing happy facial expressions (Fig. 5, Table 1). The ASD group showed deactivation only in visual cortex V1 and right temporal FFA, while the controls showed deactivation in various regions. The largest differential cluster of deactivation between groups was found in the left temporal lobe primary auditory

(A1) and secondary somatosensory (S2) areas extending to the planum temporale. This area was uniformly deactivated in the controls, while deactivation was absent in participants with ASD. The controls also showed more deactivation in the right opercular cortex. The difference between the groups in this left temporal lobe was particularly complex: the anterior (IFG) and posterior (parietal opercular cortex [POC]) part of the difference cluster showed more activation in the ASD group. At the same time, in the middle, the A1 region completely lacked deactivation in the ASD group.

Table 1. The twenty most significant differences in ASD vs. TD during facial expressions (Study I). Each entry specifies an anatomical brain area and its corresponding coverage of RSNs. Modified from Study I.

Hem	Areas // RSNs (highlighted RSN includes MI)	Volume	Mean	**MI**	**MI X**	**MI Y**	**MI Z**
L	BA21, Planum polare // **Auditory/VAN-P**, 5% (881); Motor, 4% (992); DMN/Language, 2% (423); Somatosensory, 1% (261); Salience/VAN-A, 1% (278); FPC L, 1% (181); DMN-A, 0% (51); Visual Med, 0% (6)	3122	2.77	4.27	-40	-12	-14
R	Putamen // Motor, 3% (731); Auditory/VAN-P, 3% (626); **Salience/VAN-A**, 2% (397); Somatosensory, 1% (114); DMN-A, 0% (45); FPC R, 0% (25); DMN/Language, 0% (9); FPC L, 0% (2); DAN, 0% (1)	1802	2.75	4.17	24	16	-6
L	Frontal pole, MFG // **Salience/VAN-A**, 5% (954); DMN-A, 2% (253); DMN/Language, 1% (163); Motor, 0% (71); FPC R, 0% (125); FPC L, 0% (60/17144); Somatosensory, 0% (21)	1645	2.77	5.59	-42	42	24
R	Frontal pole // FPC R, 4% (1041); **Salience/VAN-A**, 2% (349); Auditory/VAN-P, 0% (91); DMN/Language, 0% (19); FPC L, 0% (3); DMN-A, 0% (8)	1491	2.79	4.57	40	48	26
L	V5, BA37 // FPC L, 2% (281); DAN, 1% (79); Auditory/VAN-P, 1% (235); **Somatosensory**, 0% (74); DMN/Language, 0% (57); DMN-V, 0% (5); Visual Up Med, 0% (1)	781	2.72	3.70	-50	-68	8
L	SG, ant division // **Somatosensory**, 2% (377); Motor, 0% (73); FPC L, 0% (11); Auditory/VAN-P, 0% (5)	430	2.61	3.68	-58	-36	46
R	S2 per operculum // **Somatosensory**	90	2.69	3.69	50	0	12
L	MTG // **DMN/Language**	69	2.68	3.41	-54	6	-28

Hem	Areas // RSNs (highlighted RSN includes MI)	Volume	Mean	**MI**	**MI X**	**MI Y**	**MI Z**
R	IPL PFR // **Auditory/VAN-P**	37	2.48	2.82	66	-36	14
L	PMC BA6L // **Motor**	33	2.56	3.04	-46	-8	58
R	Frontal Pole // **FPC R**	17	2.52	2.73	28	64	12
L	ITG, ant division // **DMN/Language**	10	2.46	2.66	-50	-2	-36
R	TP // **DMN-A**	9	2.41	2.53	36	10	-22
L	STG, post division, TL // **DMN/Language**	9	2.45	2.64	-58	-16	-8
L	Putamen // **Motor**	6	2.58	2.87	-28	-18	0
R	Primary somatosensory cortex BA1 // **Motor**	6	2.48	2.78	66	0	20
L	ITG // **FPC L**	3	2.54	2.67	-56	-54	-22
R	Secondary somatosensory cortex // **Motor**	3	2.50	2.74	68	-6	22
R	Frontal pole // **FPC R**	2	2.34	2.36	46	52	8
R	IFG, pars opercularis // **Auditory/VAN-P**	2	2.37	2.40	54	12	12

All areas of difference (9590 voxels): Salience/VAN-A, 10% (1978/20184); Auditory/VAN-P, 10% (1838/18848); Motor, 8% (1867/23984); Somatosensory, 4% (847/21728); FPC R, 4% (1191/27224); DMN/Language, 4% (671/18072); FPC L, 3% (538/17144); DMN-A, 2% (357/15608); DAN, 1% (80/14152); Visual Med, 0% (6/19000); Visual Up Med, 0% (1/9200); DMN-V, 0% (5/12648).

Abbreviations: *Hem* hemisphere, *Volume* number of voxels (2x2x2 mm^3), *Mean* mean t-score value for the volume cluster, *Med* medial, *MI* maximum t-score intensity, *BA* Brodmann area, *DMN* default mode network, *FPC* frontoparietal cognitive control, *IFG* inferior frontal gyrus, *IPL* inferior parietal lobule, *ITG* inferior temporal gyrus, *Lat* lateral, *MTG* middle temporal gyrus, *STG* superior temporal gyrus, *TP* temporal pole, *TL* temporal lobe, *Up* upper, *PMC* premotor cortex, *PT* planum temporale, *RSN* resting state network, *VAN* ventral attention network, *-A* anterior, *L* left, *-P* posterior, *R* right, *-V* ventral. Highlighted RSN includes MI voxel.

Differences between the groups during fearful expressions

While there were many significant differences as regards happy facial expressions between the participants with ASD and the TD controls, there were no group brain activation (stimulus > mosaic) differences for fearful facial expression stimuli (Table 2). The only significant difference between the groups regarding fearful stimuli was that participants with ASD showed more deactivation (mosaic > stimulus) in the right visual cortex, V2 BA18 (Fig. 6, Table 2).

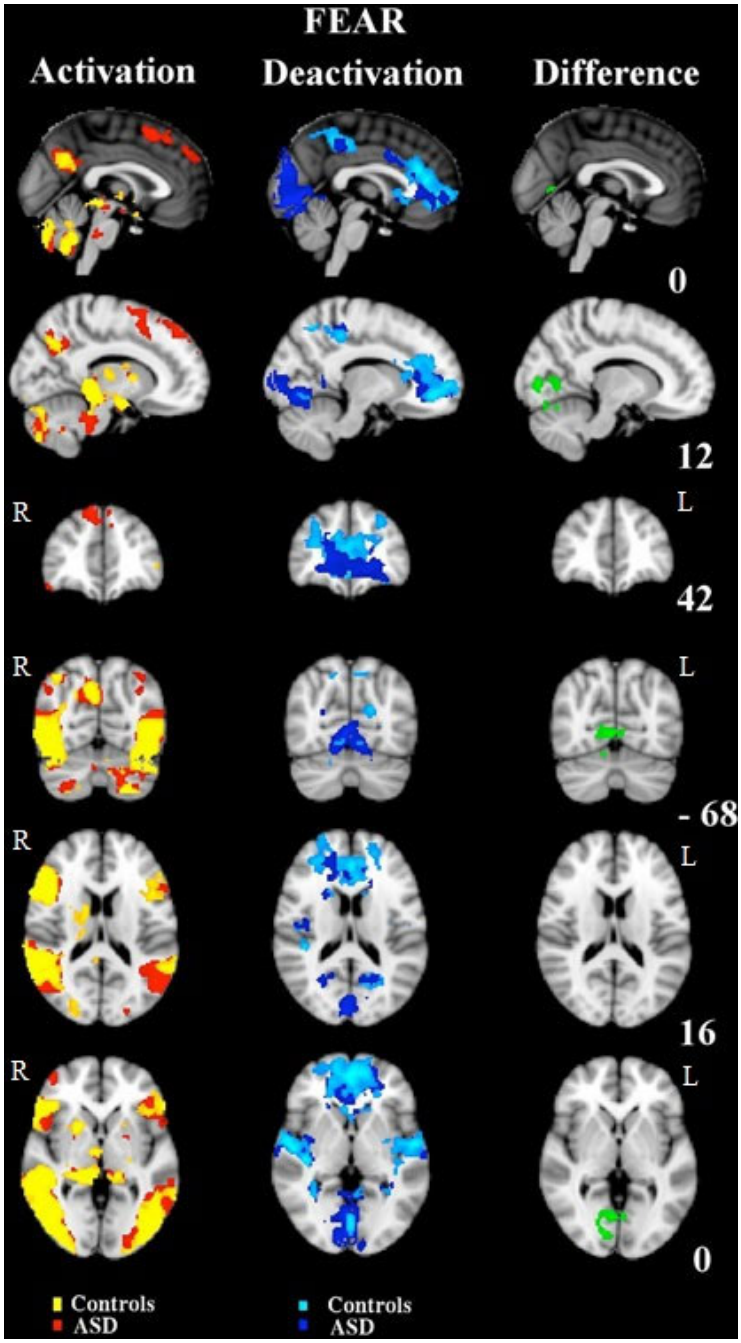

Fig. 6. Differences between the groups during fearful expressions. The only significant

difference between the groups regarding fearful stimuli was that participants with ASD showed more deactivation (mosaic > dynamic facial expression) in the right visual cortex, V2 BA18. Voxel levels were threshold-adjusted using a Z-score of > 2.3, a cluster level of p < 0.05 (corrected), and the MNI coordinates are shown on the right. Reprinted with permission of Springer Nature from Study I © 2012 Springer Nature.

Table 2. Fearful expressions ASD vs. TD controls (Study I). Modified from Study I.

Hem	Areas // RSNs	Volume	Mean	MI	MI X	MI Y	MI Z
R	Lingual Gyrus V3 // Visual Med, 3% (524/19000), FPC L 0% (1/17144)	525	2.59	3.53	18	-76	-4
R	Area VI // Motor, 0% (10/23984)	10	2.61	2.97	12	-66	-16

Abbreviations: *Hem* hemisphere, *Volume* number of voxels (2x2x2 mm^3), *Mean* mean value for the volume cluster, *MI* maximum Intensity, *RSN* resting state network. Highlighted RSN includes MI voxel.

Differences between the groups by valence (happy versus fearful expression)

The differences between valences originate from the differences in more robust activation and reduced deactivation of positive valence in the ASD group compared to TD controls. The participants with ASD showed significantly altered differences between valences in the bilateral temporal and parietal regions compared to the controls in valence-contrasted results. Symmetric differences between participants with ASD and the TD controls extended as a continuous cluster from IPLs along the fissura Sylvi all the way to TPs (Table 3).

Table 3. The ten most extensive areas of differences between the groups by valence happy versus fear (Study I). Modified from Study I.

Hem	Areas // MI RSN	Volume	Mean	MI	MI X	MI Y	MI Z
L	Insular cortex // Auditory/VAN-P	2199	2.73	4.36	-36	4	8
R	STG, post division // Motor	1930	2.78	4.44	66	-10	0
R	S1, BA3 // Motor	109	2.58	3.32	62	-10	28
L	Frontal pole // FPC L	72	2.81	3.98	-48	42	0
L	FOC, Insula // Auditory/VAN-P	14	2.42	2.64	-36	26	-6
R	S1 // Motor	9	2.43	2.67	64	-12	32
R	PG, Broca's area BA44 // FPC R	6	2.35	2.42	56	14	36
L	Frontal operculum cortex // Salience/VAN-A	4	2.44	2.52	-42	10	8
L	IFG, Broca's BA44 // Auditory/VAN-P	2	2.43	2.50	-56	28	0
L	SMG, ant division // Auditory/VAN-P	2	2.48	2.55	-62	-40	42

Hem	Areas // MI RSN	Volume	Mean	MI	MI X	MI Y	MI Z
All areas of difference (4365 voxels): Auditory/VAN-P, 7% (1396/18848); Motor, 6% (1325/23984); Somatosensory, 5% (1111/21728); Salience/VAN-A, 1% (199/20184); FPC L, 1% (128/17144); DMN/Language, 0% (70/18072); DAN, 0% (54/14152); FPC R, 0% (31/27224)							

Abbreviations: *Hem* hemisphere, *Volume* number of voxels (2x2x2 mm^3), *Mean* mean value for the volume cluster, *MI* maximum Intensity, *BA* Brodmann area, *FOC* frontal orbital cortex, *IFG* inferior frontal gyrus, *PG* precentral gyrus, *S1* primary somatosensory cortex, *SMG* supramarginal gyrus, *STG* superior temporal gyrus, *RSN* resting state network. Highlighted RSN includes MI voxel.

The insula (INS; salience/VAN-A) also showed bilateral differences between the groups with the left-side-dominance. The left hemisphere showed additional differences between the two groups in IFG and Broca's area BA 45. The right-side showed dominant differences between groups in valence-contrasted images in the superior parietal lobule (somatosensory) and precentral gyrus (FPC L) (Fig. 7).

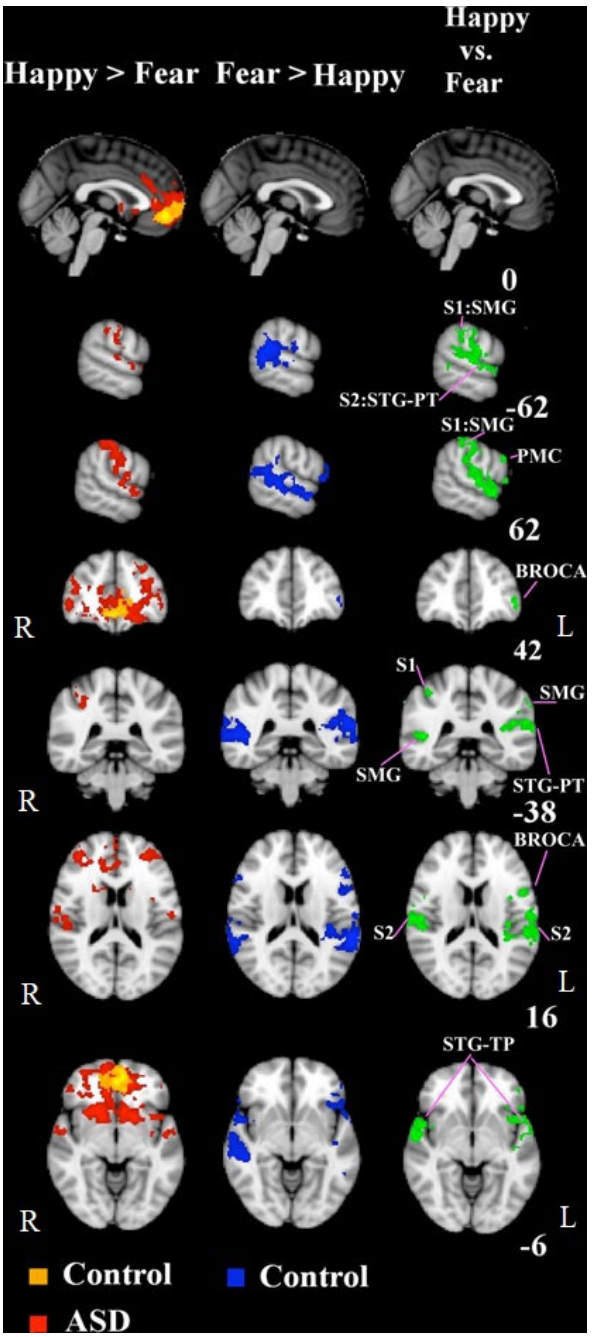

Fig. 7. Differences between the groups by the valence of facial expression (happy vs.

fearful expression, ASD > TD). Significant differences were found while viewing fearful expressions (green in right panels). The participants with ASD showed significantly altered difference between valences in bilateral temporal and parietal regions compared to the TD controls in valence contrasted results. Voxel levels were threshold-adjusted using a Z-score of > 2.3, a cluster-level of p < 0.05 (corrected), and the MNI coordinates were shown on the right. Abbreviations: *PT* planum temporale, *PMC* premotor cortex, primary (*S1*) and secondary (*S2*) somatosensory cortex, *SMG* supramarginal gyrus, *STG* superior temporal gyrus, *TP* temporal pole. Reprinted with permission of Springer Nature from Study I © 2012 Springer Nature.

5.2 Resting state fMRI

5.2.1 Static local functional connectivity: ReHo analysis

The visual impression of ReHo in the TD and ASD participants is shown in Figures 1 and 8.

The between-group difference is visualized in Figure 9. In comparison with the TD controls, the participants with ASD displayed significantly decreased ReHo in the right STS region (Figure 9. e, h), right IFG, and middle frontal gyri (MidFG) (c, e), bilateral cerebellar crus I (a, b, c, i), right insula (c, e) and right postcentral gyrus (c, g). Significantly increased ReHo was discovered in the right thalamus, mainly in its ventral posterolateral nucleus (VPL), but extending to the lateral geniculum body (Figure 9. e, g). Significantly increased ReHo was also discovered in the left IFG and anterior subcallosal gyrus (Figure 9. d) and bilateral cerebellar lobule VIII (Figure 9. a, f, i). Significantly increased ReHo in clusters, including both GM and WM, was also detected. Left cerebral hemisphere clusters included inferior occipital gyrus (IOG), MOG, SOG, and FFG with optic radiation (OR), but also the MCC with corpus callosum (CC) (Figure 9. d, e, f, i). In the right hemisphere, increased ReHo in OR with the MTG was found (Figure 9. e, i). By adding up the GM ReHo clusters (Table 1), the right-side changes totalled 6160 voxels and the left-side 1584. When WM and GM areas were included, the voxels for the right-side added up to 9128 and left to 5048.

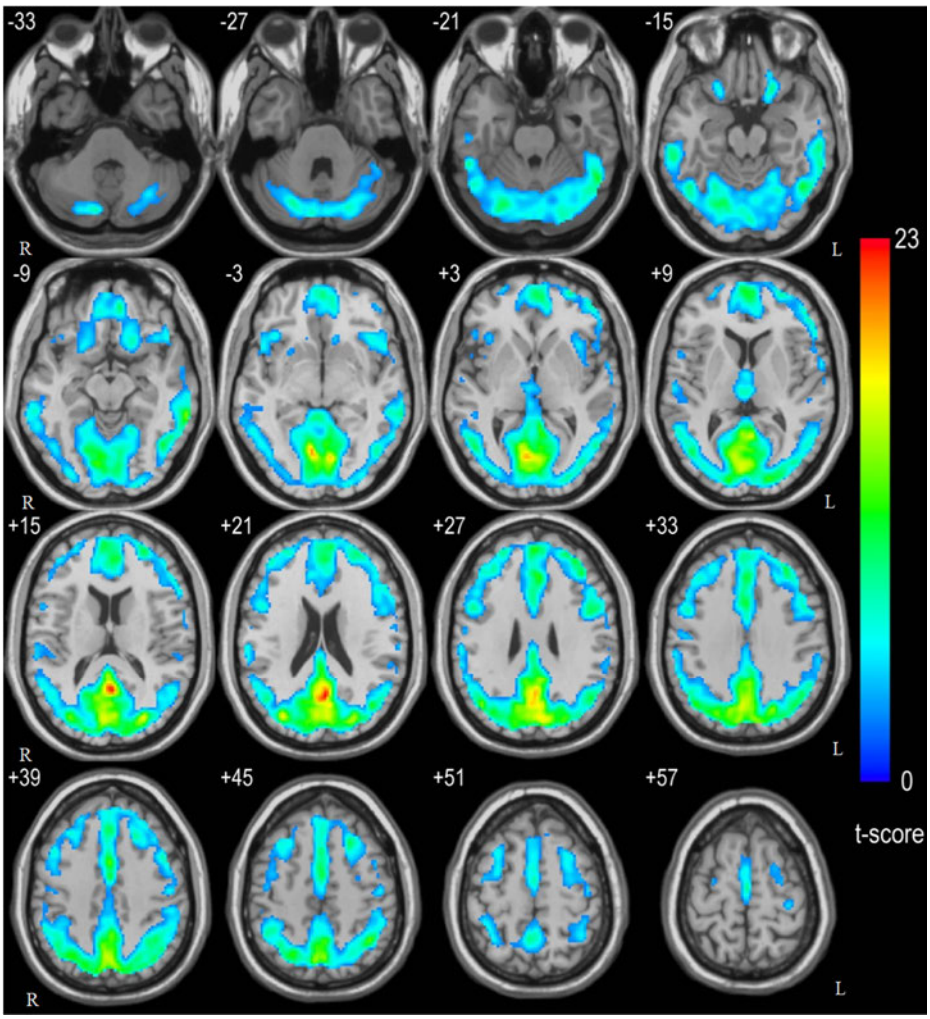

Fig. 8. Results of resting state regional homogeneity (ReHo) shown as Kendall's coefficient of concordance (KCC) map across ASD participants (one-sample t-test; $p < 0.01$, corrected for the minimum volume of 456 mm^3). The image's left-side corresponds to the brain's right-side. Z-coordinates, according to Talairach space, are shown in the upper left corner of the slices. Reprinted with permission of Elsevier from Study II © 2010 Elsevier.

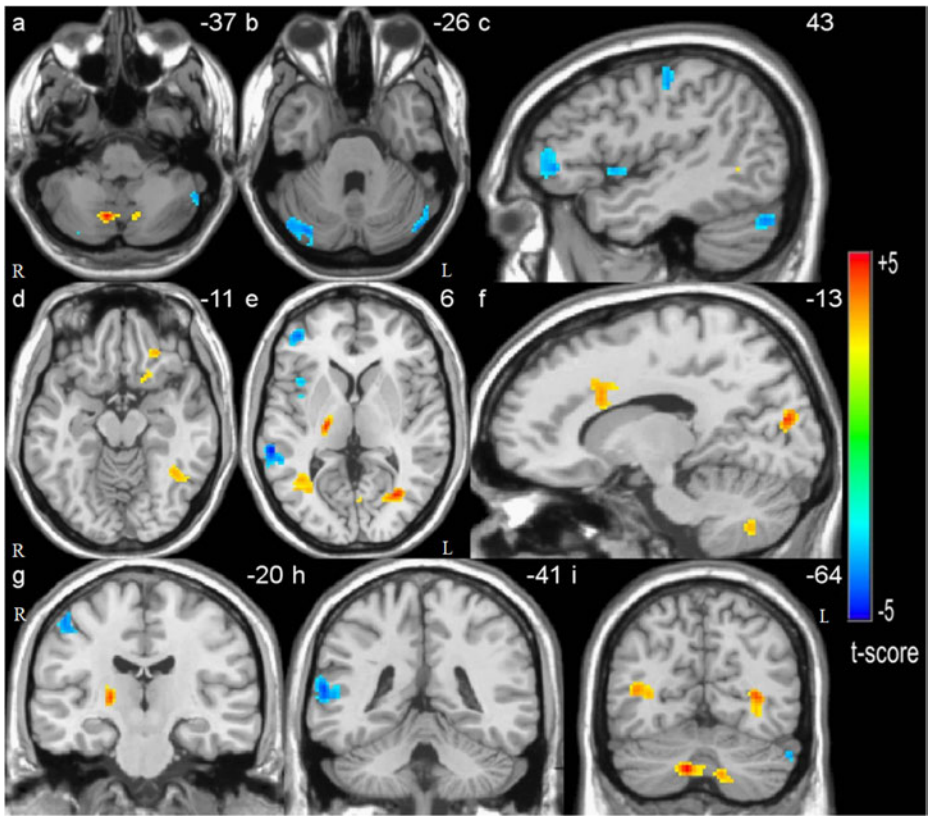

Fig. 9. T-statistical difference map between ASD participants and TD controls ($p < 0.05$, corrected). Warm and cold colors indicate ASD-related ReHo increases and decreases, respectively. The left-side of the image corresponds to the right-side of the brain in axial (a, b, d, e) and coronal (g, h, i) slices. Slice coordinates according to Talairach space are shown in the upper right corner of the slices, indicating Z-axis in axial, X-axis in sagittal, and Y-axis in coronal slices. Reprinted with permission of Elsevier from Study II © 2010 Elsevier.

Table 4. Brain areas of ReHo difference between the ASD and TD groups. The number of voxels in RSNs differs from the Study II results because they were derived from ReHo MNI space results without Talairach conversion. Modified from Study II.

Areas	Side	Volume	Peak t-value	Talairach coordinates (x, y, z)			RSN (≥ 10 voxels)
Gray Matter							
Decreased ReHo in ASD							
MTG, STG, STS	R	204	-4.81	57	-37	6	Auditory/VAN-P (251), DMN/Language (16), DMN-V (12)
Cerebellum crus 1 (Declive)	R	203	-4.34	29	−85	−22	DMN/Language (130), Visual Lat (88), FPC L (19), Salience/VAN-A (10)
MidFG, IFG	R	123	-4.09	37	43	6	FPC R (137)
Cerebellum crus 1 (Tuber)	L	84	-3.81	-45	-73	-26	FPC R (27), Visual Lat (22), Salience/VAN-A (21)
Insula	R	59	-3.59	41	1	0	Salience/VAN-A (47), Auditory/VAN-P (32)
Postcentral gyrus	R	54	-3.89	45	-19	50	Motor (60)
All areas of decreased ReHo in ASD		727					Auditory/VAN-P (288), FPC R (180), DMN/Language (151), Visual Lat (110), Salience/VAN-A (78), Motor (63), FPC L (23), DAN (21), DMN-V (12)
Increased ReHo in ASD							
Thalamus (ventral posterolateral nucleus)	R	69	4.58	19	-19	6	Motor (26)
Cerebellum lobule VIII (ISLL)	L	64	3.91	-17	-61	-42	Somatosensory (44), Motor (23)
Cerebellum lobule VIII (ISLL)	R	58	4.95	9	-65	-36	Motor (58)
IFG, SG	L	50	3.45	-25	31	-10	FPC L (47)
White and gray matter							

Areas	Side	Volume	Peak t-value	Talairach coordinates (x, y, z)			RSN (≥ 10 voxels)
Increased ReHo in ASD							
CC, OR, MOG, IOG, FFG	L	219	4.74	-31	-67	8	DAN (196), Visual Med (17), FPC L (11)
OR, MTG	R	216	5.05	37	-61	10	Auditory/VAN-P (56), DMN-V (29), DAN (23), Visual Med (20)
CC	R	155	4.27	25	-49	20	Visual Up Med (22), DMN-D (21), DMN-A (10)
OR, SOG	L	123	4.67	-15	-83	16	Visual Med (159)
CC, MCC	L	91	3.63	-13	13	26	Salience/VAN-A (45), DMN-V (14)
All areas of increased ReHo in ASD		1045					DAN (231), Visual Med (200), Motor (145), Salience/VAN-A (64), FPC L (64), Auditory/VAN-P (57), Somatosensory (48), Visual Up Med (23), DMN-D (21), DMN-A (10)

Abbreviations: *CC* corpus callosum, *FFG* fusiform gyrus, *IFG* inferior frontal gyrus, *IOG* inferior occipital gyrus, *ISLL* inferior semi-lunar lobule, *MCC* middle cingulate cortex, *MidFG* middle frontal gyrus, *MOG* middle occipital gyrus, *MTG* middle temporal gyrus, *OR* optic radiation, *RSN* resting state network, *SG* subcallosal gyrus, *SOG* superior occipital gyrus, *STG* superior temporal gyrus, *STS* superior temporal sulcus, *Volume* number of voxels (2x2x2 mm^3).

5.2.2 Time-varying functional connectivity

GICA results

We interpreted the 14 group-level ICs to represent different brain networks as follows (Figures 3 & 10). The mainly occipital visual networks were divided into three subnetworks or nodes. 1) The visual medial node. 2) The visual upper medial node. 3) The visual lateral nodes. Hierarchical clustering positioned both medial nodes in the subhierarchy with the DAN, which with this low ICA model order, included extrastriate visual areas. The visual lateral network is positioned along the subhierarchy with the auditory and posterior ventral attention networks (VAN-P) and the salience and anterior ventral attention networks (VAN-A).

The pericentral network divided into somatosensory and motor subnetworks. The DMN is divided into four subnetworks: 1) Anterior (DMN-A) in the mPFC. 2) Dorsal (DMN-D) with central bilateral PCC and precuneus nodes. 3) Ventral (DMN-V) consisting of retrosplenial, bilateral hippocampi (middle temporal gyri), and parietal nodes (angular gyri). 4) Temporoparietal nodes emphasizing the left-side (language).

The EF networks divided into four clusters that were left and right frontoparietal cognitive control networks (our FPC L/R), dorsomedial frontoparietal network, i.e., anterior control network (our Salience/VAN-A), and dorsal frontoparietal network, i.e., our DAN (Witt et al., 2021). Comparing our results to Witt et al. (2021; their Fig. 4: green dM-FPN) we can see that parts of the Salience/VAN-A and the DMN may share common task-dependent subnetwork nodes.

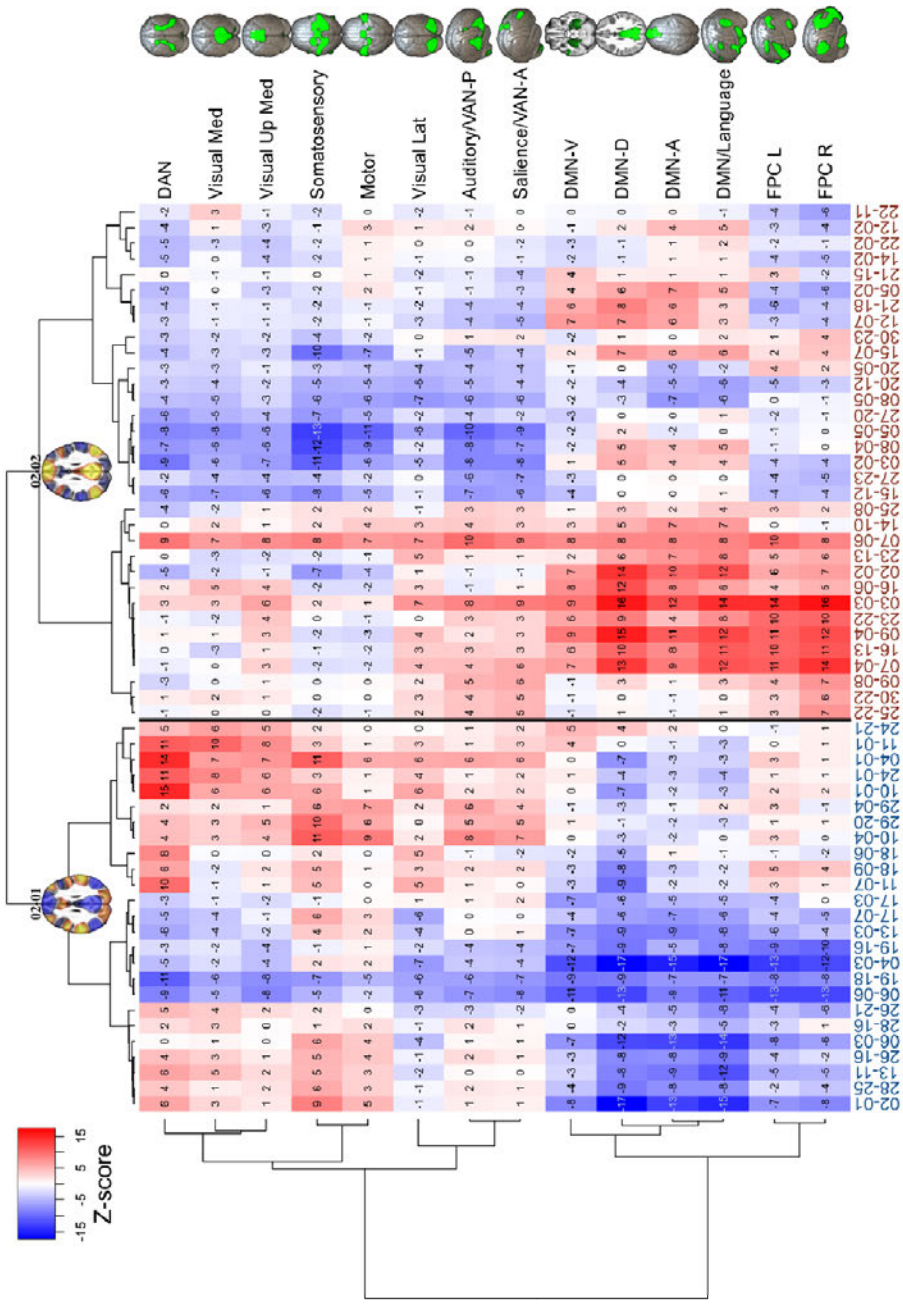

Fig. 10. Mean voxel-wise z-scores by resting state networks (as in Fig. 3) for each CAP.

On the X and Y axes, the grouping of the brain areas was determined by the hierarchical clustering (cosine distance, Ward's method) of only this particular z-score matrix. On the X axis, the CAP label colors correspond to the "DMN-negative / task-positive" (blue labels, DMN-CAPs) and "DMN-positive" (red labels, DMN+CAPs) grouping of CAPs, with a black line separating them. Network abbreviations: DAN = dorsal attention; Visual Med, Up Med, Lat = visual medial, upper medial, lateral; VAN-P/-A = ventral attention posterior/anterior; DMN-V/-D/-A = default mode ventral/dorsal/anterior, FPC L/R = frontoparietal cognitive control left/right. Views: DAN, Visual (3D elevated occipital), Somatosensory, Motor, DMN-A (3D above), Auditory, Salience, VAN, FPC R (3D right lateral), DMN-V, -D (axial slice above), DMN/Language, FPC L (3D left lateral). Reprinted under CC BY 4.0 license from Study III © 2021 The Authors.

CAP results

The median number of fMRI volumes assigned to each CAP from either the ASD or the TD participants' data were calculated with bootstrapped confidence intervals (95%, 10 000 resamples), which were overlapping (Fig. 11). The Mann-Whitney test p-value was < 0.05 in seven CAPs but became nonsignificant after FDR correction. Thus, we found no reliable ASD- or TD-specific CAPs within the cluster levels used in our study (from 2 to 30). The number of volumes in each CAP (Figures S1a–b) and the images of each CAP (Figures S2a–i), and when found, their group activation differences (Figures S2a–i), are visualized in the Supporting Information S1 of Study III (https://onlinelibrary.wiley.com/doi/full/10.1002/brb3.2174).

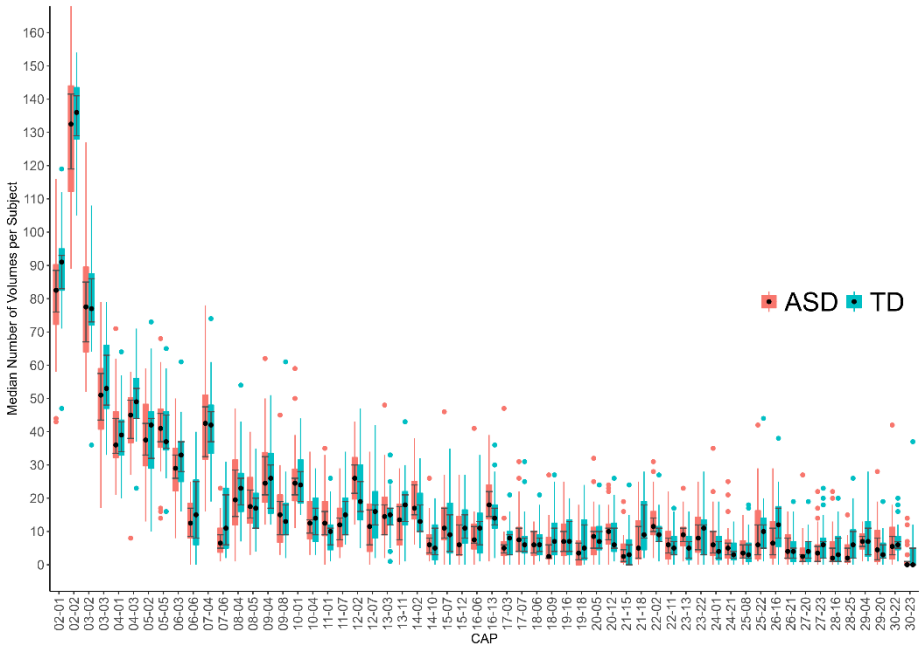

Fig. 11. The median number of fMRI volumes per participant in CAPs with confidence intervals and outlier dots. The outliers may reflect individual differences in time spent in default mode-positive or task-positive brain states. As described earlier, on average, participant-wise, censoring excluded 13 volumes more from the ASD data than from the TD data. [Under CC BY 4.0 license from Study III. Paakki J-J, Rahko JS, Kotila A, et al. Co-activation pattern alterations in autism spectrum disorder–A volume-wise hierarchical clustering fMRI study. Brain Behav. 2021;11:e02174. © 2021 The Authors]

The clustering of the whole RS-fMRI data reveals a familiar-looking division into two main cluster groups. At the highest level of the cladogram (Fig. 2), that is, the first level of branching, there are only two CAPs, and each fMRI volume belongs to one or the other. The first CAP (02-01, 39% of the 11 930 volumes) resembles a task-positive ICN as its fMRI volumes contain below-average values in the lateral visual, default mode, language, and FPC networks but above-average values in the DAN, medial visual, somatosensory, motor, auditory, salience, and VAN networks. Compared to the first CAP, the second CAP (02-02, 61% of the volumes) shows a reversal in the activity patterns with above-average values in the DMN and corresponding opposite values in other networks embodying task-negative or rather default mode-positive ICN features.

Both DMN-positive and DMN-negative (or task-positive) CAPs divide into sub-hierarchies and smaller CAPs (Fig. 2), which are distinguished from each other by different areal average values (also referred to here as activation when above average and deactivation when below average) in ICA-based RSNs (Fig. 3). This is also depicted in the heatmap of Figure 10 which illustrates the average z-score values of our study-specific RSN parcellations in different CAPs. The hierarchical clustering of this heatmap's rows and columns groups the different RSNs and CAPs by their features, respectively. This kind of review is modest in spatial accuracy but facilitates pattern recognition in group-level activation differences. The most apparent patterns are reported in the following paragraphs.

When the CAPs in Figure 2 are transformed into the heatmap of Figure 10, one can roughly detect four panels. Firstly, the DMN, language, and FPC networks exhibit mainly negative z-scores (interpreted here as network deactivation) during the default mode-negative CAPs (DMN-CAPs) and form the bluish-colored lower panel on the left. In contrast, the DAN and all the sensory, motor, salience and VAN networks mostly exhibit red-colored positive z-scores (interpreted here as task-positive network activation) and form the reddish left upper panel of the DMN-CAPs.

However, during the DMN-positive CAPs (DMN+CAPs) on the right, the DMN, language, and FPC networks predominantly exhibit positive z-scores and form the reddish right lower panel. Fourthly, the right upper panel of the DMN+CAPs consists mainly of blue-colored negative z-scores, excluding a few CAPs with activation among the auditory, visual, salience, and VAN networks.

Due to z-score averaging (of RSNs in the heatmap), the nuances of the CAPs are lost in the heatmap, and a few seemingly similar CAPs co-exist on both the left and right. Notably, some CAPs also show only activation or deactivation over all the RSNs, i.e., negative blue or positive red vertical stripes over the whole brain cortex matrix (Figures 10, 14 & 15).

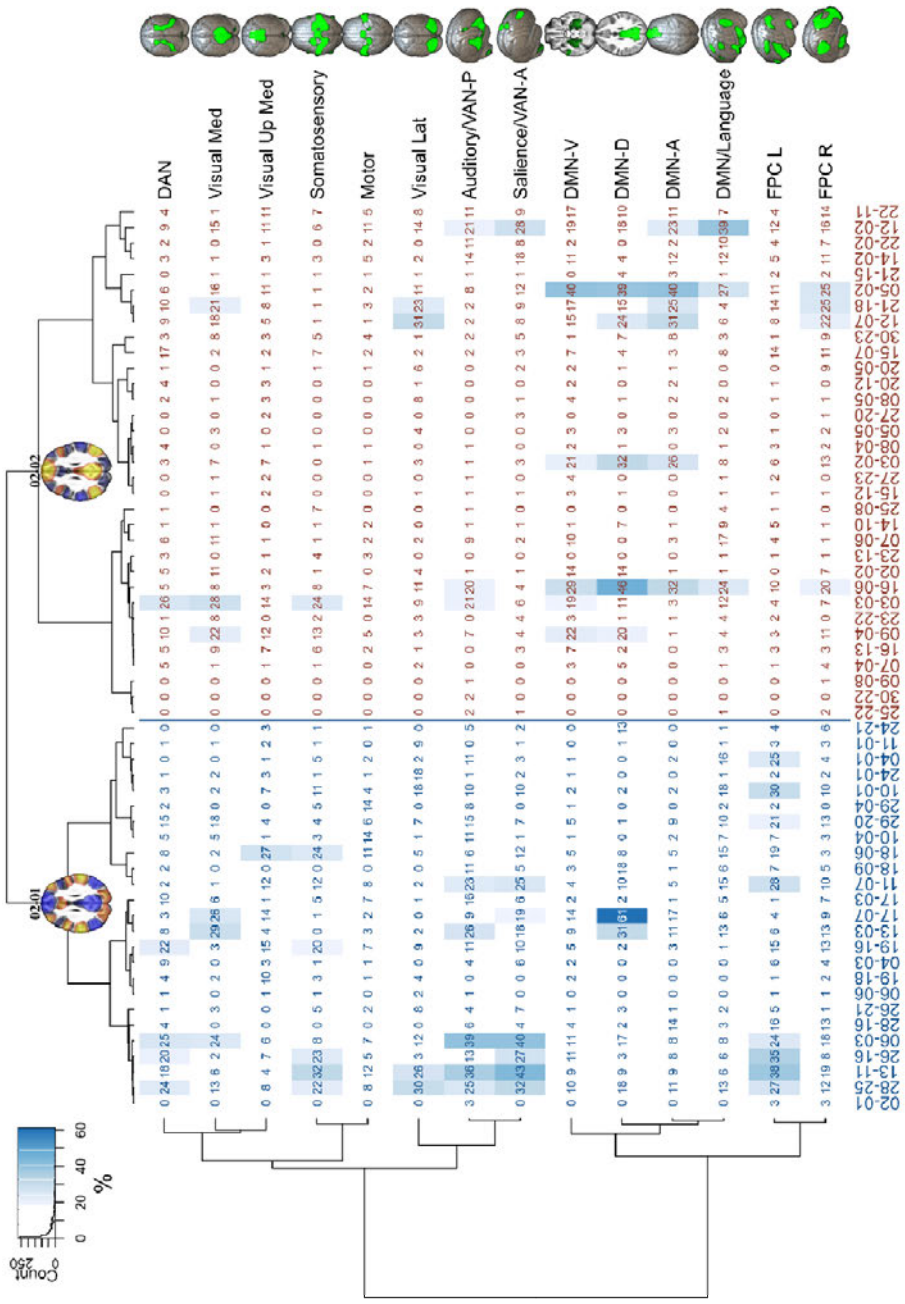

Fig. 12. Percentages of TD > ASD brain areas in CAPs. See legend of Figure 13.

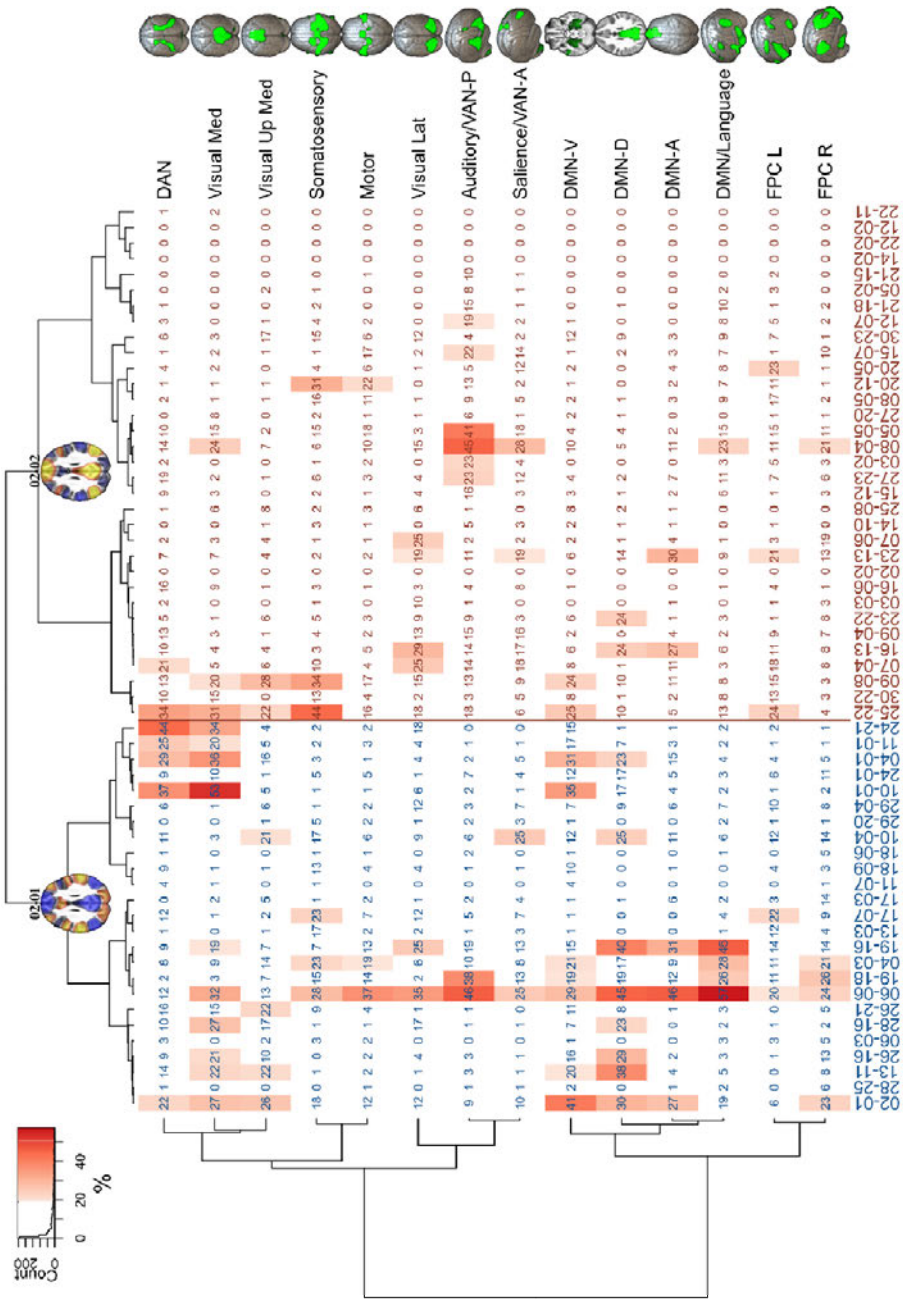

Fig. 13. Percentages of ASD > TD brain areas in CAPs. In Figure 13 the ASD and in

Figure 12 the TD group have significantly greater voxel-wise z-score values than the other group. The results are shown at q = 0.05 false discovery rate (FDR) corrected. An arbitrary threshold of the highest decile is applied to the cell background coloring (blue rectangles for TD, red for ASD) as a highlighting, where cluster areas comprise at least 19% of the corresponding IC areas. The order and origin of the X and Y axis labels are identical to those in Figure 10. Reprinted under CC BY 4.0 license from Study III © 2021 The Authors.

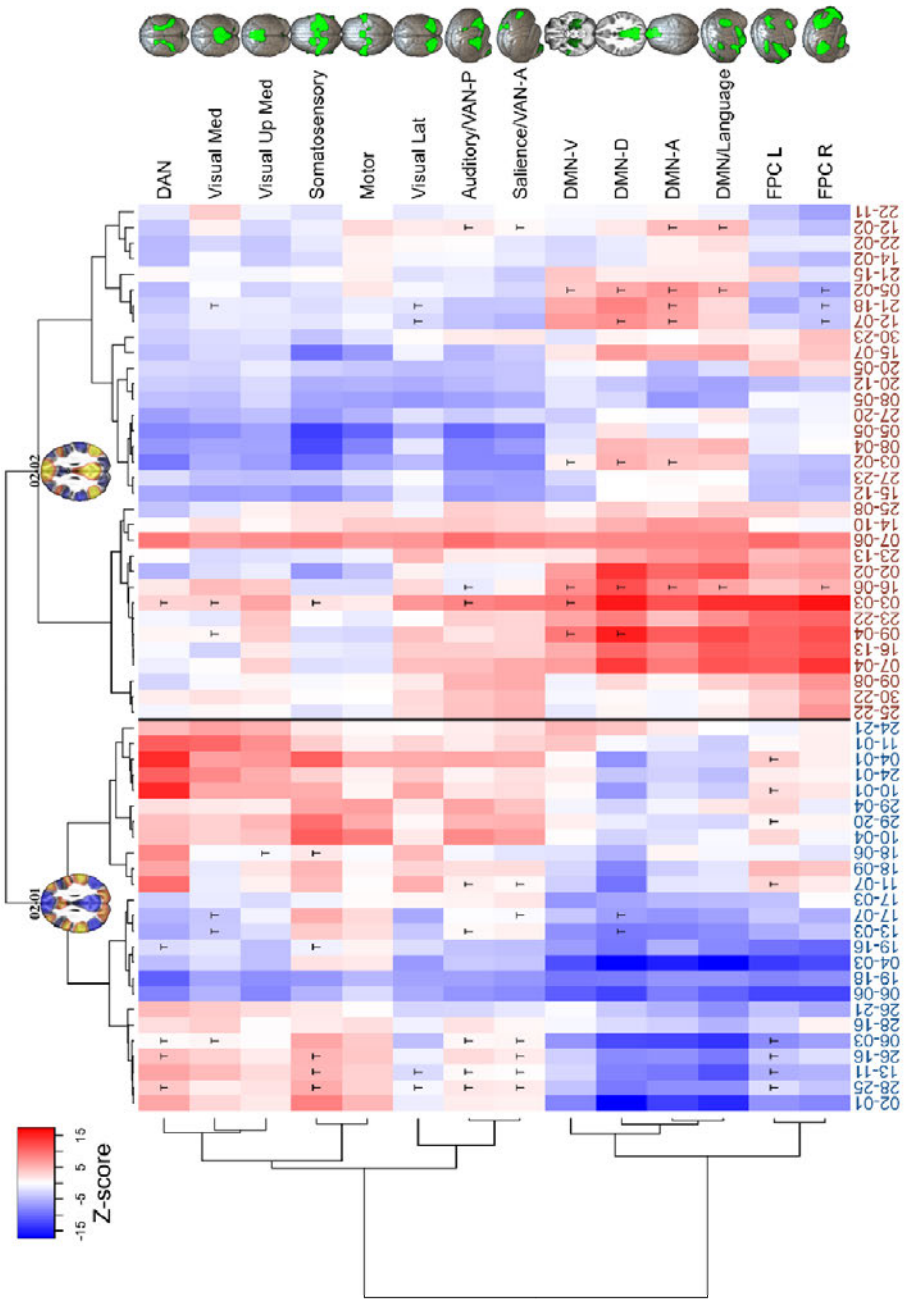

Fig. 14. Combination of Figures 10 and 12. See Legend of Figure 15.

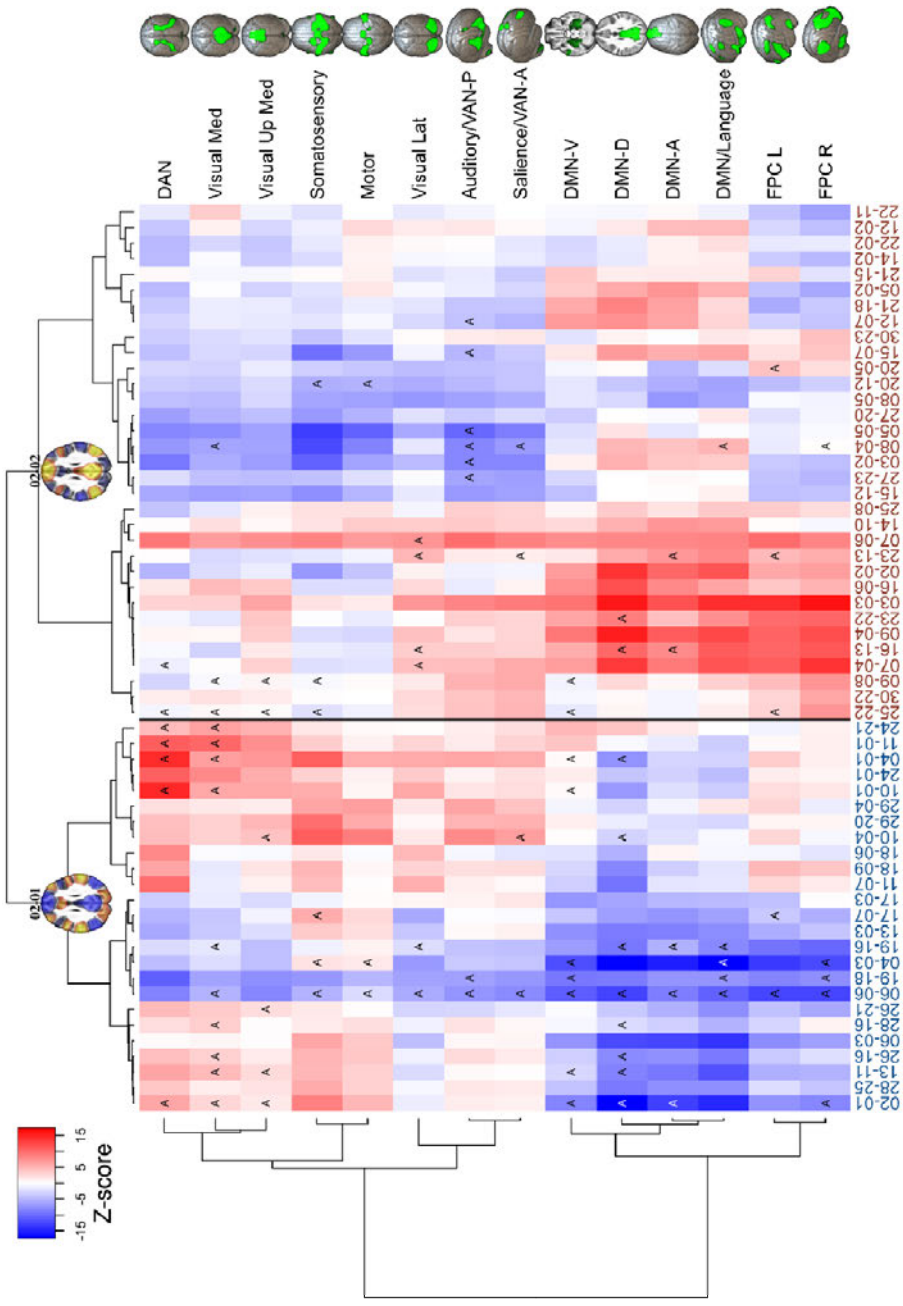

Fig. 15. Combination of Figures 10 and 13. Largest clusters (highest decile) of TD (Fig.

14) and ASD (Fig. 15) group-related CAP activity in resting state networks. The TD group-related activity is marked by the letter "T" (Fig. 14), and the ASD group-related activity by "A" (Fig. 15) over the color-coded average z-scores of the same heatmap as those in Figure 10. Reprinted under CC BY 4.0 license from Study III © 2021 The Authors.

The areas in the CAPs where the TD or ASD group has significantly greater activation than the other group are shown as a percentage of the corresponding RSN volume in Figures 12 and 13. The highlighted highest deciles of these results are projected on the earlier CAP heatmap (Fig. 10). This combination in Figures 14 and 15 finds the RSNs in the CAPs that exhibit the largest simultaneous group-related activations. The twenty largest between-group differences in CAPs are listed in Table 1. Additional descriptive figures (S1a–b, S2a–i) and detailed results in Table S1 can be found in Supporting Information S1 and S2 of Study III.

When inspecting Figure 10 through the four-panel approach described earlier, one can see that most of the largest TD group-related activations fall within the task-related networks in the upper left panel during the DMN-CAPs. In contrast, during the DMN+CAPs, the TD group-related activations are primarily within the DMN and the language and VAN networks.

The TD group-related FPC activation was left-dominant during the DMN-CAPs and right-dominant during the DMN+CAPs. The left FPC was activated while the task-related networks were also activated, and seemed to associate with the salience and VAN-A control networks in particular, but also with the auditory, somatosensory, and DAN networks. Right FPC activation related to the DMN and language networks.

The earlier four-panel approach generally showed more incoherently highlighted patterns during the ASD group-related activations than the TD group-related ones (Figures 12–15). The FPC activations in the ASD group did not demonstrate clear-cut sidedness related to the DMN-negative or DMN-positive CAPs. However, there were some repeating overactivation patterns. The DAN associated with visual networks. If the visual network was overactive but not concurrent with the DAN, it associated, in turn, with the DMN. In the TD group, the DAN overactivation was also related to other task-positive networks in a more balanced way. It also seems the ASD group did not quite reach as strong deactivations as the TD group (Figures 14 & 15). ASD group-related overactivations were found, especially in the DAN, visual and auditory networks, and the DMN. In the 06-06 CAP, which deactivated all 14 RSNs, the ASD group showed a considerably reduced deactivation pattern in nearly all (12/14) RSNs.

Table 5. The twenty biggest CAP group differences (FDR q < 0.05 corrected, two-tailed FDR adjusted p-value threshold p = 0.002). In each CAP are presented the percentages of RSNs' areas in which the ASD or TD groups had significantly greater values than the other group. Reprinted under CC BY 4.0 license from Study III © 2021 The Authors.

CAP	Effect	Volume	Clusters	RSN-areas by % (voxels of clusters area / RSN area)
06-06	ASD>TD	9565	1	DMN/Language, 57% (1298/2259); DMN-A, 46% (900/1951); Auditory/VAN-P, 46% (1086/2356); DMN-D, 45% (419/926); Motor, 37% (1113/2998); Visual Lat, 35% (530/1518); Visual Med, 32% (766/2375); DMN-V, 29% (454/1581); Somatosensory, 28% (759/2716); Salience/VAN-A, 25% (643/2523); FPC R, 24% (806/3403); FPC L, 20% (423/2143); Visual Up Med, 13% (149/1150); DAN, 12% (212/1769);
13-11	TD>ASD	6027	9	Salience/VAN-A, 43% (1087/2523); FPC L, 38% (819/2143); Auditory/VAN-P, 36% (846/2356); Somatosensory, 32% (873/2716); Visual Lat, 26% (390/1518); FPC R, 19% (636/3403); DAN, 18% (310/1769); Motor, 12% (362/2998); DMN-V, 9% (136/1581); DMN-D, 9% (80/926); DMN-A, 9% (168/1951); Visual Med, 6% (133/2375); DMN/Language, 6% (143/2259); Visual Up Med, 4% (44/1150);
02-01	ASD>TD	5631	14	DMN-V, 41% (653/1581); DMN-D, 30% (278/926); Visual Med, 27% (650/2375); DMN-A, 27% (529/1951); Visual Up Med, 26% (298/1150); FPC R, 23% (797/3403); DAN, 22% (394/1769); DMN/Language, 19% (420/2259); Somatosensory, 18% (484/2716); Visual Lat, 12% (175/1518); Motor, 12% (355/2998); Salience/VAN-A, 10% (244/2523); Auditory/VAN-P, 9% (223/2356); FPC L, 6% (119/2143);
25-22	ASD>TD	5618	15	Somatosensory, 44% (1185/2716); DAN, 34% (608/1769); Visual Med, 31% (739/2375); DMN-V, 25% (392/1581); FPC L, 24% (504/2143); Visual Up Med, 22% (251/1150); Visual Lat, 18% (268/1518); Auditory/VAN-P, 18% (423/2356); Motor, 16% (468/2998); DMN/Language, 13% (289/2259); DMN-D, 10% (96/926); Salience/VAN-A, 6% (158/2523); DMN-A, 5% (106/1951); FPC R, 4% (131/3403);
06-03	TD>ASD	5476	9	Salience/VAN-A, 40% (1014/2523); Auditory/VAN-P, 39% (930/2356); DAN, 25% (451/1769); Visual Med, 24% (568/2375); FPC L, 24% (513/2143); FPC R, 18% (623/3403); DMN-D, 17% (158/926); Visual Lat, 12% (180/1518); DMN-V, 11% (171/1581); Somatosensory, 8% (220/2716); DMN/Language, 8% (190/2259); DMN-A, 8% (162/1951); Motor, 7% (222/2998); Visual Up Med, 6% (72/1150);

CAP	Effect	Volume	Clusters	RSN-areas by % (voxels of clusters area / RSN area)
19-16	ASD>TD	5445	8	DMN/Language, 46% (1040/2259); DMN-D, 40% (373/926); DMN-A, 31% (604/1951); Visual Lat, 25% (382/1518); Visual Med, 19% (462/2375); Auditory/VAN-P, 19% (440/2356); DMN-V, 15% (235/1581); FPC R, 14% (463/3403); FPC L, 14% (294/2143); Salience/VAN-A, 13% (335/2523); Motor, 13% (375/2998); DAN, 9% (157/1769); Visual Up Med, 7% (82/1150); Somatosensory, 7% (191/2716);
28-25	TD>ASD	5340	8	Salience/VAN-A, 32% (819/2523); Visual Lat, 30% (460/1518); FPC L, 27% (569/2143); Auditory/VAN-P, 25% (588/2356); DAN, 24% (418/1769); Somatosensory, 22% (590/2716); DMN-D, 18% (163/926); Visual Med, 13% (313/2375); DMN/Language, 13% (295/2259); FPC R, 12% (414/3403); DMN-A, 11% (207/1951); DMN-V, 10% (166/1581); Visual Up Med, 8% (94/1150); Motor, 8% (244/2998);
08-04	ASD>TD	5248	12	Auditory/VAN-P, 45% (1057/2356); Salience/VAN-A, 28% (713/2523); Visual Med, 24% (574/2375); DMN/Language, 23% (519/2259); FPC R, 21% (729/3403); Visual Lat, 15% (231/1518); DAN, 14% (254/1769); FPC L, 11% (226/2143); DMN-A, 11% (208/1951); Motor, 10% (305/2998); DMN-V, 10% (158/1581); Visual Up Med, 7% (77/1150); Somatosensory, 6% (151/2716); DMN-D, 5% (46/926);
12-02	TD>ASD	5126	8	DMN/Language, 39% (875/2259); Salience/VAN-A, 28% (699/2523); DMN-A, 23% (455/1951); Auditory/VAN-P, 21% (484/2356); DMN-V, 19% (294/1581); DMN-D, 18% (166/926); FPC R, 16% (545/3403); Visual Med, 15% (363/2375); Visual Lat, 14% (217/1518); FPC L, 12% (257/2143); Visual Up Med, 11% (124/1150); Motor, 11% (332/2998); DAN, 9% (155/1769); Somatosensory, 6% (158/2716);
05-02	TD>ASD	4863	9	DMN-V, 40% (632/1581); DMN-A, 40% (776/1951); DMN-D, 39% (364/926); DMN/Language, 27% (603/2259); FPC R, 25% (859/3403); Visual Med, 16% (384/2375); Salience/VAN-A, 12% (301/2523); Visual Up Med, 11% (123/1150); Visual Lat, 11% (168/1518); FPC L, 11% (246/2143); Auditory/VAN-P, 8% (180/2356); DAN, 6% (114/1769); Motor, 2% (67/2998); Somatosensory, 1% (36/2716);
19-18	ASD>TD	4693	19	Auditory/VAN-P, 38% (907/2356); FPC R, 26% (894/3403); DMN/Language, 26% (579/2259); DMN-V, 19% (299/1581); DMN-D, 19% (173/926); Somatosensory, 15% (412/2716); Motor, 14% (425/2998); Salience/VAN-A, 13% (317/2523); DMN-A, 12% (228/1951); FPC L, 11% (234/2143); Visual Up Med, 7% (78/1150); Visual Med, 3% (76/2375); Visual Lat, 2% (36/1518); DAN, 2% (35/1769);

CAP	Effect	Volume	Clusters	RSN-areas by % (voxels of clusters area / RSN area)
09-08	ASD>TD	4525	13	Somatosensory, 34% (915/2716); Visual Up Med, 28% (321/1150); DMN-V, 24% (375/1581); Visual Med, 20% (481/2375); Motor, 17% (502/2998); Visual Lat, 15% (231/1518); FPC L, 15% (322/2143); DAN, 13% (223/1769); Auditory/VAN-P, 13% (304/2356); DMN-A, 11% (220/1951); DMN-D, 10% (93/926); Salience/VAN-A, 9% (236/2523); DMN/Language, 8% (188/2259); FPC R, 3% (108/3403);
04-03	ASD>TD	4472	18	DMN/Language, 28% (630/2259); Somatosensory, 23% (614/2716); FPC R, 21% (708/3403); DMN-V, 21% (328/1581); Motor, 19% (568/2998); DMN-D, 17% (156/926); Visual Up Med, 14% (157/1150); FPC L, 11% (227/2143); Auditory/VAN-P, 10% (236/2356); Visual Med, 9% (223/2375); DMN-A, 9% (185/1951); Salience/VAN-A, 8% (200/2523); DAN, 8% (143/1769); Visual Lat, 6% (89/1518);
16-06	TD>ASD	4426	35	DMN-D, 46% (426/926); DMN-A, 32% (622/1951); DMN-V, 29% (459/1581); DMN/Language, 24% (542/2259); FPC R, 20% (695/3403); Auditory/VAN-P, 20% (477/2356); Visual Lat, 11% (163/1518); FPC L, 10% (210/2143); Visual Med, 8% (179/2375); Somatosensory, 8% (216/2716); Motor, 7% (213/2998); DAN, 5% (81/1769); Salience/VAN-A, 4% (103/2523); Visual Up Med, 3% (39/1150);
03-03	TD>ASD	4187	17	Visual Med, 28% (667/2375); DAN, 26% (452/1769); Somatosensory, 24% (652/2716); Auditory/VAN-P, 21% (487/2356); DMN-V, 19% (301/1581); Visual Up Med, 14% (160/1150); Motor, 14% (426/2998); DMN/Language, 12% (263/2259); DMN-D, 11% (103/926); Visual Lat, 9% (134/1518); FPC R, 7% (246/3403); Salience/VAN-A, 6% (140/2523); FPC L, 4% (94/2143); DMN-A, 3% (62/1951);
05-05	ASD>TD	4151	20	Auditory/VAN-P, 41% (971/2356); Salience/VAN-A, 18% (450/2523); Motor, 18% (534/2998); Visual Med, 15% (358/2375); Somatosensory, 15% (401/2716); FPC L, 15% (319/2143); DMN/Language, 15% (345/2259); FPC R, 11% (384/3403); DAN, 10% (173/1769); DMN-V, 4% (69/1581); DMN-D, 4% (33/926); Visual Lat, 3% (51/1518); Visual Up Med, 2% (26/1150); DMN-A, 2% (37/1951);
26-16	TD>ASD	3768	16	FPC L, 35% (748/2143); Salience/VAN-A, 27% (682/2523); Somatosensory, 23% (620/2716); DAN, 20% (351/1769); Auditory/VAN-P, 13% (296/2356); DMN-V, 11% (176/1581); FPC R, 8% (257/3403); DMN-A, 8% (149/1951); Visual Up Med, 7% (83/1150); DMN/Language, 6% (131/2259); Motor, 5% (162/2998); Visual Lat, 3% (42/1518); DMN-D, 3% (25/926); Visual Med, 2% (46/2375);

CAP	Effect	Volume	Clusters	RSN-areas by % (voxels of clusters area / RSN area)
21-18	TD>ASD	3663	18	FPC R, 25% (866/3403); DMN-A, 25% (483/1951); Visual Lat, 23% (345/1518); Visual Med, 21% (498/2375); DMN-V, 17% (273/1581); DMN-D, 15% (141/926); FPC L, 14% (291/2143); DAN, 10% (179/1769); Salience/VAN-A, 9% (238/2523); Visual Up Med, 8% (89/1150); DMN/Language, 4% (86/2259); Motor, 3% (80/2998); Auditory/VAN-P, 2% (42/2356); Somatosensory, 1% (39/2716);
13-03	TD>ASD	3564	6	DMN-D, 31% (289/926); Visual Med, 29% (681/2375); Auditory/VAN-P, 26% (609/2356); Salience/VAN-A, 18% (455/2523); FPC R, 13% (434/3403); DMN/Language, 13% (300/2259); DMN-A, 11% (217/1951); DMN-V, 9% (144/1581); DAN, 8% (134/1769); FPC L, 6% (131/2143); Visual Up Med, 4% (43/1150); Motor, 3% (83/2998); Visual Lat, 2% (31/1518); Somatosensory, 0% (11/2716);
12-07	TD>ASD	3538	21	Visual Lat, 31% (466/1518); DMN-A, 31% (608/1951); DMN-D, 24% (220/926); FPC R, 22% (733/3403); Visual Med, 18% (421/2375); DMN-V, 15% (233/1581); DAN, 9% (165/1769); Salience/VAN-A, 8% (213/2523); FPC L, 8% (170/2143); DMN/Language, 6% (134/2259); Visual Up Med, 5% (63/1150); Auditory/VAN-P, 3% (59/2356); Somatosensory, 1% (21/2716); Motor, 1% (23/2998);

Abbreviations: *CAP* co-activation pattern, *Volume* number of voxels (4x4x4 mm^3), *DMN* default mode network, *FPC* frontoparietal cognitive control, *Lat* lateral, *Med* medial, *RSN* resting state network, *Up upper*, *VAN* ventral attention network, *-A* anterior, *L* left, *-P* posterior, *R* right, *-V* ventral.

6 Discussion

6.1 Brain activation while watching facial expressions

In Study I, we hypothesized that participants with ASD would demonstrate differences in the valence-dependent scaling of brain activity while observing DFEs. Two expectations were tested: (a) whether viewing DFEs reveals differences in automated valence scaling between participants with ASD and the TD controls; and (b) whether deactivation explains some of the hypothesized differences.

The TD participants present both more activation and deactivation during negative valence in comparison to positive facial expression valence. The participants with ASD showed significantly altered scaling related to facial valences in the bilateral temporal and parietal regions. The difference is related to abnormalities detected during happy DFEs. The positive, happy valence induced stronger activation and reduced deactivations over cortical and sub-cortical structures compared to the TD participants. Negative valence showed excess deactivation in the right visual cortex in the ASD participants.

Insula and salience processing

Based on the observed alterations in both RS connectivity and stimuli activation responses on the right INS, salience processing in the ASD group differs, leading to reduced valence scaling in this study. We found activation alterations in the right insula (INS), one key node in the salience network (Sridharan et al., 2008; Uddin, 2015; Uddin et al., 2019; Uddin & Menon, 2009). We have also found evidence of baseline activity abnormality, i.e., decreased local FC in the very same region in RS analyses (Study II). This supports the presence of a salience network related alteration during both task and resting conditions. Since the resting state is usually the baseline to which task activations are compared, we argue that the baseline activity of salience is already altered, which may interfere with related task activation. This can also be seen in Study III (Figures 12–15), where the associated activations of auditory/VAN/salience and other networks clearly differ between the ASD and TD groups.

In the TD participants, happy expressions activate more and deactivate less than fearful stimuli, thus presenting valence-related brain activity scaling (Rahko et al., 2010). In contrast, in the ASD participants, both stimuli strongly activate

brain areas. Thus, valence scaling of expression processing in participants with ASD is not observable. Impairments in modulating incoming sensory input have also been widely reported in the literature concerning autism characteristics (Adrien et al., 1992, 1993; Baranek, 1999; Dahlgren & Gillberg, 1989; Kientz & Dunn, 1997; Osterling & Dawson, 1994).

Activation versus deactivation

One hypothesis is that ASD is caused by an increased ratio of E-I ratio throughout the brain (Antoine, 2022; Manyukhina et al., 2022; Milovanovic & Grujicic, 2021; Port et al., 2019; Rubenstein & Merzenich, 2003). Kennedy et al. (2006) have shown that deactivation is absent in cases of ASD during the Stroop test (Stroop, 1935). Our results support the finding of abnormalities in the deactivation of neuronal activity (in the BOLD sense) in ASD. We detected a failure to deactivate during positive valence in happy facial expression, while the brain was shown to overly deactivate during negative valence processing in the right visual cortex.

The participants with ASD may have difficulty automatically determining the salience of expressions; therefore, the valence scaling of brain activity does not manifest similarly to the TD participants. The lack of automatic salience detection may engage additional cognitive processing, including both activation and deactivation. Group differences are not solely due to an absence of activation in both trial types in the ASD group.

Mirror neuron system (MNS)

There was an interesting difference between the groups in part of the superior temporal sulcus (STS / A1) due to a complete lack of deactivation during happy expressions in the ASD group. In addition, Study II also showed an alteration of the baseline regional coherence of the identical brain area. The STS areas are commonly related to the MNS and the processing of biological motion (Caspers et al., 2010; Dapretto et al., 2006; Hadjikhani et al., 2006, 2007). As far as we know, valence-specific deactivation disturbances and RS alterations had not previously been described in the MNS in identical areas.

Another part of the MNS showed altered processing of facial valences. The anterior (IFG) and posterior (POC) part of the difference cluster showed more activation in the ASD group, which is the opposite of results reported by Dapretto et al. (2006), but more in line with the results of Bastiaansen et al. (2011), Martineau

et al. (2010) and the meta-analysis by Philip et al. (2012). The p.op of the IFG has been reported to be consistently active during imitation, action observation, and intention understanding (Iacoboni, 2005; Iacoboni et al., 1999; Johnson-Frey et al., 2003). This difference between Dapretto's results and our later results may be related to dynamic versus still image processing and other aspects of the stimulus. Interestingly, we also found a valence specificity in the IFG abnormality, as there was no difference for fearful stimuli, only for the positive, happy valence.

Valence and primary visual areas

Differences were almost absent for fearful stimuli, showing a slight deactivation increase in the right visual cortex in participants with ASD compared to the TD controls. The ASD group also showed DTI alterations: significantly greater fractional anisotropy in the area containing clusters of the optic radiation and the right inferior frontal-occipital fasciculus (Bode et al., 2011). Transverse diffusion was significantly reduced in the same area, which may relate to abnormal connectivity between the insular salience processing and occipital visual areas (Bode et al., 2011). The differences in deactivation may also be related to the alterations in primary visual processing in ASD shown before. The reasons for the lateralized findings warrant further investigation.

Valence versus limbic structures

In both groups, both expressions activated limbic areas such as the (bilateral) Amy, hippocampi, and thalami, and in addition, medial parts of the lentiform nuclei. However, both putamina showed altered processing in happy facial expressions. It might be that the dynamic information in realistic facial expressions increases limbic activation, so there is no activity difference between the groups, as detected in morphed stimuli of static partially covered faces. On the other hand, more hypothesis-based region-of-interest analyses aimed at specific areas, especially with higher MRI field strengths, might reveal intricate differences found earlier by others at the subcortical level. Cortical face and expression recognition areas, such as the occipitotemporal V2 and V5 regions and the fusiform cortices, were also strongly activated during both groups' interpretation of emotions (Viinikainen et al., 2010). Interestingly, as regards fearful stimuli, differences were almost wholly absent, showing a slight deactivation increase in the right visual cortex in participants with ASD.

6.2 Resting state fMRI alterations in ASD

6.2.1 Static local connectivity alterations based on ReHo analysis

As a first ASD ReHo analysis, Study II could depict several brain areas where local BOLD signal coherence was different in the participants with ASD compared to the TD controls. Decreased or increased ReHo in ASD suggests that neural function in certain regions is less or more synchronized compared to the TD controls. It also seems that activity increase leads to more synchronized function and deactivation to less synchronized, though we are unaware of published research proving this notion. Nonetheless, it is interesting to note that the majority of the ReHo changes are right-sided. GM ReHo changes indicate decreased coherence or synchronization in local, regional RS activity in the right frontal and temporal brain regions in the participants with ASD. There can be many possible explanations for this uneven activity. For example, in the language domain, earlier study results have indicated reduced hemispheric differentiation and varying lateralization in ASD (Kleinhans et al., 2008).

Compared to a meta-analysis of task-based functional neuroimaging studies of ASD (Di Martino et al., 2009), we did not detect significant ReHo differences in ACC. However, estimated from the Talairach coordinates, common areas of altered function in both the task-based meta-analysis and this RS study include the right STG, insula, thalamus, declive, and on the left FFG, the middle occipital gyrus and anterior subcallosal gyrus.

In this study, many local ReHo changes display spatial resemblance to earlier autism studies and might be interlinked. For example, several current psychological theories of autism have implicated atypical sensory processing as a core feature of autism (Iarocci & McDonald, 2006). The decreased coherence in the RS BOLD activity detected in this study in both STS and insular regions may indicate that participants with ASD integrate a multisensory input differently or that the amount of input differs. A primary social cognitive function that recruits the STS is biological motion perception, or identifying a social form from a moving entity and attributing intentions or goals to that entity (Redcay, 2008). In the language domain, the STS is involved in identifying linguistic units from a stream of auditory information and extracting the communicative significance out of these units. Redcay (2008) argued that STS performs a common function for social and speech perception by parsing rapidly changing auditory and visual input and extracting

meaning from this input, and concluded that impairments in its operation might underlie many of the social and language abnormalities seen in autism.

As mentioned earlier, the right insula in participants with ASD showed decreased ReHo. The insular cortex is a complex structure containing areas that subserve visceral sensory, motor, vestibular, and somatosensory functions (Bamiou et al., 2003; Simmons et al., 2008). The right insula is a multimodally responsive area that responds to visual, tactile, and auditory stimuli and has shown significantly greater response to a novel versus a familiar stimulus. It is involved in detecting a temporal mismatch between simple stationary auditory and visual stimuli (Bamiou et al., 2003). The right insular activation has also been linked to perceived intolerance of uncertainty; in other words, it is related to the degree to which uncertainty is processed as aversive (Simmons et al., 2008). Results also indicate that the right claustrum/insula region is differentially activated in association with multisensory integration of conceptually related common objects (Naghavi et al., 2007). In addition, the insula is a part of the inhibition network with anterior and middle cingulate gyri, and subjects with ASD have shown lower levels of synchronization between the inhibition network and the right middle and inferior frontal and right inferior parietal regions (Kana et al., 2007).

The crucial role of the insula in the salience network has been discussed. Sridharan et al. (2008) showed that the right frontoinsular cortex (rFIC) also plays a critical and causal role in switching between the executive functions (EF / CEN) and the DMN. They propose that a transient signal from rFIC engages the brain's attentional, working memory, and higher-order control processes while disengaging other systems that are not task-relevant. Local decreased ReHo in the right insula, and IFG may indicate disruptions to these processes, which participate in balancing one's attention between external events (CEN) and internal reflections (DMN). Considering its diverse connectivity and versatile functions, the insula is one possible key area in the neurobiology of ASD.

The insula also connects with several ventral thalamic nuclei, such as the VPL, which are part of cerebello-thalamo-cortical pathways. The VPL relays somatosensory information to the postcentral area (Mizuno et al., 2006; L.-H. Wang et al., 2022). We found increased ReHo in the VPL of the participants with ASD but decreased ReHo in the postcentral gyrus.

In the ASD group, we found bilateral increased ReHo in cerebellar crus I but decreased in cerebellar lobule VIII. These cerebellar regions were among the activated areas when Dimitrova et al. (2003) evoked nociceptive leg withdrawal reflexes in healthy adults. Discrete right finger movements have been noted to

activate the right lobule HVIII, whereas continuous movements activate bilateral crus I (Habas & Cabanis, 2008). A report from 2003 involving patients performing finger movements demonstrated abnormal variability and scatter of functional maps, thus suggesting early-onset disturbances in the development of cerebellar-thalamo-cortical pathways in autism (Müller et al., 2003). In addition, certain nonmotor functional deficits, as seen in an attention task study by G. Allen and Courchesne (2003), may be related to cerebellar abnormalities in ASD. Indeed, it has become evident that the cerebellum is also involved in higher cognitive functions and plays an important social role (Castellazzi et al., 2014; Guell & Schmahmann, 2020; Hirjak et al., 2016; Marek et al., 2018; Ramnani, 2006; Van Overwalle et al., 2020). The posterior cerebellum supports social mentalizing (e.g., Crus I and II; Van Overwalle et al., 2020). The models of how the cerebellum processes information from the motor cortex might be extended to explain how it could also process information from the prefrontal cortex (Ramnani, 2006). Prefrontal and motor cortices connect via pontine nuclei, respectively, to cerebellar lobules crus I and VIII (among others) and loop back via the thalamus (Ramnani, 2006).

Compared with the controls, the participants with ASD had significantly decreased ReHo in the right IFG and MidFG. The frontal lobe hosts many essential higher functions. Based on macro- and microscopic anatomy, and fMRI studies, it has been proposed that in ASD, connectivity within this region is both excessive and disorganized, which may lead to a desynchronization between the frontal cortex and other systems (Courchesne & Pierce, 2005). Later functional studies have also shown the impact of methodological differences, even considering that the overall impression of functional connectivity changes is heterogeneous (Hull et al., 2017). We did not find any significant ReHo changes in the p.op part of IFG, which is considered an important part of the mirror neuron system, but there were decreases located more anteriorly in the pars orbitalis and p.tr. Furthermore, also insula is related to this system, acting as an interface between the frontal component of the mirror neuron system and the limbic system (Dapretto et al., 2006).

One of the clinical findings in ASD is the lack of apparent recognition of faces. The fMRI studies of face recognition have shown weaker fusiform activity in the subjects with ASD, but dysfunction of the modulating areas has also been suspected (Hughes, 2007). We detected increased ReHo in the ASD group, including part of the left FFG. Task fMRI may have advantages over RS fMRI (see also M. Liu et al., 2021) as DP participants with face recognition impairment and strong autism traits (high AQ) exhibit deficient face emotion recognition and decreased pSTS

selectivity in task fMRI, while RS fMRI showed only similarly reduced face-selective network connectivity in both DP groups compared with controls (Fry et al., 2022).

Epilepsy and ASD comorbidity range between 5 and 46%, but its temporal relationship, causal mechanisms, and interplay with an intellectual disability still lack concluding evidence (Milovanovic & Grujicic, 2021; Santarone et al., 2023). One interesting aspect related to right temporal lobe ReHo differences has emerged from EEG research. In a retrospective review, Chez et al. (2006) showed that 60.7% of 889 ASD patients displayed abnormal EEG epileptiform activity in sleep with no difference based on clinical regression. The most frequent sites of epileptiform abnormalities were localized over the right temporal region, where we found decreased ReHo. It can be speculated that in some individuals, this decreased local coherence in the right temporal lobe spontaneous activity (compared to the TD population) could lower the threshold of epileptiform activity or reflect this kind of activity. Because discharges are usually regarded as focal, and the seizures require some spread from this focus, one ASD feature may be the deficiency of cortico-cortical fibers to account for this presumed lack of spread (Hughes, 2007).

In another retrospective review of 292 routine polysomnographic EEG tracings of preschool children (age < 6 years) with ASD, the background activity during wakefulness and sleep, the presence and the characteristics (focal or diffuse) of the slow-waves abnormalities and the interictal epileptiform discharges were evaluated (Santarone et al., 2023). The EEG recordings were abnormal in 78.0% of cases, particularly during sleep. Paroxysmal slowing and epileptiform abnormalities were found in 28.4% of the subjects, confirming the high percentage of abnormal polysomnographic EEG recordings in children with ASD (Santarone et al., 2023). EEG microstate alterations also in awake pediatric ASD participants have been shown, suggesting specific alterations in synchronized activities of large-scale networks, namely the DMN and salience networks (Takarae et al., 2022).

Kennedy and Courchesne (2008) found specific abnormalities in the mPFC and left AG using resting FC. Though the ReHo method is more sensitive to activity within the task-negative network than the task-positive network (Long et al., 2008), we could not detect any significant differences in these areas between the ASD group and the TD controls. As noted earlier in this discussion, we found no evidence of Reho or local connectivity abnormalities in the ACC. However, the ReHo method cannot identify such connectivity disruption to more distant networks, as Kennedy and Courchesne (2008) found. This fact limits the comparison of our study to current fMRI evidence suggesting that autism is a

distributed systemwide brain disorder, manifesting a mixed FC pattern of under- and overconnectivity (Harikumar et al., 2021; Hull et al., 2017), in contrast with for example ADHD mostly showing stronger FC (Harikumar et al., 2021).

While there is doubt about the validity of the BOLD signal in WM (Logothetis & Wandell, 2004), studies have shown activation of the CC (Mosier & Bereznaya, 2001; Tettamanti et al., 2002). The WM and GM can be segmented on their temporal signal features (Mezer et al., 2009). Similarly, ReHo reflects the temporal homogeneity of the regional BOLD signal rather than its intensity. In an ABIDE subsample (88 ASD, 87 TD) study, the ASD group showed significantly decreased ReHo in the left superior corona radiata and left posterior limb of the internal capsule and reduced ReHo in the left anterior corona radiata with a trend level of significance (L. Ma et al., 2022). Significantly weaker structural-functional coupling was observed in the left superior corona radiata and left posterior limb of the internal capsule in the ASD participants. These findings suggested the possibility of using WM ReHo to investigate the pathophysiological mechanisms of ASD (L. Ma et al., 2022). Deshpande et al. (2009) compared ReHo, and another measure of local coherence called integrated local correlation (ILC) by examining their ability to discriminate between GM and WM in the RS data. ILC was more sensitive, and it would be interesting to compare these two techniques on this data.

6.2.2 Time-varying connectivity alterations based on CAP analysis

As individual CAPs reflect the continuous flow of time-varying co-activations within functional brain networks (X. Liu et al., 2018), in Study III, we wanted to find out whether the effects of restricted, narrow focusing of attention to limited sensory information sources typical to ASD can be detected in the clustering of CAPs. To determine possible CAP differences between adolescents with ASD and TD controls, we compared the distribution of the ASD and TD groups' volumes in CAPs as well as their voxel-wise means. This enabled us to determine the differences between the (de)activation patterns of the two groups. The number of CAPs in earlier studies ranges from 4 (X. Li et al., 2015) to 30 (X. Liu et al., 2013), and we addressed this range accordingly.

Our Study III provides complementary information and an alternative perspective to FC analysis by gathering non-sequentially brief instances of similar fMRI brain volumes into larger CAP clusters. This method may be especially beneficial before group comparisons in RS studies, in which no external synchronization is provided by tasks or stimuli. We found the DMN+CAPs and

DMN-CAPs (61% and 39% of the fMRI volumes, respectively) to be spatially similar in the TD and ASD groups as the clustering algorithm gathered volumes to each CAP from both groups without significant group-wise differences in time spent in each CAP.

While the CAP clustering, comparisons, and statistics between the groups were calculated voxel-wise, we then used GICA-derived RSNs as masks forming a simple 14-parcellation brain atlas. This provided some sort of area averaging filters for visualization and aided in interpreting differing RSN activity levels inside the CAPs. We found focused between-group alterations of internal activity levels among many RSNs, including the following (In Figures 14–15 activated RSNs red and deactivated RSNs blue; Figures 12–13 are also of interest):

1) ASD-related activations during the DMN-CAPs occurred considerably in the DMN and during DMN+CAPs in other RSNs.

2) The ASD group showed visual network overactivation during the DMN-CAPs, simultaneous with the overactivation of either the DAN or DMN.

3) ASD-related FPC activations were incoherent and showed hemispherical shifts.

4) The ASD participants may have higher baseline activation levels in the auditory, DMN and language RS networks since these showed less deactivation (compared to the TD) in CAPs with these RSNs deactivated (= blue).

The TD group-related alterations can be assessed similarly: in general, the TD group showed greater activation in the task-positive RSNs during the DMN-CAPs and in the positively activated DMN during the DMN+CAPs than the ASD group. During the DMN-CAPs, auditory activation reached higher levels in the TD group. In addition, DAN activation was also more evenly related to other sensory (auditory, somatosensory), salience, and VAN networks, even though DAN in our study included extrastriate visual areas. FPC overactivation was consistently asymmetric in the TD group: predominantly left-sided during the DMN-CAPs and right-sided during the DMN+CAPs.

Comparing the group-related changes in Figures 14 and 15 shows that the ASD participants demonstrated overactivation of medial visual areas during the DMN-CAPs. Simultaneous overactivation with a visual network was detected among the DAN and/or DMN. This tendency might have been related to increased reliance on posterior brain areas in ASD when mediating visuospatial tasks (Kana et al., 2013). In an MEG study, the ASD group presented early enhanced activity in the occipital region, suggesting that impaired face processing in ASD might be sustained by atypical responses in primary visual areas (Kovarski et al., 2019). Anecdotal

experiences from individuals with ASD report overwhelming sensations of visual details in everyday environments which they cannot seem to get past. Abnormal simultaneous overactivation of the visual networks with the DAN and the DMNs detected in our study could reflect such a propensity. In a general deactivation CAP 06-06, the ASD group showed a considerably reduced deactivation pattern in nearly all (12/14) RSNs, maybe reflecting a different E-I ratio.

People on the autism spectrum experience trouble filtering torrents of information, which hijacks their concentration, and this may explain why prolonged simultaneous multisensory events cause fatigue sooner for people with ASD. On the other hand, it could be speculated that neurotypical people may be unable to concentrate with similar intensity or for equal periods under normal levels of stimuli. It would be interesting to study further whether the neurobiological potential for concentration in ASD could be reflected in task-related DMN activation. Such a study could utilize a validated attention ability paradigm (e.g., Fortenbaugh et al., 2018) to study attentional stability and RSNs in ASD.

Concentration, mindfulness, and task-unrelated mind-wandering are examples of alternating states of mind that may be better captured in dynamical temporal analysis than static methods. The more mindful youths transitioned more between brain states, spent less time in a particular connectivity state, and showed a state-specific reduction in connectivity between salience and central executive (i.e., frontoparietal cognitive control, FPC) networks (Marusak et al., 2018).

From the RS networks, our study detected the strongest salience and FPC mean activations during DMN+CAPs (Fig. 10; similar colors in salience/VAN-A and FPC L/R). In the TD group, we found salience and FPC association during the DMN-CAPs, but in contrast, in the ASD group, only during two DMN+CAPs (Figures 12–15).

Similarly, in the ASD group, we found interesting reversals in associations between DMN-D, the other parts of the DMN, and FPC. DMN-D associations with other DMN components were more frequent in the TD group during DMN+CAPs, but again, in contrast to the ASD group where it was more frequent during DMN-CAPs. In participants without neuropsychiatric disorders, increased connectivity during task performance has been found between the precuneus (in our study part of the DMN-D) and the FPC L, whereas rest increased connectivity between the precuneus and other parts of the DMN (Utevsky et al., 2014).

Parallel top-down volitional attention is influenced by the DAN (Vossel et al., 2014; Yamasaki et al., 2017). The dorsal frontoparietal areas can causally modulate visual areas' activity (Vossel et al., 2014). One hypothetical explanation for our

study results could be that this modulating effect may be more substantial among ASD individuals: for ASD, during the DMN-CAPs associated with DAN RSN activation, there was a repeated simultaneous overactivation of the DAN and the visual medial network (Fig. 15: CAPs 24-21, 13-11, 11-01, 10-01, 04-01, and 02-01; also Supporting Information S1 of Study III: Figures S2a–i).

However, we detected visual overactivation during many DMN-CAPs, and the CAP method cannot infer causality. Yamasaki et al. (2017) reviewed studies using visual evoked potentials and the DTI MRI of visual and attention networks in ASD. They found that (1) enhanced and impaired processing co-exist within the lower visual area (V1), (2) that local information integration from lower visual areas (V1) is impaired in higher-level visual areas after V4 and V5/MT, and (3) that the DAN is impaired while the VAN is intact in ASD. The VAN contains key nodes in the temporoparietal junction and ventral frontal cortices related to automatically produced and quicker bottom-up attention (Yamasaki et al., 2017). Despite the results of Yamasaki et al. (2017), some fMRI studies have found ASD-related differences in the VAN as well (Bernas et al., 2018; Farrant & Uddin, 2016; Fitzgerald et al., 2015).

Moreover, a study by Feczko et al. (2018) hints that some ASD subgroups have altered visual processing, attention mechanisms, or both. In addition to overwhelming sensory experiences, altered connectivity of visual and attention networks may contribute to impaired social communication in ASD. Early disordered FC involving the visual network may engender later disruptions in higher order behaviors. McKinnon et al. (2019) showed that aberrant functional connectivity between the visual, control, DMN, DAN, and subcortical networks are also associated with certain restricted and repetitive behaviors among children with ASD at 12 and 24 months of age. Also, Bi et al. (2018), Fitzgerald et al. (2015), and Gabrielsen et al. (2018) have found abnormal attention mechanisms in ASD. While ASD may offer advantages in various visual-attentional tasks, the predisposition to intense attentional focus may come at the cost of resistance to task disengagement and other behavioral symptoms such as overfocusing and restricted interests (Kaldy et al., 2016).

In the TD group, highlighted simultaneous DAN and visual network overactivation were detected only during task-positive CAP 06-03 and DMN-positive CAP 03-03. The former, unlike the CAPs mentioned in the previous paragraph, exhibits mainly motor and somatosensory activation. In addition to the DAN and visual medial networks, TD group-related overactivation is more comprehensive and detected among the auditory, salience, VAN, and FPC networks.

Despite hearing protection, noisy MRI environments may cause more auditory than somatosensory input in a supine patient lying still. In healthy participants, connectivity reductions related to MRI coil noise have been detected in both the right auditory and sensory-motor networks (Pellegrino et al., 2022). Tactile and auditory hypersensitivity among children raises the risk of ASD diagnosis 34- and 22-fold, respectively (Jussila et al., 2019). Our results suggest higher auditory network baseline activity during deactivations in ASD and that somatosensory activations are less unambiguous.

In our study, the ASD participants showed rightward shifted FPC activation for the DMN-CAPs and leftward for the DMN+CAPs (Figures 12–15). ASD-related functional brain asymmetry has been detected during RS by, for example, Cardinale et al. (2013) and Subbaraju et al. (2018), who have shown rightward asymmetry shifts of functional networks and atypical hemispherical lateralization, respectively. Diffusion imaging has found inversion or diminishing of typical left-right asymmetry among ASD individuals (Carper et al., 2016; Conti et al., 2016; Wei et al., 2018).

Earlier evidence of reduced functional integration of the DMN, especially weaker coherence of connectivity between the posterior and anterior subsystems (Joshi et al., 2017; Starck et al., 2013), may be mirrored in our study as higher baseline activity during the DMN-CAPs, especially in the dorsal and ventral components of the DMN. Still, the inferences between FC and CAP analysis remain unclear.

6.3 Comparing task and resting state results

The brain network changes were not identical during the task and RSs. The greatest areal changes during the happy facial expression viewing (Table 1) were elicited, respectively, in the Salience, VAN, Auditory, Motor, Somatosensory, FPC, DMN, and Language networks. Surprisingly, the smallest difference areas were detected in the DAN and Visual areas, which in CAP RS analysis showed altered activations. Fearful facial expression, however, deactivated more Visual Med network in ASD. As DMN-CAPs showed heightened Visual Med activation, it would have been easier to explain less ASD deactivation instead of more, or maybe the deactivation depicts the greater overall delta difference in ASD. It would be interesting to run CAP analysis for the facial expression task and inspect ICN activations at shorter periods. Most differences between happy versus fear valence (Table 3) were found in the Auditory/VAN-P and Motor networks.

Increased ReHo (Table 4) highlighted, respectively, the DAN, Visual Med, Motor, Salience/VAN-A, FPC L, and Auditory/VAN-P networks. Decreased ReHo highlighted, respectively, the Auditory/VAN-P, FPC R, DMN/Language, Visual Lat, Salience/VAN-A, and Motor networks.

6.4 Reliability and validity

6.4.1 Strengths of the study

To limit computing time, especially in dynamic FC analysis, voxel-wise fMRI data is usually summed into larger mean time series parcels or ROIs. We used accurate voxel-wise data despite the increased computer memory use and analysis time, especially with the FSL randomise tool.

6.4.2 Limitations of the study and future directions

All of the studies

The data SNR and resolution would have been higher at 3.0T MRI, but we only had access to a lower 1.5T field strength device. We lacked the equipment to record and model optimally physiological parameters such as heart and respiratory rate and their impact on results. We did not have a video-based real-time eye-tracking system that would have shown the gaze position and verified if the eyes were open or closed. This information would have been valuable since mere eye movements potentially cause complex brain activations. Also, ASD individuals may look less at faces and eyes (Schultz, 2005) as their social attention is reduced and has different temporal dynamics (Del Bianco et al., 2021).

The number of participants was different between the task and RS studies. The fMRI sequence parameters differed between the face expression viewing task and the resting state. As the analysis period was long, the preprocessing methods between studies differed.

We lacked the authorization to correlate the ASD assessment measures ADOS and ADIR with the fMRI findings. Due to the recruitment process, not all ASD participants had all the same measures, such as ASSQ or SRS, in addition to ADOS and ADIR. Future studies could benefit from correlating such measures with fMRI findings to assess different dimensions of ASD.

Reproducible brain-wide association studies may require thousands of participants because, in smaller studies, the results may be more inflated and unreliable than previously thought (Marek et al., 2022). However, Marek et al. (2022) note: ”Neuroimaging-only studies are typically adequately powered at small sample sizes. For example, central tendencies of human functional brain organization among groups can be accurately represented by averaging within small samples (that is, n = 25). Precise individual-specific RSFC and fMRI activation brain maps can be generated by repeatedly sampling the same individual”. The estimates for the amount of data needed for reliable characterization of individual-specific RSFC measures vary, depending on the specific measure (Gordon et al., 2017; White et al., 2014).

Study I

The first limitation of the study was that the participants simply watched the emotional stimuli passively without having to respond. This was, however, deliberate since recognition of facial expressions was hypothesized to be reduced in ASD, and we wanted to reduce any potential anxiety related to an inability to recognize expressions. Including additional observational tasks related to attentional processes might have strengthened the interpretation of the current findings. We found that the participants paid attention in the free viewing task due to good stimulus-related activation of known areas connected to facial emotion and deactivation in attention-related default mode areas in the ACC. In addition, we found that the same participants' performance in the following N-back task was still very accurate, with marginal differences between the groups (Rahko et al., 2016).

The second limitation was that we did not use a dynamic mosaic mask because as a continuous video it was visually disturbing for the participants. Therefore, we used stable mosaic images to reduce the participants’ eye blinking and gaze wandering in the relatively challenging fMRI environment. Possibly there would have been better stimulus alternatives (Stojanoski & Cusack, 2014). We did not strive for separation of DFE areas per se but rather for differences between groups highlighted by stronger activation due to dynamic facial stimuli. A set of static facial expression images would have been a useful control since contrasting dynamic versus static images would have given more information on how much the dynamic nature of the expressions contributes to the results. The stimuli employed have been optimized to be as natural and recognizable as possible (for further information, see Kätsyri, 2006).

Study II

The traditional slow repetition time RS imaging leads to signal aliasing and quantifying the source of ReHo changes as originating from VLF or cardiorespiratory differences is compromised (Huotari et al., 2019). Also, the motion could have been handled better (Ciric et al., 2017; Power et al., 2015), and the Talairach conversion was unnecessary.

Study III

RS studies have found it challenging to show unambiguous brain FC changes in ASD (Hull et al., 2017). Even though local (e.g., ReHo) and more distant changes of FC have been shown (Hull et al., 2017; Jao Keehn et al., 2018; Nair et al., 2018), legitimate concern has arisen that motion during RS examinations might at least partly explain the detected under- and/or overconnectivity (Jo et al., 2013; Power et al., 2014). Comparisons suggest that censoring and ICA-AROMA perform well across most preprocessing quality benchmarks (Parkes et al., 2018). Whereas earlier dual-regression ICA and FC analysis has revealed only hypo-/underconnectivity within the DMN sub-networks of our study participants with ASD (Starck et al., 2013), we found significant differences in many CAPs. When similarly activated brain BOLD fMRI volumes are accumulated into CAPs, between-group comparisons may become more powerful than, for example, sliding window methods, in which each window of sequential volumes includes more heterogeneous brain activation patterns. When discussing results, one should remember that hierarchical clusters are nested, and thus volumes accumulate as we move up the hierarchy into lower-numbered cluster levels. Depending on the different spatial (de)activation signal amplitudes of the clusters (CAPs) combined and the difference in the brain areas' activation behavior between the groups, some of the spatial between-group differences may fade, and others may increase from one hierarchical level to another.

It should be remembered that hierarchical clustering is an exploratory method and imposes a hierarchical structure regardless of whether one exists in the data (Friedman et al., 2001). Accordingly, the results should be interpreted cautiously. However, based on previous research about alternating rest and task states of brain function and our results, this method can yield meaningful complementary information on the "natural" occurrence of CAPs and their relations to each other during RS-fMRI. The coarse division in our data showed that 61% of the volumes

had default mode-positive RSN features. RS data certainly also include varying epochs with genuine task-positive ICN activations, as the MRI environment is noisy and disruptive (Stogiannos et al., 2022), especially to young individuals, and we imaged RS with the participants' eyes open. Empirical evidence suggests that eyes-open brain states are better controlled than eyes-closed states (Patriat et al., 2013; Zou et al., 2015), but as stated earlier, eye status affects local connectivity: the eyes-open state highlights overconnectivity in posterior, visual regions and underconnectivity in the cingulate gyrus (Nair et al., 2018).

We did not compare RS with task data, and the relationship between the CAPs of the rest and task data should be addressed in the future to determine the proportions of DMN-positive and task-positive activity in combined data and the various settings: in other words we should determine whether specific CAPs and their between-group differences persist during tasks and how they are modified. In this context, there is evidence that functional hierarchies in the pediatric brain are stable and similar during rest and task (Harrewijn et al., 2020). It would have been interesting to study separately whether hierarchical RSN groupings differ in ASD and TD groups.

As stated earlier, due to RSN z-score averaging in the Fig. 10 heatmap, the voxel-wise nuances of CAPs are lost, and a few seemingly similar CAPs co-exist on both the DMN-negative (DMN-CAPs) and DMN-positive (DMN+CAPs) sides of the clustering results. In addition to averaging, the weaknesses of the chosen method and arbitrary low ICA model order may predispose to this phenomenon. The clustering procedure itself is, of course, unaware of this interpretive naming convention and simplification aimed to facilitate the understanding of complex network interactions.

There are several linkage methods in hierarchical clustering. We chose Ward's method as it shares a common principle with k-means, providing a basis for current research and comparison to earlier research. We found high Pearson correlation coefficients (as implemented in the FSL fslcc tool) with the CAPs from X. Liu et al. (2013) (results not shown), though their results were acquired after global mean removal. Using GSR could eliminate artifacts even more efficiently than censoring and ICA-AROMA alone (Byrge & Kennedy, 2018; Ciric et al., 2017; Murphy & Fox, 2017; Power et al., 2015). Possible anticorrelations in the CAPs might not be as problematic as with FC measures, as signal amplitudes are compared. Our educated guess is that using GSR would reduce the portion of CAPs that exhibit whole brain-wide activation or deactivation. Unfortunately, censoring reduces degrees of freedom and may also remove the signal of interest from the data. For

example, Syed et al. (2017) found that although the DMN provided the highest discriminability between the control and ASD groups, the motor network regions with the midcingulate cortex and temporal-parietal junction were also discriminatory. Moreover, the choice of clustering distance measure (cosine, Euclidean, Pearson correlation, etc.) may potentially increase or decrease GSR-like effects.

Besides distance and linkage adjustments, combining other statistical procedures, such as permutational methods to hierarchical clustering, could achieve results closer to the ground truth. Based on our study, efforts to refine volume-wise methods are worth pursuing. Hierarchical and k-means are only two standard, older clustering methods, and more efficient algorithms that can utilize fMRI-specific data features probably exist. For example, random forest methods could be used volume-wise instead of measures from temporally stationary FC (Feczko et al., 2018; Fernández-Delgado et al., 2014). Though FC and ICA RS metrics are not substantially affected by different TRs, faster imaging methods such as MREG with 10-20 Hz temporal resolution show "neural avalanches", which in traditional 0.5–1 Hz fMRI temporal resolutions are only seen as aliased images and could enable the study of higher cluster numbers and shorter CAPs (Huotari et al., 2019; Rajna et al., 2015), though the inherently slow HRF may act as a limiting bottleneck (Bolton et al., 2020). Faster imaging and dynamic lag analysis (Kotila et al., 2020; Raatikainen et al., 2020) or causality analysis methods (Bernas et al., 2018; Bielczyk et al., 2019; Borchers et al., 2012; H. Chen et al., 2016; Deshpande & Hu, 2012; Kaminski et al., 2016; L. Li et al., 2020) may shed light on interactions between the attention, visual and other brain networks. MREG fMRI coupled with simultaneous EEG analysis (Ding et al., 2022; Hiltunen et al., 2014; J. Li et al., 2019; Ridley et al., 2017) could clarify the relationship between the neural avalanches and the brain's electrical activity in the future.

As each volume is a time point in the imaging time series and is assigned with cluster membership, this method could map the changes at the individual level. The current study could be extended using a network or Markov chain analysis to determine whether there are repetitive sequences or states in the occurrence of the CAPs (J. E. Chen et al., 2015; X. Liu et al., 2013; Zhuang et al., 2018), as some ASD studies indicate (Kupis et al., 2020; Malaia et al., 2016; J. Zhang et al., 2016).

Even if independent RSNs seemed to activate normally, CAP analysis might reveal aberrant in-between network interactions and their timing. FC analysis could be supplemented by CAP analysis. It may find CAPs that exhibit the most significant differences between the voxels with aberrant connectivity, pinpoint the

moments at which the differences lie, and detect simultaneous patterns in other intrinsic networks and their activity levels. This knowledge may help find new approaches to ASD rehabilitation: for example, using customized stimuli targeting brain network combinations that have been found to have abnormal interactions or inappropriate timing in interaction situations.

Preprocessing methods changed during the long study period and affected the results. In Study III, noise reduction techniques were more advanced, but the choice of censoring motion may have reduced the visibility of motor network activity. It is known that ASD also affects motor control (J. L. Cook et al., 2013). Preprocessing methods evolve continuously. For example, instead of earlier co-existence of volume- and surface-based registration and analysis methods, there are strong exhortations to adopt the latter approach for more reliable results (Coalson et al., 2018).

7 Conclusions

7.1 Main findings

The main finding of Study I was that in the ASD group, the passive valence scaling of dynamic facial expressions was different compared to the TD group. Positive valence induces both lower deactivation and abnormally strong activation in ASD. Negative valence increased deactivation in the right visual areas in participants with ASD compared to TD controls. Participants with ASD may have difficulty in an unconscious, passive processing of valence-related dynamic facial information in brain areas involved in mirroring emotions and determining the salience of expressions. As the valence scaling and the evaluation of salience fails, the participants with ASD cannot use dynamic facial information as an automated modulator of brain activity during social interaction.

The main finding of Study II was that participants with ASD have right dominant ReHo alterations of RS brain activity in areas known to present altered functionality in the stimulus or task-based fMRI studies compared to the TD group. The decreased coherence or synchronization in local, regional RS BOLD activity detected in participants with ASD in both the right STS and insular regions may reflect atypical sensory processing and problems integrating multisensory input. Similarly, decreased ReHo in the right insula and IFG may be related to attention abnormalities, as rFIC has been shown to play a critical role in switching between internally and externally oriented brain networks. The significant differences in the right thalamus and bilateral cerebellum may be related to abnormal or relatively overactive cerebello-thalamo-cortical pathways or the cerebellum's role in nonmotor functional deficits. Our results demonstrated potential in utilizing the ReHo method in fMRI analyses of ASD.

The main finding of Study III was that while we did not find ASD-specific CAPs, the CAPs showed focused alterations of internal activity levels among many RSNs. ASD-related activations during the DMN-CAPs considerably occurred in the DMN, and during DMN+CAPs, in other RSNs. The ASD group showed visual network overactivation during the DMN-CAPs, simultaneously with the overactivation of either the DAN or DMN. ASD participants may have higher baseline activation levels in the auditory, DMN, and language RS networks since these showed less deactivation compared to the TD participants in CAPs with these

RSNs deactivated. ASD-related FPC activations were incoherent and showed hemispherical shifts.

7.2 Implications for research

The studies utilized three different and complementary methods to characterize and pioneeringly compare BOLD brain function between ASD and TD populations. All three studies highlighted exciting differences between the groups. Due to its dynamic network-based approach, Study III provided the most detailed information. Because myriad network combinations are possible and the signal amplitude in each network varies greatly, developing a method that could satisfyingly capture the whole dynamics of brain networks is a never-ending challenge. Based on our study experiences, we encourage the development of volume-wise approaches as an option to further characterize the TVFC changes in brain networks.

7.3 Implications for clinical practice

As a result of ongoing study efforts, earlier and more accurate imaging diagnostics may help clarify the mechanisms and etiology of ASD and guide the targeting of possible interventions. Concurrently, it is possible to identify behavioral and neurological biomarkers that indicate an increased likelihood of ASD as early as six months of age before the consolidation of autistic characteristics into a clinical diagnosis (Grzadzinski et al., 2021). A preemptive 10-session infant-parent social communication intervention (iBASIS-VIPP) with a trained therapist was able to reduce ASD diagnostic behaviors when used at the time that atypical development first emerges during infancy (Whitehouse et al., 2021). Infants receiving the intervention had lower odds of meeting the diagnostic criteria of ASD, with a number needed to treat of 7. Also, physical activity interventions improve executive function among participants with neurodevelopmental disorders, but in practice, behavioral measures are used to detect the impact (Sung et al., 2022), rarely fMRI (Chaddock-Heyman et al., 2013). Transcranial magnetic stimulation (TMS), usually over the dorsolateral prefrontal cortex (DLPC), has been used to modulate the gamma band activity with the idea of improving cognitive functions and attendant social behaviors (Casanova et al., 2020). Some studies have addressed motor areas (SMA, M1), others frontal or temporal areas (Casanova et al., 2020). To our knowledge, there do not exist therapies targeting certain ICNs or their interactions in ASD in the neuroimaging sense, but the TMS studies above indicate

that it could be possible. In ADHD, tailored TMS and its effect on the key network measures modifying the brain dynamics have been simulated successfully (Iravani et al., 2021). Lesion network mapping (LNM), a technique used to aid localization by mapping lesion-induced symptoms to brain circuits rather than individual brain regions, has been applied to more than 40 different symptoms or symptom complexes (Joutsa, Corp, et al., 2022). Lesion locations were combined with an atlas of human brain connections (the human connectome) to map heterogeneous lesion locations causing the same symptom to a common brain circuit. This approach has lent insight into symptoms that have been difficult to localize, for example tobacco or alcohol addictions and identified testable treatment targets for circuit-based and symptom-based neuromodulation (Joutsa, Corp, et al., 2022; Joutsa, Moussawi, et al., 2022).

Environmental risk factors can be mitigated but never completely evaded, nor can the effect of complex genetics. As even prenatal children can be studied, growing evidence supports the idea that ASD is prenatally wired (Bonnet-Brilhault et al., 2018; Caly et al., 2021; Grzadzinski et al., 2021; Panisi et al., 2021). Once an aberrant trajectory in brain development commences, it may be impossible to stop or reverse. In this context, patient organizations have reminded that instead of emphasizing recovery or cures, the focus should always be kept on accommodating the needs of autistic people and helping them learn new skills. For example, focused interests can be utilized as an educational tool for positive engagement and interaction. Social skills training may be helpful, but caution in concluding the efficacy of the current training methods and continued efforts to improve them are needed, with simultaneous training for neurotypical peers to increase knowledge of ASD and decrease stigma (Bottema-Beutel et al., 2018; Choque Olsson et al., 2017). And while an autistic person's different style of social interaction may present an impediment on one's way to professional life, supportive and accommodative work environments can also convert ASD traits into strengths (Des Roches Rosa, 2016; Diener et al., 2020; Kaldy et al., 2016; Sipola, 2020; Verasai, 2017; Wong et al., 2018).

References

Abou-Elseoud, A., Littow, H., Remes, J., Starck, T., Nikkinen, J., Nissilä, J., Timonen, M., Tervonen, O., & Kiviniemi, V. (2011). Group-ICA model order highlights patterns of functional brain connectivity. *Frontiers in Systems Neuroscience*, *5*. https://doi.org/bkd34h

Abou-Elseoud, A., Starck, T., Remes, J., Nikkinen, J., Tervonen, O., & Kiviniemi, V. (2010). The effect of model order selection in group PICA. *Human Brain Mapping*, *31*(8), 1207–1216. https://doi.org/10.1002/hbm.20929

Adolphs, R. (2002). Recognizing emotion from facial expressions: Psychological and neurological mechanisms. *Behavioral and Cognitive Neuroscience Reviews*, *1*(1), 21–62. https://doi.org/10.1177/1534582302001001003

Adrien, J. L., Lenoir, P., Martineau, J., Perrot, A., Hameury, L., Larmande, C., & Sauvage, D. (1993). Blind ratings of early symptoms of autism based upon family home movies. *Journal of the American Academy of Child & Adolescent Psychiatry*, *32*(3), 617–626. https://doi.org/bf23nb

Adrien, J. L., Perrot, A., Sauvage, D., Leddet, I., Larmande, C., Hameury, L., & Barthelemy, C. (1992). Early symptoms in autism from family home movies. Evaluation and comparison between 1st and 2nd year of life using I.B.S.E. scale. *Acta Paedopsychiatrica*, *55*(2), 71–75.

Agelink van Rentergem, J. A., Deserno, M. K., & Geurts, H. M. (2021). Validation strategies for subtypes in psychiatry: A systematic review of research on autism spectrum disorder. *Clinical Psychology Review*, *87*, 102033. https://doi.org/gj9pwd

Ali, M. T., ElNakieb, Y., Elnakib, A., Shalaby, A., Mahmoud, A., Ghazal, M., Yousaf, J., Abu Khalifeh, H., Casanova, M., Barnes, G., & El-Baz, A. (2022). The role of structure MRI in diagnosing autism. *Diagnostics*, *12*(1), 165. https://doi.org/kdw2

Allen, E. A., Damaraju, E., Plis, S. M., Erhardt, E. B., Eichele, T., & Calhoun, V. D. (2014). Tracking whole-brain connectivity dynamics in the resting state. *Cerebral Cortex*, *24*(3), 663–676. https://doi.org/10.1093/cercor/bhs352

Allen, E. J., St-Yves, G., Wu, Y., Breedlove, J. L., Prince, J. S., Dowdle, L. T., Nau, M., Caron, B., Pestilli, F., Charest, I., Hutchinson, J. B., Naselaris, T., & Kay, K. (2022). A massive 7T fMRI dataset to bridge cognitive neuroscience and artificial intelligence. *Nature Neuroscience*, *25*(1), 116–126. https://doi.org/gnspnw

Allen, G., & Courchesne, E. (2003). Differential effects of developmental cerebellar abnormality on cognitive and motor functions in the cerebellum: An fMRI study of autism. *American Journal of Psychiatry*, *160*(2), 262–273. https://doi.org/cndxbw

Altschuler, M. R., Trevisan, D. A., Wolf, J. M., Naples, A. J., Foss-Feig, J. H., Srihari, V. H., & McPartland, J. C. (2021). Face perception predicts affective theory of mind in autism spectrum disorder but not schizophrenia or typical development. *Journal of Abnormal Psychology*, *130*(4), 413–422. https://doi.org/10.1037/abn0000621

Amaro, E., & Barker, G. J. (2006). Study design in fMRI: Basic principles. *Brain and Cognition*, *60*(3), 220–232. https://doi.org/10.1016/j.bandc.2005.11.009

American Psychiatric Association. (2000). *Diagnostic and statistical manual of mental disorders (4th ed., text revision)*. https://doi.org/j9t8

American Psychiatric Association. (2013). *Diagnostic and statistical manual of mental disorders (5th ed.)*. https://doi.org/brfw

Amico, E., Gomez, F., Di Perri, C., Vanhaudenhuyse, A., Lesenfants, D., Boveroux, P., Bonhomme, V., Brichant, J.-F., Marinazzo, D., & Laureys, S. (2014). Posterior cingulate cortex-related co-activation patterns: A resting state fMRI study in propofol-induced loss of consciousness. *PLoS ONE*, *9*(6), e100012. https://doi.org/gfvrxj

Anderson, A. N., King, J. B., & Anderson, J. S. (2019). Neuroimaging in psychiatry and neurodevelopment: Why the emperor has no clothes. *The British Journal of Radiology*, *92*(1101), 20180910. https://doi.org/gp93w6

Anderson, M. J., & Robinson, J. (2001). Permutation Tests for Linear Models. *Australian & New Zealand Journal of Statistics*, *43*(1), 75. https://doi.org/10.1111/1467-842X.00156

Andersson, J., Jenkinson, M., & Smith, S. (2007). *Non-Linear registration aka spatial normalisation FMRIB technical report TR07JA2.* Https://Www.Fmrib.Ox.Ac.Uk/Datasets/Techrep/.

Antoine, M. W. (2022). Paradoxical Hyperexcitability in Disorders of Neurodevelopment. *Frontiers in Molecular Neuroscience*, *15*, 826679. https://doi.org/j9t9

Aurich, N. K., Alves Filho, J. O., Marques da Silva, A. M., & Franco, A. R. (2015). Evaluating the reliability of different preprocessing steps to estimate graph theoretical measures in resting state fMRI data. *Frontiers in Neuroscience*, *9*. https://doi.org/10.3389/fnins.2015.00048

Bai, D., Yip, B. H. K., Windham, G. C., Sourander, A., Francis, R., Yoffe, R., Glasson, E., Mahjani, B., Suominen, A., Leonard, H., Gissler, M., Buxbaum, J. D., Wong, K., Schendel, D., Kodesh, A., Breshnahan, M., Levine, S. Z., Parner, E. T., Hansen, S. N., … Sandin, S. (2019). Association of genetic and environmental factors with autism in a 5-country cohort. *JAMA Psychiatry*, *76*(10), 1035–1043. https://doi.org/gf7t22

Bamiou, D.-E., Musiek, F. E., & Luxon, L. M. (2003). The insula (Island of Reil) and its role in auditory processing: Literature review. *Brain Research Reviews*, *42*(2), 143–154. https://doi.org/10.1016/S0165-0173(03)00172-3

Baranek, G. T. (1999). Autism during infancy: A retrospective video analysis of sensory-motor and social behaviors at 9–12 months of age. *Journal of Autism and Developmental Disorders*, *29*(3), 213–224. https://doi.org/czntps

Baron-Cohen, S., & Wheelwright, S. (2001). The “Reading the Mind in the Eyes” test revised version: A study with normal adults, and adults with Asperger syndrome or high-functioning autism. *Journal of Child Psychology & Psychiatry & Allied Disciplines*, *42*(2), 241. https://doi.org/bng8xf

Baron-Cohen, S., Wheelwright, S., Skinner, R., Martin, J., & Clubley, E. (2001). The Autism-Spectrum Quotient (AQ): Evidence from Asperger syndrome/high-functioning autism, males and females, scientists and mathematicians. *Journal of Autism and Developmental Disorders*, *31*(1), 5–17. https://doi.org/cmgjjn

Bastiaansen, J. A., Thioux, M., Nanetti, L., van der Gaag, C., Ketelaars, C., Minderaa, R., & Keysers, C. (2011). Age-related increase in inferior frontal gyrus activity and social functioning in autism spectrum disorder. *Biological Psychiatry*, *69*(9), 832–838. https://doi.org/10.1016/j.biopsych.2010.11.007

Beckmann, C. F., DeLuca, M., Devlin, J. T., & Smith, S. M. (2005). Investigations into resting-state connectivity using independent component analysis. *Philosophical Transactions of the Royal Society B: Biological Sciences*, *360*(1457), 1001–1013. https://doi.org/10.1098/rstb.2005.1634

Beckmann, C. F., Jenkinson, M., & Smith, S. M. (2003). General multilevel linear modeling for group analysis in FMRI. *NeuroImage*, *20*(2), 1052–1063. https://doi.org/10.1016/S1053-8119(03)00435-X

Beckmann, C. F., & Smith, S. M. (2004). Probabilistic independent component analysis for functional magnetic resonance imaging. *IEEE Transactions on Medical Imaging*, *23*(2), 137–152. https://doi.org/10.1109/TMI.2003.822821

Behrmann, M., Thomas, C., & Humphreys, K. (2006). Seeing it differently: Visual processing in autism. *Trends in Cognitive Sciences*, *10*(6), 258–264. https://doi.org/10.1016/j.tics.2006.05.001

Bengtsson, H. (2016). *R.matlab: Read and Write MAT Files and Call MATLAB from Within R* (3.6.0). https://CRAN.R-project.org/package=R.matlab

Benjamini, Y., & Hochberg, Y. (1995). Controlling the false discovery rate: A practical and powerful approach to multiple testing. *Journal of the Royal Statistical Society: Series B (Methodological)*, *57*(1), 289–300. https://doi.org/gfpkdx

Bernas, A., Barendse, E. M., Aldenkamp, A. P., Backes, W. H., Hofman, P. A. M., Hendriks, M. P. H., Kessels, R. P. C., Willems, F. M. J., de With, P. H. N., Zinger, S., & Jansen, J. F. A. (2018). Brain resting-state networks in adolescents with high-functioning autism: Analysis of spatial connectivity and temporal neurodynamics. *Brain and Behavior*, *8*(2). https://doi.org/10.1002/brb3.878

Berto, S., Treacher, A. H., Caglayan, E., Luo, D., Haney, J. R., Gandal, M. J., Geschwind, D. H., Montillo, A. A., & Konopka, G. (2022). Association between resting-state functional brain connectivity and gene expression is altered in autism spectrum disorder. *Nature Communications*, *13*(1), 3328. https://doi.org/10.1038/s41467-022-31053-5

Besseling, R., Lamerichs, R., Michels, B., Heunis, S., de Louw, A., Tijhuis, A., Bergmans, J., & Aldenkamp, B. (2018). Functional network abnormalities consistent with behavioral profile in Autism Spectrum Disorder. *Psychiatry Research: Neuroimaging*, *275*, 43–48. https://doi.org/10.1016/j.pscychresns.2018.02.006

Best, C. T., Womer, J. S., & Queen, H. F. (1994). Hemispheric asymmetries in adults' perception of infant emotional expressions. *Journal of Experimental Psychology: Human Perception and Performance*, *20*(4), 751–765. https://doi.org/b42j3r

Bi, X., Zhao, J., Xu, Q., Sun, Q., & Wang, Z. (2018). Abnormal functional connectivity of resting state network detection based on linear ICA analysis in autism spectrum disorder. *Frontiers in Physiology*, *9*. https://doi.org/gdntdf

Bielczyk, N. Z., Uithol, S., van Mourik, T., Anderson, P., Glennon, J. C., & Buitelaar, J. K. (2019). Disentangling causal webs in the brain using functional magnetic resonance imaging: A review of current approaches. *Network Neuroscience (Cambridge, Mass.)*, *3*(2), 237–273. https://doi.org/10.1162/netn_a_00062

Bird, G., Silani, G., Brindley, R., White, S., Frith, U., & Singer, T. (2010). Empathic brain responses in insula are modulated by levels of alexithymia but not autism. *Brain*, *133*(5), 1515–1525. https://doi.org/10.1093/brain/awq060

Bishop, S. R., Lau, M., Shapiro, S., Carlson, L., Anderson, N. D., Carmody, J., Segal, Z. V., Abbey, S., Speca, M., Velting, D., & Devins, G. (2004). Mindfulness: A proposed operational definition. *Clinical Psychology: Science and Practice*, *11*(3), 230–241. https://doi.org/10.1093/clipsy.bph077

Biswal, B., Zerrin Yetkin, F., Haughton, V. M., & Hyde, J. S. (1995). Functional connectivity in the motor cortex of resting human brain using echo-planar MRI. *Magnetic Resonance in Medicine*, *34*(4), 537–541. https://doi.org/crmzr2

Bloch, F. (1946). Nuclear Induction. *Physical Review*, *70*(7–8), 460–474. https://doi.org/c8ds9b

Bode, M. K., Mattila, M.-L., Kiviniemi, V., Rahko, J., Moilanen, I., Ebeling, H., Tervonen, O., & Nikkinen, J. (2011). White matter in autism spectrum disorders – evidence of impaired fiber formation. *Acta Radiologica*, *52*(10), 1169–1174. https://doi.org/cwhpnx

Bojorquez, J. Z., Bricq, S., Acquitter, C., Brunotte, F., Walker, P. M., & Lalande, A. (2017). What are normal relaxation times of tissues at 3 T? *Magnetic Resonance Imaging*, *35*, 69–80. https://doi.org/10.1016/j.mri.2016.08.021

Bolt, T., Nomi, J. S., Bzdok, D., Salas, J. A., Chang, C., Thomas Yeo, B. T., Uddin, L. Q., & Keilholz, S. D. (2022). A parsimonious description of global functional brain organization in three spatiotemporal patterns. *Nature Neuroscience*, *25*(8), 1093–1103. https://doi.org/10.1038/s41593-022-01118-1

Bolton, T. A. W., Tuleasca, C., Wotruba, D., Rey, G., Dhanis, H., Gauthier, B., Delavari, F., Morgenroth, E., Gaviria, J., Blondiaux, E., Smigielski, L., & Van De Ville, D. (2020). TbCAPs: A toolbox for co-activation pattern analysis. *NeuroImage*, *211*, 116621. https://doi.org/10.1016/j.neuroimage.2020.116621

Bonnet-Brilhault, F., Rajerison, T. A., Paillet, C., Guimard-Brunault, M., Saby, A., Ponson, L., Tripi, G., Malvy, J., & Roux, S. (2018). Autism is a prenatal disorder: Evidence from late gestation brain overgrowth. *Autism Research*, *11*(12), 1635–1642. https://doi.org/10.1002/aur.2036

Borchers, S., Himmelbach, M., Logothetis, N., & Karnath, H.-O. (2012). Direct electrical stimulation of human cortex—The gold standard for mapping brain functions? *Nature Reviews Neuroscience*, *13*(1), 63–70. https://doi.org/10.1038/nrn3140

Bottema-Beutel, K., Kapp, S. K., Lester, J. N., Sasson, N. J., & Hand, B. N. (2021). Avoiding ableist language: Suggestions for autism researchers. *Autism in Adulthood*, *3*(1), 18–29. https://doi.org/10.1089/aut.2020.0014

Bottema-Beutel, K., Park, H., & Kim, S. Y. (2018). Commentary on social skills training curricula for individuals with ASD: Social interaction, authenticity, and stigma. *Journal of Autism and Developmental Disorders*, *48*(3), 953–964. https://doi.org/gc46p7

Bourguignon, M., De Tiège, X., de Beeck, M. O., Pirotte, B., Van Bogaert, P., Goldman, S., Hari, R., & Jousmäki, V. (2011). Functional motor-cortex mapping using corticokinematic coherence. *NeuroImage*, *55*(4), 1475–1479. https://doi.org/bfrpr5

Bowring, A., Nichols, T. E., & Maumet, C. (2022). Isolating the sources of pipeline-variability in group-level task-fMRI results. *Human Brain Mapping*, *43*(3), 1112–1128. https://doi.org/10.1002/hbm.25713

Bray, S., Arnold, A. E. G. F., Levy, R. M., & Iaria, G. (2015). Spatial and temporal functional connectivity changes between resting and attentive states. *Human Brain Mapping*, *36*(2), 549–565. https://doi.org/10.1002/hbm.22646

Breedlove, J. L., St-Yves, G., Olman, C. A., & Naselaris, T. (2020). Generative feedback explains distinct brain activity codes for seen and mental images. *Current Biology*, *30*(12), 2211-2224.e6. https://doi.org/10.1016/j.cub.2020.04.014

Bremmer, F., Schlack, A., Shah, N. J., Zafiris, O., Kubischik, M., Hoffmann, K.-P., Zilles, K., & Fink, G. R. (2001). Polymodal motion processing in posterior parietal and premotor cortex: A human fMRI study strongly implies equivalencies between humans and monkeys. *Neuron*, *29*(1), 287–296. https://doi.org/bqxvrz

Bright, M. G., Whittaker, J. R., Driver, I. D., & Murphy, K. (2020). Vascular physiology drives functional brain networks. *NeuroImage*, *217*, 116907. https://doi.org/ghbhdn

Buckner, R. L., Andrews-Hanna, J. R., & Schacter, D. L. (2008). The brain's default network. *Annals of the New York Academy of Sciences*, *1124*(1), 1–38. https://doi.org/bp6p6p

Buxton, R. B. (2012). Dynamic models of BOLD contrast. *NeuroImage*, *62*(2), 953–961. https://doi.org/10.1016/j.neuroimage.2012.01.012

Buxton, R. B., Uludağ, K., Dubowitz, D. J., & Liu, T. T. (2004). Modeling the hemodynamic response to brain activation. *NeuroImage*, *23*, S220–S233. https://doi.org/dqtwz8

Buxton, R. B., Wong, E. C., & Frank, L. R. (1998). Dynamics of blood flow and oxygenation changes during brain activation: The balloon model. *Magnetic Resonance in Medicine*, *39*(6), 855–864. https://doi.org/10.1002/mrm.1910390602

Byrge, L., & Kennedy, D. P. (2018). Identifying and characterizing systematic temporally-lagged BOLD artifacts. *NeuroImage*, *171*, 376–392. https://doi.org/gc8h4t

Caballero-Gaudes, C., & Reynolds, R. C. (2017). Methods for cleaning the BOLD fMRI signal. *NeuroImage*, *154*, 128–149. https://doi.org/f8jn7h

Caly, H., Rabiei, H., Coste-Mazeau, P., Hantz, S., Alain, S., Eyraud, J.-L., Chianea, T., Caly, C., Makowski, D., Hadjikhani, N., Lemonnier, E., & Ben-Ari, Y. (2021). Machine learning analysis of pregnancy data enables early identification of a subpopulation of newborns with ASD. *Scientific Reports*, *11*(1), 6877. https://doi.org/10.1038/s41598-021-86320-0

Campatelli, G., Federico, R. R., Apicella, F., Sicca, F., & Muratori, F. (2013). Face processing in children with ASD: Literature review. *Research in Autism Spectrum Disorders*, *7*(3), 444–454. https://doi.org/10.1016/j.rasd.2012.10.003

Cao, L., Xu, J., Yang, X., Li, X., & Liu, B. (2018). Abstract Representations of Emotions Perceived From the Face, Body, and Whole-Person Expressions in the Left Postcentral Gyrus. *Frontiers in Human Neuroscience*, *12*, 419. https://doi.org/gfmfdb

Cardinale, R. C., Shih, P., Fishman, I., Ford, L. M., & Müller, R.-A. (2013). Pervasive rightward asymmetry shifts of functional networks in autism spectrum disorder. *JAMA Psychiatry*, *70*(9), 975. https://doi.org/f5cvdt

Caron, M.-J., Mottron, L., Berthiaume, C., & Dawson, M. (2006). Cognitive mechanisms, specificity and neural underpinnings of visuospatial peaks in autism. *Brain: A Journal of Neurology*, *129*(Pt 7), 1789–1802. https://doi.org/10.1093/brain/awl072

Carper, R. A., Treiber, J. M., DeJesus, S. Y., & Müller, R.-A. (2016). Reduced hemispheric asymmetry of white matter microstructure in autism spectrum disorder. *Journal of the American Academy of Child and Adolescent Psychiatry*, *55*(12), 1073–1080. https://doi.org/f9dq63

Casanova, M. F., Sokhadze, E. M., Casanova, E. L., & Li, X. (2020). Transcranial magnetic stimulation in autism spectrum disorders: Neuropathological underpinnings and clinical correlations. *Seminars in Pediatric Neurology*, *35*, 100832. https://doi.org/kdw6

Caspers, S., Schleicher, A., Bacha-Trams, M., Palomero-Gallagher, N., Amunts, K., & Zilles, K. (2013). Organization of the human inferior parietal lobule based on receptor architectonics. *Cerebral Cortex (New York, NY)*, *23*(3), 615–628. https://doi.org/f4kkv5

Caspers, S., Zilles, K., Laird, A. R., & Eickhoff, S. B. (2010). ALE meta-analysis of action observation and imitation in the human brain. *NeuroImage*, *50*(3), 1148–1167. https://doi.org/10.1016/j.neuroimage.2009.12.112

Castellazzi, G., Palesi, F., Casali, S., Vitali, P., Sinforiani, E., Wheeler-Kingshott, C. A. M., & D'Angelo, E. (2014). A comprehensive assessment of resting state networks: Bidirectional modification of functional integrity in cerebro-cerebellar networks in dementia. *Frontiers in Neuroscience*, *8*. https://doi.org/10.3389/fnins.2014.00223

Chaddock-Heyman, L., Erickson, K., Voss, M., Knecht, A., Pontifex, M., Castelli, D., Hillman, C., & Kramer, A. (2013). The effects of physical activity on functional MRI activation associated with cognitive control in children: A randomized controlled intervention. *Frontiers in Human Neuroscience*, *7*. https://doi.org/hqd7

Chang, C., & Glover, G. H. (2010). Time–frequency dynamics of resting-state brain connectivity measured with fMRI. *NeuroImage*, *50*(1), 81–98. https://doi.org/10.1016/j.neuroimage.2009.12.011

Chavhan, G. B., Babyn, P. S., Thomas, B., Shroff, M. M., & Haacke, E. M. (2009). Principles, techniques, and applications of T2*-based MR imaging and its special applications. *RadioGraphics*, *29*(5), 1433–1449. https://doi.org/cbcwf8

Chen, H., Nomi, J. S., Uddin, L. Q., Duan, X., & Chen, H. (2017). Intrinsic functional connectivity variance and state-specific under-connectivity in autism. *Human Brain Mapping*, *38*(11), 5740–5755. https://doi.org/10.1002/hbm.23764

Chen, H., Uddin, L. Q., Zhang, Y., Duan, X., & Chen, H. (2016). Atypical effective connectivity of thalamo-cortical circuits in autism spectrum disorder. *Autism Research*, *9*(11), 1183–1190. https://doi.org/10.1002/aur.1614

Chen, J. E., Chang, C., Greicius, M. D., & Glover, G. H. (2015). Introducing co-activation pattern metrics to quantify spontaneous brain network dynamics. *NeuroImage*, *111*, 476–488. https://doi.org/10.1016/j.neuroimage.2015.01.057

Chen, J. E., Glover, G. H., Fultz, N. E., Rosen, B. R., Polimeni, J. R., & Lewis, L. D. (2021). Investigating mechanisms of fast BOLD responses: The effects of stimulus intensity and of spatial heterogeneity of hemodynamics. *NeuroImage*, *245*, 118658. https://doi.org/10.1016/j.neuroimage.2021.118658

Chen, J. E., Lewis, L. D., Chang, C., Tian, Q., Fultz, N. E., Ohringer, N. A., Rosen, B. R., & Polimeni, J. R. (2020). Resting-state "physiological networks." *NeuroImage*, *213*, 116707. https://doi.org/10.1016/j.neuroimage.2020.116707

Chen, Z., & Calhoun, V. (2018). Effect of spatial smoothing on task fMRI ICA and functional connectivity. *Frontiers in Neuroscience*, *12*. https://doi.org/gc2m47

Cheng, W., Rolls, E. T., Gu, H., Zhang, J., & Feng, J. (2015). Autism: Reduced connectivity between cortical areas involved in face expression, theory of mind, and the sense of self. *Brain*, *138*(5), 1382–1393. https://doi.org/10.1093/brain/awv051

Cherkassky, V. L., Kana, R. K., Keller, T. A., & Just, M. A. (2006). Functional connectivity in a baseline resting-state network in autism. *NeuroReport*, *17*(16), 1687–1690. https://doi.org/10.1097/01.wnr.0000239956.45448.4c

Chez, M. G., Chang, M., Krasne, V., Coughlan, C., Kominsky, M., & Schwartz, A. (2006). Frequency of epileptiform EEG abnormalities in a sequential screening of autistic patients with no known clinical epilepsy from 1996 to 2005. *Epilepsy & Behavior*, *8*(1), 267–271. https://doi.org/10.1016/j.yebeh.2005.11.001

Choque Olsson, N., Flygare, O., Coco, C., Görling, A., Råde, A., Chen, Q., Lindstedt, K., Berggren, S., Serlachius, E., Jonsson, U., Tammimies, K., Kjellin, L., & Bölte, S. (2017). Social skills training for children and adolescents with autism spectrum disorder: A randomized controlled trial. *Journal of the American Academy of Child and Adolescent Psychiatry*, *56*(7), 585–592. https://doi.org/gbn2d4

Ciarrusta, J., Dimitrova, R., Batalle, D., O'Muircheartaigh, J., Cordero-Grande, L., Price, A., Hughes, E., Kangas, J., Perry, E., Javed, A., Demilew, J., Hajnal, J., Edwards, A. D., Murphy, D., Arichi, T., & McAlonan, G. (2020). Emerging functional connectivity differences in newborn infants vulnerable to autism spectrum disorders. *Translational Psychiatry*, *10*(1), 131. https://doi.org/10.1038/s41398-020-0805-y

Ciarrusta, J., O'Muircheartaigh, J., Dimitrova, R., Batalle, D., Cordero-Grande, L., Price, A., Hughes, E., Steinweg, J. K., Kangas, J., Perry, E., Javed, A., Stoencheva, V., Akolekar, R., Victor, S., Hajnal, J., Murphy, D., Edwards, D., Arichi, T., & McAlonan, G. (2019). Social brain functional maturation in newborn infants with and without a family history of autism spectrum disorder. *JAMA Network Open*, *2*(4), e191868. https://doi.org/gkd84m

Cifre, I., Miller Flores, M. T., Penalba, L., Ochab, J. K., & Chialvo, D. R. (2021). Revisiting nonlinear functional brain co-activations: Directed, dynamic, and delayed. *Frontiers in Neuroscience*, *15*, 700171. https://doi.org/kdw9

Ciric, R., Wolf, D. H., Power, J. D., Roalf, D. R., Baum, G. L., Ruparel, K., Shinohara, R. T., Elliott, M. A., Eickhoff, S. B., Davatzikos, C., Gur, R. C., Gur, R. E., Bassett, D. S., & Satterthwaite, T. D. (2017). Benchmarking of participant-level confound regression strategies for the control of motion artifact in studies of functional connectivity. *NeuroImage*, *154*, 174–187. https://doi.org/gbm7g3

Clements, C. C., Zoltowski, A. R., Yankowitz, L. D., Yerys, B. E., Schultz, R. T., & Herrington, J. D. (2018). Evaluation of the social motivation hypothesis of autism: A systematic review and meta-analysis. *JAMA Psychiatry*, *75*(8), 797–808. https://doi.org/ghk765

Coalson, T. S., Van Essen, D. C., & Glasser, M. F. (2018). The impact of traditional neuroimaging methods on the spatial localization of cortical areas. *Proceedings of the National Academy of Sciences*, *115*(27), E6356–E6365. https://doi.org/gdts5b

Conti, E., Calderoni, S., Gaglianese, A., Pannek, K., Mazzotti, S., Rose, S., Scelfo, D., Tosetti, M., Muratori, F., Cioni, G., & Guzzetta, A. (2016). Lateralization of brain networks and clinical severity in toddlers with autism spectrum disorder: A HARDI diffusion MRI study. *Autism Research: Official Journal of the International Society for Autism Research*, *9*(3), 382–392. https://doi.org/f8f23n

Contractor, A., Ethell, I. M., & Portera-Cailliau, C. (2021). Cortical interneurons in autism. *Nature Neuroscience*, *24*(12), 1648–1659. https://doi.org/10.1038/s41593-021-00967-6

Cook, J. L., Blakemore, S.-J., & Press, C. (2013). Atypical basic movement kinematics in autism spectrum conditions. *Brain: A Journal of Neurology*, *136*(Pt 9), 2816–2824. https://doi.org/10.1093/brain/awt208

Cook, R., Brewer, R., Shah, P., & Bird, G. (2013). Alexithymia, not autism, predicts poor recognition of emotional facial expressions. *Psychological Science*, *24*(5), 723–732. https://doi.org/f4x27m

Courchesne, E., & Pierce, K. (2005). Why the frontal cortex in autism might be talking only to itself: Local over-connectivity but long-distance disconnection. *Current Opinion in Neurobiology*, *15*(2), 225–230. https://doi.org/bgqnqs

Cox, R. W. (1996). AFNI: Software for analysis and visualization of functional magnetic resonance neuroimages. *Computers and Biomedical Research, an International Journal*, *29*(3), 162–173. https://doi.org/10.1006/cbmr.1996.0014

Cox, R. W., & Hyde, J. S. (1997). Software tools for analysis and visualization of fMRI data. *NMR in Biomedicine*, *10*(4–5), 171–178. https://doi.org/cms7mx

Dahlgren, S. O., & Gillberg, C. (1989). Symptoms in the first two years of life. *European Archives of Psychiatry and Neurological Sciences*, *238*(3), 169–174. https://doi.org/10.1007/BF00451006

Dai, R., Huang, Z., Weng, X., & He, S. (2022). Early visual exposure primes future cross-modal specialization of the fusiform face area in tactile face processing in the blind. *NeuroImage*, *253*, 119062. https://doi.org/10.1016/j.neuroimage.2022.119062

Dajani, D. R., & Uddin, L. Q. (2016). Local brain connectivity across development in autism spectrum disorder: A cross-sectional investigation. *Autism Research*, *9*(1), 43–54. https://doi.org/10.1002/aur.1494

Damoiseaux, J. S., Rombouts, S. A. R. B., Barkhof, F., Scheltens, P., Stam, C. J., Smith, S. M., & Beckmann, C. F. (2006). Consistent resting-state networks across healthy subjects. *Proceedings of the National Academy of Sciences*, *103*(37), 13848–13853. https://doi.org/10.1073/pnas.0601417103

Dapretto, M., Davies, M. S., Pfeifer, J. H., Scott, A. A., Sigman, M., Bookheimer, S. Y., & Iacoboni, M. (2006). Understanding emotions in others: Mirror neuron dysfunction in children with autism spectrum disorders. *Nature Neuroscience*, *9*(1), 28–30. https://doi.org/10.1038/nn1611

Davey, C. G., Pujol, J., & Harrison, B. J. (2016). Mapping the self in the brain's default mode network. *NeuroImage*, *132*, 390–397. https://doi.org/f8jn7h

Davidson, R. J., & Irwin, W. (1999). Neuroanatomy of emotion and affective style. *Trends in Cognitive Sciences*, *3*(1), 11.

Dawson, G., Franz, L., & Brandsen, S. (2022). At a crossroads—Reconsidering the goals of autism early behavioral intervention from a neurodiversity perspective. *JAMA Pediatrics*, *176*(9), 839–840. https://doi.org/kdxb

De Tiège, X., Bourguignon, M., Piitulainen, H., & Jousmäki, V. (2020). Sensorimotor mapping with MEG: An update on the current state of clinical research and practice with considerations for clinical practice guidelines. *Journal of Clinical Neurophysiology*, *37*(6), 564–573. https://doi.org/gjhw4h

de Vignemont, F., & Singer, T. (2006). The empathic brain: How, when and why? *Trends in Cognitive Sciences*, *10*(10), 435–441. https://doi.org/dj44v6

Del Bianco, T., Mason, L., Charman, T., Tillman, J., Loth, E., Hayward, H., Shic, F., Buitelaar, J., Johnson, M. H., Jones, E. J. H., Ahmad, J., Ambrosino, S., Banaschewski, T., Baron-Cohen, S., Baumeister, S., Beckmann, C. F., Bölte, S., Bourgeron, T., Bours, C., … Zwiers, M. P. (2021). Temporal profiles of social attention are different across development in autistic and neurotypical people. *Biological Psychiatry: Cognitive Neuroscience and Neuroimaging*, *6*(8), 813–824. https://doi.org/gnprh4

Delaidelli, A., & Moiraghi, A. (2017). Respiration: A new mechanism for CSF circulation? *Journal of Neuroscience*, *37*(30), 7076–7078. https://doi.org/kdxd

DeMayo, M. M., Pokorski, I., Song, Y. J. C., Thapa, R., Patel, S., Ambarchi, Z., Soligo, D., Sadeli, I., Thomas, E. E., Hickie, I. B., & Guastella, A. J. (2022). The feasibility of magnetic resonance imaging in a non-selective comprehensive clinical trial in pediatric autism spectrum disorder. *Journal of Autism and Developmental Disorders*, *52*(3), 1211–1222. https://doi.org/kdxf

Deruelle, C., Hubert, B., Santos, A., & Wicker, B. (2008). Negative emotion does not enhance recall skills in adults with autistic spectrum disorders. *Autism Research: Official Journal of the International Society for Autism Research*, *1*(2), 91–96. https://doi.org/10.1002/aur.13

Des Roches Rosa, S. (2016, January 26). Before talking about autism, listen to families. *Spectrum | Autism Research News*. https://www.spectrumnews.org/opinion/viewpoint/before-talking-about-autism-listen-to-families/

Deshpande, G., & Hu, X. (2012). Investigating effective brain connectivity from fMRI data: Past findings and current issues with reference to Granger causality analysis. *Brain Connectivity*, *2*(5), 235–245. https://doi.org/10.1089/brain.2012.0091

Deshpande, G., LaConte, S., Peltier, S., & Hu, X. (2009). Integrated local correlation: A new measure of local coherence in fMRI data. *Human Brain Mapping*, *30*(1), 13–23. https://doi.org/10.1002/hbm.20482

Di Martino, A., Ross, K., Uddin, L. Q., Sklar, A. B., Castellanos, F. X., & Milham, M. P. (2009). Functional Brain Correlates of Social and Nonsocial Processes in Autism Spectrum Disorders: An Activation Likelihood Estimation Meta-Analysis. *Biological Psychiatry*, *65*(1), 63–74. https://doi.org/10.1016/j.biopsych.2008.09.022

Di Martino, A., Yan, C.-G., Li, Q., Denio, E., Castellanos, F. X., Alaerts, K., Anderson, J. S., Assaf, M., Bookheimer, S. Y., Dapretto, M., Deen, B., Delmonte, S., Dinstein, I., Ertl-Wagner, B., Fair, D. A., Gallagher, L., Kennedy, D. P., Keown, C. L., Keysers, C., … Milham, M. P. (2014). The autism brain imaging data exchange: Towards a large-scale evaluation of the intrinsic brain architecture in autism. *Molecular Psychiatry*, *19*(6), 659–667. https://doi.org/10.1038/mp.2013.78

Di Perri, C., Amico, E., Heine, L., Annen, J., Martial, C., Larroque, S. K., Soddu, A., Marinazzo, D., & Laureys, S. (2017). Multifaceted brain networks reconfiguration in disorders of consciousness uncovered by co-activation patterns: Dynamic connectivity in disorders of consciousness. *Human Brain Mapping*. https://doi.org/gmfkcm

Diamond, A. (2013). Executive Functions. *Annual Review of Psychology*, *64*(1), 135–168. https://doi.org/10.1146/annurev-psych-113011-143750

Diener, M. L., Wright, C. A., Taylor, C., D'Astous, V., & Lasrich, L. (2020). Dual perspectives in autism spectrum disorders and employment: Toward a better fit in the workplace. *Work (Reading, Mass.)*, *67*(1), 223–237. https://doi.org/10.3233/WOR-203268

Dimitrova, A., Kolb, F. P., Elles, H.-G., Maschke, M., Forsting, M., Diener, H. C., & Timmann, D. (2003). Cerebellar responses evoked by nociceptive leg withdrawal reflex as revealed by event-related fMRI. *Journal of Neurophysiology*, *90*(3), 1877–1886. https://doi.org/b9vnhj

Ding, L., Shou, G., Cha, Y.-H., Sweeney, J. A., & Yuan, H. (2022). Brain-wide neural co-activations in resting human. *NeuroImage*, *260*, 119461. https://doi.org/kdxg

Douaud, G., Smith, S., Jenkinson, M., Behrens, T., Johansen-Berg, H., Vickers, J., James, S., Voets, N., Watkins, K., Matthews, P. M., & James, A. (2007). Anatomically related grey and white matter abnormalities in adolescent-onset schizophrenia. *Brain*, *130*(9), 2375–2386. https://doi.org/10.1093/brain/awm184

Dreha-Kulaczewski, S., Joseph, A. A., Merboldt, K.-D., Ludwig, H.-C., Gärtner, J., & Frahm, J. (2015). Inspiration is the major regulator of human CSF flow. *The Journal of Neuroscience: The Official Journal of the Society for Neuroscience*, *35*(6), 2485–2491. https://doi.org/10.1523/JNEUROSCI.3246-14.2015

D'Souza, N. S., Nebel, M. B., Wymbs, N., Mostofsky, S. H., & Venkataraman, A. (2020). A joint network optimization framework to predict clinical severity from resting state functional MRI data. *NeuroImage*, *206*, 116314. https://doi.org/gnfdv4

Du, Y., He, X., Kochunov, P., Pearlson, G., Hong, L. E., van Erp, T. G. M., Belger, A., & Calhoun, V. D. (2022). A new multimodality fusion classification approach to explore the uniqueness of schizophrenia and autism spectrum disorder. *Human Brain Mapping*, *43*(12), 3887–3903. https://doi.org/10.1002/hbm.25890

Dubois, J., Alison, M., Counsell, S. J., Hertz-Pannier, L., Hüppi, P. S., & Benders, M. J. N. L. (2021). MRI of the neonatal brain: A review of methodological challenges and neuroscientific advances. *Journal of Magnetic Resonance Imaging*, *53*(5), 1318–1343. https://doi.org/ggxf5t

Ehlers, S., Gillberg, C., & Wing, L. (1999). A screening questionnaire for Asperger syndrome and other high-functioning autism spectrum disorders in school age children. *Journal of Autism and Developmental Disorders*, *29*(2), 129–141.

Eickhoff, S. B., Paus, T., Caspers, S., Grosbras, M.-H., Evans, A. C., Zilles, K., & Amunts, K. (2007). Assignment of functional activations to probabilistic cytoarchitectonic areas revisited. *NeuroImage*, *36*(3), 511–521. https://doi.org/bnhtgx

Ekman, P., & Friesen, W. V. (1978). *Pictures of facial affect*. Palo Alto, CA: Consulting Psychologist Press.

Elster, A. D. (2023). *MRI Questions & Answers; MR imaging physics & technology*. Questions and Answers in MRI. http://mriquestions.com/

Falahpour, M., Thompson, W. K., Abbott, A. E., Jahedi, A., Mulvey, M. E., Datko, M., Liu, T. T., & Müller, R.-A. (2016). Underconnected, but not broken? Dynamic functional connectivity MRI shows underconnectivity in autism is linked to increased intra-individual variability across time. *Brain Connectivity*, *6*(5), 403–414. https://doi.org/ggmpgx

Farrant, K., & Uddin, L. Q. (2016). Atypical developmental of dorsal and ventral attention networks in autism. *Developmental Science*, *19*(4), 550–563. https://doi.org/f8wfxr

Feczko, E., Balba, N. M., Miranda-Dominguez, O., Cordova, M., Karalunas, S. L., Irwin, L., Demeter, D. V., Hill, A. P., Langhorst, B. H., Grieser Painter, J., Van Santen, J., Fombonne, E. J., Nigg, J. T., & Fair, D. A. (2018). Subtyping cognitive profiles in Autism Spectrum Disorder using a Functional Random Forest algorithm. *NeuroImage*, *172*, 674–688. https://doi.org/10.1016/j.neuroimage.2017.12.044

Fernández-Delgado, M., Cernadas, E., Barro, S., & Amorim, D. (2014). Do we need hundreds of classifiers to solve real world classification problems? *The Journal of Machine Learning Research*, *15*(1), 3133–3181.

First, M. B., Gaebel, W., Maj, M., Stein, D. J., Kogan, C. S., Saunders, J. B., Poznyak, V. B., Gureje, O., Lewis-Fernández, R., Maercker, A., Brewin, C. R., Cloitre, M., Claudino, A., Pike, K. M., Baird, G., Skuse, D., Krueger, R. B., Briken, P., Burke, J. D., … Reed, G. M. (2021). An organization- and category-level comparison of diagnostic requirements for mental disorders in ICD-11 and DSM-5. *World Psychiatry*, *20*(1), 34–51. https://doi.org/10.1002/wps.20825

Fitzgerald, J., Johnson, K., Kehoe, E., Bokde, A. L. W., Garavan, H., Gallagher, L., & McGrath, J. (2015). Disrupted functional connectivity in dorsal and ventral attention networks during attention orienting in autism spectrum disorders. *Autism Research: Official Journal of the International Society for Autism Research*, *8*(2), 136–152. https://doi.org/10.1002/aur.1430

Floris, D. L., Filho, J. O. A., Lai, M.-C., Giavasis, S., Oldehinkel, M., Mennes, M., Charman, T., Tillmann, J., Dumas, G., Ecker, C., Dell'Acqua, F., Banaschewski, T., Moessnang, C., Baron-Cohen, S., Durston, S., Loth, E., Murphy, D. G. M., Buitelaar, J. K., Beckmann, C. F., … Di Martino, A. (2021). Towards robust and replicable sex differences in the intrinsic brain function of autism. *Molecular Autism*, *12*, 19. https://doi.org/10.1186/s13229-021-00415-z

Fortenbaugh, F. C., Rothlein, D., McGlinchey, R., DeGutis, J., & Esterman, M. (2018). Tracking behavioral and neural fluctuations during sustained attention: A robust replication and extension. *NeuroImage*, *171*, 148–164. https://doi.org/gc8hch

Fox, M. D., & Raichle, M. E. (2007). Spontaneous fluctuations in brain activity observed with functional magnetic resonance imaging. *Nature Reviews Neuroscience*, *8*(9), 700–711. https://doi.org/10.1038/nrn2201

Fox, M. D., Snyder, A. Z., Vincent, J. L., Corbetta, M., Van Essen, D. C., & Raichle, M. E. (2005). The human brain is intrinsically organized into dynamic, anticorrelated functional networks. *Proceedings of the National Academy of Sciences*, *102*(27), 9673–9678. https://doi.org/10.1073/pnas.0504136102

Fox, M. D., Zhang, D., Snyder, A. Z., & Raichle, M. E. (2009). The global signal and observed anticorrelated resting state brain networks. *Journal of Neurophysiology*, *101*(6), 3270–3283. https://doi.org/c3kmrk

Fox, P. T., & Raichle, M. E. (1986). Focal physiological uncoupling of cerebral blood flow and oxidative metabolism during somatosensory stimulation in human subjects. *Proceedings of the National Academy of Sciences of the United States of America*, *83*(4), 1140–1144. https://doi.org/10.1073/pnas.83.4.1140

Freyd, J. J. (1987). Dynamic mental representations. *Psychological Review*, *94*(4), 427–438.

Friedman, J., Hastie, T., & Tibshirani, R. (2001). *The elements of statistical learning* (Vol. 1). Springer series in statistics Springer, Berlin. http://statweb.stanford.edu/~tibs/book/preface.ps

Friston, K. J. (1994). Functional and effective connectivity in neuroimaging: A synthesis. *Human Brain Mapping*, *2*(1–2), 56–78. https://doi.org/10.1002/hbm.460020107

Friston, K. J., Holmes, A. P., Worsley, K. J., Poline, J.-P., Frith, C. D., & Frackowiak, R. S. J. (1994). Statistical parametric maps in functional imaging: A general linear approach. *Human Brain Mapping*, *2*(4), 189–210. https://doi.org/10.1002/hbm.460020402

Friston, K. J., Jezzard, P., & Turner, R. (1994). Analysis of functional MRI time-series. *Human Brain Mapping*, *1*(2), 153–171. https://doi.org/10.1002/hbm.460010207

Friston, K. J., Mechelli, A., Turner, R., & Price, C. J. (2000). Nonlinear Responses in fMRI: The Balloon Model, Volterra Kernels, and Other Hemodynamics. *NeuroImage*, *12*(4), 466–477. https://doi.org/10.1006/nimg.2000.0630

Fry, R., Li, X., Evans, T. C., Esterman, M., Tanaka, J., & DeGutis, J. (2022). Investigating the influence of autism spectrum traits on face processing mechanisms in developmental prosopagnosia. *Journal of Autism and Developmental Disorders*. https://doi.org/kdxh

Gabrielsen, T. P., Anderson, J. S., Stephenson, K. G., Beck, J., King, J. B., Kellems, R., Top, D. N., Russell, N. C. C., Anderberg, E., Lundwall, R. A., Hansen, B., & South, M. (2018). Functional MRI connectivity of children with autism and low verbal and cognitive performance. *Molecular Autism*, *9*(1), 67. https://doi.org/ggdr9g

Galili, T. (2015). dendextend: An R package for visualizing, adjusting and comparing trees of hierarchical clustering. *Bioinformatics*, *31*(22), 3718–3720. https://doi.org/gc4n3d

Garroway, A. N., Grannell, P. K., & Mansfield, P. (1974). Image formation in NMR by a selective irradiative process. *Journal of Physics C: Solid State Physics*, *7*(24), L457. https://doi.org/10.1088/0022-3719/7/24/006

Genovese, C. R., Lazar, N. A., & Nichols, T. (2002). Thresholding of statistical maps in functional neuroimaging using the false discovery rate. *NeuroImage*, *15*(4), 870–878. https://doi.org/10.1006/nimg.2001.1037

Georgopoulos, M. A., Brewer, N., Lucas, C. A., & Young, R. L. (2022). Speed and accuracy of emotion recognition in autistic adults: The role of stimulus type, response format, and emotion. *Autism Research*, *15*(9). https://doi.org/10.1002/aur.2713

Gold, S., Christian, B., Arndt, S., Zeien, G., Cizadlo, T., Johnson, D. L., Flaum, M., & Andreasen, N. C. (1998). Functional MRI statistical software packages: A comparative analysis. *Human Brain Mapping*, *6*(2), 73–84.

Goldman, M. (2001). Formal Theory of Spin–Lattice Relaxation. *Journal of Magnetic Resonance*, *149*(2), 160–187. https://doi.org/10.1006/jmre.2000.2239

Gomez, J., Barnett, M. A., Natu, V., Mezer, A., Palomero-Gallagher, N., Weiner, K. S., Amunts, K., Zilles, K., & Grill-Spector, K. (2017). Microstructural proliferation in human cortex is coupled with the development of face processing. *Science (New York, N.Y.)*, *355*(6320), 68–71. https://doi.org/10.1126/science.aag0311

Good, C. D., Johnsrude, I. S., Ashburner, J., Henson, R. N. A., Friston, K. J., & Frackowiak, R. S. J. (2001). A voxel-based morphometric study of ageing in 465 normal adult human brains. *NeuroImage*, *14*(1), 21–36. https://doi.org/btr3wm

Gopnik, A., & Meltzoff, A. N. (1994). Minds, bodies, and persons: Young children's understanding of the self and others as reflected in imitation and theory of mind research. In *Self-awareness in animals and humans: Developmental perspectives* (pp. 166–186). Cambridge University Press. https://doi.org/10.1017/CBO9780511565526.012

Gordon, E. M., Laumann, T. O., Gilmore, A. W., Newbold, D. J., Greene, D. J., Berg, J. J., Ortega, M., Hoyt-Drazen, C., Gratton, C., Sun, H., Hampton, J. M., Coalson, R. S., Nguyen, A. L., McDermott, K. B., Shimony, J. S., Snyder, A. Z., Schlaggar, B. L., Petersen, S. E., Nelson, S. M., & Dosenbach, N. U. F. (2017). Precision functional mapping of individual human brains. *Neuron*, *95*(4), 791-807.e7. https://doi.org/gdcdv2

Gotts, S. J., Saad, Z. S., Jo, H. J., Wallace, G. L., Cox, R. W., & Martin, A. (2013). The perils of global signal regression for group comparisons: A case study of autism spectrum disorders. *Frontiers in Human Neuroscience*, *7*. https://doi.org/ggqp97

Greicius, M. D., Krasnow, B., Reiss, A. L., & Menon, V. (2003). Functional connectivity in the resting brain: A network analysis of the default mode hypothesis. *Proceedings of the National Academy of Sciences of the United States of America*, *100*(1), 253–258. https://doi.org/10.1073/pnas.0135058100

Greicius, M. D., Srivastava, G., Reiss, A. L., Menon, V., & Raichle, M. E. (2004). Default-mode network activity distinguishes Alzheimer's disease from healthy aging: Evidence from functional MRI. *Proceedings of the National Academy of Sciences of the United States of America*, *101*(13), 4637–4642.

Grèzes, J., Wicker, B., Berthoz, S., & de Gelder, B. (2009). A failure to grasp the affective meaning of actions in autism spectrum disorder subjects. *Neuropsychologia*, *47*(8–9), 1816–1825. https://doi.org/10.1016/j.neuropsychologia.2009.02.021

Griffanti, L., Douaud, G., Bijsterbosch, J., Evangelisti, S., Alfaro-Almagro, F., Glasser, M. F., Duff, E. P., Fitzgibbon, S., Westphal, R., Carone, D., Beckmann, C. F., & Smith, S. M. (2017). Hand classification of fMRI ICA noise components. *NeuroImage*, *154*, 188–205. https://doi.org/10.1016/j.neuroimage.2016.12.036

Groot, J. M., Boayue, N. M., Csifcsák, G., Boekel, W., Huster, R., Forstmann, B. U., & Mittner, M. (2021). Probing the neural signature of mind wandering with simultaneous fMRI-EEG and pupillometry. *NeuroImage*, *224*, 117412. https://doi.org/gh27gv

Gruber, B., Froeling, M., Leiner, T., & Klomp, D. W. J. (2018). RF coils: A practical guide for nonphysicists: RF Coils. *Journal of Magnetic Resonance Imaging*, *48*(3), 590–604. https://doi.org/10.1002/jmri.26187

Grzadzinski, R., Amso, D., Landa, R., Watson, L., Guralnick, M., Zwaigenbaum, L., Deák, G., Estes, A., Brian, J., Bath, K., Elison, J., Abbeduto, L., Wolff, J., & Piven, J. (2021). Pre-symptomatic intervention for autism spectrum disorder (ASD): Defining a research agenda. *Journal of Neurodevelopmental Disorders*, *13*(1). Scopus. https://doi.org/kdxj

Gu, Z., Jamison, K. W., Khosla, M., Allen, E. J., Wu, Y., St-Yves, G., Naselaris, T., Kay, K., Sabuncu, M. R., & Kuceyeski, A. (2022). NeuroGen: Activation optimized image synthesis for discovery neuroscience. *NeuroImage*, *247*, 118812. https://doi.org/kdxk

Guell, X., & Schmahmann, J. (2020). Cerebellar functional anatomy: A didactic summary based on human fMRI evidence. *The Cerebellum*, *19*(1), 1–5. https://doi.org/gnp982

Guillon, Q., Hadjikhani, N., Baduel, S., & Rogé, B. (2014). Visual social attention in autism spectrum disorder: Insights from eye tracking studies. *Neuroscience & Biobehavioral Reviews*, *42*, 279–297. https://doi.org/10.1016/j.neubiorev.2014.03.013

Guo, X., Wang, J., Wang, X., Liu, W., Yu, H., Xu, L., Li, H., Wu, J., Dong, M., Tan, W., Chen, W., Yang, Y., & Chen, Y. (2022). Diagnosing autism spectrum disorder in children using conventional MRI and apparent diffusion coefficient based deep learning algorithms. *European Radiology*, *32*(2), 761–770. https://doi.org/10.1007/s00330-021-08239-4

Gurd, J. M., Amunts, K., Weiss, P. H., Zafiris, O., Zilles, K., Marshall, J. C., & Fink, G. R. (2002). Posterior parietal cortex is implicated in continuous switching between verbal fluency tasks: An fMRI study with clinical implications. *Brain*, *125*(5), 1024–1038. https://doi.org/10.1093/brain/awf093

Gusnard, D. A., Akbudak, E., Shulman, G. L., & Raichle, M. E. (2001). Medial prefrontal cortex and self-referential mental activity: Relation to a default mode of brain function. *Proceedings of the National Academy of Sciences*, *98*(7), 4259–4264. https://doi.org/10.1073/pnas.071043098

Gutierrez-Barragan, D., Basson, M. A., Panzeri, S., & Gozzi, A. (2019). Infraslow state fluctuations govern spontaneous fMRI network dynamics. *Current Biology*, *29*(14), 2295-2306.e5. https://doi.org/ghcnqp

Habas, C., & Cabanis, E. A. (2008). Neural correlates of simple unimanual discrete and continuous movements: A functional imaging study at 3 T. *Neuroradiology*, *50*(4), 367–375. https://doi.org/10.1007/s00234-007-0354-6

Habayeb, S., Tsang, T., Saulnier, C., Klaiman, C., Jones, W., Klin, A., & Edwards, L. A. (2021). Visual traces of language acquisition in toddlers with autism spectrum disorder during the second year of life. *Journal of Autism and Developmental Disorders*, *51*(7), 2519–2530. https://doi.org/gp2rjw

Hadjikhani, N., Joseph, R. M., Snyder, J., & Tager-Flusberg, H. (2006). Anatomical Differences in the Mirror Neuron System and Social Cognition Network in Autism. *Cerebral Cortex*, *16*(9), 1276–1282. https://doi.org/10.1093/cercor/bhj069

Hadjikhani, N., Joseph, R. M., Snyder, J., & Tager-Flusberg, H. (2007). Abnormal activation of the social brain during face perception in autism. *Human Brain Mapping*, *28*(5), 441–449. https://doi.org/10.1002/hbm.20283

Hale, J. R., Brookes, M. J., Hall, E. L., Zumer, J. M., Stevenson, C. M., Francis, S. T., & Morris, P. G. (2010). Comparison of functional connectivity in default mode and sensorimotor networks at 3 and 7T. *Magnetic Resonance Materials in Physics, Biology and Medicine*, *23*(5), 339–349. https://doi.org/10.1007/s10334-010-0220-0

Hamilton, A. F. de C. (2013). Reflecting on the mirror neuron system in autism: A systematic review of current theories. *Developmental Cognitive Neuroscience*, *3*, 91–105. https://doi.org/10.1016/j.dcn.2012.09.008

Han, S., Eun, S., Cho, H., Uludağ, K., & Kim, S.-G. (2022). Improved laminar specificity and sensitivity by combining SE and GE BOLD signals. *NeuroImage*, *264*, 119675. https://doi.org/10.1016/j.neuroimage.2022.119675

Hanke, M., Halchenko, Y. O., Sederberg, P. B., Hanson, S. J., Haxby, J. V., & Pollmann, S. (2009). PyMVPA: A Python toolbox for multivariate pattern analysis of fMRI data. *Neuroinformatics*, *7*(1), 37–53. https://doi.org/c7q9tx

Hari, R., Bourguignon, M., Piitulainen, H., Smeds, E., De Tiège, X., & Jousmäki, V. (2014). Human primary motor cortex is both activated and stabilized during observation of other person's phasic motor actions. *Philosophical Transactions of the Royal Society B: Biological Sciences*, *369*(1644), 20130171. https://doi.org/kdx5

Hari, R., & Kujala, M. V. (2009). Brain basis of human social interaction: From concepts to brain imaging. *Physiological Reviews*, *89*(2), 453–479. https://doi.org/bjzz6h

Harikumar, A., Evans, D. W., Dougherty, C. C., Carpenter, K. L. H., & Michael, A. M. (2021). A review of the default mode network in autism spectrum disorders and attention deficit hyperactivity disorder. *Brain Connectivity*, *11*(4), 253–263. https://doi.org/kdxm

Harrewijn, A., Abend, R., Linke, J., Brotman, M. A., Fox, N. A., Leibenluft, E., Winkler, A. M., & Pine, D. S. (2020). Combining fMRI during resting state and an attention bias task in children. *NeuroImage*, *205*, 116301. https://doi.org/gqpkmb

He, B. J., Snyder, A. Z., Zempel, J. M., Smyth, M. D., & Raichle, M. E. (2008). Electrophysiological correlates of the brain's intrinsic large-scale functional architecture. *Proceedings of the National Academy of Sciences*, *105*(41), 16039–16044. https://doi.org/10.1073/pnas.0807010105

He, N., Palaniyappan, L., Linli, Z., & Guo, S. (2022). Abnormal hemispheric asymmetry of both brain function and structure in attention deficit/hyperactivity disorder: A meta-analysis of individual participant data. *Brain Imaging and Behavior*, *16*(1), 54–68. https://doi.org/10.1007/s11682-021-00476-x

Herrero, M. J., Velmeshev, D., Hernandez-Pineda, D., Sethi, S., Sorrells, S., Banerjee, P., Sullivan, C., Gupta, A. R., Kriegstein, A. R., & Corbin, J. G. (2020). Identification of amygdala-expressed genes associated with autism spectrum disorder. *Molecular Autism*, *11*(1), 39. https://doi.org/10.1186/s13229-020-00346-1

Hillman, E. M. C. (2014). Coupling mechanism and significance of the BOLD signal: A status report. *Annual Review of Neuroscience*, *37*, 161–181. https://doi.org/ggmd2f

Hiltunen, T., Kantola, J., Abou Elseoud, A., Lepola, P., Suominen, K., Starck, T., Nikkinen, J., Remes, J., Tervonen, O., Palva, S., Kiviniemi, V., & Palva, J. M. (2014). Infra-slow EEG fluctuations are correlated with resting-state network dynamics in fMRI. *Journal of Neuroscience*, *34*(2), 356–362. https://doi.org/f5pcw7

Hindriks, R., Adhikari, M. H., Murayama, Y., Ganzetti, M., Mantini, D., Logothetis, N. K., & Deco, G. (2016). Can sliding-window correlations reveal dynamic functional connectivity in resting-state fMRI? *NeuroImage*, *127*, 242–256. https://doi.org/f786fz

Hirjak, D., Thomann, P. A., Kubera, K. M., Stieltjes, B., & Wolf, R. C. (2016). Cerebellar contributions to neurological soft signs in healthy young adults. *European Archives of Psychiatry and Clinical Neuroscience*, *266*(1), 35–41. https://doi.org/10.1007/s00406-015-0582-4

Hirvikoski, T., Boman, M., Chen, Q., D'Onofrio, B. M., Mittendorfer-Rutz, E., Lichtenstein, P., Bölte, S., & Larsson, H. (2020). Individual risk and familial liability for suicide attempt and suicide in autism: A population-based study. *Psychological Medicine*, *50*(9), 1463–1474. https://doi.org/10.1017/S0033291719001405

Howarth, C., Gleeson, P., & Attwell, D. (2012). Updated energy budgets for neural computation in the neocortex and cerebellum. *Journal of Cerebral Blood Flow & Metabolism*, *32*(7), 1222–1232. https://doi.org/10.1038/jcbfm.2012.35

Howarth, C., Mishra, A., & Hall, C. N. (2021). More than just summed neuronal activity: How multiple cell types shape the BOLD response. *Philosophical Transactions of the Royal Society B: Biological Sciences*, *376*(1815), 20190630. https://doi.org/ghknx2

Hudetz, A. G., Liu, X., & Pillay, S. (2015). Dynamic repertoire of intrinsic brain states is reduced in propofol-induced unconsciousness. *Brain Connectivity*, *5*(1), 10–22. https://doi.org/kdxn

Hughes, J. R. (2007). Autism: The first firm finding = underconnectivity? *Epilepsy & Behavior*, *11*(1), 20–24. https://doi.org/10.1016/j.yebeh.2007.03.010

Hull, J. V., Jacokes, Z. J., Torgerson, C. M., Irimia, A., & Van Horn, J. D. (2017). Resting-State Functional Connectivity in Autism Spectrum Disorders: A Review. *Frontiers in Psychiatry*, *7*. https://doi.org/10.3389/fpsyt.2016.00205

Huotari, N., Raitamaa, L., Helakari, H., Kananen, J., Raatikainen, V., Rasila, A., Tuovinen, T., Kantola, J., Borchardt, V., Kiviniemi, V. J., & Korhonen, V. O. (2019). Sampling Rate Effects on Resting State fMRI Metrics. *Frontiers in Neuroscience*, *13*. https://doi.org/10.3389/fnins.2019.00279

Huotari, N., Tuunanen, J., Raitamaa, L., Raatikainen, V., Kananen, J., Helakari, H., Tuovinen, T., Järvelä, M., Kiviniemi, V., & Korhonen, V. (2022). Cardiovascular Pulsatility Increases in Visual Cortex Before Blood Oxygen Level Dependent Response During Stimulus. *Frontiers in Neuroscience*, *16*. https://www.frontiersin.org/articles/10.3389/fnins.2022.836378

Hutchison, R. M., Womelsdorf, T., Allen, E. A., Bandettini, P. A., Calhoun, V. D., Corbetta, M., Penna, S. D., Duyn, J. H., Glover, G. H., Gonzalez-Castillo, J., Handwerker, D. A., Keilholz, S., Kiviniemi, V., Leopold, D. A., de Pasquale, F., Sporns, O., Walter, M., & Chang, C. (2013). Dynamic functional connectivity: Promise, issues, and interpretations. *NeuroImage*, *80*. https://doi.org/10.1016/j.neuroimage.2013.05.079

Hyvärinen, A., & Oja, E. (2000). Independent component analysis: Algorithms and applications. *Neural Networks*, *13*(4–5), 411–430. https://doi.org/10.1016/S0893-6080(00)00026-5

Iacoboni, M. (2005). Neural mechanisms of imitation. *Current Opinion in Neurobiology*, *15*(6), 632–637. https://doi.org/10.1016/j.conb.2005.10.010

Iacoboni, M., Woods, R. P., Brass, M., Bekkering, H., Mazziotta, J. C., & Rizzolatti, G. (1999). Cortical mechanisms of human imitation. *Science*, *286*(5449), 2526–2528. https://doi.org/ckjgmg

Iarocci, G., & McDonald, J. (2006). Sensory integration and the perceptual experience of persons with autism. *Journal of Autism & Developmental Disorders*, *36*(1), 77–90. https://doi.org/b69f72

Iraji, A., Faghiri, A., Fu, Z., Kochunov, P., Adhikari, B. M., Belger, A., Ford, J. M., McEwen, S., Mathalon, D. H., Pearlson, G. D., Potkin, S. G., Preda, A., Turner, J. A., Van Erp, T. G. M., Chang, C., & Calhoun, V. D. (2022). Moving beyond the 'CAP' of the Iceberg: Intrinsic connectivity networks in fMRI are continuously engaging and overlapping. *NeuroImage*, *251*, 119013. https://doi.org/10.1016/j.neuroimage.2022.119013

Iravani, B., Arshamian, A., Fransson, P., & Kaboodvand, N. (2021). Whole-brain modelling of resting state fMRI differentiates ADHD subtypes and facilitates stratified neuro-stimulation therapy. *NeuroImage*, *231*, 117844. https://doi.org/gjkhdz

Iwabuchi, S. J., Krishnadas, R., Li, C., Auer, D. P., Radua, J., & Palaniyappan, L. (2015). Localized connectivity in depression: A meta-analysis of resting state functional imaging studies. *Neuroscience & Biobehavioral Reviews*, *51*, 77–86. https://doi.org/10.1016/j.neubiorev.2015.01.006

Jain, A. K. (2010). Data clustering: 50 years beyond K-means. *Pattern Recognition Letters*, *31*(8), 651–666. https://doi.org/10.1016/j.patrec.2009.09.011

Jansson-Verkasalo, E., Kujala, T., Jussila, K., Mattila, M. L., Moilanen, I., Näätänen, R., Suominen, K., & Korpilahti, P. (2005). Similarities in the phenotype of the auditory neural substrate in children with Asperger syndrome and their parents. *The European Journal of Neuroscience*, *22*(4), 986–990. https://doi.org/10.1111/j.1460-9568.2005.04216.x

Jao Keehn, R. J., Nair, S., Pueschel, E. B., Linke, A. C., Fishman, I., & Müller, R.-A. (2018). Atypical local and distal patterns of occipito-frontal functional connectivity are related to symptom severity in autism. *Cerebral Cortex*. https://doi.org/gd4dh2

Jenkinson, M., Bannister, P., Brady, M., & Smith, S. (2002). Improved optimization for the robust and accurate linear registration and motion correction of brain images. *NeuroImage*, *17*(2), 825–841. https://doi.org/10.1016/s1053-8119(02)91132-8

Jenkinson, M., Beckmann, C. F., Behrens, T. E. J., Woolrich, M. W., & Smith, S. M. (2012). FSL. *NeuroImage*, *62*(2), 782–790. https://doi.org/10.1016/j.neuroimage.2011.09.015

Jenkinson, M., & Smith, S. (2001). A global optimisation method for robust affine registration of brain images. *Medical Image Analysis*, *5*(2), 143–156. https://doi.org/10.1016/s1361-8415(01)00036-6

Ji, J. L., Spronk, M., Kulkarni, K., Repovš, G., Anticevic, A., & Cole, M. W. (2019). Mapping the human brain's cortical-subcortical functional network organization. *NeuroImage*, *185*, 35–57. https://doi.org/10.1016/j.neuroimage.2018.10.006

Jiang, L., Hou, X.-H., Yang, N., Yang, Z., & Zuo, X.-N. (2015). Examination of local functional homogeneity in autism. *BioMed Research International*, *2015*, e174371. https://doi.org/10.1155/2015/174371

Jiang, L., & Zuo, X.-N. (2016). Regional homogeneity: A multimodal, multiscale neuroimaging marker of the human connectome. *The Neuroscientist*, *22*(5), 486–505. https://doi.org/10.1177/1073858415595004

Jin, K., Xu, D., Shen, Z., Feng, G., Zhao, Z., Lu, J., Lyu, H., Pan, F., Shang, D., Chen, J., Hu, S., & Huang, M. (2021). Distinguishing hypochondriasis and schizophrenia using regional homogeneity: A resting-state fMRI study and support vector machine analysis. *Acta Neuropsychiatrica*, *33*(4), 182–190. https://doi.org/10.1017/neu.2021.9

Jo, H. J., Gotts, S. J., Reynolds, R. C., Bandettini, P. A., Martin, A., Cox, R. W., & Saad, Z. S. (2013). Effective preprocessing procedures virtually eliminate distance-dependent motion artifacts in resting state fMRI. *Journal of Applied Mathematics*, *2013*, 1–9. https://doi.org/10.1155/2013/935154

Jo, H. J., Saad, Z. S., Simmons, W. K., Milbury, L. A., & Cox, R. W. (2010). Mapping sources of correlation in resting state fMRI, with artifact detection and removal. *NeuroImage*, *52*(2), 571–582. https://doi.org/10.1016/j.neuroimage.2010.04.246

Johnson, M. H., Griffin, R., Csibra, G., Halit, H., Farroni, T., De Haan, M., Tucker, L. A., Baron–Cohen, S., & Richards, J. (2005). The emergence of the social brain network: Evidence from typical and atypical development. *Development and Psychopathology*, *17*(03). https://doi.org/10.1017/S0954579405050297

Johnson-Frey, S. H., Maloof, F. R., Newman-Norlund, R., Farrer, C., Inati, S., & Grafton, S. T. (2003). Actions or hand-object interactions? Human inferior frontal cortex and action observation. *Neuron*, *39*(6), 1053–1058. https://doi.org/fptbbz

Joseph, R. M., & Tanaka, J. (2003). Holistic and part-based face recognition in children with autism. *Journal of Child Psychology and Psychiatry*, *44*(4), 529–542. https://doi.org/dkxd99

Joshi, G., Arnold Anteraper, S., Patil, K. R., Semwal, M., Goldin, R. L., Furtak, S. L., Chai, X. J., Saygin, Z. M., Gabrieli, J. D. E., Biederman, J., & Whitfield-Gabrieli, S. (2017). Integration and segregation of default mode network resting-state functional connectivity in transition-age males with high-functioning autism spectrum disorder: A proof-of-concept study. *Brain Connectivity*, *7*(9), 558–573. https://doi.org/ggth49

Jousmäki, V. (2000). Tracking functions of cortical networks on a millisecond timescale. *Neural Networks*, *13*(8), 883–889. https://doi.org/10.1016/S0893-6080(00)00061-7

Joutsa, J., Corp, D. T., & Fox, M. D. (2022). Lesion network mapping for symptom localization: Recent developments and future directions. *Current Opinion in Neurology*, *35*(4), 453–459. https://doi.org/10.1097/WCO.0000000000001085

Joutsa, J., Moussawi, K., Siddiqi, S. H., Abdolahi, A., Drew, W., Cohen, A. L., Ross, T. J., Deshpande, H. U., Wang, H. Z., Bruss, J., Stein, E. A., Volkow, N. D., Grafman, J. H., van Wijngaarden, E., Boes, A. D., & Fox, M. D. (2022). Brain lesions disrupting addiction map to a common human brain circuit. *Nature Medicine*, *28*(6), 1249–1255. https://doi.org/10.1038/s41591-022-01834-y

Jung, M., Mody, M., Saito, D. N., Tomoda, A., Okazawa, H., Wada, Y., & Kosaka, H. (2015). Sex differences in the default mode network with regard to autism spectrum traits: A resting state fMRI study. *PLOS ONE*, *10*(11), e0143126. https://doi.org/f8dxkp

Jussila, K., Junttila, M., Kielinen, M., Ebeling, H., Joskitt, L., Moilanen, I., & Mattila, M.-L. (2019). Sensory abnormality and quantitative autism traits in children with and without autism spectrum disorder in an epidemiological population. *Journal of Autism and Developmental Disorders*. https://doi.org/kdxt

Just, M. A., Cherkassky, V. L., Buchweitz, A., Keller, T. A., & Mitchell, T. M. (2014). Identifying autism from neural representations of social interactions: Neurocognitive markers of autism. *PLOS ONE*, *9*(12), e113879. https://doi.org/gng7jx

Just, M. A., Cherkassky, V. L., Keller, T. A., Kana, R. K., & Minshew, N. J. (2007). Functional and Anatomical Cortical Underconnectivity in Autism: Evidence from an fMRI Study of an Executive Function Task and Corpus Callosum Morphometry. *Cerebral Cortex*, *17*(4), 951–961. https://doi.org/10.1093/cercor/bhl006

Kadesjö, B., Gillberg, C., & Hagberg, B. (1999). Brief report: Autism and Asperger syndrome in seven-year-old children: a total population study. *Journal of Autism and Developmental Disorders*, *29*(4), 327–331. https://doi.org/10.1023/a:1022115520317

Kala, S., Rolison, M. J., Trevisan, D. A., Naples, A. J., Pelphrey, K., Ventola, P., & McPartland, J. C. (2021). Brief report: Preliminary evidence of the N170 as a biomarker of response to treatment in autism spectrum disorder. *Frontiers in Psychiatry*, *12*. https://doi.org/gk864h

Kaldy, Z., Giserman, I., Carter, A. S., & Blaser, E. (2016). The mechanisms underlying the ASD advantage in visual search. *Journal of Autism and Developmental Disorders*, *46*(5), 1513–1527. https://doi.org/f8hs97

Kam, T.-E., Suk, H.-I., & Lee, S.-W. (2017). Multiple functional networks modeling for autism spectrum disorder diagnosis. *Human Brain Mapping*, *38*(11), 5804–5821. https://doi.org/gm9v6v

Kaminski, M., Brzezicka, A., Kaminski, J., & Blinowska, K. J. (2016). Measures of coupling between neural populations based on Granger causality principle. *Frontiers in Computational Neuroscience*, *10*, 114. https://doi.org/gdvhtv

Kamps, F. S., Hendrix, C. L., Brennan, P. A., & Dilks, D. D. (2020). Connectivity at the origins of domain specificity in the cortical face and place networks. *Proceedings of the National Academy of Sciences of the United States of America*, *117*(11), 6163–6169. https://doi.org/10.1073/pnas.1911359117

Kana, R. K., Keller, T. A., Minshew, N. J., & Just, M. A. (2007). Inhibitory control in high-functioning autism: Decreased activation and underconnectivity in inhibition networks. *Biological Psychiatry*, *62*(3), 198–206. https://doi.org/d5v3mn

Kana, R. K., Liu, Y., Williams, D. L., Keller, T. A., Schipul, S. E., Minshew, N. J., & Just, M. A. (2013). The local, global, and neural aspects of visuospatial processing in autism spectrum disorders. *Neuropsychologia*, *51*(14), 2995–3003. https://doi.org/f5pcqb

Karahanoğlu, F. I., & Van De Ville, D. (2015). Transient brain activity disentangles fMRI resting-state dynamics in terms of spatially and temporally overlapping networks. *Nature Communications*, *6*, 7751. https://doi.org/10.1038/ncomms8751

Kätsyri, J. (2006, December 15). *Human Recognition of Basic Emotions from Posed and Animated Dynamic Facial Expressions*. Doctoral Thesis. http://lib.tkk.fi/Diss/2006/isbn951228538X/

Kätsyri, J., & Sams, M. (2008). The effect of dynamics on identifying basic emotions from synthetic and natural faces. *International Journal of Human-Computer Studies*, *66*(4), 233–242. https://doi.org/10.1016/j.ijhcs.2007.10.001

Kaufman, J., Birmaher, B., Brent, D., Rao, U., Flynn, C., Moreci, P., Williamson, D., & Ryan, N. (1997). Schedule for affective disorders and schizophrenia for school-age children-present and lifetime version (K-SADS-PL): Initial reliability and validity data. *Journal of the American Academy of Child & Adolescent Psychiatry*, *36*(7), 980–988. https://doi.org/dbr6hc

Kauppi, J.-P., Pajula, J., & Tohka, J. (2014). A versatile software package for inter-subject correlation based analyses of fMRI. *Frontiers in Neuroinformatics*, *8*. https://doi.org/kdxv

Keilholz, S. D., Pan, W.-J., Billings, J., Nezafati, M., & Shakil, S. (2017). Noise and non-neuronal contributions to the BOLD signal: Applications to and insights from animal studies. *NeuroImage*, *154*, 267–281. https://doi.org/10.1016/j.neuroimage.2016.12.019

Kendall, M., & Gibbons, J. D. (1990). *Rank Correlation Methods (5th Edition)*. Edward Arnold, London.

Kennedy, D. P., & Courchesne, E. (2008a). Functional abnormalities of the default network during self- and other-reflection in autism. *Social Cognitive & Affective Neuroscience*, *3*(2), 177–190. https://doi.org/10.1093/scan/nsn011

Kennedy, D. P., & Courchesne, E. (2008b). The intrinsic functional organization of the brain is altered in autism. *NeuroImage*, *39*(4), 1877–1885. https://doi.org/ckr535

Kennedy, D. P., Redcay, E., & Courchesne, E. (2006). Failing to deactivate: Resting functional abnormalities in autism. *Proceedings of the National Academy of Sciences*, *103*(21), 8275–8280. https://doi.org/bkfgdp

Keown, C. L., Shih, P., Nair, A., Peterson, N., Mulvey, M. E., & Müller, R.-A. (2013). Local functional overconnectivity in posterior brain regions Is associated with symptom severity in autism spectrum disorders. *Cell Reports*, *5*(3), 567–572. https://doi.org/ggkdxz

Khodatars, M., Shoeibi, A., Sadeghi, D., Ghaasemi, N., Jafari, M., Moridian, P., Khadem, A., Alizadehsani, R., Zare, A., Kong, Y., Khosravi, A., Nahavandi, S., Hussain, S., Acharya, U. R., & Berk, M. (2021). Deep learning for neuroimaging-based diagnosis and rehabilitation of Autism Spectrum Disorder: A review. *Computers in Biology and Medicine*, *139*, 104949. https://doi.org/10.1016/j.compbiomed.2021.104949

Kientz, M. A., & Dunn, W. (1997). A comparison of the performance of children with and without autism on the Sensory Profile. *The American Journal of Occupational Therapy: Official Publication of the American Occupational Therapy Association*, *51*(7), 530–537. https://doi.org/10.5014/ajot.51.7.530

Kim, M., Kim, H., Huang, Z., Mashour, G. A., Jordan, D., Ilg, R., & Lee, U. (2021). Criticality creates a functional platform for network transitions between internal and external processing modes in the human brain. *Frontiers in Systems Neuroscience*, *15*. https://doi.org/kdxw

Kim, S.-G., & Ogawa, S. (2012). Biophysical and physiological origins of blood oxygenation level-dependent fMRI signals. *Journal of Cerebral Blood Flow and Metabolism*, *32*(7), 1188–1206. https://doi.org/10.1038/jcbfm.2012.23

Kiviniemi, V., Kantola, J.-H., Jauhiainen, J., Hyvärinen, A., & Tervonen, O. (2003). Independent component analysis of nondeterministic fMRI signal sources. *NeuroImage*, *19*(2), 253–260. https://doi.org/10.1016/S1053-8119(03)00097-1

Kiviniemi, V., Starck, T., Remes, J., Long, X., Nikkinen, J., Haapea, M., Veijola, J., Moilanen, I., Isohanni, M., Zang, Y.-F., & Tervonen, O. (2009). Functional segmentation of the brain cortex using high model order group PICA. *Human Brain Mapping*, *30*(12), 3865–3886.

Kiviniemi, V., Vire, T., Remes, J., Elseoud, A. A., Starck, T., Tervonen, O., & Nikkinen, J. (2011). A sliding time-window ICA reveals spatial variability of the default mode network in time. *Brain Connectivity*, *1*(4), 339–347. https://doi.org/ccj8wq

Kiviniemi, V., Wang, X., Korhonen, V., Keinänen, T., Tuovinen, T., Autio, J., LeVan, P., Keilholz, S., Zang, Y.-F., Hennig, J., & Nedergaard, M. (2016). Ultra-fast magnetic resonance encephalography of physiological brain activity—Glymphatic pulsation mechanisms? *Journal of Cerebral Blood Flow and Metabolism: Official Journal of the International Society of Cerebral Blood Flow and Metabolism*, *36*(6), 1033–1045. https://doi.org/10.1177/0271678X15622047

Kleinhans, N. M., Müller, R.-A., Cohen, D. N., & Courchesne, E. (2008). Atypical functional lateralization of language in autism spectrum disorders. *Brain Research*, *1221*, 115–125. https://doi.org/10.1016/j.brainres.2008.04.080

Koehler, R. C., Roman, R. J., & Harder, D. R. (2009). Astrocytes and the regulation of cerebral blood flow. *Trends in Neurosciences*, *32*(3), 160–169. https://doi.org/c8jb2k

Kotila, A., Järvelä, M., Korhonen, V., Loukusa, S., Hurtig, T., Ebeling, H., Kiviniemi, V., & Raatikainen, V. (2020). Atypical inter-network deactivation associated with the posterior default-mode network in autism spectrum disorder. *Autism Research*, *14*(2). https://doi.org/kdxx

Kovarski, K., Mennella, R., Wong, S. M., Dunkley, B. T., Taylor, M. J., & Batty, M. (2019). Enhanced early visual responses during implicit emotional faces processing in autism spectrum disorder. *Journal of Autism and Developmental Disorders*, *49*(3), 871–886. https://doi.org/kdxz

Kozhemiako, N., Nunes, A. S., Vakorin, V., Iarocci, G., Ribary, U., & Doesburg, S. M. (2020). Alterations in local connectivity and their developmental trajectories in autism spectrum disorder: Does being female matter? *Cerebral Cortex*, *30*(9), 5166–5179. https://doi.org/10.1093/cercor/bhaa109

Krasnow, B., Tamm, L., Greicius, M. D., Yang, T. T., Glover, G. H., Reiss, A. L., & Menon, V. (2003). Comparison of fMRI activation at 3 and 1.5 T during perceptual, cognitive, and affective processing. *NeuroImage*, *18*(4), 813–826. https://doi.org/10.1016/S1053-8119(03)00002-8

Krüger, G., Kastrup, A., & Glover, G. H. (2001). Neuroimaging at 1.5 T and 3.0 T: Comparison of oxygenation-sensitive magnetic resonance imaging. *Magnetic Resonance in Medicine*, *45*(4), 595–604. https://doi.org/10.1002/mrm.1081

Kucyi, A., Schrouff, J., Bickel, S., Foster, B. L., Shine, J. M., & Parvizi, J. (2018). Intracranial electrophysiology reveals reproducible intrinsic functional connectivity within human brain networks. *The Journal of Neuroscience*, *38*(17), 4230–4242. https://doi.org/10.1523/JNEUROSCI.0217-18.2018

Kupis, L., Goodman, Z. T., Kircher, L., Romero, C., Dirks, B., Chang, C., Nomi, J. S., & Uddin, L. Q. (2021). Altered patterns of brain dynamics linked with body mass index in youth with autism. *Autism Research*, *14*(5), 873–886. https://doi.org/10.1002/aur.2488

Kupis, L., Romero, C., Dirks, B., Hoang, S., Parladé, M. V., Beaumont, A. L., Cardona, S. M., Alessandri, M., Chang, C., Nomi, J. S., & Uddin, L. Q. (2020). Evoked and intrinsic brain network dynamics in children with autism spectrum disorder. *NeuroImage: Clinical*, *28*, 102396. https://doi.org/10.1016/j.nicl.2020.102396

Kuusikko, S., Haapsamo, H., Jansson-Verkasalo, E., Hurtig, T., Mattila, M.-L., Ebeling, H., Jussila, K., Bölte, S., & Moilanen, I. (2009). Emotion recognition in children and adolescents with autism spectrum disorders. *Journal of Autism and Developmental Disorders*, *39*(6), 938–945. https://doi.org/10.1007/s10803-009-0700-0

Kuusikko, S., Pollock-Wurman, R., Jussila, K., Carter, A. S., Mattila, M.-L., Ebeling, H., Pauls, D. L., & Moilanen, I. (2008). Social anxiety in high-functioning children and adolescents with autism and Asperger syndrome. *Journal of Autism and Developmental Disorders*, *38*(9), 1697–1709. https://doi.org/bqpdf4

Kwong, K. K., Belliveau, J. W., Chesler, D. A., Goldberg, I. E., Weisskoff, R. M., Poncelet, B. P., Kennedy, D. N., Hoppel, B. E., Cohen, M. S., & Turner, R. (1992). Dynamic magnetic resonance imaging of human brain activity during primary sensory stimulation. *Proceedings of the National Academy of Sciences*, *89*(12), 5675–5679. https://doi.org/10.1073/pnas.89.12.5675

LaBar, K. S., Crupain, M. J., Voyvodic, J. T., & McCarthy, G. (2003). Dynamic perception of facial affect and identity in the human brain. *Cerebral Cortex*, *13*(10), 1023–1033. https://doi.org/cp8pft

Lan, Z., Xu, S., Wu, Y., Xia, L., Hua, K., Li, M., Liu, M., Yin, Y., Li, C., Huang, S., Feng, Y., Jiang, G., & Wang, T. (2021). Alterations of regional homogeneity in preschool boys with autism spectrum disorders. *Frontiers in Neuroscience*, *15*. https://doi.org/kdx2

Lanka, P., Rangaprakash, D., Dretsch, M. N., Katz, J. S., Denney, T. S., & Deshpande, G. (2020). Supervised machine learning for diagnostic classification from large-scale neuroimaging datasets. *Brain Imaging and Behavior*, *14*(6), 2378–2416. https://doi.org/10.1007/s11682-019-00191-8

Lanka, P., Rangaprakash, D., Gotoor, S. S. R., Dretsch, M. N., Katz, J. S., Denney, T. S., & Deshpande, G. (2020). MALINI (Machine Learning in NeuroImaging): A MATLAB toolbox for aiding clinical diagnostics using resting-state fMRI data. *Data in Brief*, *29*, 105213. https://doi.org/10.1016/j.dib.2020.105213

Lassalle, A., Zürcher, N. R., Porro, C. A., Benuzzi, F., Hippolyte, L., Lemonnier, E., Åsberg Johnels, J., & Hadjikhani, N. (2019). Influence of anxiety and alexithymia on brain activations associated with the perception of others' pain in autism. *Social Neuroscience*, *14*(3), 359–377. https://doi.org/10.1080/17470919.2018.1468358

Laumann, T. O., Snyder, A. Z., Mitra, A., Gordon, E. M., Gratton, C., Adeyemo, B., Gilmore, A. W., Nelson, S. M., Berg, J. J., Greene, D. J., McCarthy, J. E., Tagliazucchi, E., Laufs, H., Schlaggar, B. L., Dosenbach, N. U. F., & Petersen, S. E. (2017). On the stability of BOLD fMRI correlations. *Cerebral Cortex*, *27*(10), 4719–4732. https://doi.org/f9p8v2

Lauterbur, P. C. (1973). Image formation by induced local interactions: Examples employing nuclear magnetic resonance. *Nature*, *242*(5394), 190–191. https://doi.org/dznwr5

Legendre, P. (2010). Coefficient of concordance. In *Encyclopedia of Research Design* (Vol. 1, pp. 164–169). SAGE Publications, Inc. http://adn.biol.umontreal.ca/ ~numericalecology/ Reprints/Legendre_Coefficient_of_concordance_2010.pdf

Lewis, L. D., Setsompop, K., Rosen, B. R., & Polimeni, J. R. (2018). Stimulus-dependent hemodynamic response timing across the human subcortical-cortical visual pathway identified through high spatiotemporal resolution 7T fMRI. *NeuroImage*, *181*, 279–291. https://doi.org/10.1016/j.neuroimage.2018.06.056

Li, G., Rossbach, K., Jiang, W., & Du, Y. (2018). Resting-state brain activity in Chinese boys with low functioning autism spectrum disorder. *Annals of General Psychiatry*, *17*(1), 47. https://doi.org/10.1186/s12991-018-0217-z

Li, J., Kronemer, S. I., Herman, W. X., Kwon, H., Ryu, J. H., Micek, C., Wu, Y., Gerrard, J., Spencer, D. D., & Blumenfeld, H. (2019). Default mode and visual network activity in an attention task: Direct measurement with intracranial EEG. *NeuroImage*, *201*, 116003. https://doi.org/10.1016/j.neuroimage.2019.07.016

Li, L., He, C., Jian, T., Guo, X., Xiao, J., Li, Y., Chen, H., Kang, X., Chen, H., & Duan, X. (2020). Attenuated link between the medial prefrontal cortex and the amygdala in children with autism spectrum disorder: Evidence from effective connectivity within the "social brain." *Progress in Neuro-Psychopharmacology & Biological Psychiatry*, 110147. https://doi.org/10.1016/j.pnpbp.2020.110147

Li, T., Fu, Z., Liu, X., Qi, S., Calhoun, V. D., & Sui, J. (2019). Multimodal neuroimaging patterns associated with social responsiveness impairment in autism: A replication study. *2019 IEEE 16th International Symposium on Biomedical Imaging (ISBI 2019)*, 409–413. https://doi.org/kdx6

Li, X., Zang, Y.-F., & Zhang, H. (2015). Exploring dynamic brain functional networks using continuous "state-related" functional MRI. *BioMed Research International*, *2015*, 1–8. https://doi.org/gb85kk

Liang, Y., Liu, B., & Zhang, H. (2021). A convolutional neural network combined with prototype learning framework for brain functional network classification of autism spectrum disorder. *IEEE Transactions on Neural Systems and Rehabilitation Engineering*, *29*, 2193–2202. https://doi.org/kdx7

Liu, D., Dong, Z., Zuo, X., Wang, J., & Zang, Y. (2013). Eyes-open/Eyes-closed dataset sharing for reproducibility evaluation of resting state fMRI data analysis methods. *Neuroinformatics*, *11*(4), 469–476. https://doi.org/ggbwfj

Liu J., Mei T., Yan C., Zhou H., Chen X., Li L., Lu B., Shen Y., & Chen N. (2018). Aberrant dynamics of spontaneous brain activity and its integration in patients with autism spectrum disorder. *Chinese Science Bulletin*, *63*(15), 1452–1463. https://doi.org/gprjkb

Liu, M., Li, B., & Hu, D. (2021). Autism spectrum disorder studies using fMRI data and machine learning: A review. *Frontiers in Neuroscience*, *15*. https://doi.org/kdx8

Liu, T. T. (2017). Reprint of 'Noise contributions to the fMRI signal: An Overview'. *NeuroImage*, *154*, 4–14. https://doi.org/10.1016/j.neuroimage.2017.05.031

Liu, X., Chang, C., & Duyn, J. H. (2013). Decomposition of spontaneous brain activity into distinct fMRI co-activation patterns. *Frontiers in Systems Neuroscience*, *7*. https://doi.org/10.3389/fnsys.2013.00101

Liu, X., & Duyn, J. H. (2013). Time-varying functional network information extracted from brief instances of spontaneous brain activity. *Proceedings of the National Academy of Sciences*, *110*(11), 4392–4397. https://doi.org/10.1073/pnas.1216856110

Liu, X., Zhang, N., Chang, C., & Duyn, J. H. (2018). Co-activation patterns in resting-state fMRI signals. *NeuroImage*, *180*, 485–494. https://doi.org/gd6zxq

Liu, X., Zhu, X.-H., Qiu, P., & Chen, W. (2012). A correlation-matrix-based hierarchical clustering method for functional connectivity analysis. *Journal of Neuroscience Methods*, *211*(1), 94–102. https://doi.org/10.1016/j.jneumeth.2012.08.016

Liu, Y., Wang, K., Yu, C., He, Y., Zhou, Y., Liang, M., Wang, L., & Jiang, T. (2008). Regional homogeneity, functional connectivity and imaging markers of Alzheimer's disease: A review of resting-state fMRI studies. *Neuropsychologia*, *46*(6), 1648–1656. https://doi.org/10.1016/j.neuropsychologia.2008.01.027

Logothetis, N. K. (2008). What we can do and what we cannot do with fMRI. *Nature*, *453*(7197), 869–878. https://doi.org/10.1038/nature06976

Logothetis, N. K., Pauls, J., Augath, M., Trinath, T., & Oeltermann, A. (2001). Neurophysiological investigation of the basis of the fMRI signal. *Nature*, *412*(6843), 150–157. https://doi.org/10.1038/35084005

Logothetis, N. K., & Wandell, B. A. (2004). Interpreting the BOLD signal. *Annual Review of Physiology*, *66*(1), 735–769. https://doi.org/d7m4d5

Long, X.-Y., Zuo, X.-N., Kiviniemi, V., Yang, Y., Zou, Q.-H., Zhu, C.-Z., Jiang, T.-Z., Yang, H., Gong, Q.-Y., Wang, L., Li, K.-C., Xie, S., & Zang, Y.-F. (2008). Default mode network as revealed with multiple methods for resting-state functional MRI analysis. *Journal of Neuroscience Methods*, *171*(2), 349–355. https://doi.org/cpr8cj

Loomes, R., Hull, L., & Mandy, W. P. L. (2017). What is the male-to-female ratio in autism spectrum disorder? A systematic review and meta-analysis. *Journal of the American Academy of Child & Adolescent Psychiatry*, *56*(6), 466–474. https://doi.org/gbg9sz

Lord, C., Charman, T., Havdahl, A., Carbone, P., Anagnostou, E., Boyd, B., Carr, T., de Vries, P. J., Dissanayake, C., Divan, G., Freitag, C. M., Gotelli, M. M., Kasari, C., Knapp, M., Mundy, P., Plank, A., Scahill, L., Servili, C., Shattuck, P., … McCauley, J. B. (2022). The Lancet Commission on the future of care and clinical research in autism. *The Lancet*, *399*(10321), 271–334. https://doi.org/10.1016/S0140-6736(21)01541-5

Lord, C., Rutter, M., DiLavore, P. C., & Risi, S. (2000). *Autism diagnostic observation schedule (ADOS)*. Los Angeles: Western Psychological Services.

Lord, C., Rutter, M., & LeCouteur, A. (1995). *Autism diagnostic interview-revised (3rd ed.)*. Los Angeles: Western Psychological Services.

Lowe, M. J., Mock, B. J., & Sorenson, J. A. (1998). Functional connectivity in single and multislice echoplanar imaging using resting-state fluctuations. *NeuroImage*, *7*(2), 119–132. https://doi.org/10.1006/nimg.1997.0315

Lu, J., Liu, H., Zhang, M., Wang, D., Cao, Y., Ma, Q., Rong, D., Wang, X., Buckner, R. L., & Li, K. (2011). Focal pontine lesions provide evidence that intrinsic functional connectivity reflects polysynaptic anatomical pathways. *Journal of Neuroscience*, *31*(42), 15065–15071. https://doi.org/bbf2jk

Ludwig, H. C., Dreha-Kulaczewski, S., & Bock, H. C. (2021). Neurofluids-Deep inspiration, cilia and preloading of the astrocytic network. *Journal of Neuroscience Research*, *99*(11), 2804–2821. https://doi.org/10.1002/jnr.24935

Lurie, D. J., Kessler, D., Bassett, D. S., Betzel, R. F., Breakspear, M., Kheilholz, S., Kucyi, A., Liégeois, R., Lindquist, M. A., McIntosh, A. R., Poldrack, R. A., Shine, J. M., Thompson, W. H., Bielczyk, N. Z., Douw, L., Kraft, D., Miller, R. L., Muthuraman, M., Pasquini, L., … Calhoun, V. D. (2020). Questions and controversies in the study of time-varying functional connectivity in resting fMRI. *Network Neuroscience*, *4*(1), 30–69. https://doi.org/10.1162/netn_a_00116

Ma, D., Peng, L., & Gao, X. (2023). Adaptive noise depression for functional brain network estimation. *Frontiers in Psychiatry*, *13*. https://www.frontiersin.org/articles/ 10.3389/fpsyt.2022.1100266

Ma, L., Liu, M., Xue, K., Ye, C., Man, W., Cheng, M., Liu, Z., Zhu, D., Liu, F., & Wang, J. (2022). Abnormal regional spontaneous brain activities in white matter in patients with autism spectrum disorder. *Neuroscience*, *490*, 1–10. https://doi.org/kdx9

Ma, X., Gu, H., & Zhao, J. (2021). Atypical gaze patterns to facial feature areas in autism spectrum disorders reveal age and culture effects: A meta-analysis of eye-tracking studies. *Autism Research*, *14*(12), 2625–2639. https://doi.org/10.1002/aur.2607

Maenner, M. J. (2020). Prevalence of autism spectrum disorder among children aged 8 years—Autism and developmental disabilities monitoring network, 11 sites, United States, 2016. *MMWR. Surveillance Summaries*, *69*. https://doi.org/d2jd

Mahmood, U., Rahman, M. M., Fedorov, A., Lewis, N., Fu, Z., Calhoun, V. D., & Plis, S. M. (2020). Whole MILC: Generalizing learned dynamics across tasks, datasets, and populations. In A. L. Martel, P. Abolmaesumi, D. Stoyanov, D. Mateus, M. A. Zuluaga, S. K. Zhou, D. Racoceanu, & L. Joskowicz (Eds.), *Medical Image Computing and Computer Assisted Intervention – MICCAI 2020* (pp. 407–417). Springer International Publishing. https://doi.org/kdzb

Mahmoudi, A., Takerkart, S., Regragui, F., Boussaoud, D., & Brovelli, A. (2012). Multivoxel pattern analysis for fMRI data: A review. *Computational and Mathematical Methods in Medicine*, *2012*, e961257. https://doi.org/gb8ng6

Malaia, E., Bates, E., Seitzman, B., & Coppess, K. (2016). Altered brain network dynamics in youths with autism spectrum disorder. *Experimental Brain Research*, *234*(12), 3425–3431. https://doi.org/10.1007/s00221-016-4737-y

Maltbie, E., Yousefi, B., Zhang, X., Kashyap, A., & Keilholz, S. (2022). Comparison of resting-state functional MRI methods for characterizing brain dynamics. *Frontiers in Neural Circuits*, *16*. https://www.frontiersin.org/article/10.3389/ fncir.2022.681544

Manning, C. D., Raghavan, P., & Schütze, H. (2008). *Introduction to information retrieval*. Cambridge University Press.

Manyukhina, V. O., Prokofyev, A. O., Galuta, I. A., Goiaeva, D. E., Obukhova, T. S., Schneiderman, J. F., Altukhov, D. I., Stroganova, T. A., & Orekhova, E. V. (2022). Globally elevated excitation–inhibition ratio in children with autism spectrum disorder and below-average intelligence. *Molecular Autism*, *13*(1), 20. https://doi.org/10.1186/s13229-022-00498-2

Marek, S., Siegel, J. S., Gordon, E. M., Raut, R. V., Gratton, C., Newbold, D. J., Ortega, M., Laumann, T. O., Adeyemo, B., Miller, D. B., Zheng, A., Lopez, K. C., Berg, J. J., Coalson, R. S., Nguyen, A. L., Dierker, D., Van, A. N., Hoyt, C. R., McDermott, K. B., … Dosenbach, N. U. F. (2018). Spatial and temporal organization of the individual human cerebellum. *Neuron*, *100*(4), 977-993.e7. https://doi.org/gfgk3g

Marek, S., Tervo-Clemmens, B., Calabro, F. J., Montez, D. F., Kay, B. P., Hatoum, A. S., Donohue, M. R., Foran, W., Miller, R. L., Hendrickson, T. J., Malone, S. M., Kandala, S., Feczko, E., Miranda-Dominguez, O., Graham, A. M., Earl, E. A., Perrone, A. J., Cordova, M., Doyle, O., … Dosenbach, N. U. F. (2022). Reproducible brain-wide association studies require thousands of individuals. *Nature*, *603*(7902), 654–660. https://doi.org/10.1038/s41586-022-04492-9

Margulies, D. S., Ghosh, S. S., Goulas, A., Falkiewicz, M., Huntenburg, J. M., Langs, G., Bezgin, G., Eickhoff, S. B., Castellanos, F. X., Petrides, M., Jefferies, E., & Smallwood, J. (2016). Situating the default-mode network along a principal gradient of macroscale cortical organization. *Proceedings of the National Academy of Sciences*, *113*(44), 12574–12579. https://doi.org/10.1073/pnas.1608282113

Marina, N., Christie, I. N., Korsak, A., Doronin, M., Brazhe, A., Hosford, P. S., Wells, J. A., Sheikhbahaei, S., Humoud, I., Paton, J. F. R., Lythgoe, M. F., Semyanov, A., Kasparov, S., & Gourine, A. V. (2020). Astrocytes monitor cerebral perfusion and control systemic circulation to maintain brain blood flow. *Nature Communications*, *11*(1), 131. https://doi.org/10.1038/s41467-019-13956-y

Markicevic, M., Fulcher, B. D., Lewis, C., Helmchen, F., Rudin, M., Zerbi, V., & Wenderoth, N. (2020). Cortical excitation:inhibition imbalance causes abnormal brain network dynamics as observed in neurodevelopmental disorders. *Cerebral Cortex*, *30*(9), 4922–4937. https://doi.org/10.1093/cercor/bhaa084

Marshall, E., Nomi, J. S., Dirks, B., Romero, C., Kupis, L., Chang, C., & Uddin, L. Q. (2020). Coactivation pattern analysis reveals altered salience network dynamics in children with autism spectrum disorder. *Network Neuroscience*, *4*(4), 1219–1234. https://doi.org/10.1162/netn_a_00163

Martineau, J., Andersson, F., Barthélémy, C., Cottier, J.-P., & Destrieux, C. (2010). Atypical activation of the mirror neuron system during perception of hand motion in autism. *Brain Research*, *1320*, 168–175. https://doi.org/10.1016/j.brainres.2010.01.035

Martini, M. I., Kuja-Halkola, R., Butwicka, A., Du Rietz, E., D'Onofrio, B. M., Happé, F., Kanina, A., Larsson, H., Lundström, S., Martin, J., Rosenqvist, M. A., Lichtenstein, P., & Taylor, M. J. (2022). Sex differences in mental health problems and psychiatric hospitalization in autistic young adults. *JAMA Psychiatry*, *79*(12), 1188–1198. https://doi.org/10.1001/jamapsychiatry.2022.3475

Marusak, H. A., Elrahal, F., Peters, C. A., Kundu, P., Lombardo, M. V., Calhoun, V. D., Goldberg, E. K., Cohen, C., Taub, J. W., & Rabinak, C. A. (2018). Mindfulness and dynamic functional neural connectivity in children and adolescents. *Behavioural Brain Research*, *336*, 211–218. https://doi.org/10.1016/j.bbr.2017.09.010

Matsui, T., Pham, T. Q., Jimura, K., & Chikazoe, J. (2022). On co-activation pattern analysis and non-stationarity of resting brain activity. *NeuroImage*, *249*, 118904. https://doi.org/10.1016/j.neuroimage.2022.118904

Mattila, M.-L., Hurtig, T., Haapsamo, H., Jussila, K., Kuusikko-Gauffin, S., Kielinen, M., Linna, S.-L., Ebeling, H., Bloigu, R., Joskitt, L., Pauls, D. L., & Moilanen, I. (2010). Comorbid psychiatric disorders associated with Asperger syndrome/high-functioning autism: A community- and clinic-based study. *Journal of Autism and Developmental Disorders*, *40*(9), 1080–1093. https://doi.org/10.1007/s10803-010-0958-2

Mattila, M.-L., Jussila, K., Kuusikko, S., Kielinen, M., Linna, S.-L., Ebeling, H., Bloigu, R., Joskitt, L., Pauls, D., & Moilanen, I. (2009). When does the Autism Spectrum Screening Questionnaire (ASSQ) predict autism spectrum disorders in primary school-aged children? *European Child & Adolescent Psychiatry*, *18*(8), 499–509. https://doi.org/10.1007/s00787-009-0044-5

Mattila, M.-L., Jussila, K., Linna, S.-L., Kielinen, M., Bloigu, R., Kuusikko-Gauffin, S., Joskitt, L., Ebeling, H., Hurtig, T., & Moilanen, I. (2012). Validation of the Finnish Autism Spectrum Screening Questionnaire (ASSQ) for clinical settings and total population screening. *Journal of Autism and Developmental Disorders*, *42*(10), 2162–2180. https://doi.org/10.1007/s10803-012-1464-5

Mattila, M.-L., Kielinen, M., Jussila, K., Linna, S.-L., Bloigu, R., Ebeling, H., & Moilanen, I. (2007). An epidemiological and diagnostic study of Asperger syndrome according to four sets of diagnostic criteria. *Journal of the American Academy of Child & Adolescent Psychiatry*, *46*(5), 636–646. https://doi.org/10.1097/chi.0b013e318033ff42

Mattila, M.-L., Kielinen, M., Linna, S.-L., Jussila, K., Ebeling, H., Bloigu, R., Joseph, R. M., & Moilanen, I. (2011). Autism spectrum disorders according to DSM-IV-TR and comparison with DSM-5 draft criteria: An epidemiological study. *Journal of the American Academy of Child & Adolescent Psychiatry*, *50*(6), 583-592.e11. https://doi.org/c7r348

Maximo, J. O., Keown, C. L., Nair, A., & Müller, R.-A. (2013). Approaches to local connectivity in autism using resting state functional connectivity MRI. *Frontiers in Human Neuroscience*, *7*. https://doi.org/10.3389/fnhum.2013.00605

McKinnon, C. J., Eggebrecht, A. T., Todorov, A., Wolff, J. J., Elison, J. T., Adams, C. M., Snyder, A. Z., Estes, A. M., Zwaigenbaum, L., Botteron, K. N., McKinstry, R. C., Marrus, N., Evans, A., Hazlett, H. C., Dager, S. R., Paterson, S. J., Pandey, J., Schultz, R. T., Styner, M. A., … Pruett, J. R. (2019). Restricted and repetitive behavior and brain functional connectivity in infants at risk for developing autism spectrum disorder. *Biological Psychiatry: Cognitive Neuroscience and Neuroimaging*, *4*(1), 50–61. https://doi.org/ggsdx6

Meigel, F. J., Cha, P., Brenner, M. P., & Alim, K. (2019). Robust increase in supply by vessel dilation in globally coupled microvasculature. *Physical Review Letters*, *123*(22), 228103. https://doi.org/10.1103/PhysRevLett.123.228103

Meyer, H. S., Schwarz, D., Wimmer, V. C., Schmitt, A. C., Kerr, J. N. D., Sakmann, B., & Helmstaedter, M. (2011). Inhibitory interneurons in a cortical column form hot zones of inhibition in layers 2 and 5A. *Proceedings of the National Academy of Sciences*, *108*(40), 16807–16812. https://doi.org/10.1073/pnas.1113648108

Mezer, A., Yovel, Y., Pasternak, O., Gorfine, T., & Assaf, Y. (2009). Cluster analysis of resting-state fMRI time series. *NeuroImage*, *45*(4), 1117–1125. https://doi.org/10.1016/j.neuroimage.2008.12.015

Miao, X., Li, Y., Zhou, X., Luo, Y., Paez, A. G., Liu, D., van Zijl, P. C. M., & Hua, J. (2023). Evaluation of T2-prepared blood oxygenation level dependent functional magnetic resonance imaging with an event-related task: Hemodynamic response function and reproducibility. *Frontiers in Neuroscience*, *17*, 1114045. https://doi.org/10.3389/fnins.2023.1114045

Miller, K. J., Weaver, K. E., & Ojemann, J. G. (2009). Direct electrophysiological measurement of human default network areas. *Proceedings of the National Academy of Sciences*, *106*(29), 12174–12177. https://doi.org/10.1073/pnas.0902071106

Milovanovic, M., & Grujicic, R. (2021). Electroencephalography in Assessment of Autism Spectrum Disorders: A Review. *Frontiers in Psychiatry*, *12*. https://www.frontiersin.org/articles/10.3389/fpsyt.2021.686021

Ministry of Social Affairs and Health. (2022, June 8). *The Client and Patient Safety Strategy and Implementation Plan 2022–2026* [Serial publication]. Ministry of Social Affairs and Health. https://julkaisut.valtioneuvosto.fi/handle/10024/164212

Mizuno, A., Villalobos, M. E., Davies, M. M., Dahl, B. C., & Müller, R.-A. (2006). Partially enhanced thalamocortical functional connectivity in autism. *Brain Research*, *1104*(1), 160–174. https://doi.org/10.1016/j.brainres.2006.05.064

Moon, H. S., Jiang, H., Vo, T. T., Jung, W. B., Vazquez, A. L., & Kim, S.-G. (2021). Contribution of excitatory and inhibitory neuronal activity to BOLD fMRI. *Cerebral Cortex*, *31*(9), 4053–4067. Scopus. https://doi.org/10.1093/cercor/bhab068

Morris, J. S., Ohman, A., & Dolan, R. J. (1998). Conscious and unconscious emotional learning in the human amygdala. *Nature*, *393*(6684), 467–470. https://doi.org/10.1038/30976

Morris, J. S., Öhman, A., & Dolan, R. J. (1999). A subcortical pathway to the right amygdala mediating "unseen" fear. *Proceedings of the National Academy of Sciences*, *96*(4), 1680–1685. https://doi.org/10.1073/pnas.96.4.1680

Mosier, K., & Bereznaya, I. (2001). Parallel cortical networks for volitional control of swallowing in humans. *Experimental Brain Research*, *140*(3), 280–289. https://doi.org/10.1007/s002210100813

Müller, R.-A., Kleinhans, N., Kemmotsu, N., Pierce, K., & Courchesne, E. (2003). Abnormal variability and distribution of functional maps in autism: An fMRI study of visuomotor learning. *American Journal of Psychiatry*, *160*(10), 1847–1862. https://doi.org/d53czv

Müllner, D. (2013). fastcluster: Fast hierarchical, agglomerative clustering routines for R and Python. *Journal of Statistical Software*, *53*(9), 1–18.

Murphy, K., & Fox, M. D. (2017). Towards a consensus regarding global signal regression for resting state functional connectivity MRI. *NeuroImage*, *154*, 169–173. https://doi.org/10.1016/j.neuroimage.2016.11.052

Murtagh, F., & Contreras, P. (2011). Methods of hierarchical clustering. *ArXiv Preprint ArXiv:1105.0121*. http://arxiv.org/abs/1105.0121

Murtagh, F., & Legendre, P. (2014). Ward's hierarchical agglomerative clustering method: Which algorithms implement Ward's criterion? *Journal of Classification*, *31*(3), 274–295. https://doi.org/10.1007/s00357-014-9161-z

Naghavi, H. R., Eriksson, J., Larsson, A., & Nyberg, L. (2007). The claustrum/insula region integrates conceptually related sounds and pictures. *Neuroscience Letters*, *422*(1), 77–80. https://doi.org/10.1016/j.neulet.2007.06.009

Nair, S., Jao Keehn, R. J., Berkebile, M. M., Maximo, J. O., Witkowska, N., & Müller, R.-A. (2018). Local resting state functional connectivity in autism: Site and cohort variability and the effect of eye status. *Brain Imaging and Behavior*, *12*(1), 168–179. https://doi.org/10.1007/s11682-017-9678-y

Naselaris, T., & Kay, K. N. (2015). Resolving ambiguities of MVPA using explicit models of representation. *Trends in Cognitive Sciences*, *19*(10), 551–554. https://doi.org/gfrhwp

Ne'eman, A. (2021). When disability is defined by behavior, outcome measures should not promote "passing." *AMA Journal of Ethics*, *23*(7), 569–575. https://doi.org/kdzc

Nelson, S. B., & Valakh, V. (2015). Excitatory/inhibitory balance and circuit homeostasis in autism spectrum disorders. *Neuron*, *87*(4), 684–698. https://doi.org/gg4t74

Neufeld, J., Hsu, C.-T., & Chakrabarti, B. (2019). Atypical reward-driven modulation of mimicry-related neural activity in autism. *Frontiers in Psychiatry*, *10*. https://doi.org/ggdscb

Neuwirth, E. (2014). *RColorBrewer: ColorBrewer Palettes*. https://CRAN.R-project.org/package=RColorBrewer

Nichols, T. E. (2013). *Notes on creating a standardized version of DVARS*. http://citeseerx.ist.psu.edu/viewdoc/download?doi=10.1.1.411.9059&rep=rep1&type=pdf

Nichols, T. E., & Holmes, A. P. (2002). Nonparametric permutation tests for functional neuroimaging: A primer with examples. *Human Brain Mapping*, *15*(1), 1–25. https://doi.org/10.1002/hbm.1058

Nobel Prize Outreach AB. (2023a). *The Nobel Prize in Physics 1952*. NobelPrize.Org. https://www.nobelprize.org/prizes/physics/1952/summary/

Nobel Prize Outreach AB. (2023b). *The Nobel Prize in Physiology or Medicine 2003*. NobelPrize.Org. https://www.nobelprize.org/prizes/medicine/2003/press-release/

Nomura, M., Ohira, H., Haneda, K., Iidaka, T., Sadato, N., Okada, T., & Yonekura, Y. (2004). Functional association of the amygdala and ventral prefrontal cortex during cognitive evaluation of facial expressions primed by masked angry faces: An event-related fMRI study. *NeuroImage*, *21*(1), 352–363. https://doi.org/fh7x3c

Numssen, O., Bzdok, D., & Hartwigsen, G. (2021). Functional specialization within the inferior parietal lobes across cognitive domains. *ELife*, *10*, e63591. https://doi.org/10.7554/eLife.63591

Ogawa, S., Lee, T. M., Kay, A. R., & Tank, D. W. (1990). Brain magnetic resonance imaging with contrast dependent on blood oxygenation. *Proceedings of the National Academy of Sciences*, *87*(24), 9868–9872. https://doi.org/10.1073/pnas.87.24.9868

Ogawa, S., Tank, D. W., Menon, R., Ellermann, J. M., Kim, S. G., Merkle, H., & Ugurbil, K. (1992). Intrinsic signal changes accompanying sensory stimulation: Functional brain mapping with magnetic resonance imaging. *Proceedings of the National Academy of Sciences*, *89*(13), 5951–5955. https://doi.org/10.1073/pnas.89.13.5951

Oliveira, Í. A. F., van der Zwaag, W., Raimondo, L., Dumoulin, S. O., & Siero, J. C. W. (2021). Comparing hand movement rate dependence of cerebral blood volume and BOLD responses at 7T. *NeuroImage*, *226*, 117623. https://doi.org/kdzf

Osterling, J., & Dawson, G. (1994). Early recognition of children with autism: A study of first birthday home videotapes. *Journal of Autism & Developmental Disorders*, *24*(3), 247–257. https://doi.org/10.1007/BF02172225

Pan, P., Zhan, H., Xia, M., Zhang, Y., Guan, D., & Xu, Y. (2017). Aberrant regional homogeneity in Parkinson's disease: A voxel-wise meta-analysis of resting-state functional magnetic resonance imaging studies. *Neuroscience & Biobehavioral Reviews*, *72*, 223–231. https://doi.org/10.1016/j.neubiorev.2016.11.018

Panisi, C., Guerini, F. R., Abruzzo, P. M., Balzola, F., Biava, P. M., Bolotta, A., Brunero, M., Burgio, E., Chiara, A., Clerici, M., Croce, L., Ferreri, C., Giovannini, N., Ghezzo, A., Grossi, E., Keller, R., Manzotti, A., Marini, M., Migliore, L., … Fanos, V. (2021). Autism spectrum disorder from the womb to adulthood: Suggestions for a paradigm shift. *Journal of Personalized Medicine*, *11*(2), 70. https://doi.org/kdzg

Paradis, E., & Schliep, K. (2018). ape 5.0: An environment for modern phylogenetics and evolutionary analyses in R. *Bioinformatics*, *35*, 526–528.

Parkes, L., Fulcher, B., Yücel, M., & Fornito, A. (2018). An evaluation of the efficacy, reliability, and sensitivity of motion correction strategies for resting-state functional MRI. *NeuroImage*, *171*, 415–436. https://doi.org/10.1016/j.neuroimage.2017.12.073

Patenaude, B., Smith, S. M., Kennedy, D. N., & Jenkinson, M. (2011). A Bayesian model of shape and appearance for subcortical brain segmentation. *NeuroImage*, *56*(3), 907–922. https://doi.org/10.1016/j.neuroimage.2011.02.046

Patriat, R., Molloy, E. K., Meier, T. B., Kirk, G. R., Nair, V. A., Meyerand, M. E., Prabhakaran, V., & Birn, R. M. (2013). The effect of resting condition on resting-state fMRI reliability and consistency: A comparison between resting with eyes open, closed, and fixated. *NeuroImage*, *78*, 463–473. https://doi.org/f43c25

Pellegrino, G., Schuler, A.-L., Arcara, G., Di Pino, G., Piccione, F., & Kobayashi, E. (2022). Resting state network connectivity is attenuated by fMRI acoustic noise. *NeuroImage*, *247*, 118791. https://doi.org/10.1016/j.neuroimage.2021.118791

Pelphrey, K. A., Morris, J. P., McCarthy, G., & LaBar, K. S. (2007). Perception of dynamic changes in facial affect and identity in autism. *Social Cognitive and Affective Neuroscience*, *2*(2), 140–149. https://doi.org/10.1093/scan/nsm010

Pfeifer, J. H., Iacoboni, M., Mazziotta, J. C., & Dapretto, M. (2008). Mirroring others' emotions relates to empathy and interpersonal competence in children. *NeuroImage*, *39*(4), 2076–2085. https://doi.org/10.1016/j.neuroimage.2007.10.032

Philip, R. C. M., Dauvermann, M. R., Whalley, H. C., Baynham, K., Lawrie, S. M., & Stanfield, A. C. (2012). A systematic review and meta-analysis of the fMRI investigation of autism spectrum disorders. *Neuroscience & Biobehavioral Reviews*, *36*(2), 901–942. https://doi.org/10.1016/j.neubiorev.2011.10.008

Picci, G., Gotts, S. J., & Scherf, K. S. (2016). A theoretical rut: Revisiting and critically evaluating the generalized under/over-connectivity hypothesis of autism. *Developmental Science*, *19*(4), 524–549. https://doi.org/10.1111/desc.12467

Plewes, D. B., & Kucharczyk, W. (2012). Physics of MRI: A primer. *Journal of Magnetic Resonance Imaging*, *35*(5), 1038–1054. https://doi.org/10.1002/jmri.23642

Plitt, M., Barnes, K. A., & Martin, A. (2015). Functional connectivity classification of autism identifies highly predictive brain features but falls short of biomarker standards. *NeuroImage: Clinical*, *7*, 359–366. https://doi.org/10.1016/j.nicl.2014.12.013

Polimeni, J. R., & Lewis, L. D. (2021). Imaging faster neural dynamics with fast fMRI: A need for updated models of the hemodynamic response. *Progress in Neurobiology*, *207*, 102174. https://doi.org/10.1016/j.pneurobio.2021.102174

Port, R. G., Oberman, L. M., & Roberts, T. P. (2019). Revisiting the excitation/inhibition imbalance hypothesis of ASD through a clinical lens. *The British Journal of Radiology*, *92*(1101), 20180944. https://doi.org/10.1259/bjr.20180944

Power, J. D., Mitra, A., Laumann, T. O., Snyder, A. Z., Schlaggar, B. L., & Petersen, S. E. (2014). Methods to detect, characterize, and remove motion artifact in resting state fMRI. *NeuroImage*, *84*, 320–341. https://doi.org/10.1016/j.neuroimage.2013.08.048

Power, J. D., Schlaggar, B. L., & Petersen, S. E. (2015). Recent progress and outstanding issues in motion correction in resting state fMRI. *NeuroImage*, *105*, 536–551. https://doi.org/10.1016/j.neuroimage.2014.10.044

Preti, M. G., Bolton, T. A., & Van De Ville, D. (2017). The dynamic functional connectome: State-of-the-art and perspectives. *NeuroImage*, *160*, 41–54. https://doi.org/gcj5q7

Prinsen, J., & Alaerts, K. (2022). Broken or socially mistuned mirroring in ASD? An investigation via transcranial magnetic stimulation. *Autism Research*, *15*(6). https://doi.org/kdxr

Pruim, R. H. R., Mennes, M., Buitelaar, J. K., & Beckmann, C. F. (2015). Evaluation of ICA-AROMA and alternative strategies for motion artifact removal in resting state fMRI. *NeuroImage*, *112*, 278–287. https://doi.org/10.1016/j.neuroimage.2015.02.063

Pruim, R. H. R., Mennes, M., van Rooij, D., Llera, A., Buitelaar, J. K., & Beckmann, C. F. (2015). ICA-AROMA: A robust ICA-based strategy for removing motion artifacts from fMRI data. *NeuroImage*, *112*, 267–277. https://doi.org/f68wkq

Pukki, H. (2022, October 5). Autismin ja neurokirjon uusi, syrjimätön sanasto on julkaistu. *ASY*. https://asy.fi/autismin-ja-neurokirjon-uusi-syrjimaton-sanasto-on-julkaistu/

Purcell, E. M., Torrey, H. C., & Pound, R. V. (1946). Resonance absorption by nuclear magnetic moments in a solid. *Physical Review*, *69*(1–2), 37–38. https://doi.org/b3j56n

Qing, X., Gu, L., & Li, D. (2021). Abnormalities of localized connectivity in obsessive-compulsive disorder: A voxel-wise meta-analysis. *Frontiers in Human Neuroscience*, *15*. https://doi.org/kdzh

Qiu, X., Xu, W., Zhang, R., Yan, W., Ma, W., Xie, S., & Zhou, M. (2021). Regional homogeneity brain alterations in schizophrenia: An activation likelihood estimation meta-analysis. *Psychiatry Investigation*, *18*(8), 709–717. https://doi.org/kdzj

R Core Team. (2017). *R: A Language and Environment for Statistical Computing*. R Foundation for Statistical Computing. https://www.R-project.org/

Raatikainen, V., Korhonen, V., Borchardt, V., Huotari, N., Helakari, H., Kananen, J., Raitamaa, L., Joskitt, L., Loukusa, S., Hurtig, T., Ebeling, H., Uddin, L. Q., & Kiviniemi, V. (2020). Dynamic lag analysis reveals atypical brain information flow in autism spectrum disorder. *Autism Research: Official Journal of the International Society for Autism Research*, *13*(2), 244–258. https://doi.org/10.1002/aur.2218

Rabi, I. I., Zacharias, J. R., Millman, S., & Kusch, P. (1938). A New Method of Measuring Nuclear Magnetic Moment. *Physical Review*, *53*(4), 318–318. https://doi.org/10.1103/PhysRev.53.318

Rafiee, F., Rezvani Habibabadi, R., Motaghi, M., Yousem, D. M., & Yousem, I. J. (2022). Brain MRI in autism spectrum disorder: Narrative review and recent advances. *Journal of Magnetic Resonance Imaging*, *55*(6), 1613–1624. https://doi.org/gm9m69

Rahko, J. S., Paakki, J.-J., Starck, T., Nikkinen, J., Remes, J., Hurtig, T., Kuusikko-Gauffin, S., Mattila, M.-L., Jussila, K., Jansson-Verkasalo, E., Kätsyri, J., Sams, M., Pauls, D., Ebeling, H., Moilanen, I., Tervonen, O., & Kiviniemi, V. (2010). Functional mapping of dynamic happy and fearful facial expression processing in adolescents. *Brain Imaging and Behavior*, *4*(2), 164–176. https://doi.org/b9k45h

Rahko, J. S., Vuontela, V. A., Carlson, S., Nikkinen, J., Hurtig, T. M., Kuusikko-Gauffin, S., Mattila, M.-L., Jussila, K. K., Remes, J. J., Jansson-Verkasalo, E. M., Aronen, E. T., Pauls, D. L., Ebeling, H. E., Tervonen, O., Moilanen, I. K., & Kiviniemi, V. J. (2016). Attention and working memory in adolescents with autism spectrum disorder: A functional MRI study. *Child Psychiatry & Human Development*, *47*(3), 503–517. https://doi.org/f8n7b7

Raichle, M. E., MacLeod, A. M., Snyder, A. Z., Powers, W. J., Gusnard, D. A., & Shulman, G. L. (2001). A default mode of brain function. *Proceedings of the National Academy of Sciences*, *98*(2), 676–682. https://doi.org/10.1073/pnas.98.2.676

Raimondo, L., Oliveira, Ícaro A. F., Heij, J., Priovoulos, N., Kundu, P., Leoni, R. F., & van der Zwaag, W. (2021). Advances in resting state fMRI acquisitions for functional connectomics. *NeuroImage*, *243*, 118503. https://doi.org/gmqpwk

Rajna, Z., Kananen, J., Keskinarkaus, A., Seppänen, T., & Kiviniemi, V. (2015). Detection of short-term activity avalanches in human brain default mode network with ultrafast MR encephalography. *Frontiers in Human Neuroscience*, *9*. https://doi.org/kdzm

Ramnani, N. (2006). The primate cortico-cerebellar system: Anatomy and function. *Nature Reviews Neuroscience*, *7*(7), 511–522. https://doi.org/10.1038/nrn1953

Raval, V., Nguyen, K. P., Pinho, M., Dewey, R. B., Trivedi, M., & Montillo, A. A. (2022). Pitfalls and recommended strategies and metrics for suppressing motion artifacts in functional MRI. *Neuroinformatics*, *20*(4), 879–896. https://doi.org/kdzn

Ray, L., Iliff, J. J., & Heys, J. J. (2019). Analysis of convective and diffusive transport in the brain interstitium. *Fluids and Barriers of the CNS*, *16*(1), 6. https://doi.org/kdzp

Redcay, E. (2008). The superior temporal sulcus performs a common function for social and speech perception: Implications for the emergence of autism. *Neuroscience & Biobehavioral Reviews*, *32*(1), 123–142. https://doi.org/fgrd44

Ridley, B., Wirsich, J., Bettus, G., Rodionov, R., Murta, T., Chaudhary, U., Carmichael, D., Thornton, R., Vulliemoz, S., McEvoy, A., Wendling, F., Bartolomei, F., Ranjeva, J.-P., Lemieux, L., & Guye, M. (2017). Simultaneous intracranial EEG-fMRI shows inter-modality correlation in time-resolved connectivity within normal areas but not within epileptic regions. *Brain Topography*, *30*(5), 639–655. https://doi.org/gbth9f

Rizzolatti, G., & Sinigaglia, C. (2010). The functional role of the parieto-frontal mirror circuit: Interpretations and misinterpretations. *Nature Reviews Neuroscience*, *11*(4), 264–274. https://doi.org/10.1038/nrn2805

Robison, J. E. (2020). *The Limits of Neurodiversity | Psychology Today*. https://www.psychologytoday.com/us/blog/my-life-aspergers/202003/the-limits-neurodiversity

Rodgers, J. L., & Nicewander, W. A. (1988). Thirteen ways to look at the correlation coefficient. *The American Statistician*, *42*(1), 59–66. https://doi.org/dk75t9

Rorden, C., & Brett, M. (2000). Stereotaxic display of brain lesions. *Behavioural Neurology*, *12*(4), 191–200. https://doi.org/10.1155/2000/421719

Rubenstein, J. L. R., & Merzenich, M. M. (2003). Model of autism: Increased ratio of excitation/inhibition in key neural systems. *Genes, Brain and Behavior*, *2*(5), 255–267. https://doi.org/10.1034/j.1601-183X.2003.00037.x

Russell, J. A., & Barrett, L. F. (1999). Core affect, prototypical emotional episodes, and other things called emotion: Dissecting the elephant. *Journal of Personality and Social Psychology*, *76*(5), 805–819. https://doi.org/10.1037/0022-3514.76.5.805

Saarimäki, H., Glerean, E., Smirnov, D., Mynttinen, H., Jääskeläinen, I. P., Sams, M., & Nummenmaa, L. (2022). Classification of emotion categories based on functional connectivity patterns of the human brain. *NeuroImage*, *247*, 118800. https://doi.org/10.1016/j.neuroimage.2021.118800

Sadaghiani, S., Brookes, M. J., & Baillet, S. (2022). Connectomics of human electrophysiology. *NeuroImage*, *247*, 118788. https://doi.org/gnrwhm

Sakai, R., Winand, R., Verbeiren, T., Moere, A. V., & Aerts, J. (2014). dendsort: Modular leaf ordering methods for dendrogram representations in R. *F1000Research*, *3*. https://doi.org/10.12688/f1000research.4784.1

Santana, C. P., de Carvalho, E. A., Rodrigues, I. D., Bastos, G. S., de Souza, A. D., & de Brito, L. L. (2022). rs-fMRI and machine learning for ASD diagnosis: A systematic review and meta-analysis. *Scientific Reports*, *12*(1), 6030. https://doi.org/kdzw

Santarone, M. E., Zambrano, S., Zanotta, N., Mani, E., Minghetti, S., Pozzi, M., Villa, L., Molteni, M., & Zucca, C. (2023). EEG features in autism spectrum disorder: A retrospective analysis in a cohort of preschool children. *Brain Sciences*, *13*(2), 345. https://doi.org/kdzz

Sarlo, G. L., & Holton, K. F. (2021). Brain concentrations of glutamate and GABA in human epilepsy: A review. *Seizure*, *91*, 213–227. https://doi.org/kdz7

Sarovic, D. (2021). A unifying theory for autism: The pathogenetic triad as a theoretical framework. *Frontiers in Psychiatry*, *12*. https://doi.org/gnt3k5

Sato, W., & Aoki, S. (2006). Right hemispheric dominance in processing of unconscious negative emotion. *Brain and Cognition*, *62*(3), 261–266. https://doi.org/bwf6wh

Sato, W., Kochiyama, T., Yoshikawa, S., Naito, E., & Matsumura, M. (2004). Enhanced neural activity in response to dynamic facial expressions of emotion: An fMRI study. *Cognitive Brain Research*, *20*(1), 81–91. https://doi.org/ddzh3v

Scheel, N., Keller, J. N., Binder, E. F., Vidoni, E. D., Burns, J. M., Thomas, B. P., Stowe, A. M., Hynan, L. S., Kerwin, D. R., Vongpatanasin, W., Rossetti, H., Cullum, C. M., Zhang, R., & Zhu, D. C. (2022). Evaluation of noise regression techniques in resting-state fMRI studies using data of 434 older adults. *Frontiers in Neuroscience*, *16*, 1006056. https://doi.org/10.3389/fnins.2022.1006056

Scheibner, H. J., Bogler, C., Gleich, T., Haynes, J.-D., & Bermpohl, F. (2017). Internal and external attention and the default mode network. *NeuroImage*, *148*, 381–389. https://doi.org/10.1016/j.neuroimage.2017.01.044

Schmid, F., Barrett, M. J. P., Jenny, P., & Weber, B. (2019). Vascular density and distribution in neocortex. *NeuroImage*, *197*, 792–805. https://doi.org/gfwjp2

Schulte-Rüther, M., Greimel, E., Markowitsch, H. J., Kamp-Becker, I., Remschmidt, H., Fink, G. R., & Piefke, M. (2011). Dysfunctions in brain networks supporting empathy: An fMRI study in adults with autism spectrum disorders. *Social Neuroscience*, *6*(1), 1–21. https://doi.org/10.1080/17470911003708032

Schultz, R. T. (2005). Developmental deficits in social perception in autism: The role of the amygdala and fusiform face area. *International Journal of Developmental Neuroscience*, *23*(2), 125–141. https://doi.org/10.1016/j.ijdevneu.2004.12.012

Schultz, R. T., Gauthier, I., Klin, A., Fulbright, R., Anderson, A. W., Volkmar, F., Skudlarski, P., Lacadie, C., Cohen, D. J., & Gore, J. (2000). Abnormal ventral temporal cortical activity during face discrimination among individuals with autism and Asperger syndrome. *Archives of General Psychiatry*. https://doi.org/dsqjnw

Shafritz, K. M., Bregman, J. D., Ikuta, T., & Szeszko, P. R. (2015). Neural systems mediating decision-making and response inhibition for social and nonsocial stimuli in autism. *Progress in Neuro-Psychopharmacology and Biological Psychiatry*, *60*, 112–120. https://doi.org/10.1016/j.pnpbp.2015.03.001

Shen, J. (2014). *Tools for NIfTI and ANALYZE image—File Exchange—MATLAB Central*. https://se.mathworks.com/matlabcentral/fileexchange/8797-tools-for-nifti-and-analyze-image

Shukla, D. K., Keehn, B., & Müller, R. A. (2010). Regional homogeneity of fMRI time series in autism spectrum disorders. *Neuroscience Letters*, *476*(1), 46–51. https://doi.org/10.1016/j.neulet.2010.03.080

Shulman, G. L., & Fiez, J. A. (1997). Common blood flow changes across visual tasks: II. Decreases in cerebral cortex. *Journal of Cognitive Neuroscience*, *9*(5), 648. https://doi.org/10.1162/jocn.1997.9.5.648

Sigman, M., Dijamco, A., Gratier, M., & Rozga, A. (2004). Early detection of core deficits in autism. *Mental Retardation and Developmental Disabilities Research Reviews*, *10*(4), 221–233. https://doi.org/10.1002/mrdd.20046

Simmons, A., Matthews, S. C., Paulus, M. P., & Stein, M. B. (2008). Intolerance of uncertainty correlates with insula activation during affective ambiguity. *Neuroscience Letters*, *430*(2), 92–97. https://doi.org/10.1016/j.neulet.2007.10.030

Singhal, A. (2001). Modern information retrieval: A brief overview. *IEEE Data Eng. Bull.*, *24*(4), 35–43.

Sipola, T. (2020). *Aspergerin oireyhtymä voi olla vahvuus työelämässä – esimerkiksi tarkassa koodarin työssä autismin kirjon ihminen pärjää paremmin kuin moni muu*. Yle Uutiset. https://yle.fi/uutiset/3-11197771

Smith, S. M. (2002). Fast robust automated brain extraction. *Human Brain Mapping*, *17*(3), 143–155. https://doi.org/10.1002/hbm.10062

Smith, S. M., Fox, P. T., Miller, K. L., Glahn, D. C., Fox, P. M., Mackay, C. E., Filippini, N., Watkins, K. E., Toro, R., Laird, A. R., & others. (2009). Correspondence of the brain's functional architecture during activation and rest. *Proceedings of the National Academy of Sciences*, *106*(31), 13040–13045.

Smith, S. M., Jenkinson, M., Woolrich, M. W., Beckmann, C. F., Behrens, T. E. J., Johansen-Berg, H., Bannister, P. R., De Luca, M., Drobnjak, I., Flitney, D. E., Niazy, R. K., Saunders, J., Vickers, J., Zhang, Y., De Stefano, N., Brady, J. M., & Matthews, P. M. (2004). Advances in functional and structural MR image analysis and implementation as FSL. *NeuroImage*, *23*, S208–S219. https://doi.org/cbsrtg

Song, X.-W., Dong, Z.-Y., Long, X.-Y., Li, S.-F., Zuo, X.-N., Zhu, C.-Z., He, Y., Yan, C.-G., & Zang, Y.-F. (2011). REST: A toolkit for resting-state functional magnetic resonance imaging data processing. *PLOS ONE*, *6*(9), e25031. https://doi.org/c9vgbr

Sridharan, D., Levitin, D. J., & Menon, V. (2008). A critical role for the right fronto-insular cortex in switching between central-executive and default-mode networks. *Proceedings of the National Academy of Sciences of the United States of America*, *105*(34), 12569–12574. https://doi.org/10.1073/pnas.0800005105

Starck, T., Nikkinen, J., Rahko, J. S., Remes, J., Hurtig, T., Haapsamo, H., Jussila, K., Kuusikko-Gauffin, S., Mattila, M.-L., Jansson-Verkasalo, E., Pauls, D. L., Ebeling, H., Moilanen, I., Tervonen, O., & Kiviniemi, V. J. (2013). Resting state fMRI reveals a default mode dissociation between retrosplenial and medial prefrontal subnetworks in ASD despite motion scrubbing. *Frontiers in Human Neuroscience*, *7*. https://doi.org/10.3389/fnhum.2013.00802

Stark, C. E. L., & Squire, L. R. (2001). When zero is not zero: The problem of ambiguous baseline conditions in fMRI. *Proceedings of the National Academy of Sciences*, *98*(22), 12760–12766. https://doi.org/10.1073/pnas.221462998

Stephan, K. E., Weiskopf, N., Drysdale, P. M., Robinson, P. A., & Friston, K. J. (2007). Comparing hemodynamic models with DCM. *NeuroImage*, *38*(3), 387–401. https://doi.org/10.1016/j.neuroimage.2007.07.040

Stiernman, L. J., Grill, F., Hahn, A., Rischka, L., Lanzenberger, R., Lundmark, V. P., Riklund, K., Axelsson, J., & Rieckmann, A. (2021). Dissociations between glucose metabolism and blood oxygenation in the human default mode network revealed by simultaneous PET-fMRI. *Proceedings of the National Academy of Sciences of the United States of America*, *118*(27). https://doi.org/gk3vnv

Stogiannos, N., Carlier, S., Harvey-Lloyd, J. M., Brammer, A., Nugent, B., Cleaver, K., McNulty, J. P., dos Reis, C. S., & Malamateniou, C. (2022). A systematic review of person-centred adjustments to facilitate magnetic resonance imaging for autistic patients without the use of sedation or anaesthesia. *Autism*, *26*(4), 782–797. https://doi.org/10.1177/13623613211065542

Stojanoski, B., & Cusack, R. (2014). Time to wave good-bye to phase scrambling: Creating controlled scrambled images using diffeomorphic transformations. *Journal of Vision*, *14*(12), 6. https://doi.org/10.1167/14.12.6

Stroop, J. R. (1935). Studies of interference in serial verbal reactions. *Journal of Experimental Psychology*, *18*(6), 643–662. https://doi.org/10.1037/h0054651

Subbaraju, V., Sundaram, S., & Narasimhan, S. (2018). Identification of lateralized compensatory neural activities within the social brain due to autism spectrum disorder in adolescent males. *European Journal of Neuroscience*, *47*(6), 631–642. https://doi.org/10.1111/ejn.13634

Sung, M.-C., Ku, B., Leung, W., & MacDonald, M. (2022). The effect of physical activity interventions on executive function among people with neurodevelopmental disorders: A meta-analysis. *Journal of Autism and Developmental Disorders*, *52*(3), 1030–1050. https://doi.org/gnfq3w

Supekar, K., Ryali, S., Yuan, R., Kumar, D., de los Angeles, C., & Menon, V. (2022). Robust, generalizable, and interpretable artificial intelligence–derived brain fingerprints of autism and social communication symptom severity. *Biological Psychiatry*, *92*(8), 643–653. https://doi.org/kdz6

Syed, M. A., Yang, Z., Hu, X. P., & Deshpande, G. (2017). Investigating brain connectomic alterations in autism using the reproducibility of independent components derived from resting state functional MRI data. *Frontiers in Neuroscience*, *11*. https://doi.org/gfpjhs

Tagliazucchi, E., Balenzuela, P., Fraiman, D., & Chialvo, D. R. (2012). Criticality in large-scale brain fMRI dynamics unveiled by a novel point process analysis. *Frontiers in Physiology*, *3*. https://doi.org/10.3389/fphys.2012.00015

Tagliazucchi, E., Siniatchkin, M., Laufs, H., & Chialvo, D. R. (2016). The voxel-wise functional connectome can be efficiently derived from co-activations in a sparse spatio-temporal point-process. *Frontiers in Neuroscience*, *10*. https://doi.org/kd2b

Takarae, Y., Zanesco, A., Keehn, B., Chukoskie, L., Müller, R.-A., & Townsend, J. (2022). EEG microstates suggest atypical resting-state network activity in high-functioning children and adolescents with autism spectrum development. *Developmental Science*, *25*(4), e13231. https://doi.org/10.1111/desc.13231

Talairach, J., & Tournoux, P. (1988). *Co-planar Stereotaxic Atlas of the Human Brain: 3-dimensional Proportional System: An Approach to Cerebral Imaging*. G. Thieme. https://books.google.fi/books?id=pYFiQgAACAAJ

Tang, J. S. (2022). Editorial comment on “Diagnosing autism spectrum disorder in children using conventional MRI and apparent diffusion coefficient based deep learning algorithms.” *European Radiology*, *32*(2), 759–760. https://doi.org/gp6j99

Tettamanti, M., Paulesu, E., Scifo, P., Maravita, A., Fazio, F., Perani, D., & Marzi, C. A. (2002). Interhemispheric transmission of visuomotor information in humans: FMRI evidence. *Journal of Neurophysiology*, *88*(2), 1051–1058. https://doi.org/kd2c

Teunisse, J.-P., & de Gelder, B. (2003). Face processing in adolescents with autistic disorder: The inversion and composite effects. *Brain and Cognition*, *52*(3), 285–294. https://doi.org/10.1016/S0278-2626(03)00042-3

Thirion, B., Varoquaux, G., Dohmatob, E., & Poline, J.-B. (2014). Which fMRI clustering gives good brain parcellations? *Frontiers in Neuroscience*, *8*. https://doi.org/ggb6pr

Thomas, R. M., Gallo, S., Cerliani, L., Zhutovsky, P., El-Gazzar, A., & van Wingen, G. (2020). Classifying autism spectrum disorder using the temporal statistics of resting-state functional MRI data with 3D convolutional neural networks. *Frontiers in Psychiatry*, *11*, 440. https://doi.org/gk7q46

Thornburgh, C. L., Narayana, S., Rezaie, R., Bydlinski, B. N., Tylavsky, F. A., Papanicolaou, A. C., Choudhri, A. F., & Völgyi, E. (2017). Concordance of the resting state networks in typically developing, 6-to 7-year-old children and healthy adults. *Frontiers in Human Neuroscience*, *11*. https://doi.org/kd2d

Tong, Y., Hocke, L. M., & Frederick, B. B. (2019). Low frequency systemic hemodynamic “noise” in resting state BOLD fMRI: Characteristics, causes, implications, mitigation strategies, and applications. *Frontiers in Neuroscience*, *13*, 787. https://doi.org/kd2f

Trautmann, S. A., Fehr, T., & Herrmann, M. (2009). Emotions in motion: Dynamic compared to static facial expressions of disgust and happiness reveal more widespread emotion-specific activations. *Brain Research*, *1284*, 100–115. https://doi.org/bcm7vc

Trautwein, F.-M., Kanske, P., Böckler, A., & Singer, T. (2020). Differential benefits of mental training types for attention, compassion, and theory of mind. *Cognition*, *194*, 104039. https://doi.org/10.1016/j.cognition.2019.104039

Uddin, L. Q. (2015). Salience processing and insular cortical function and dysfunction. *Nature Reviews Neuroscience*, *16*(1), 55–61. https://doi.org/10.1038/nrn3857

Uddin, L. Q., Davies, M. S., Scott, A. A., Zaidel, E., Bookheimer, S. Y., Iacoboni, M., & Dapretto, M. (2008). Neural basis of self and other representation in autism: An fMRI study of self-face recognition. *PLOS ONE*, *3*(10), e3526. https://doi.org/bqt9jm

Uddin, L. Q., & Menon, V. (2009). The anterior insula in autism: Under-connected and under-examined. *Neuroscience & Biobehavioral Reviews*, *33*(8), 1198–1203. https://doi.org/10.1016/j.neubiorev.2009.06.002

Uddin, L. Q., Supekar, K., Lynch, C. J., Cheng, K. M., Odriozola, P., Barth, M. E., Phillips, J., Feinstein, C., Abrams, D. A., & Menon, V. (2015). Brain state differentiation and behavioral inflexibility in autism. *Cerebral Cortex*, *25*(12), 4740–4747. https://doi.org/f74hdg

Uddin, L. Q., Yeo, B. T. T., & Spreng, R. N. (2019). Towards a universal taxonomy of macro-scale functional human brain networks. *Brain Topography*, *32*(6), 926–942. https://doi.org/ggrvw5

Urchs, S., Armoza, J., Moreau, C., Benhajali, Y., St-Aubin, J., Orban, P., & Bellec, P. (2019). MIST: A multi-resolution parcellation of functional brain networks. *MNI Open Research*, *1*, 3. https://doi.org/10.12688/mniopenres.12767.2

Utevsky, A. V., Smith, D. V., & Huettel, S. A. (2014). Precuneus is a functional core of the default-mode network. *The Journal of Neuroscience*, *34*(3), 932–940. https://doi.org/f5pb6h

van der Linden, D., Tops, M., & Bakker, A. B. (2021). Go with the flow: A neuroscientific view on being fully engaged. *European Journal of Neuroscience*, *53*(4), 947–963. https://doi.org/10.1111/ejn.15014

Van Overwalle, F., Manto, M., Cattaneo, Z., Clausi, S., Ferrari, C., Gabrieli, J. D. E., Guell, X., Heleven, E., Lupo, M., Ma, Q., Michelutti, M., Olivito, G., Pu, M., Rice, L. C., Schmahmann, J. D., Siciliano, L., Sokolov, A. A., Stoodley, C. J., van Dun, K., … Leggio, M. (2020). Consensus Paper: Cerebellum and Social Cognition. *The Cerebellum*, *19*(6), 833–868. https://doi.org/10.1007/s12311-020-01155-1

Vanni, S., Henriksson, L., & James, A. C. (2005). Multifocal fMRI mapping of visual cortical areas. *NeuroImage*, *27*(1), 95–105. https://doi.org/c65m7k

Vanni, S., Sharifian, F., Heikkinen, H., & Vigário, R. (2015). Modeling fMRI signals can provide insights into neural processing in the cerebral cortex. *Journal of Neurophysiology*, *114*(2), 768–780. https://doi.org/10.1152/jn.00332.2014

Verasai, A. (2017, April). *Autistic Workers are your Strength, not Weakness*. The HR Digest. https://www.thehrdigest.com/autistic-workers-strength-not-weakness/

Vigneshwaran, S., Mahanand, B. S., Suresh, S., & Sundararajan, N. (2015). Using regional homogeneity from functional MRI for diagnosis of ASD among males. *2015 International Joint Conference on Neural Networks (IJCNN)*, 1–8. https://doi.org/10.1109/IJCNN.2015.7280562

Viinikainen, M., Jääskeläinen, I. P., Alexandrov, Y., Balk, M. H., Autti, T., & Sams, M. (2010). Nonlinear relationship between emotional valence and brain activity: Evidence of separate negative and positive valence dimensions. *Human Brain Mapping*, *31*(7), 1030–1040. https://doi.org/10.1002/hbm.20915

Vossel, S., Geng, J. J., & Fink, G. R. (2014). Dorsal and ventral attention systems. *The Neuroscientist*, *20*(2), 150–159. https://doi.org/10.1177/1073858413494269

Walker, N. (2014). Neurodiversity: Some basic terms & definitions. *Neuroqueer*. https://neuroqueer.com/neurodiversity-terms-and-definitions/

Walker, N. (2016). Autism & the pathology paradigm. *Neuroqueer*. https://neuroqueer.com/autism-and-the-pathology-paradigm/

Wallis, C. (2022). *Autism Treatment Shifts Away from "Fixing" the Condition*. Scientific American. https://doi.org/10.1038/scientificamerican1222-25

Wang, L.-H., Ding, W.-Q., & Sun, Y.-G. (2022). Spinal ascending pathways for somatosensory information processing. *Trends in Neurosciences*, *45*(8), 594–607. https://doi.org/10.1016/j.tins.2022.05.005

Wang, Q., Li, H.-Y., Li, Y.-D., Lv, Y.-T., Ma, H.-B., Xiang, A.-F., Jia, X.-Z., & Liu, D.-Q. (2021). Resting-state abnormalities in functional connectivity of the default mode network in autism spectrum disorder: A meta-analysis. *Brain Imaging and Behavior*, *15*(5), 2583–2592. https://doi.org/10.1007/s11682-021-00460-5

Wang, Y., & Li, T.-Q. (2013). Analysis of whole-brain resting-state fMRI data using hierarchical clustering approach. *PloS One*, *8*(10), e76315.

Wang, Y., Msghina, M., & Li, T.-Q. (2016). Studying sub-dendrograms of resting-state functional networks with voxel-wise hierarchical clustering. *Frontiers in Human Neuroscience*, *10*. https://doi.org/f3vg8f

Wardlaw, J., Brindle, W., Casado, A., Shuler, K., Henderson, M., Thomas, B., Macfarlane, J., Muñoz Maniega, S., Lymer, K., Morris, Z., Pernet, C., Nailon, W., Ahearn, T., Mumuni, A. N., Mugruza, C., McLean, J., Chakirova, G., Tao, Y., Simpson, J., & Hernandez, M. (2012). A systematic review of the utility of 1.5 versus 3 Tesla magnetic resonance brain imaging in clinical practice and research. *European Radiology*, *22*, 2295–2303. https://doi.org/10.1007/s00330-012-2500-8

Warnes, G. R., Bolker, B., Bonebakker, L., Gentleman, R., Liaw, W. H. A., Lumley, T., Maechler, M., Magnusson, A., Moeller, S., Schwartz, M., & Venables, B. (2020). *gplots: Various R Programming Tools for Plotting Data*. https://CRAN.R-project.org/package=gplots

Wechsler, D. (1991). *Wechsler intelligence scale for children (WISC-III)*. New York: The Psychological Corporation.

Wei, L., Zhong, S., Nie, S., & Gong, G. (2018). Aberrant development of the asymmetry between hemispheric brain white matter networks in autism spectrum disorder. *European Neuropsychopharmacology: The Journal of the European College of Neuropsychopharmacology*, *28*(1), 48–62. https://doi.org/gcswgf

Weiss, L. A., Arking, D. E., Gene Discovery Project of Johns Hopkins & the Autism Consortium, Daly, M. J., & Chakravarti, A. (2009). A genome-wide linkage and association scan reveals novel loci for autism. *Nature*, *461*(7265), 802–808. https://doi.org/10.1038/nature08490

White, T., Muetzel, R., Schmidt, M., Langeslag, S. J. E., Jaddoe, V., Hofman, A., Calhoun, V. D., Verhulst, F. C., & Tiemeier, H. (2014). Time of acquisition and network stability in pediatric resting-state functional magnetic resonance imaging. *Brain Connectivity*, *4*(6), 417–427. https://doi.org/10.1089/brain.2013.0195

Whitehead, J. C., & Armony, J. L. (2018). Singing in the brain: Neural representation of music and voice as revealed by fMRI. *Human Brain Mapping*, *39*(12), 4913–4924. https://doi.org/10.1002/hbm.24333

Whitehouse, A. J. O., Varcin, K. J., Pillar, S., Billingham, W., Alvares, G. A., Barbaro, J., Bent, C. A., Blenkley, D., Boutrus, M., Chee, A., Chetcuti, L., Clark, A., Davidson, E., Dimov, S., Dissanayake, C., Doyle, J., Grant, M., Green, C. C., Harrap, M., … Hudry, K. (2021). Effect of preemptive intervention on developmental outcomes among infants showing early signs of autism: A randomized clinical trial of outcomes to diagnosis. *JAMA Pediatrics*, e213298. https://doi.org/gmv3s8

Wicker, B., Keysers, C., Plailly, J., Royet, J.-P., Gallese, V., & Rizzolatti, G. (2003). Both of us disgusted in my insula: The common neural basis of seeing and feeling disgust. *Neuron*, *40*(3), 655–664. https://doi.org/dxk5p7

Wickham, H. (2011). The split-apply-combine strategy for data analysis. *Journal of Statistical Software*, *40*(1), 1–29. https://doi.org/10.18637/jss.v040.i01

Wickham, H. (2016). *ggplot2: Elegant Graphics for Data Analysis*. Springer-Verlag New York. https://ggplot2.tidyverse.org

Wickham, H., François, R., Henry, L., & Müller, K. (2020). *dplyr: A Grammar of Data Manipulation*. https://CRAN.R-project.org/package=dplyr

Winkler, A. M., Ridgway, G. R., Webster, M. A., Smith, S. M., & Nichols, T. E. (2014). Permutation inference for the general linear model. *NeuroImage*, *92*, 381–397. https://doi.org/10.1016/j.neuroimage.2014.01.060

Witt, S. T., van Ettinger-Veenstra, H., Salo, T., Riedel, M. C., & Laird, A. R. (2021). What executive function network is that? An image-based meta-analysis of network labels. *Brain Topography*, *34*(5), 598–607. https://doi.org/gjxxd2

Wong, P., Donelly, M., Neck, P., & Boyd, B. (2018). Positive autism: Investigation of workplace characteristics leading to a strengths-based approach to employment of people with autism. *Review of International Comparative Management*, *19*(1), 15–30. https://doi.org/kd2q

Woolrich, M. W., Behrens, T. E. J., Beckmann, C. F., Jenkinson, M., & Smith, S. M. (2004). Multilevel linear modelling for FMRI group analysis using Bayesian inference. *NeuroImage*, *21*(4), 1732–1747. https://doi.org/c7hpkz

Woolrich, M. W., Behrens, T. E. J., & Smith, S. M. (2004). Constrained linear basis sets for HRF modelling using Variational Bayes. *NeuroImage*, *21*(4), 1748–1761. https://doi.org/10.1016/j.neuroimage.2003.12.024

Woolrich, M. W., Ripley, B. D., Brady, M., & Smith, S. M. (2001). Temporal autocorrelation in univariate linear modeling of fMRI data. *NeuroImage*, *14*(6), 1370–1386. https://doi.org/10.1006/nimg.2001.0931

World Health Organization. (2020). *International statistical classification of diseases and related health problems (11th Revision)*. World Health Organization. https://icd.who.int/

Wu, G.-R., Colenbier, N., Van Den Bossche, S., Clauw, K., Johri, A., Tandon, M., & Marinazzo, D. (2021). rsHRF: A toolbox for resting-state HRF estimation and deconvolution. *NeuroImage*, *244*. https://doi.org/gn2zks

Yamasaki, T., Maekawa, T., Fujita, T., & Tobimatsu, S. (2017). Connectopathy in autism spectrum disorders: A review of evidence from visual evoked potentials and diffusion magnetic resonance imaging. *Frontiers in Neuroscience*, *11*. https://doi.org/gckq75

Yang, G., Ye, Q., & Xia, J. (2022). Unbox the black-box for the medical explainable AI via multi-modal and multi-centre data fusion: A mini-review, two showcases and beyond. *An International Journal on Information Fusion*, *77*, 29–52. https://doi.org/10.1016/j.inffus.2021.07.016

Yao, Z., Hu, B., Xie, Y., Zheng, F., Liu, G., Chen, X., & Zheng, W. (2016). Resting-state time-varying analysis reveals aberrant variations of functional connectivity in autism. *Frontiers in Human Neuroscience*, *10*. https://doi.org/gg4v65

Yeo, B. T. T., Krienen, F. M., Sepulcre, J., Sabuncu, M. R., Lashkari, D., Hollinshead, M., Roffman, J. L., Smoller, J. W., Zöllei, L., Polimeni, J. R., Fischl, B., Liu, H., & Buckner, R. L. (2011). The organization of the human cerebral cortex estimated by intrinsic functional connectivity. *Journal of Neurophysiology*, *106*(3), 1125–1165. https://doi.org/10.1152/jn.00338.2011

Yeo, B. T. T., Tandi, J., & Chee, M. W. L. (2015). Functional connectivity during rested wakefulness predicts vulnerability to sleep deprivation. *NeuroImage*, *111*, 147–158. https://doi.org/10.1016/j.neuroimage.2015.02.018

Yu, G., Smith, D. K., Zhu, H., Guan, Y., & Lam, T. T.-Y. (2017). ggtree: An r package for visualization and annotation of phylogenetic trees with their covariates and other associated data. *Methods in Ecology and Evolution*, *8*(1), 28–36. https://doi.org/10.1111/2041-210X.12628

Yue, X., Zhang, G., Li, X., Shen, Y., Wei, W., Bai, Y., Luo, Y., Wei, H., Li, Z., Zhang, X., & Wang, M. (2022). Brain functional alterations in prepubertal boys with autism spectrum disorders. *Frontiers in Human Neuroscience*, *16*. https://doi.org/kd2r

Zang, Y., Jiang, T., Lu, Y., He, Y., & Tian, L. (2004). Regional homogeneity approach to fMRI data analysis. *NeuroImage*, *22*(1), 394–400. https://doi.org/crfqfs

Zhang, J., Cheng, W., Liu, Z., Zhang, K., Lei, X., Yao, Y., Becker, B., Liu, Y., Kendrick, K. M., Lu, G., & Feng, J. (2016). Neural, electrophysiological and anatomical basis of brain-network variability and its characteristic changes in mental disorders. *Brain*, *139*(8), 2307–2321. https://doi.org/10.1093/brain/aww143

Zhang, X., Pan, W.-J., & Keilholz, S. D. (2020). The relationship between BOLD and neural activity arises from temporally sparse events. *NeuroImage*, *207*, 116390. https://doi.org/10.1016/j.neuroimage.2019.116390

Zhao, X., Zhu, S., Cao, Y., Cheng, P., Lin, Y., Sun, Z., Li, Y., Jiang, W., & Du, Y. (2022). Regional homogeneity of adolescents with high-functioning autism spectrum disorder and its association with symptom severity. *Brain and Behavior*, *12*(8), e2693. https://doi.org/10.1002/brb3.2693

Zhuang, X., Walsh, R. R., Sreenivasan, K., Yang, Z., Mishra, V., & Cordes, D. (2018). Incorporating spatial constraint in co-activation pattern analysis to explore the dynamics of resting-state networks: An application to Parkinson's disease. *NeuroImage*, *172*, 64–84. https://doi.org/10.1016/j.neuroimage.2018.01.019

Zou, Q., Miao, X., Liu, D., Wang, D. J. J., Zhuo, Y., & Gao, J.-H. (2015). Reliability comparison of spontaneous brain activities between BOLD and CBF contrasts in eyes-open and eyes-closed resting states. *NeuroImage*, *121*, 91–105. https://doi.org/10.1016/j.neuroimage.2015.07.044

Zou, Q., Wu, C. W., Stein, E. A., Zang, Y., & Yang, Y. (2009). Static and dynamic characteristics of cerebral blood flow during the resting state. *NeuroImage*, *48*(3), 515–524. https://doi.org/10.1016/j.neuroimage.2009.07.006

Zuberer, A., Kucyi, A., Yamashita, A., Wu, C. M., Walter, M., Valera, E. M., & Esterman, M. (2021). Integration and segregation across large-scale intrinsic brain networks as a marker of sustained attention and task-unrelated thought. *NeuroImage*, *229*, 117610. https://doi.org/10.1016/j.neuroimage.2020.117610

Original publications

I Rahko, J. S., Paakki, J.-J., Starck, T. H., Nikkinen, J., Pauls, D. L., Kätsyri, J. V., Jansson-Verkasalo, E. M., Carter, A. S., Hurtig, T. M., Mattila, M.-L., Jussila, K. K., Remes, J. J., Kuusikko-Gauffin, S. A., Sams, M. E., Bölte, S., Ebeling, H. E., Moilanen, I. K., Tervonen, O., & Kiviniemi, V. (2012). Valence scaling of dynamic facial expressions is altered in high-functioning subjects with autism spectrum disorders: an fMRI study. *Journal of Autism and Developmental Disorders*, *42*(6), 1011–1024. https://doi.org/10.1007/s10803-011-1332-8

II Paakki, J.-J., Rahko, J., Long, X., Moilanen, I., Tervonen, O., Nikkinen, J., Starck, T., Remes, J., Hurtig, T., Haapsamo, H., Jussila, K., Kuusikko-Gauffin, S., Mattila, M.-L., Zang, Y., & Kiviniemi, V. (2010). Alterations in regional homogeneity of resting-state brain activity in autism spectrum disorders. *Brain Research*, *1321*, 169–179. https://doi.org/10.1016/j.brainres.2009.12.081

III Paakki, J.-J., Rahko, J. S., Kotila, A., Mattila, M.-L., Miettunen, H., Hurtig, T. M., Jussila, K. K., Kuusikko-Gauffin, S. A., Moilanen, I. K., Tervonen, O., & Kiviniemi, V. J. (2021). Co-activation pattern alterations in autism spectrum disorder – a volume-wise hierarchical clustering fMRI study. *Brain and Behavior, 2021;11:e02174.* https://doi.org/10.1002/brb3.2174

Original publications are not included in the electronic version of the dissertation.

Book orders:
Virtual book store
https://verkkokauppa.omapumu.com/fi/

UNIVERSITY OF OULU P.O. Box 8000 FI-90014 UNIVERSITY OF OULU FINLAND

ACTA UNIVERSITATIS OULUENSIS

ISBN 978-952-62-3741-1 (Paperback)
ISBN 978-952-62-3742-8 (PDF)
ISSN 0355-3221 (Print)
ISSN 1796-2234 (Online)

UNIVERSITY OF OULU